



The Application of Pulsed Wave Doppler Tissue
Imaging in the Evaluation of Cardiac Function in
Cats with Primary Cardiomyopathy and Disease
States Linked to Specific **Cardiomyopathies** in
Human-beings

Kerry Simpson

The University of Edinburgh

PhD

May 2005



Declaration

Dr D Shaw gave statistical advice and guidance. Four abstracts have been published; two in the Journal of Veterinary Internal Medicine, one in the 46th Annual Proceedings of the British Small Animal Veterinary Association and one in the European Journal of Ultrasound. The rest of this thesis has been entirely composed by the author, Kerry Simpson, and has not been presented to any university other than the University of Edinburgh.

Kerry E Simpson
May 2005

Abstract

Cardiac dysfunction is commonly identified in geriatric cats. Disease may be primary, typically hypertrophic cardiomyopathy (HCM), or may occur in association with a number of specific diseases, such as hyperthyroidism or hypertension.

Doppler Tissue Imaging (DTI) techniques allow for the non-invasive assessment of myocardial dynamics. These techniques have previously demonstrated regional and global diastolic impairment in various forms of human cardiomyopathy and in cats with HCM.

The aim of this study was to characterise the echocardiographic findings in healthy geriatric cats and to compare these to the changes seen in geriatric cats with primary cardiomyopathy and disease states linked to specific cardiomyopathies in human beings. It was predicted that from this it might be possible to derive disease specific cardiac changes. In addition, it may be possible to elucidate the affect of medication on disease processes.

A total of 134 cats, aged eight years or above, were studied. Each cat underwent a conventional echocardiographic examination (two-dimensional, spectral Doppler, and M-mode) and a more advanced assessment of diastolic function (pulsed-wave Doppler tissue imaging [pw-DTI], colour M-mode propagation velocity and spectral Doppler assessment of the isovolumetric relaxation time). The cats were grouped according to either the disease process, or the diastolic filling pattern, and groups were then compared.

Pulsed-wave DTI tracings (of both radial and longitudinal velocity) were successfully recorded from the feline myocardium. The repeatability of these measurements was assessed, and generally found to be comparable to the variability reported in human beings. There was no evidence that pw-DTI velocities are affected by age in a normal geriatric cat population. Furthermore, there was no significant difference in the relationship between pw-DTI velocities and age in cats within any of the disease groups studied, although there was some variation with heart rate (as assessed by the R-R interval). In addition, it was demonstrated that when grouped according to the transmitral diastolic flow pattern and the ratio of transmitral A-wave duration to pulmonary venous atrial reversal duration, the pw-DTI flow pattern recorded from the apical four chamber view (at either the lateral aspect of the mitral annulus, or mid-lateral wall) was able to differentiate normal from impaired relaxation and pseudonormal flow patterns.

Analysis of echocardiographic data demonstrated that there was an increase in the thickness of the basilar interventricular septum in the majority of cats studied. Compared to unaffected cats, cats with HCM had a decrease in the E' velocity (recorded by pw-DTI at the interventricular septum) and a tendency towards a decrease at the lateral aspect of the mitral annulus (recorded from the left apical four-chamber view). A similar decrease in the E' velocity in cats and people with HCM has been reported previously, and is thought to suggest diastolic dysfunction in affected individuals. Cats with chronic renal failure demonstrated some mild 2-dimensional and spectral Doppler abnormalities; however, no pw-DTI changes were detected in this group. The hyperthyroid cats demonstrated increased S' velocities, suggesting an increased inotropic state. In addition, the hyperthyroid cats

demonstrated increased A' velocities, the cause of which was undetermined, but which may suggest mild diastolic dysfunction or an increase in atrial systolic function. A comparison of treated and untreated hyperthyroid cats was performed. This found that the treated hyperthyroid cats generally demonstrated less variation from the normal cats, compared to the untreated hyperthyroid cats, this may suggest that the use of carbimazole improves the function of the feline myocardium in thyrotoxic cardiomyopathy.

This work, for the first time, uses novel ultrasound techniques to investigate the myocardial dynamics in normal geriatric cats, cats with primary hypertrophy and cats with a range of disease states linked to specific cardiomyopathies in human beings. The use of these techniques has provided us with a new insight into these disease processes and has evaluated the use of this clinically applicable tool for the evaluation of feline myocardial dynamics.

Albert Einstein, when asked to describe radio, replied: "You see, wire telegraph is a kind of a very, very long cat. You pull his tail in New York and his head is meowing in Los Angeles. Do you understand this? And radio operates exactly the same way: you send signals here, they receive them there. The only difference is that there is no cat."

To my parents, with love

Acknowledgements

I would like to thank Petplan Charitable Trust for the Scholarship that enabled me to carry out this work.

I am indebted to all those who supervised me in the preparation of this thesis. To Brendan Corcoran for his trust and support, to Jo Dukes McEwan for her invaluable input and advice and to Carmel Moran for her technical expertise. I am especially grateful to Anne French for providing the training that allowed me to pursue this project, and for her time, patience and enthusiasm; and to Danielle Gunn-Moore, for her faith, support, encouragement and perceptiveness, I cannot thank her enough; although perhaps to this end I should also thank Frank for his understanding.

There are many people within the university who have helped in the preparation of this thesis. Particularly, I would like to thank Craig Devine for his help with both the repeatability study, and the encouragement that he provided for the main project. I would like to thank and acknowledge Graham Thomas for advice and support, ideas and understanding and Darren Shaw for his invaluable statistical advise and guidance. I must also thank the staff and clinicians within the Large Animal Hospital for allowing me endless access to the Vivid FiVe™ ultrasound machine.

I am grateful to all those who assisted in the clinical care of the cases described in this study and to all the nurses, and students who assisted in holding the cats. I am particularly indebted to Mo Clarke, of Dundas Veterinary Group, Elliot Beattie, of Armac Veterinary Group and Nicola Reed, from the first opinion service of the Royal (Dick) School of Veterinary Studies, for providing a constant stream of cases for inclusion in this project.

Thanks must go to my family and friends who have put up with me during the writing of this thesis; to Le Rayol, for its solitude and to Steven for his unwavering love, support and understanding.

Finally, I would like to thank the cats (and their owners) for participating in this study, without whom, this project would not have been possible.

Contents

ABSTRACT.....	II
ACKNOWLEDGEMENTS.....	VI
LIST OF ABBREVIATIONS USED IN TEXT AND ILLUSTRATIONS	XII
 Chapter 1: General Review	1
 SECTION 1 HYPERTROPHIC CARDIOMYOPATHY	2
1.1 INTRODUCTION: HYPERTROPHIC CARDIOMYOPATHY IN HUMAN BEINGS	2
1.1.1 AETIOLOGY OF HYPERTROPHIC CARDIOMYOPATHY IN HUMAN BEINGS	3
1.1.2 NATURALLY OCCURRING HYPERTROPHIC CARDIOMYOPATHY IN ANIMALS	5
1.1.3 AETIOLOGY OF FELINE HYPERTROPHIC CARDIOMYOPATHY	5
1.1.4 FELINE HYPERTROPHIC CARDIOMYOPATHY: CLINICAL FEATURES OF THE DISEASE	6
SECTION 2 DISEASE STATES LINKED TO SPECIFIC CARDIOMYPATHIES IN HUMAN BEINGS 15	
1.2.1 HYPERTENSIVE CARDIOMYOPATHY	15
1.2.2 URAEMIC CARDIOMYOPATHY	24
1.2.3 THYROTOXIC CARDIOMYOPATHY	33
1.2.4 DIABETIC CARDIOMYOPATHY	43
SECTION 3 ECHOCARDIOGRAPHY AND ITS APPLICATION IN THE ASSESSMENT OF DIASTOLIC FUNCTION	49
1.3.1 INTRODUCTION	49
1.3.1.1 THE USE OF ECHOCARDIOGRAPHY IN THE ASSESSMENT OF DIASTOLIC FUNCTION	49
1.3.2 TECHNIQUES USED TO ASSESS MYOCARDIAL EXCURSION	65
1.3.2.1 MEASUREMENT OF MYOCARDIAL EXCURSION AND DISPLACEMENT	65
1.3.2.2 MYOCARDIAL FIBRE ORIENTATION	66
1.3.2.3 RATE OF CHANGE OF WALL THICKNESS	67
1.3.2.4 MITRAL ANNULUS MOTION	68
1.3.2.5 DOPPLER TISSUE IMAGING	68
SECTION 4 ECHOCARDIOGRAPHY IN THE CAT	82
1.4 INTRODUCTION	82
1.4.1 THE FELINE ECHOCARDIOGRAM	82
 Hypothesis.....	87
 Aim	87
 Chapter 2	88
 Measurement of variability in feline echocardiography: An assessment of traditional and pulse-wave Doppler tissue imaging techniques.....	88

IN ORDER TO COMPREHEND THE CLINICAL SIGNIFICANCE OF CHANGES WITHIN THE FELINE ECHOCARDIOGRAM, IT IS FIRST NECESSARY TO UNDERSTAND THE REPEATABILITY AND REPRODUCIBILITY OF THE MEASURED VARIABLES.....	88
ABSTRACT.....	89
INTRODUCTION.....	90
MATERIALS AND METHODS	92
RESULTS	100
DISCUSSION	103

Chapter 3: Age related variation in pulsed-wave Doppler tissue imaging velocities in normal geriatric cats and geriatric cats with primary cardiomyopathies or disease states linked to specific cardiomyopathies in human beings..... 116

ABSTRACT.....	117
INTRODUCTION.....	119
MATERIALS AND METHODS	121
RESULTS	129
DISCUSSION	131

Chapter 4: Heart rate-related variation in pulsed-wave Doppler tissue imaging velocities in normal geriatric cats and geriatric cats with primary cardiomyopathies or disease states linked to specific cardiomyopathies in human beings..... 141

ABSTRACT.....	142
INTRODUCTION.....	143
MATERIALS AND METHODS	145
RESULTS	146
DISCUSSION	148

Chapter 5 157

The application of pulsed wave Doppler tissue imaging and conventional echocardiographic techniques, in the evaluation of cardiac function in normal geriatric cats and aged cats with primary cardiomyopathies or disease states linked to specific cardiomyopathies in human beings. 157

ABSTRACT.....	159
INTRODUCTION.....	161
MATERIALS AND METHODS	166
RESULTS	169
DISCUSSION	175

Chapter 6 189

The application of pulsed wave Doppler tissue imaging, and conventional echocardiographic techniques, in the evaluation of cardiac function in treated and untreated hyperthyroid cats	189
ABSTRACT.....	190
MATERIALS AND METHODS	199
RESULTS	201
DISCUSSION	206
 Chapter 7	 222
 The clinical application of pulsed-wave Doppler tissue imaging and colour M-mode propagation velocity for the assessment of left ventricular relaxation ...	 222
ABSTRACT.....	223
INTRODUCTION.....	225
MATERIALS AND METHODS	236
RESULTS	238
DISCUSSION	244
 General Discussion	 264
 Appendix 1: Haematology and Serum Biochemistry Profile	 271
 Reference List	 272

Figures:

FIGURE 1: PATTERNS OF TRANSMITRAL FLOW	56
FIGURE 2: COLOUR M-MODE PROPAGATION VELOCITY	63
FIGURE 3: A TYPICAL PULSED-WAVE DOPPLER TISSUE IMAGING (PW-DTI) TRACING.....	114
FIGURE 4: PLACEMENT OF SAMPLING GATE FOR ACQUISITION OF PULSED-WAVE DOPPLER TISSUE IMAGING (PW-DTI) VELOCITIES.....	115
FIGURE 5: LINEAR REGRESSION ANALYSIS OF UNAFFECTED AND DISEASED CATS	137
FIGURE 6: LINEAR REGRESSION ANALYSIS OF UNAFFECTED AND DISEASED CATS (CONTINUED)	138
FIGURE 7: LINEAR REGRESSION ANALYSIS OF DIFFERENT DISEASED GROUPS.....	139
FIGURE 8: LINEAR REGRESSION ANALYSIS OF DIFFERENT DISEASED GROUPS (CONTINUED)	140
FIGURE 9: LINEAR REGRESSION ANALYSIS OF UNAFFECTED AND DISEASED CATS	154
FIGURE 10: LINEAR REGRESSION ANALYSIS OF DIFFERENT DISEASED GROUPS	155
FIGURE 11: LINEAR REGRESSION ANALYSIS OF DIFFERENT DISEASED GROUPS (CONTINUED)	156
FIGURE 12: RIGHT PARASTERNAL LONG-AXIS VIEW DEMONSTRATING A LOCALISED BASILAR SEPTAL BULGE IN A CAT.....	187
FIGURE 13: MULTIPLE COMPARISONS BY THE TUKEY METHOD.....	188
FIGURE 14: MULTIPLE COMPARISONS BY THE TUKEY METHOD.....	221
FIGURE 15: THE EFFECT OF VARYING DIASTOLIC FUNCTION OF TRANSMITRAL, PULMONARY VENOUS AND PULSED WAVE DOPPLER TISSUE IMAGING (PW-DTI) VELOCITIES	258
FIGURE 16: SIGNIFICANT VARIATIONS BETWEEN GROUPS	261
FIGURE 17: SIGNIFICANT VARIATIONS BETWEEN GROUPS (CONTINUED).....	262
FIGURE 18: SIGNIFICANT VARIATIONS BETWEEN GROUPS (CONTINUED).....	263

Tables:

TABLE 1: INTRAOPERATOR VARIABILITY	111
TABLE 2: INTRAOBSERVER VARIABILITY	112
TABLE 3: INTEROBSERVER VARIABILITY	113
TABLE 4: LINEAR REGRESSION ANALYSIS ASSESSING THE RELATIONSHIP BETWEEN AGE AND PULSED-WAVE DOPPLER TISSUE IMAGING (PW-DTI) VELOCITIES.....	135
TABLE 5: LINEAR REGRESSION ANALYSIS ASSESSING THE RELATIONSHIP BETWEEN AGE AND PULSED-WAVE DOPPLER TISSUE IMAGING (PW-DTI) VELOCITIES (CONTINUED)	136
TABLE 6: LINEAR REGRESSION ANALYSIS ASSESSING THE RELATIONSHIP BETWEEN R-R INTERVAL AND PULSED-WAVE DOPPLER TISSUE IMAGING (PW-DTI) VELOCITIES.....	152
TABLE 7: LINEAR REGRESSION ANALYSIS ASSESSING THE RELATIONSHIP BETWEEN R-R INTERVAL AND PULSED-WAVE DOPPLER TISSUE IMAGING (PW-DTI) VELOCITIES (CONTINUED)	153
TABLE 8: INVESTIGATION INTO ECHOCARDIOGRAPHIC DIFFERENCES BETWEEN GROUPS ..	186
TABLE 9: POPULATION CHARACTERISTICS.....	219
TABLE 10: ONE-WAY ANALYSIS OF VARIANCE (ANOVA) ASSESSING THE VARIATION BETWEEN GROUPS.....	220
TABLE 11: THE ASSOCIATION BETWEEN DISEASE AND DIASTOLIC FLOW PATTERN.....	259
TABLE 12: RESULTS OF THE ONE-WAY ANALYSIS OF VARIANCE (ANOVA) ASSESSING THE DIFFERENCES IN ECHOCARDIOGRAPHIC MEASUREMENTS BETWEEN THE GROUPS	260

List of Abbreviations Used in Text and Illustrations

A	Late Diastolic Flow
A'	Velocity of Myocardial Motion During the Late Diastolic Phase
ACE	Angiotensin Converting Enzyme
ALDO	Aldosterone
ALT	Alanine transferase
AngII	Angiotensin II
ANOVA	Analysis of Variance
Ao	Aortic Diameter
AP	Alkaline phosphatase
Ar	Pulmonary venous flow: Atrial Reversal Velocity
ARVC	Arrhythmogenic Right Ventricular Cardiomyopathy
AT	Aortic Thromboembolism
ATP	Adenosine Tri-Phosphate
AV	Aortic Velocity
AV Block	Atrioventricular Block
BP	Blood Pressure
bpm	Breaths per Minute (with regard to RR)
bpm	Beats per Minute (with regard to HR)
BSB	Lone Basilar Septal Bulge
BSH	British Shorthair
Ca ²⁺	Calcium
cAMP	Cyclic Adenosine Monophosphate
CBZ	Carbimazole
c-DTI	Colour DTI
c-erb A	Cellular Erythroblastosis A
CoA	Co-enzyme A
Crea	Creatinine
CRF	Chronic Renal Failure
CsA	Cyclosporin A
d	Diastole
D	Diastolic Peak
DCM	Dilated Cardiomyopathy
dl	decilitre
DLH	Domestic Longhair
DM	Diabetes Mellitus
DNA	Deoxyribose nucleic acid
DSH	Domestic Shorthair
DTI	Doppler Tissue Imaging

Dur	Duration
E	Early Diastolic Flow
E@A	E wave velocity at the point of partial summation
E'	Velocity of Myocardial Motion During the Early Diastolic Phase
E+A	Completely summated E and A wave velocity
ECG	Electrocardiogram
EDV	End Diastolic Volume
EF	Ejection Fraction
ESV	End Systolic Volume
ET-1	Endothelin-1
F	Variance Ratio (ANOVA)
fl	femtolitre
FN	Female Neutered
FPA	Flat Phased Array
FS	Fractional Shortening
g	grams
HCM	Hypertrophic Cardiomyopathy
HiBP	Hypertension
HiT4	Hyperthyroidism
HPRF	High Pulse Repetition Frequency
HR	Heart Rate
Hz	Hertz
IGF-1	Insulin-like Growth Factor 1
IU/L	International units per litre
IVC'	Myocardial motion during the Isovolumetric Contraction Phase
IVCb	IVC' away from the transducer
IVCr	IVC' toward the transducer
IVR'	Myocardial motion during the Isovolumetric Relaxation Phase
IVRb	IVR' away from the transducer
IVRr	IVR' toward the transducer
IVRT	Isovolumetric Relaxation Time
IVS	Interventricular Septum
K ⁺	Potassium
kg	Kilogrammes
l	litre
LAD	Left Atrial Diameter
LAFB	Left Anterior Fascicular Block
LCAC	Long Chain Acyl Carnitines
LPRF	Low Pulse Repetition Frequency
LVD	Left Ventricular Diameter

LVFw	Left Ventricular Free Wall
LVOT	Left Ventricular Outflow Tract
MAM	Mitral Annulus Motion
MCHC	Mean corpuscle haemoglobin content
MCV	Mean corpuscle volume
MHC	Myosin Heavy Chain
mmHg	Millimetres of Mercury
mmol	millimoles
MMV	Mean Myocardial Velocity
MN	Male Neutered
MRI	Magnetic Resonance Imaging
mRNA	Messenger Ribonucleic Acid
MVA	Transmitral A Wave
MVE	Transmitral E Wave
MVG	Myocardial Velocity Gradient
MYL	Myosin Regulatory Light Chain
N	Number
n	Number of Observations
Na ⁺	Sodium
NAD	No Abnormalities Detected
NFκB	Nuclear Factor-κB
nmol	nanomoles
NO	Nitric Oxide
NYHA	New York Heart Association
p	Probability
P	P wave (With regard to ECGs)
PAS	Periodic Acid-Schiff
PCV	Packed Cell Volume
PCV	Packed Cell Volume
PKD	Polycystic Kidney Disease
PRA	Plasma Renin Activity
PRF	Pulse Repetition Frequency
PSS	Post Systolic Shortening
PST	Post Systolic Thickening
PTH	Parathyroid Hormone
PV	Pulmonic Velocity
PVf	Pulmonary Venous Flow
pw-DTI	Pulsed Wave DTI
R	R wave
R(D)SVS	Royal (Dick) School of Veterinary Studies

RAAS	Renin-Angiotensin-Aldosterone System
RBBB	Right Bundle Branch Block
RBC	Red blood cell
RCM	Restrictive Cardiomyopathy
RCWT	Rate of Change of Wall Thickness
RR	Respiratory Rate
R-R	R-R Interval (assessed on the ECG)
rT3	Reverse T3
RVOT	Right Ventricular Outflow Tract
s	Systole
s.d.	Standard deviation
S'	Velocity of Myocardial Motion During Systole
S ₁	First Systolic Peak
S ₂	Second Systolic Peak
SAM	Systolic Anterior Motion
seg	Segmented
S·E _v	Sample Variance (95% Confidence Intervals)
SNX	Sub-total Nephrectomy
SPCs	Supraventricular Premature Complexes
STZ	Streptozotocin
T3	Tri-iodothyronine
T4	Thyroxine
TA	Trans-tricuspid A Wave
TE	Trans-tricuspid E Wave
TnC	Troponin C
TnI	Troponin I
TnT	Troponin T
TRH	Thyroid Releasing Hormone
TSH	Thyroid Stimulating Hormone
UCM	Unclassified Cardiomyopathy
V	Velocity
V (stat)	Coefficient of Variation
V tach	Ventricular Tachycardia
V _p	Propagation Velocity
VPCs	Ventricular Premature Complexes
WBC	White blood cell
x	Cross
yrs	Years
λ	Acquisitional Frequency

μmol	micromoles
τ	Tau

Chapter 1: General Review

The purpose of this review is to provide a brief overview of the information available on the feline primary cardiomyopathy and disease states linked to specific cardiomyopathies in human beings, drawing on comparative information from descriptions of recognised disease in human beings. In particular, those aspects pertinent to the understanding of the echocardiographic features of these diseases are highlighted.

Section 1 Hypertrophic Cardiomyopathy

1.1 Introduction: Hypertrophic Cardiomyopathy in Human Beings

In 1980, the World Health Organisation defined the cardiomyopathies as a group of myocardial diseases of unknown aetiology (WHO/ISFC task force 1980). The committee made the distinction between cardiomyopathies and 'specific heart muscle disease', in which myocardial dysfunction occurred secondary to a known aetiology. However, within the last decade, an increased understanding of the aetiology and pathogenesis of the cardiomyopathies has led to the revision of this classification.

In 1996, the new classification system was published (Richardson, et al 1996). This states that the cardiomyopathies are defined as diseases of the myocardium associated with cardiac dysfunction. They are classified as dilated cardiomyopathy (DCM), hypertrophic cardiomyopathy (HCM), restrictive cardiomyopathy (RCM), and arrhythmogenic right ventricular cardiomyopathy (ARVC). It was also decided to introduce the term 'specific cardiomyopathies' to describe myocardial diseases associated with specific cardiac or systemic disorders. These are further divided according to the underlying aetiology, giving rise to terms such as hypertensive cardiomyopathy and metabolic cardiomyopathy. In addition, the term unclassified cardiomyopathy (UCM) was introduced to accommodate cases in which salient features of more than one disease group may be present.

Hypertrophic cardiomyopathy in human beings was further defined as a disease characterised by ventricular hypertrophy, which may involve either the left and/or right ventricle, is usually symmetrical and involves the interventricular septum (Richardson, et al 1996). Systolic interventricular gradients may be identified and

typically the left ventricular volume is normal or reduced. It is predominantly a familial disease, transmitted as an autosomal dominant trait, typically caused by mutations within the genes encoding for the sarcomeric proteins. Pathological changes include myocyte hypertrophy and disarray with areas of increased loose connective tissue (Richardson, et al 1996).

1.1.1 Aetiology of Hypertrophic Cardiomyopathy in Human Beings

In human beings, HCM is, in the majority of cases, an inherited genetic disorder, with *de novo* mutations occurring frequently (Maron, et al 1995). A genetic basis for HCM was first reported in 1989, when it was discovered that a mutation within the gene encoding beta myosin heavy chain (β MHC) resulted in familial HCM (Jarcho, et al 1989). Since that time, more than 140 mutations have been associated with clinical HCM. These mutations are predominantly in genes encoding for cardiac sarcomeric proteins, although mutations of the mitochondrial genome have also been identified (Ommen and Tajik 2001).

Unfortunately, the phenotypic diversity witnessed in HCM is not explained solely by the plethora of genetic mutations. It is acknowledged that certain mutations, such as those involving the cardiac β MHC gene (MYH7), tend to result in severe hypertrophy and advanced clinical signs at an early age (Havudrup, et al 2002), while others such as mutations in the myosin binding protein C gene (MYPBC3), culminate in mild hypertrophy, and late onset of clinical signs (Havudrup, et al 2002). Furthermore, certain mutations such as those of the cardiac troponin T (TnT) gene (Fujino, et al 2002) or α -tropomyosin (V95A) (Yamauchi-Takahara, et al 1996,

Karibe, et al 2001) typically engender moderate hypertrophy, but carry a poor prognosis. Phenotypic diversity has also been identified in individuals affected by identical mutations (Havudrup, et al 2002). This has led to the assumption that environmental stimuli and/or modifier genes may participate in the onset or expression of clinical disease.

While the effect of environmental stimuli is difficult to assess in the natural setting, there is some evidence that modifier genes may be involved in the clinical heterogeneity witnessed in HCM. It has been demonstrated that polymorphisms of the genes encoding the components of the renin-angiotensin-aldosterone-system (RAAS) influence not only the penetrance but also the degree of hypertrophy in related individuals with familial HCM (Ortlepp, et al 2002). Notably, one recent study has suggested that the overall prognosis with HCM due to β MHC mutation may be altered depending on which functional domain is affected by the missense mutation; a worse prognosis being associated with mutations of the actin binding site or the rod portion of the β MHC in which there was a change in the charge of the amino acid (Woo, et al 2003).

The majority of studies of HCM suggest that hypertrophy is a compensatory response and that the underlying aberration is sarcomere/myocyte hypofunction. This theory is supported by work demonstrating that isolated feline cardiac myocytes expressing the β MHC mutation, Arg⁴⁰³Gln, demonstrate disruption of sarcomere assembly, and myofibrillar disarray (Marian, et al 1995). Furthermore, isolated feline cardiac myocytes expressing the TnT mutation, Arg⁹²Gln, demonstrate decreased fractional shortening and decreased peak shortening velocity, although in

this model there was no observed disruption to the sarcomeric assembly (Marian, et al 1997). In vivo, tissue Doppler echocardiography has demonstrated a decrease in myocardial function prior to the onset of hypertrophy in individuals with mutations encoding for HCM (Nagueh, et al 2001a). In addition, expression profiling of cardiac genes in HCM has shown that not only are a diverse array of genes upregulated, many markers of ‘secondary’ hypertrophy are also increased. This suggests that there may be common pathways involved in the appearance of hypertrophy in HCM and in ‘specific cardiomyopathies’ as would be expected if hypertrophy were merely a compensatory mechanism (Lim, et al 2001).

1.1.2 Naturally Occurring Hypertrophic Cardiomyopathy in Animals

In addition to human beings, HCM has been reported to occur in the dog (Liu, et al 1979, Thomas, et al 1984, Liu, et al 1993), pig (Van Vleet and Ferrans 1986), and in the cat (Lord, et al 1974, Liu, et al 1981, Nishimura, et al 1989b, Kittleson 1998, Fox 1999, Baty, et al 2001). However, the condition is most commonly seen in the cat.

1.1.3 Aetiology of Feline Hypertrophic Cardiomyopathy

Although the aetiology of feline HCM remains undetermined, there have been many studies which have suggested that, like in human beings, there may be a genetic predisposition. In 1999, Kittleson and colleagues identified a family of Maine Coon cats with HCM and an autosomal dominant mode of inheritance, where 100% penetrance was demonstrated (Kittleson, et al 1999). Further studies have

demonstrated left ventricular hypertrophy in a closed colony of Persian cats (Martin, et al 1994), and a familial predisposition for HCM and aortic thromboembolism (AT) in a family of (American) domestic shorthaired cats (Baty, et al 2001). In addition, a family of American shorthaired cats has been identified with a familial tendency for HCM and/or systolic anterior motion of the mitral valve (SAM) (Meurs, et al 1997). In all these studies the pattern of inheritance was consistent with that of an autosomal dominant trait. Polymorphisms of both the feline TnT gene (Magnon, et al 2000a) and the feline myosin regulatory light chain gene (MYL2) (Magnon, et al 2000b) have been identified. Furthermore, it has been found that Myomesin (an M-band sarcomeric protein) was decreased or absent in Maine Coon cats with HCM, compared to control cats (Meurs, et al 2001).

Although genetic mutation remains the most likely aetiology of HCM in cats, several alternative hypotheses have been put forward, including viral, bacterial and nutritional causes (Meurs, et al 1998). Notably, recent work by Meurs and colleagues has resulted in the isolation of feline panleukopenia virus DNA from the hearts of cats with ‘cardiomyopathy’ (Meurs, et al 1998).

1.1.4 Feline Hypertrophic Cardiomyopathy: Clinical Features of the Disease

Prior to 1970, the feline cardiomyopathies were recognised only in association with aortic thromboembolism. In 1970, Liu published the first report describing acquired cardiac lesions which culminated in congestive heart failure (Liu 1970). Over the subsequent decade, various reports were published detailing the gross anatomical and histological features of the feline cardiomyopathies (Lord, et al 1974, Liu 1977,

Wilkins 1977, Van Vleet, et al 1980). At that time, cardiomyopathy was detected in 8.5% of cats that underwent post-mortem examination (Liu 1977). In addition, it was found that the classification system described in human beings suitably differentiated the disease groups described in cats, namely; DCM, HCM, RCM, ARVC, UCM and persistent moderator band cardiomyopathy (Liu, et al 1981, Van Vleet and Ferrans 1986, Fox, et al 1995, Fox, et al 1997). Initially, DCM and HCM were reported to be the most prevalent of the feline cardiomyopathies (Fox 1999). However, in 1987, Pion and colleagues discovered a causal relationship between decreased plasma taurine levels and feline myocardial failure (Pion, et al 1987). With the supplementation of commercial cat food with taurine, the incidence of feline 'DCM' has decreased. Today, the most prevalent feline cardiomyopathy is HCM (Fox 1999).

The prevalence of HCM is reported to be between 27% (Fox 1999) and 67% (Tilley 1976) of all feline cardiomyopathies, the wide variation possibly being due to the misclassification of 'specific cardiomyopathies' in the earlier reports. There appears to be a male predisposition with an odds ratio of 3:1 often being reported (Atkins, et al 1992, Rush, et al 2002), although there are also reports stating that there is no sex predisposition (Rozengurt and Hayward 1984, Martin, et al 1994, Meurs, et al 1997, Ferasin, et al 2003). It has been proposed that this apparent contradiction may arise from a variation in the severity of the disease expressed by the different genders. In his 1999 paper, Kittleson and colleagues noted that affected males displayed more severe clinical signs than affected females (Kittleson, et al 1999). Since most of the statistics alluding to disease prevalence arise from secondary, or tertiary, referral

clinics, the presumed male predisposition may merely reflect a younger or more severely affected group, with these animals possibly being more likely to be referred.

Cats have been diagnosed as having HCM from the age of two months (Fijii, et al 2001) to 24 years (Liu, et al 1975), with a reported mean age of naturally occurring HCM being between 4.8 years (Martin, et al 1994) and seven years (Fox, et al 1995).

The most commonly reported affected 'breeds' are the domestic shorthaired (DSH) and longhaired (DLH) cats (Rush, et al 2002). In addition, Persian cats have been reported as being predisposed to HCM (Tilley and Liu 1975), although this is not universally accepted (Atkins, et al 1992). A high incidence of disease has also been reported in the Maine Coon, the Birman (Fox 1999) and the Ragdoll breeds (Saunders, et al 2001). The Siamese, Burmese and Abyssinian breeds may be under-represented (Fox 1999).

Clinical Findings

Feline HCM is a highly heterogenous disease (Bright, et al 1992, Peterson, et al 1993) and therefore, the associated clinical signs are highly variable. Since many cats are asymptomatic, apparent unexpected sudden death may occur (Atkins, et al 1992). In others, stress may induce dyspnoea, with acute pulmonary oedema or pleural effusion being seen (Liu, et al 1975). Other reported clinical signs include tachypnoea, anorexia, vomiting, syncope or paresis, which is typically posterior paresis, lethargy or cachexia and occasionally ascites (Liu, et al 1975, Tilley and Liu 1975).

Physical examination may reveal a normal or hyperdynamic apical pulse (Luis Fuentes 1992). There may be systolic murmurs or an audible S4, also known as a 'gallop' sound. When present, murmurs are usually the result of either dynamic outflow tract obstruction or atrioventricular valve regurgitation (Rush, et al 2002). In some instances these may occur concurrently; turbulence within the left ventricular outflow tract causing systolic displacement of the septal leaflet of the mitral valve (by the Venturi effect) and with this mitral valve insufficiency: This phenomenon is known as systolic anterior motion or SAM (Kittleson 1995). Arrhythmias, typically tachyarrhythmias, are not uncommon (Luis Fuentes 1992). If congestive heart failure is present there may be moist pulmonary rales (Bond and Fox 1984), decreased thoracic compressibility and/or a decrease in thoracic resonance (Dukes McEwan 1996). In such cases, heart and lung sounds may be muffled. Pulse quality may be reduced, or pulses may be absent if there is thromboembolic disease (Liu, et al 1975). One study of thromboembolic disease in cats demonstrated that this was associated with HCM in 58% of cases (Laste and Harpster 1995). If there is severe right heart disease, there may be abnormal jugular pulses and distended jugular veins (Bright, et al 1992). Occasionally cachexia and/or ascites are reported (Fox 1999).

Diagnosis

A diverse spectrum of electrocardiographic changes have been reported in HCM in cats. All of these are non-specific (Fox 1999). Amongst the most common findings are the presence of a left anterior fascicular block, which has been reported to occur in between 11% (Fox 1999) and 33% (Bright, et al 1992) of cats with HCM.

Reported abnormal rhythms include sinus tachycardia, atrial fibrillation, supraventricular tachycardias and ventricular premature complexes (Harpster 1990, Bright, et al 1992). Increased amplitude and/or duration of individual electrocardiographic (ECG) waveforms is commonly reported. These are thought to represent enlargement of one or more chambers (Harpster 1986).

Radiographic changes are also highly variable and non-diagnostic. With mild disease radiographic changes may be absent or subtle. However, survey radiographs are required to evaluate pulmonary parenchymal and vascular changes (Fox 1999). If congestive heart failure is present, radiographs may reveal pulmonary vascular congestion with interstitial or alveolar oedema (Rush, et al 2002). Frequently, there may be fluid within the pleural space (Rush, et al 2002). Unlike dogs, cats may develop pleural effusion with left or right sided congestive heart failure (Kittleson 1998). It is thought that this may be due to an anatomical variation, in that the blood supply to the visceral pleura is supplied by the pulmonary arteries, whereas in the dog the bronchial arteries provide this blood supply (McLaughlin, et al 1961). It has been hypothesised that since the pulmonary arteries provide the blood supply for the visceral pleura, the pulmonary vein may be involved in drainage; thereby, increased pulmonary pressures may lead to pleural effusion (Kittleson 1998). With generalised or right-sided heart failure, hepatosplenomegaly and/or ascites may also be present (Rush, et al 2002).

If the cardiac silhouette can be imaged adequately, enlargement of one or more chambers may be observed. This is frequently the left atrium, or left auricular appendage (Bond, et al 1988). Although biatrial enlargement, with right ventricular

enlargement and shifting of the apex toward the midline of a dorsoventral projection, (the 'valentine shaped' heart) has been described as a classical finding in HCM (Lord, et al 1974, Tilley 1976), some authors now dispute this as a frequent finding (Fox 1999).

Definitive diagnosis of HCM requires the demonstration of inappropriate ventricular hypertrophy. This can be provided by echocardiography, angiography or post mortem examination. However, echocardiography is the procedure of choice. Techniques by which echocardiography can be utilised in the investigation of HCM will be discussed in Section 4.

Pathology of HCM

It is important to understand the pathological alterations that occur in HCM. This is because it is the alterations in the composition of the myocardium that are responsible for many of the echocardiographic changes seen. Macroscopic post mortem examination reveals an increase in cardiac mass. The normal heart weight in relation to body weight has been reported to be in the range of 4.8 ± 0.1 g/kg, whereas in cats with HCM the range was significantly greater (6.4 ± 0.1 g/kg) (Liu, et al 1993). In addition, one or more of the ventricular walls and the papillary muscles are hypertrophied; the left ventricular chamber being normal or decreased in size (Liu, et al 1981). The pattern of hypertrophy in HCM is typically symmetrical, the free wall and interventricular septum both being affected. In some cases there may also be involvement of the right ventricle (Van Vleet, et al 1980). However, in

approximately 31% of cases there may be disproportionate involvement of the interventricular septum; termed asymmetric septal hypertrophy (Liu, et al 1993). This is in contrast to human beings in which asymmetric hypertrophy accounts for approximately 81% of cases (Liu, et al 1993). When present, this asymmetry may be striking. The upper portion of the septum, adjacent to the anterior leaflet of the mitral valve, is frequently affected (Liu 1977). This localised area of hypertrophy may impinge on the left ventricular outflow tract. In such cases an endocardial mural plaque may be present on the basal interventricular septum and there may be fibrosis of the ventral leaflet of the mitral valve (Liu 1977, Fox 2003) .

Enlargement and hypertrophy of the left (and occasionally right) atrium may be present and in some cases ball thrombi may be found within the atrium (Lord, et al 1974). When present, thromboemboli may be located elsewhere in the body, but are most typically located at the aortic trifurcation (Lord, et al 1974).

If congestive heart failure is present, the lungs may be moist and heavy, with foamy fluid easily expressed from the parenchyma (Van Vleet, et al 1980). Free fluid may be present in the abdomen, thorax or pericardium. Occasionally there may be hepatic congestion (termed nutmeg liver) (Van Vleet, et al 1980).

Histological examination reveals hypertrophy of the cardiac myocytes, which have rectangular hyperchromatic nuclei (Liu, et al 1981). There is an increase in the interstitial connective tissue, with areas of the endocardium being replaced by fibroplasia and there may be interruption of the atrioventricular Purkinje cells with collagen fibres (Liu, et al 1981).

In the majority of cats with asymmetric HCM, microscopic examination of the myocardium reveals myofibrillar disarray affecting at least five per cent of a hypertrophied section (Liu, et al 1981). This disorganisation is predominantly of a “pinwheel” configuration in which myocytes are aligned perpendicularly or obliquely to one another (Liu, et al 1981). The nuclei of some myocytes may be hypertrophied and hyperchromatic. Other areas of non-hypertrophied myocardium may demonstrate similar changes, although these are less prevalent (Liu, et al 1981).

Myofibrillar disarray is a common finding in human HCM, with over 90% of individuals demonstrating this phenomenon in excess of five per cent of the myocardium (Liu, et al 1993). It appears to be an uncommon finding in cats with symmetric hypertrophy, but common in cats with asymmetric hypertrophy (Liu, et al 1993).

Abnormal coronary arteries are reported with equal frequencies in human beings, cats and dogs (Liu, et al 1993). These are most commonly located in the interventricular septum, but may be found elsewhere. The abnormal intramural arteries display thickening of both the tunica media and tunica intima and therefore, a reduction in the luminal diameter. The wall thickening results from increased mucopolysaccharide deposits, increases in smooth muscle cells, fibrous tissue and elastic fibres (Liu, et al 1993).

These abnormalities are found in a large proportion of the vessels in areas in which there is substantial interstitial fibrosis. This is a common inter-species finding and it has been hypothesised in human beings and cats that this relationship may reflect a

causal relationship, the decreased blood flow resulting in myocardial ischaemia and necrosis (Liu, et al 1993).

Section 2 Disease states linked to specific cardiomyopathies in human beings

There are many forms of 'specific' cardiomyopathy described (Richardson, et al 1996). However, many of these are seen principally in human beings. For the purpose of this study, a brief overview of the diseases that may secondarily affect the feline myocardium will be given; these include hypertension, hyperthyroidism, chronic renal failure and diabetes mellitus.

1.2.1 Hypertensive Cardiomyopathy

Cardiac Effects of Hypertension in Human Beings

One of the main changes to occur as a result of systemic hypertension is cardiac hypertrophy. In human beings, this acts as an independent predictor of morbidity and mortality (Weber, et al 1991, Lip, et al 2000). It has been shown that even once the hypertension has been corrected, hypertrophy may remain (Sen 1999, Lip, et al 2000). This has led some investigators to suggest that it is neurohumoral activation that causes the hypertrophy rather than a direct response to the pressure overload (Dhalla, et al 1999, Olivetti, et al 2000).

The classic pattern of hypertrophy described in hypertension is concentric hypertrophy. However, eccentric hypertrophy can also be seen (Frochlich, et al 1992). Diastolic dysfunction has been demonstrated in people with hypertension,

and with essential hypertension, the diastolic filling patterns can identify people at increased cardiovascular risk (Schillaci, et al 2002).

Histologically, hypertensive cardiomyopathy produces cardiac myocytes which are enlarged, there is an increase in the amount of fibrosis and coronary vessels are remodelled demonstrating perivascular fibrosis, and thickening of the tunica media (Yamazaki, et al 1999a). However, if these changes were produced solely as a result of pressure overload, similar changes would be expected in other conditions in which pressure overload is the salient feature. One such condition is aortic stenosis. However, while this condition also causes left ventricular pressure overload, it does not produce the same changes, for example: Intramyocardial arteriole wall thickening and perivascular fibrosis are not features seen in aortic stenosis (Lip, et al 2000).

There have been many studies undertaken which attempt to demonstrate which changes are due to pressure overload and which are due to humoral activation, with conflicting results. Several factors have been implicated in the formation of myocardial hypertrophy, among which the renin-angiotensin-aldosterone system (RAAS) seems to have a central role (Basset, et al 2001). It has been shown that stretching cardiac myocytes increases the production of angiotensin II (AngII) (Kim and Iwao 2000). It has also been demonstrated, by some investigators, that both angiotensin converting enzyme (ACE) inhibitors and the angiotensin receptor I (AT₁) antagonists can suppress the development of hypertrophy and promote its regression if loading conditions improve (Kim and Iwao 2000). However, other investigators have failed to demonstrate this (Kent and McDermott 1996). In addition, studies in

rats have demonstrated that even in the presence of AT₁ blockade AngII mediated proliferation of medial vascular smooth muscle cells and adventitial/interstitial fibroblasts of intramyocardial coronary arteries is inhibited, but AngII mediated proliferation of myoendothelial cells is unaffected (McEwan, et al 1998). Therefore, it appears that AngII plays a role in cardiac hypertrophy, although its activation may not be mandatory (Kent and McDermott 1996, Lorell 1999). Notably, in an experimental study examining the effects of AT₁ receptor blockade by losartan and AngII blockade by the ACE inhibitor captopril on feline cardiac hypertrophy induced by pulmonary artery banding, neither treatment group differed significantly from the control group (Koide, et al 1999). This result suggests that in feline pressure overload the ACE inhibitor captopril may have minimal effects on right ventricular remodelling.

Our understanding is further complicated by studies that have demonstrated that the angiotensin receptor II (AT₂) is the predominant receptor in the diseased heart (Lorell 1999). While its role is still unclear, it does appear to provide an antigrowth response, at least in normal tissue (Lorell 1999). However, it has been shown that in AT₂ receptor knockout mice, pressure overload fails to produce the expected hypertrophy and cardiac function remains normal (Senbonmatsu, et al 2000). This suggests that AT₂ receptors may play a role in the murine hypertrophic response.

Aldosterone (ALDO) and AngII have been shown to precipitate fibrosis (Weber, et al 1991, Fiebeler, et al 2001), the degree of which is decreased in response to both ACE inhibition and spironolactone (an ALDO inhibitor).

In the presence of hypertension the sympathetic nervous system is activated. This leads to myocardial α and β receptors activating intracellular signalling pathways that ultimately lead to cardiac hypertrophy (Kent, et al 1991). One of the results of the activation of these pathways is the increase in intracellular calcium (Iaccarino, et al 2001).

Calcineurin is a calcium-sensitive phosphatase, which has recently been implicated in the development of hypertensive hypertrophy. Calcineurin is activated in response to an increased load (Zou, et al 2001) and remains activated long-term. It can be inhibited by cyclosporin A (CsA). Inhibited models of pressure overload have failed to produce the expected hypertrophy (Avdonin, et al 1999, Lim, et al 2000). Suggesting that, as an intracellular regulatory mediator, calcineurin is involved in AngII induced hypertrophy (Murat, et al 2000).

In addition, it has been demonstrated, in experimental models, that a rise in the endothelin-1 (ET-1) level induces cardiac hypertrophy in the presence of volume overload (Kedzierski and Yanagisawa 2001). It has been hypothesised that AngII may promote hypertrophy partly through upregulation of ET-1 transcription (Massart, et al 1999). Furthermore, it has been shown that in the presence of damaged endothelium, ET-1 is secreted by the vascular smooth muscle cells in addition to the endothelial cells (Kedzierski and Yanagisawa 2001). Therefore, once the endothelium is damaged, for example, by continuous stretch, the level of vasoconstriction provided by the endothelin system is upregulated, causing further damage to the endothelium (Opie 1998b).

As in the normal subject, some of the increased activity of AngII and ET-1 is negated by nitric oxide (NO) mediated vasodilation (Moreno, et al 1996). Moreover, it is hypothesised that some forms of essential hypertension, as described in human beings, may in fact be due to an imbalance in the level of NO compared to AngII (Raij 2001).

Feline Hypertension

In the cat, essential (primary) hypertension is rarely encountered. Most cases of hypertension have been documented secondary to other diseases, the most common of which is chronic renal failure (CRF). Between 61% (Kobayashi, et al 1990) and 73% (Lesser, et al 1992) of cats diagnosed with systemic hypertension are azotaemic. However, in one study investigating the incidence of hypertension in a population of cats with CRF, only 19.4% of cats were hypertensive (Syme, et al 2002). Notably, there was no association between the degree of azotaemia and the incidence of hypertension (Syme, et al 2002). Other documented causes of feline hypertension include hyperthyroidism (Kobayashi, et al 1990), diabetes mellitus, acromegaly, pheochromocytoma, hyperadrenocorticism, primary hyperaldosteronism (Flood, et al 1999), hyperparathyroidism and hypercalcaemia, anaemia and polycythaemia (Dukes 1992). There are also some reports of essential hypertension (Littman 1994, Elliot, et al 2001). However, at this stage it is still unclear whether or not this is a primary disorder comparable to essential hypertension in human beings, since it is difficult to rule out all possible differentials.

Whatever the inciting cause of the elevation in blood pressure, there is always one common feature; pressure overload of the circulatory system. In addition, there are many effects on the neuroendocrine systems. Some of these may be specific to the precipitating disease; others may be stimulated by organ damage secondary to the pressure overload.

Measurement of Feline Blood Pressure

Blood pressure can be measured by direct or indirect methods. Direct blood pressure determination is the gold standard, but requires the placement of an indwelling catheter into a peripheral artery; a technique which is very difficult in the unsedated feline patient (Brown and Henik 1998). Therefore, indirect methods of blood pressure measurement have been evaluated in the cat (Dukes 1992, Grandy, et al 1992, Lesser, et al 1992, Beardow 1993, Sawyer 1993, Branson, et al 1997, Henik 1997, Brown and Henik 1998, Sparkes, et al 1999). These include Doppler, oscillometric and photoplethysmographic methods. Auscultatory techniques, as used commonly in human medicine, are not applicable to cats since the arterial (Korotkoff) sounds are of low amplitude and frequency, making auditory identification inaccurate (Brown and Henik 1998).

All of the methods of indirect blood pressure measurement require an inflatable cuff to be wrapped around an extremity and the cuff to be inflated to a pressure at which arterial blood flow is occluded. The cuff is then gradually deflated and the pressure at which arterial flow recommences is measured. This measurement can be made by

a variety of methods. A Doppler flowmeter, placed distal to the cuff will detect the presence of a Doppler shift marking the recommencement of arterial flow (Grandy, et al 1992). Alternatively, an oscillometric device can be used to measure a change in the pressure within the cuff resulting from arterial pulse pressure (Branson, et al 1997) or infrared radiation can be used to measure arterial volume as in the photoplethysmographic technique (Brown and Henik 1998).

Evaluation of these indirect methods has yielded inconsistent results when assessing veterinary patients. It has generally been found that, in the feline patient, the oscillometric technique is the least accurate (Branson, et al 1997). Evaluation of the photoplethysmograph on anaesthetised patients showed this to be the most accurate of the non-invasive techniques (Brown and Henik 1998). However, there are few reports on the use of this technique in the conscious cat. The Doppler technique is widely available, and has been assessed in conscious cats (Lesser, et al 1992). Unfortunately, this technique does tend to under-estimate high blood pressure and over-estimate low blood pressure (Grandy, et al 1992, Lesser, et al 1992), as do all indirect techniques. Measurements of diastolic blood pressure have proved difficult and highly operator dependent and therefore, are generally not measured in cats (Sawyer 1993).

Systemic blood pressure measurements are affected by the size of cuff used: An oversized cuff tends to produce lower values, while an undersized cuff tends to produce higher values (Henik 1997, Sparkes, et al 1999). It has been extrapolated from the human and canine literature that the ideal cuff width is 40% of the circumference of the limb. However, it has been demonstrated that in cats a figure

closer to 30% may yield more accurate results (Grandy, et al 1992). Unfortunately, at present, the published reference ranges for feline blood pressure measurement, have been deduced using the 40% rule.

There is some disagreement over the ideal site for cuff placement. Studies have demonstrated small, but insignificant, variations between oscillometric measurements recorded over the coccygeal, brachial and medial arteries (Sawyer 1993, Branson, et al 1997). Branson and colleagues also demonstrated that, whether the fur was clipped, or not, did not significantly alter the blood pressure measurement (Branson, et al 1997). Since it is well recognised that cats experience anxiety induced hypertension, it is considered best to keep the stressful stimuli to a minimum (Sparkes, et al 1999), and these include, where possible, avoiding the use of clippers. This in turn may influence the site of cuff placement.

In the veterinary literature, reports citing abnormal values for the blood pressure in the cat are plentiful (Morgan 1986, Kobayashi, et al 1990, Lesser, et al 1992, Littman 1994, Sansom, et al 1994, Branson, et al 1997, Henik 1997, Brown and Henik 1998, Bartges, et al 1999, Sparkes, et al 1999). However, there is an immense variation between authors as to what should be considered normal. These vary not only with the technique used but also when, apparently, the same technique has been used. Although, the actual range of normal feline systolic blood pressure is not known, it has been demonstrated that end organ damage can occur secondary to a raised blood pressure (Morgan 1986, Kobayashi, et al 1990, Lesser, et al 1992, Littman 1994, Sansom, et al 1994, Sansom 1997, Bartges, et al 1999, Crispin and Mould 2001, Elliot, et al 2001). It is generally considered that a cat is hypertensive if the systolic

blood pressure exceeds 160mmHg (when measured using an indirect technique) (Hypertension Consensus Panel 2002).

Cardiac Affects of Feline Hypertension

Reports of hypertension in cats allude to a relationship between high blood pressure and cardiac murmurs, gallops or cardiomegaly (Littman 1994, Snyder, et al 2001). In one such study, 81% of the cats examined were found to have cardiomegaly (Littman 1994). Furthermore, within a population of cats with left ventricular hypertrophy 47.5% were found to be hypertensive (Lesser, et al 1992).

Recently, more detailed reports of the echocardiographic changes in hypertensive cats have been published. It has been found that compared to age matched control cats, cats with an elevated systolic blood pressure, typically demonstrate hypertrophy of the interventricular septum, free wall or both (Nelson, et al 2002, Chetboul, et al 2003b). However, the degree of hypertrophy appears variable, with some affected cats being within the published reference ranges (Nelson, et al 2002). In some cases the ascending aorta has been reported to be dilated (Nelson, et al 2002), as have the atria (Snyder, et al 2001). Notably, two different groups have commented that a common feature in hypertensive cats is a localised area of hypertrophy affecting the basilar septum (Nelson, et al 2002, Chetboul, et al 2003b).

The pathology of feline hypertensive cardiomyopathy has not been fully described. Of two cats with hypertension that had a post mortem examination performed, it was found that the tunica media of the coronary arterioles demonstrated hypertrophy

(Littman 1994). This finding is also reported in human hypertensive hypertrophy, but is not a feature of conditions with precipitate pressure overload (Yamazaki, et al 1999b, Lip, et al 2000).

In addition to its effects on the heart, hypertension has many other effects on other organs including the kidneys (Bartges, et al 1999). Increasing the renal perfusion pressure elicits damage to the glomerulus, hyaline nephrosclerosis (Henik 1997), and may eventually cause renal failure. It is still unclear as to whether or not the high incidence of azotaemia within the hypertensive feline population is a primary or secondary problem (Bartges, et al 1999). This is frequently complicated because hypertension is not diagnosed until ocular signs, such as retinal haemorrhage are seen, at which time the blood pressure is often highly elevated, and may have been so for some time.

1.2.2 Uraemic Cardiomyopathy

Evidence for a Specific Uraemic Cardiomyopathy

Uraemic cardiomyopathy is a term used in human medicine to describe the myocardial changes that occur secondary to CRF (Lewis, et al 1976). In human beings, it is recognised that individuals who are undergoing dialysis are at a higher risk of dying from cardiovascular disease than any other condition (Levin, et al 1999); the risk within this population is five to ten times greater than that within the normal population (Kunz, et al 1998). It has also been demonstrated that there is

cardiac dysfunction in many patients with CRF prior to the commencement of dialysis and it is not merely a side effect of the procedure (Kunz, et al 1998). Abnormal diastolic function was demonstrated in approximately half of the patients in one study, with the other half suffering systolic dysfunction and dilation (Kunz, et al 1998). Furthermore, it has been shown that even after renal transplantation, there remains a degree of cardiac dysfunction (Kunz, et al 1998). Pericardial inflammation and effusion is reported as a common sequel to CRF (Pastan and Braunwald 1988). Although several groups have tried to identify a specific uraemic toxin responsible for these effects, to date, it has not been possible to do so. The present consensus is, that there are in fact several variables which can precipitate cardiac disease, and the dysfunction seen is due to combinations of these factors (Amann, et al 1998, Levin and Foley 2000). This may explain why there are many different types of cardiomyopathy, with either concentric or eccentric changes, identified in CRF patients.

In some cases of CRF, a hypoproliferative anaemia is identified (Levin and Foley 2000). The aetiology of this anaemia is multifactorial. However, the principle constituent appears to be a relative deficiency in the plasma levels of erythropoietin (Al-Ahmad, et al 2001). It remains to be established whether this is due to a decrease in production, an alteration in the threshold below which increased production occurs, or an increase in plasma proteolytic activity resulting in degradation of this hormone (Polzin, et al 1995). Other factors that can play a role in the precipitation of anaemia in the uraemic individual include an increased risk of gastrointestinal haemorrhage (often secondary to gastrointestinal ulceration), a poor

nutritional status, and a mild haemolytic tendency (possibly secondary to a structural alteration within the membrane of the red blood cells, which results in an intolerance to oxidative stress) (Polzin, et al 1995).

Anaemia imposes several effects upon the cardiovascular system. Primarily, there is a decrease in the circulating level of haemoglobin and therefore a relative hypoxaemia (Levin and Foley 2000). It has been demonstrated in CRF patients that there is a significant correlation between the circulating level of haemoglobin, the degree of left ventricular dilation and left ventricular mass (Levin, et al 1999). The hypoxia also leads to stimulation of the RAAS, which in turn stimulates myocyte growth, apoptosis, and interstitial fibrosis (Levin, et al 1999). In human beings, it has been demonstrated that even a limited correction of anaemia leads to a partial regression of left ventricular hypertrophy (Lewis, et al 1976).

A second factor hypothesised to play a role in uraemic cardiomyopathy is hypertension (Brahimi, et al 2000). In CRF induced hypertension the cardiopulmonary baroreceptor influence upon renal haemodynamics is impaired, resulting in less inhibition of sympathetic control (Opie 1998b). Systolic blood pressure has shown a weak correlation with left ventricular hypertrophy within a human population with CRF (Kunz, et al 1998). However, many human studies are complicated by the fact that the majority of patients are undergoing dialysis (Kunz, et al 1998). This alters the arterial compliance and the synchronisation of arterial reflex waves, factors that in themselves are independent determinants of left ventricular hypertrophy (Kunz, et al 1998). In these patients, it has been found that hypertension is a determinant of left ventricular mass. However, diastolic function is

not significantly different between hypertensive and normotensive dialysis patients; being impaired in both groups to the same degree. These results suggest that there are alterations seen in the diastolic function of CRF dialysis patients, out-with those seen secondary to hypertension or anaemia. Furthermore, it has been demonstrated that correction of hypertension fails to reduce cardiac mass to normal (Mall, et al 1990).

Experimental studies have demonstrated a rise in blood pressure following sub-total nephrectomy (SNX). Comparisons between SNX rats and rats with renovascular hypertension have demonstrated that whilst the SNX rats show an increased expression of various growth factors and their receptors, rats with renovascular hypertension (Goldblatt rats) do not. This supports the existence of a specific uraemic cardiomyopathy (Amann, et al 1998).

Moreover, histological studies have identified myocardial interstitial fibrosis in people suffering from uraemia. This fibrosis was distinct from replacement, or ischaemic fibrosis and was independent of hypertension, diabetes mellitus, anaemia, heart weight and the presence or absence of dialysis (Mall, et al 1990). It is recognised that many cats with ventricular hypertrophy have myocardial interstitial fibrosis (Liu 1970), but to date no studies have looked for an association with uraemia.

It has also been hypothesised that an increase in the circulating level of parathyroid hormone (PTH) may be responsible for myocardial dysfunction (Slatopolsky, et al 1980). Hyperparathyroidism is a common feature in human CRF (Slatopolsky, et al 1980). Under normal conditions PTH is involved primarily in calcium homeostasis.

It enhances calcium release from bone by initiating proliferation of the osteoprogenitor cells to form more osteoclasts and thereby increases the rate of bone resorption (Slatopolsky, et al 1980). Reciprocally, PTH acts on the kidney, decreasing both proximal and distal reabsorption of phosphate and increasing the permeability of the proximal tubule, whilst decreasing sodium and calcium reabsorption (Hanley and Sherwood 1978). However, this is reversed in the distal nephron where the reabsorption of calcium is enhanced, resulting in an overall decrease in calcium excretion (Slatopolsky, et al 1980). In addition, PTH affects the reabsorption of several other electrolytes, including magnesium and bicarbonate, and is responsible for the activation of 1-hydroxylase, which is the enzyme responsible for the formation of 1,25-dihydrocholcalciferol (Slatopolsky, et al 1980).

The aetiopathogenesis of renal secondary hyperparathyroidism is incredibly complex and has yet to be fully explained. The chief cells of the parathyroid gland synthesise PTH from pro-parathyroid hormone (Hanley and Sherwood 1978). The main stimulus for secretion of which is a reduction in the circulating level of ionised calcium. The liver and kidney are the principle organs involved in the cleavage of intact PTH, giving rise to PTH fragments. The activity of these fragments varies depending on how they have been cleaved (Slatopolsky, et al 1980). Within the kidney, the biologically active fragments are removed by peritubular uptake and glomerular filtration, while the biologically inactive forms are removed by glomerular filtration and tubular reabsorption. The liver contributes to the removal of only the inactive fragments (Slatopolsky, et al 1980). It has been demonstrated that in uraemic dogs the hepatic uptake of intact PTH is decreased and the renal

clearance of PTH is greatly reduced, in proportion to the decrease in renal plasma flow (Crass, et al 1985).

In human beings, it is thought that the main pathogenic mechanism initiating secondary hyperparathyroidism is phosphate retention; but as the glomerular filtration rate declines, there are also alterations in the metabolism of 1,25-dihydrocholcalciferol, which may be responsible for the development of skeletal resistance to PTH.

In addition, the renal degradation of intact and biologically inactive PTH fragments becomes impaired (Slatopolsky, et al 1980). At present it is not known if these fragments can impose biological actions when present at high concentrations. It is thought that the build up of these metabolites may influence carbohydrate and lipid metabolism, as well as acid-base balance and may be responsible for the calcification of soft tissues, including the blood vessels (Hanley and Sherwood 1978). It has been suggested that this calcification of blood vessels may play a role in cardiac hypertrophy. This is because the replacement of the canine aorta with a non-elastic tube will induce left ventricular hypertrophy despite a constant mean arterial pressure (Kunz, et al 1998). There is also some evidence that in human beings, PTH may promote bone marrow fibrosis and with it, anaemia (Klahr and Slatopolsky 1986). This is a common finding in primary hyperparathyroidism and may be a feature of secondary renal hyperparathyroidism. However, at present it is not possible to deduce whether this anaemia is secondary to the effects of PTH or a direct result of the renal impairment (Slatopolsky, et al 1980), via the mechanisms discussed previously.

Finally, it has been demonstrated that autonomic dysfunction, including a decreased responsiveness of α and β -adrenoreceptors, a reduction in baroreceptor sensitivity and an increase in the circulating level of noradrenaline, may be present in human haemodialysis patients (Dhein, et al 2000). This decrease in β -receptor responsiveness has also been demonstrated in a SNZ model of CRF in rats and has been hypothesised to have been caused by either, an “uncoupling” of the receptor or by inhibition of the receptor by the uraemic toxins (Dhein, et al 2000). Clinically, the blunted β -adrenoceptor responsiveness may functionally contribute to the impaired baroreflex function (Dhein, et al 2000).

Feline Uraemic Cardiomyopathy

To date, CRF is not a recognised cause of feline cardiomyopathy. While it is recognised that CRF is common in aged cats (Elliot, et al 2000), there are no reports of feline uraemic cardiomyopathy. However, since there is a high incidence of both cardiac and renal disease within the aged feline population, a possible association between these conditions is not implausible.

As discussed previously, hypertension associated with CRF is not uncommon in the cat. It has been demonstrated that between 19.4% (Elliot, et al 2001) and 69% (Bartges, et al 1996) of cats with CRF are hypertensive. In one study, cats with CRF had blood pressure measurement approximately 20mmHg higher than the normal group of cats (Mishina, et al 1998). Furthermore, it has been shown that in this sub-

group the renin, AngI, AngII and ALDO levels were increased compared to normal (Mishina, et al 1998). However, this finding is disputed by the findings of Jensen and colleagues, who demonstrated only an increase in ALDO levels (Jensen, et al 1997). Notably, one recent study has reported that cats with polycystic kidney disease (PKD) have a higher systemic blood pressure than unaffected cats (Pedersen, et al 2003). Furthermore, the cats with PKD have a higher ALDO to renin ratio, suggesting either a raised ALDO or decreased renin concentration. It was found that the plasma renin activity (PRA) tended to be lower in cats with PKD (Pedersen, et al 2003). Therefore, the role of the RAAS in feline CRF and hypertension remains unclear.

Pathological studies of cats with renal failure have demonstrated an increase in the number of renin containing epithelioid cells, as well as an increase in the distribution of these cells in cases of mild to moderate renal failure. In addition, they have also shown a reduction in the renin content of those cells with marked renal dysfunction (Taugner, et al 1996). To date, this is the only species in which epithelioid cells secreting renin have been identified within the centrilobular mesangium in addition to their normal distribution (which is within the afferent arteriole of the juxtaglomerular apparatus) (Taugner, et al 1996). This may perhaps indicate an augmented capability of renin synthesis in the cat (Taugner, et al 1996). These researchers observed a 46.6% incidence of left ventricular hypertrophy within the cats with CRF. However, no data were presented documenting the incidence of hypertension within this group. Unfortunately, this study was unable to correlate the proportion of renin containing epithelioid cells with the degree of cardiac hypertrophy in cats with CRF (Taugner, et al 1996). They did, however, report an

increased distribution of these cells, and hypothesised that there may have been previous activation in the severely azotaemic cats, followed by quiescence in the later stages of CRF (Taugner, et al 1996). It is perhaps notable that the same group have found a correlation between the percentage of renin positive cells within the juxtaglomerular apparatus and the occurrence of feline HCM (Taugner 2001).

As in human beings with CRF, secondary renal hyperparathyroidism is also a common occurrence in CRF cats. In one study 84% of cats with CRF also had elevated levels of PTH (Barber and Elliot 1998).

While the aetiopathogenesis of cardiac changes secondary to CRF may still be unclear, the presence of pathological changes has been documented. Pathological studies have identified an increased cardiac mass in cats with concomitant CRF (Taugner, et al 1996), while an echocardiographic study has reported an increase in the diastolic thickness of both basilar interventricular septum and free wall, in addition to left atrial enlargement (Adin, et al 2000). In addition, Rush and colleagues, reported uraemic pericarditis in 11% of cats, which were found to have pericardial disease at post mortem examination (Rush, et al 2002). Furthermore, an increased incidence of right ventricular outflow tract turbulence has been reported in cats with azotaemia, with or without hypertension (Rishniw and Thomas 2002).

Unfortunately, as yet, there have been no studies undertaken to ascertain whether or not a specific uraemic cardiomyopathy exists within the feline population; nor any studies undertaken to investigate the effect of raised PTH, or lowered haematocrit on the feline heart. However, since it is documented that cats with CRF have an increased incidence of hypertension (Elliot, et al 2001), cats with PKD have a higher

systemic blood pressure than unaffected cats (Pedersen, et al 2003), the RAAS may be activated in cats with CRF (Taugner, et al 1996, Mishina, et al 1998), and secondary renal hyperparathyroidism is common in cats (Barber and Elliot 1998); extrapolation from the human literature makes it reasonable to hypothesise that a specific 'uraemic cardiomyopathy' may also exist in cats.

1.2.3 Thyrotoxic Cardiomyopathy

Thyrotoxic Cardiomyopathy in Human Beings

Hyperthyroidism is a commonly recognised endocrine disorder, which results in an overproduction of thyroxine (T4) and tri-iodothyronine (T3). It is generally thought that most actions of the thyroid hormones are mediated by T3 and that T4 plays a role primarily as a pro-hormone. Evidence for this assumption comes from the discovery of nuclear T3 receptors, but not T4, in tissues responsive to thyroid hormone, specifically the heart (Dillmann 1990). There have been several different T3, and T4, isomers identified; the different isomers show varying degrees of biological activity. The initial events precipitating these actions are the energy dependant transport of thyroid hormone across the sarcolemma and the nuclear membrane. The majority of actions elicited by T3 appear to take place in the nucleus, where T3 receptor proteins are located. These are members of the cellular erythroblastosis A (c-erb A) proto-oncogene family (Bahouth 1991). By binding to the receptors, the transcription of specific genes is affected. The type and number of genes affected is widespread, perhaps explaining the multiple changes seen in organs

systems under the influence of thyroid stimulation. The effects of T3 on the heart are mediated by three general mechanisms: (1) the direct effect of thyroid hormone on cardiac tissues, (2) an interaction between the thyroid hormones and the sympathoadrenal system, and (3) the consequence of increased peripheral oxygen consumption and blood flow (Dillmann 1983). In the last three decades, many investigators have attempted to identify which genes are affected by T3 receptor binding, whether they are up or down regulated, and what effect these changes have on cardiac function.

The force and degree with which a muscle, including cardiac muscle, contracts depends upon interactions between thick and thin filaments and calcium ions. Thyroid hormones act at several levels to affect this process and ultimately to increase the force and rate of contraction. The thick filaments are composed mainly of myosin, the thin filaments of actin, troponin (I, C and T forms) and tropomyosin. These filaments are surrounded by the sarcoplasmic reticulum, which accumulates and releases calcium during diastole and systole (Opie 1998a).

The cardiac myosin heavy chain (MHC) isoforms are products of two genes on which the effects of T3 have been studied extensively. These genes code for α and β MHC. Thyroid hormone has been shown to upregulate the production of α MHC and down-regulate β MHC (Tiska, et al 1990). One of the effects of this is to increase the level of myosin V₁ isoenzyme and to decrease the level of myosin V₃, thereby leading to an increased velocity of contraction and diastolic relaxation. Other genes which T3 has been shown to upregulate include cardiac Troponin (Tn) (Averyhart-Fullard, et al 1994), which is a thin filament contractile protein, which displays

isoforms TnT, TnC and TnI. During diastole, tropomyosin binds with actin to prevent an actin-myosin interaction, and therefore, contraction. In order for a contraction to take place it is necessary for calcium stored in the sarcoplasmic reticulum to be released, and this is mediated by a cellular influx of sodium and calcium. When this occurs calcium binds to TnC and this initiates changes which lead to the detachment of tropomyosin from actin, allowing systole to occur. To terminate the contraction, it is necessary to lower the cytoplasmic calcium concentration, which is achieved by a Ca^{2+} -ATPase pump in the sarcoplasmic reticulum. The inhibitory subunit of the Tn complex is TnI. This is an element in transduction of the Ca-binding signal from TnC to TnT-Tropomyosin-actin, and this results in activation of the thin filament cross-bridge reaction (Opie 1998a). In hyperthyroid rats TnI is upregulated at a transcriptional level; thus increasing cardiac cross-bridge cycling (Dieckman and Solaro 1990).

In the hyperthyroid heart, the activity of Ca^{2+} -ATPase is increased. This causes a greater build up of calcium in the sarcoplasmic reticulum during diastole, resulting in an enhanced relaxation. When, during systole, this calcium is released, the increased availability results in more cross-bridge formation and therefore, an enhanced force of contraction (Suko 1973).

In addition, increased levels of T3 are responsible for the upregulation of Na^+ , K^+ -ATPase α_2 , α_3 , and β -isoforms resulting in an increase in the concentration of sarcolemmal Na^+ , K^+ -ATPase isozymes (although, to date, this has only been demonstrated in neonates) (Orlowski and Lingrel 1990). One of the actions of this is to maintain Na^+ and K^+ gradients across the plasma membrane, playing an essential

role in the electroactivity of muscle. Therefore, it is thought that alterations in the expression of these isoforms may play a role in modulating myocardial function and ionotrophy (Dieckman and Solaro 1990).

Expression of the glucose transporter GLUT-4 is promoted by T3 whereas GLUT-1 expression is decreased (Castello 1993). The GLUT-1 receptors are found on the cell surface and are thought to be responsible for the basal uptake of glucose whereas GLUT-4 are intracellular, under basal conditions, and are thought to translocate to the cell surface under the influence of insulin; being responsible for the increase in glucose uptake in response to insulin. It is demonstrated that there is an upregulation in the expression of GLUT-4 messenger ribonucleic acid (mRNA) in the hyperthyroid heart (Sugden, et al 1992).

Exposure of ventricular myocytes to T3 has also been shown to increase the number of β_1 -adrenergic receptors per cell (Bahouth 1991). It is perhaps notable that the number of β_2 receptors remain unaltered (Bahouth 1991). This increase in β_1 -receptors may result in tachycardia and an increase in inotropic response.

Thyroid hormone also exerts several extranuclear effects. Examples of these include an increase in calcium uptake (Segal 1990), an effect that is seen within fifteen seconds of the addition of T3 to rat heart slices, and is independent of extracellular calcium concentration. It is blocked in vitro by inorganic, but not organic, calcium channel blockers, suggesting that it is independent of sarcolemmal depolarisation. It is thought that this is probably associated with a phosphorylation related activation of the calcium channels (Segal 1990).

It has also been shown that T3 produces a rapid increase in 2-deoxyglucose uptake in cardiac myocytes from several species (Segal 1989). This effect is independent of new protein synthesis, but is dependent on the uptake of extracellular calcium (Segal 1990). This is followed by an increase in the cellular cyclic adenosine monophosphate (cAMP) concentration, which in turn is thought to increase the intrinsic activity of plasma membrane sugar transporters (Segal 1989).

A consequence of the influence of T3 on the myocyte is to increase the utilisation of adenosine triphosphate (ATP). However, less of the chemical energy of ATP is utilised in contraction, instead more is converted to heat, which leads to a decreased efficiency of contraction in the hyperthyroid heart (Dillmann 1990, Bing 1994, Han 1994).

The changes noticed in the cardiovascular system in response to an increased level of T3 bear striking resemblances to those seen as a result of an increase in the activity of the sympathetic nervous system. Furthermore, many of these effects can be abolished by the use of β -blocking drugs such as propranolol (Forfar 1982). Evidence surrounding this issue still provokes controversy. Whilst it has been demonstrated that T3 up regulates cardiac β_1 receptors, it seems unlikely that this is the only interaction between the two systems. Some investigators consider it possible that there is an increase in the activity of the sympathoadrenal system. However this seems unlikely since the discovery that plasma and urine levels of catecholamines are either low or normal in hyperthyroidism (Dillmann 1983). There is also data to suggest that the sympathomimetic features of hyperthyroidism may be due to an altered affinity of the ligands for their receptors or to a modification of a post-

receptor processing (Hammond 1987). Although it appears that there are interactions between the two systems, the precise nature of these relationships remains unclear.

The increases in thyroid hormones do not only have a direct effect on the myocardium, but also interact with many different systems. Some of these interactions in turn have an effect on the heart. Hyperthyroidism results in an increase in tissue oxygen consumption, this leads to a peripheral vasodilation, and together these demand an increase in circulatory dynamics (Dillmann 1983). However, since the cardiac output is increased in excess of that seen in other hypermetabolic states, such as exercise, it is thought that the direct changes listed above play the greater role in altering cardiac output (Dillmann 1983).

Aetiology of Hyperthyroidism

The aetiology of feline multinodular adenomatous goitre remains unknown. Goitre arises from multiplication of follicular epithelial cells to form new follicles. Growth-stimulating immunoglobulins, thyroid stimulating hormone (TSH) or other growth factors already present at low concentrations may trigger replication of these cells. In human beings, it is known that thyrotrophin acts as a growth stimulator for normal thyroid cells, acting both directly through the cAMP pathways and indirectly by increasing the sensitivity of thyrocytes to other growth factors such as insulin-like growth factor 1 (IGF-1). It has also been hypothesised that there may be a loss of some of the inhibitory effects of growth modulators and that the development of follicular-cell adenomas may be the result of preferential growth of cell clones

(Gerber, et al 1994). Other authors suggest that environmental factors may play a role in the disease process; these may be toxic, infectious or dietary (Kass, et al 1999). The most common form of hyperthyroidism in human beings is 'Graves disease', an immune-mediated disorder, which is not thought to occur in the cat. Evidence for this is supported in that if feline goitres are transplanted into mice they continue to grow, indicating that if humoral factors are involved in the initiation of the disorder, they are not necessary for maintenance (Gerber, et al 1994). While serum anti-nuclear antibodies and serum thyroid microsomal antibodies have been found in affected cats, immunoglobulins which stimulate thyroid function have not been identified (Kennedy and Thoday 1988, Brown, et al 1992).

Feline Hyperthyroidism

Hyperthyroidism is now recognised as the most commonly occurring endocrine disorder in the domestic cat, the incidence of which is approximately one to two per cent (Fox, et al 1999). It is a disorder of the thyroid gland leading to overproduction of T4 and T3. This is usually caused by a functional thyroid adenoma involving one (30%) or both thyroid lobes (70%), with less than two per cent of cases being caused by a follicular or papillary carcinoma (Feldman and Nelson 2004).

Clinical Features of Feline Hyperthyroidism

Hyperthyroidism is a disease that generally affects cats between the ages of six and 20 years (mean age 11-12 yrs). The most common reasons for initial presentation are polyphagia, weight loss, diarrhoea, intermittent vomiting, hyperactivity, polyuria and/or polydipsia. On physical examination a palpable thyroid goitre is often noted (70-90% of cases), affected cats are usually thin, with reduced muscle mass, may be short tempered, often have a raised resting heart rate, can be hypertensive and may have a systolic heart murmur (Fox, et al 1999). Diagnosis is usually made by demonstrating increased circulating levels of total T4. However, 2-10% of hyperthyroid cats have a resting T4 in the normal range and in these cats it is necessary to demonstrate the over activity of the thyroid gland by means of a thyrotrophin releasing hormone (TRH) stimulation test or a T3 suppression test (Feldman and Nelson 2004).

It has been reported that abnormalities of the cardiovascular system can be found on physical examination, in 95% of hyperthyroid cats (Santilli, et al 2000), and that most cats examined show changes similar to those seen in HCM (with only occasional cases resembling DCM). For this reason hyperthyroidism is sometimes said to cause a form of secondary cardiomyopathy. The most common alterations within the cardiovascular system are hyperkinetic femoral pulses (91.2%), systolic murmurs (44.7%), gallop sounds (31.5%) and sinus tachycardia (26%) (Santilli, et al 2000).

In an attempt to find an accurate non-invasive diagnostic method to evaluate the cardiovascular status of these patients, many studies have been performed to look at

the electrocardiographic, echocardiographic and radiographic changes of affected individuals.

Electrocardiographic studies have reported a sinus tachycardia in 20-34% of cats (Moise and Dietze 1986, Fox, et al 1993, Santilli, et al 2000). Frequently, (in 7%-22% of cats) a left ventricular (LV) enlargement pattern is noticed (Moise and Dietze 1986, Fox, et al 1993, Santilli, et al 2000). Various arrhythmias and conduction disturbances such as left anterior fascicular block and right bundle branch block have also been reported although with a much lower incidence, 8 and 9% respectively (Fox, et al 1993).

Radiographic assessment often reveals cardiac enlargement (in approximately 60% of cases) (Moise and Dietze 1986, Santilli, et al 2000). It will occasionally reveal other changes, such as pulmonary oedema or pleural effusion.

Echocardiographic examinations have revealed that a proportion of cats with hyperthyroidism demonstrate hypertrophy of the LV free wall and/or the interventricular septum, left atrial dilatation, and an increase in left atrium to aortic diameter (Moise and Dietze 1986). In addition to these changes, other authors have also reported an increase in left ventricular end diastolic diameter (but not left ventricular end systolic diameter), and an increase in the indices of contraction such as the percentage change in the ventricular diameter (Bond, et al 1988). This indicates that, in patients not in congestive heart failure, hyperthyroidism is associated with an increased inotropic state (Bond, et al 1988).

Histological examination of cats with cardiac changes secondary to hyperthyroidism has revealed cardiac myocytes of various sizes (some with enlarged nuclei), interstitial fibrosis of the myocardium (predominantly in the left atrium), plus granulation, coagulation and vacuolisation of the sarcoplasm in the left ventricular free wall, septum and right ventricular free wall (Liu, et al 1984). Some cats were found to have fibrosis and degeneration of the atrioventricular node. This may explain the predisposition to arrhythmia seen in hyperthyroid cats (Liu, et al 1984).

Although, in the majority of cats the cardiac muscle cells of the ventricular septum and LV free wall have been found to be in normal parallel alignment, a small minority of cases show foci of marked disorganisation. In these cases the ventricular septum to free wall thickness ratio has been shown to be >1.1 (Liu, et al 1984, Van Vleet and Ferrans 1986). This disorganisation has the same appearance as that seen in asymmetric HCM. However, it has yet to be proven as to whether individuals demonstrating these changes have an underlying primary cardiomyopathy or develop the histological changes secondary to their hyperthyroidism (Liu, et al 1984).

Hyperthyroidism is a readily treatable disorder. Post-treatment the majority of cardiac signs usually resolve and most cats do not require maintenance on cardiac medications (Friedman 1982). Studies have demonstrated that the majority, but not all, of the cardiac alterations reverse if a stable euthyroid state is maintained (Moise and Dietze 1986). The remaining changes may be due to damage invoked by the increased activity that has been imposed on the heart, or it may be because hyperthyroidism is a disease of older cats and they may have had a mild underlying cardiac condition that the hyperkinetic state has exacerbated (Lewis, et al 1979).

1.2.4 Diabetic Cardiomyopathy

Evidence for a Diabetic Cardiomyopathy in Human Beings and Experimental Models

Diabetes mellitus (DM) is characterised by a relative or absolute deficiency of pancreatic insulin production, or activity. Most of the evidence that DM can be responsible for cardiac dysfunction arises from the human literature. The demonstration of an increased risk of congestive heart failure in diabetic people (even when factors such as coronary artery disease, obesity, hypertension and hypercholesterolaemia are taken into consideration), has lead to the conclusion that a specific diabetic cardiomyopathy exists in human beings (Kannel, et al 1974, Annonu, et al 2001).

One of the leading causes of mortality in people with either Type I or II DM is myocardial disease (Annonu, et al 2001). There is also an increased incidence of systemic hypertension and coronary atherosclerosis (Mildenberger, et al 1984). In addition, coronary heart disease is associated with particularly large infarcts and a high index of mortality (Atkins 1991). The increased cardiac dysfunction was originally thought to be the result of atherosclerosis. However, the Framingham study demonstrated an increased risk of congestive heart failure in diabetic patients, even in the absence of clinical coronary artery disease (Kannel, et al 1974). Furthermore, experimental studies of rats with DM and hypertension have revealed significantly more post mortem changes than those with hypertension alone (Factor,

et al 1981). This finding is reflected in clinical DM, where it is recognised that people with DM and hypertension are at an increased risk for cardiovascular disease (Giles and Sander 1989).

It is recognised that both macroangiopathy and microangiopathy occur in diabetics (Tahiliani and McNeill 1986). Macroangiopathy is caused by the accumulation of hyaline substances, cholesterol, calcium and glycoproteins within large blood vessels. This results in thickening of the tunica intima and luminal reduction (Tahiliani and McNeill 1986). In microangiopathy there is both endothelial and subendothelial proliferation, and accumulation of periodic acid-Schiff (PAS) positive material within the small blood vessels within the kidney, eye and in the intramural coronary arteries (Tahiliani and McNeill 1986).

The pathogenesis of these changes remains undetermined. However, a variety of studies have been undertaken using diabetic models such as streptozotocin (STZ) or alloxan treated animals. These studies suggest that myocardial function (particularly diastolic function) is impaired soon after the onset of diabetes; and show that supplementing the animals with insulin can reverse the majority of these changes (Tahiliani and McNeill 1986). Changes that occur include accumulations of lipids and glycogen, loss of myofilament structure, and interstitial fibrosis (Tahiliani and McNeill 1986). Furthermore, studies have demonstrated that the hearts of diabetic animals are more susceptible to ischaemia than non-diabetic controls (Tahiliani and McNeill 1986). Some of these changes are explained by the biochemical abnormalities present within the diabetic myocardium.

It is recognised that in DM, there is functional disruption of the sarcoplasmic reticulum. This is thought to result from the elevated levels of fatty acids present in DM (Tahiliani and McNeill 1986). The long chain acyl carnitines (LCAC) are responsible for transport of fatty acids into the mitochondria. In vitro, the LCACs have been shown to depress the uptake of calcium by the sarcoplasmic reticulum (Tahiliani and McNeill 1986). Furthermore, in diabetic rat hearts, the expression of long-chain fatty-acyl CoA is increased. This occurs in parallel with a decrease in the myocardial levels of ATP. It is hypothesised that this decrease in ATP may result from inhibition of adenine-nucleotide translocase, which is responsible for transporting ATP from the mitochondrion to the cytoplasm (Tahiliani and McNeill 1986).

However, the myocardial alterations occurring in DM are not limited to the sarcoplasmic reticulum. In human beings, DM can induce both hyper- and hypothyroidism. It has been demonstrated that there is a decrease in the circulating level of T3 and an increase in reverse T3 (rT3) in diabetic ketoacidosis and uncontrolled DM. These alterations are thought to arise from alterations in the monodeiodination pathways of T4. Furthermore, hypothalamic regulation of thyroid-pituitary feedback may be defective and there is thought to be an impaired response of the thyroid gland to TSH (Bagchi 1982). The resulting decrease in T3 leads to an alteration in the expression of myosin isoforms, with the expression of the V3 isoform increasing (Tahiliani and McNeill 1986). Myosin V3 is the slowest isoform and therefore, this alteration in the expression of V3 is thought to play a role in slowing the velocity of myocardial contraction (Tahiliani and McNeill 1986).

In addition to the direct effects upon the myocardium, DM causes an autonomic neuropathy. Typically, this affects the parasympathetic nervous system before there is sympathetic dysfunction (Atkins 1991). Due to the loss of parasympathetic control, there is an increase in the resting heart rate in diabetic subjects. This does not respond well to vagal manoeuvres or pharmacological perturbation (Atkins 1991).

Many of the manifestations of diabetic cardiomyopathy can be reversed by insulin supplementation. In addition to its effect on substrate metabolism, insulin appears to have many other important roles, including effects of nerve function, lipoprotein metabolism and vascular function (Sundell and Knuuti 2003). In normal people insulin acts as a vasodilator. This is mediated primarily through the endothelin system with insulin inducing NO formation from endothelial cells (Sundell and Knuuti 2003).

Furthermore, insulin increases the activity of the sympathetic nervous system. It appears that inhibiting centrally mediated sympathetic activity can abolish the insulin-induced vasodilation within the skeletal muscle of normal subjects (Sundell and Knuuti 2003). However, the effect of insulin upon coronary vasodilation is not affected by this mechanism (Sundell and Knuuti 2003).

In people with Type II DM, endothelium-dependant vasodilation has been shown to increase after insulin therapy (Sundell and Knuuti 2003). However, to date, no studies have conclusively demonstrated a direct effect of insulin upon myocardial perfusion.

Despite its effects on myocardial perfusion, insulin concentration has not been determined to be an independent predictor of left ventricular mass in non-diabetic humans (Paternostro, et al 1999). It therefore appears that the cardiac dysfunction witnessed in DM is not merely due to a decreased insulin concentration.

Myocardial dynamics have been studied in human beings with DM. It has been found that even in young, otherwise healthy diabetic patients, there may be left ventricular dysfunction (Mildenberger, et al 1984). This may be manifest as abnormalities of the mitral annulus motion (MAM) (Sanderson, et al 1979), the ratio of pre-ejection period to left ventricular ejection time (Seneviratne 1977), transmitral E:A ratio (Annonu, et al 2001), or peak exercise ejection-fraction (Mildenberger, et al 1984). It remains unknown which of the above, or perhaps other as yet undefined, factors are responsible for this myocardial impairment.

Diabetes Mellitus in the Cat

After hyperthyroidism, DM is the most common feline endocrine disorder. The prevalence is estimated to be approximately 0.25% (Panciera, et al 1990). Both age and gender are recognised risk factors; older male cats being particularly predisposed (Panciera, et al 1990). Other predisposing factors include obesity, and medicating with diabetogenic drugs such as corticosteroids or progestogens (Nelson, et al 1999). Studies in both the UK and Australia have suggested that the Burmese breed of cat is predisposed to DM (Rand, et al 1997, McCann, et al 2005). The human classification system, differentiating DM into Types I and II, has been applied to

feline diabetics (Kirk, et al 1993). However, the validity of this system within the feline diabetic population is disputed (Rand 2002).

To date, there are no reports suggesting an increased incidence of cardiomyopathy in diabetic cats. It has been noted that, unlike humans, cats with DM do not appear to be predisposed to hypertension (Sennello, et al 2003), although there is a high incidence of renal disease within the feline diabetic population. The lack of reported cardiac involvement in feline DM may stem from the relatively high incidence of concurrent disease in this population, masking signs of diabetic cardiomyopathy, or it may be that compared to humans, cats show relatively few signs attributable to cardiomyopathy. It is clear that DM demonstrates many interspecies disparities and diabetic cardiomyopathy may be one such variation.

Section 3 Echocardiography and Its Application in the Assessment of Diastolic Function

1.3.1 Introduction

This section will review the application and utility of echocardiography in the assessment of diastolic dysfunction. In HCM, and many of the specific cardiomyopathies, diastolic dysfunction is believed to be the principle derangement. Therefore, for the purposes of this review, little attention will be paid to the assessment of systolic function. Furthermore, detail will be given to the application of the more novel Doppler tissue imaging techniques in the assessment of myocardial function as they are particularly applicable to this study.

1.3.1.1 The use of Echocardiography in the Assessment of Diastolic Function

Diastole is the period between aortic valve closure and mitral valve closure (Nishimura, et al 1989a). This can be further divided into isovolumic relaxation (the period between aortic valve closure and mitral valve opening), rapid ventricular filling, diastasis (the slow filling phase dependent on the passive filling properties of the heart), and atrial systole (Nishimura, et al 1989b, Appleton, et al 2000). Historically, diastole was largely ignored and thought of simply as the interval in which ventricular filling occurred passively. Gradually, it was recognised that left ventricular stroke volume was dependent on left ventricular end diastolic volume (the Frank-Starling mechanism) and that systole and diastole were in fact part of a dynamic continuum. In the last two decades, diastolic dysfunction has been

recognised as playing a major role in producing the signs of heart failure (Nishimura, et al 1989a). Approximately one third of people with congestive heart failure have normal systolic function, and it is thought that their symptoms are due to diastolic dysfunction (Nishimura, et al 1989b). Furthermore, in many disease states diastolic abnormalities have been shown to precede systolic dysfunction (Nishimura, et al 1989b). Diastolic dysfunction acts to increase intraventricular pressure during diastole. In turn, this increases the pressure in the left atrium and ultimately in the pulmonary circulation, leading to signs of congestive heart failure (Nishimura, et al 1989a). Compensatory mechanisms may decrease the volume filling the heart, leading to a decreased cardiac output and signs of forward failure, even in the presence of normal systolic function (Nishimura, et al 1989a).

Classically, assessment of diastolic function was performed in a catheterisation laboratory. However, in 1982, Kitabatake first speculated that Doppler echocardiography could be used for the non-invasive assessment of left ventricular diastolic filling (Kitabatake, et al 1982). The Doppler indices measured have been validated by comparison with invasive measurements. For this reason, a brief overview of the invasive measurements, movement and pressure changes associated with diastole, is given.

Left ventricular filling can be described in terms of the rate of left ventricular relaxation and ventricular compliance. Relaxation of the left ventricle is measured as the rate of pressure decline during isovolumic relaxation. From this the time constant of isovolumic relaxation, tau (τ), can be calculated from the line fitting the monoexponential equation from the maximal negative change in pressure over

change in time (dP/dt), to 5 mmHg above the left ventricular end-diastolic pressure (Appleton, et al 2000). Furthermore, if left ventricular end-diastolic pressure is plotted against left ventricular end diastolic volume, the corresponding curve can be used to calculate left ventricular compliance (dV/dP) (Appleton, et al 2000). This is the inverse of ventricular wall stiffness and therefore, has an effect on both the left atrial and left ventricular pressures.

Rushmer and colleagues first described the functional anatomy of ventricular contraction in 1952 (Rushmer, et al 1953). In their experiments a series of pins were placed within the different layers comprising the wall of the canine ventricle. Changes in orientation of these pins were observed using cinefluorography, angiography and fluoroscopy. They found that the left ventricular free wall tended to move obliquely toward the apex and the interventricular septum. They demonstrated a base-apex gradient, with the apex remaining almost stationary throughout the cardiac cycle. In addition, these investigators demonstrated that the endocardial surface of the ventricular myocardium moved to a greater extent than the epicardial surface (the transmural gradient). Other investigators later verified these findings (LeWinter, et al 1975, Gallagher, et al 1985).

It was evidence of these dynamic variations that prompted investigations into the interventricular pressure-volume relationship, which is used to assess diastolic mechanisms.



Transmitral Flow

When investigators first began to describe echocardiographic methods of assessing the interventricular pressure-volume relationship, they studied the velocity of blood flow across the mitral valve. The measurements obtained by such a technique are representative of global ventricular filling and do not require assessment of ventricular asynchrony. The rate of flow through the mitral valve is altered by both changes in ventricular compliance and the rate of ventricular relaxation (Nishimura and Appleton 1996).

Transmitral flow can normally be divided into early filling flow, the so-called E wave, followed by flow occurring as a result of atrial systole, the A wave (Figure 1). This can be measured by placing a small sample volume between the tips of the mitral valve leaflets and measuring the velocity of the blood flow using pulsed wave Doppler (Appleton, et al 1988). In a normal subject, the predominant force controlling filling is the rate of ventricular relaxation. The rate of relaxation is a determinant of the atrioventricular pressure gradient. Once the mitral valve opens blood flows freely from the atrium into the ventricle, along this gradient. Therefore, the E wave is dominant. The contribution of atrial systole (the A wave) is small as the volume of blood within the left atrium is not substantial (Appleton, et al 1988). In the initial stages of diastolic impairment there is reduced ventricular compliance, slowing the rate of relaxation. This decreases the atrioventricular pressure gradient and less blood enters the ventricle during early diastole. Therefore, atrial systole plays a more substantial role in ventricular filling, and the corresponding transmitral flow pattern demonstrates a small E wave, prolonged E wave deceleration, and tall A

wave (Appleton, et al 1988). As diastolic impairment worsens the left atrial pressure increases. The elevated left atrial pressure restores the atrioventricular pressure gradient and with this early diastolic filling once more becomes the predominant force involved in ventricular filling. In this situation the transmitral flow pattern mirrors that of a normal subject (pseudonormalisation). Assessment of left ventricular pressures and calculation of τ and dP/dt has led to the realisation that patients demonstrating these filling patterns have increased filling pressures; therefore, the resulting pattern is known as a pseudonormal filling pattern (Appleton, et al 1988). Finally, when diastolic function is severely impaired, and the left atrial pressures are massively elevated, there is an increased atrioventricular pressure gradient. This results in a tall E wave with a sharp deceleration, and a small A wave. In this instance the ratio of E to A is at least two to one (Appleton, et al 2000) (Figure 1).

With the realisation that transmitral flow represented a non-invasive method of assessing diastolic function there began a flux of studies into the effects of different physiological conditions and disease states on these variables. It was found that although transmitral flow generally demonstrated a reasonable correlation with invasive measurements, these patterns are subject to alteration under a variety of conditions: These include changes in mitral inertance (Thomas, et al 1991, Steen and Steen 1994), alterations in loading conditions (Choong, et al 1987, Choong, et al 1988, Stoddard, et al 1989, Thomas and Weyman 1991), heart rate (Smith, et al 1989, Appleton, et al 1991), body weight (Schober and Luis Fuentes 2001a) and age (Schirmer, et al 2000).

It had been presumed that during transmitral flow there was a linear flow through an area of constant cross-sectional area. However, the mitral annulus has been demonstrated as having an increasing area during diastole (Nishimura, et al 1989a). Mitral inertance is the hydro-dynamic force acting upon the acceleration of blood through the orifice (Thomas and Weyman 1991). Therefore, acceleration rate is directly related to atrial pressure as well as mitral inertance. Furthermore, it has been demonstrated both mathematically and invasively that the waveform deceleration rate is directly related to the mitral valve area and the net atrioventricular stiffness. It is independent of the pressure gradient across the mitral valve (Thomas, et al 1990, Thomas, et al 1991). In a study investigating the effects of various physiological variables on mitral filling patterns, the deceleration of the E wave was found to be influenced by both heart rate (Smith, et al 1989, Appleton, et al 1991) and body weight (Schober and Luis Fuentes 2001a). Peak velocity depends on the balance between acceleration and deceleration and can be affected by the aforementioned variables.

Studies have been performed in which left ventricular pressure and transmitral flow patterns were recorded simultaneously. It has been demonstrated that a reduction in preload results in a decreased E velocity and prolongation of the E wave deceleration time, without corresponding changes in the A wave (Choong, et al 1987, Stoddard, et al 1989, Nishimura, et al 1990); whereas, an increase in preload results in an increased E velocity, an increased A velocity, and a decrease in the E wave deceleration time (Stoddard, et al 1989, Nishimura, et al 1990). A decrease in preload is able to alter the E:A ratio without corresponding alterations in τ (Choong, et al 1987, Stoddard, et al 1989).

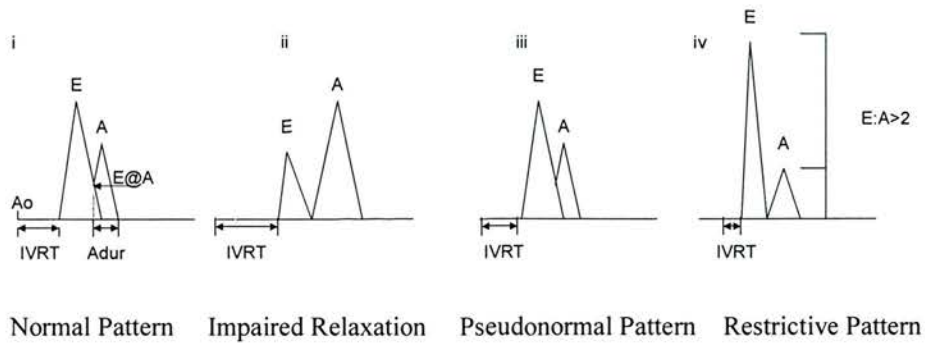
In human beings, it has been shown that different diastolic filling patterns are expected for different age groups (Schirmer, et al 2000). In healthy young subjects elastic recoil is vigorous and the myocardium relaxes rapidly. The majority of filling occurs in early diastole with only a small volume of blood entering the ventricle during atrial systole. With ageing, the amplitude of blood flow slowly alters and the velocities achieved during atrial contraction become more and more significant. A healthy person in their seventies will show an impaired relaxation pattern since the recoil and rate of relaxation have naturally slowed to a state where atrial contraction is responsible for an equal or greater velocity (Schirmer, et al 2000). Recognition of these age related alterations, or the 'natural history' of mitral flow velocity, has led to the formation of age-related reference values for human beings.

Accepting these limitations, attaining spectral Doppler tracings that are a valid representation of transmitral flow has its own inherent difficulties. Initially, flow through the mitral valve is directed centrally but then changes to a posterolateral orientation. This angle of alteration becomes more obtuse with ventricular enlargement, making accurate alignment even harder. This is best corrected by looking for smooth sharp envelopes with a near linear downward slope, and listening for the best flow signal (Appleton, et al 1997). Additionally, at high heart rates, the transmitral E and A waves may become summated, making interpretation impossible.

These diastolic filling patterns are not a direct measure of diastolic function. Since mitral velocity and its respective gradients are determined by the complex interplay between multiple factors, assumptions made with respect to compliance and

relaxation should be interpreted with caution. For this reason, other diastolic modalities are now considered alongside mitral inflow in order to gain a better oversight into cardiac dynamics.

Figure 1: Patterns of transmitral flow



E, Early Filling; A, Filling due to atrial systole; Ao, Aortic valve closure;
 IVRT, Isovolumic relaxation time; Adur, A wave duration; E@A, E velocity at point of (incomplete) summation.

Trans-tricuspid Flow

Diastolic dysfunction does not only affect the left side of the heart. In order to assess global cardiac function tricuspid flow patterns should also be analysed. The tricuspid diastolic velocities are slightly lower than those associated with transmitral flow, but in other respects are similar (Nishimura, et al 1989a). Trans-tricuspid flow is however, subject to greater variation with respiration; velocities increasing during inspiration and decreasing at expiration. It is therefore important to average measurements over several cardiac cycles and where possible to record velocities during apnoea (Appleton, et al 1997).

Measurement of tricuspid flow velocities is undertaken from the four chamber apical view by placing a small (1-2mm) sample size between the tips of the tricuspid valve leaflets (Appleton, et al 1997). Problems in achieving optimal recordings are the same as those for recording mitral flow. Interpretation of tricuspid flow velocities also follows the same principles as interpretation of transmitral flow, and these variables can likewise be subject to alteration by the same physiological determinants (Nishimura, et al 1989b). However, the number of studies analysing trans-tricuspid flow is limited.

Pulmonary Venous Flow

The pulsatile nature of flow through the pulmonary capillary bed has long been recognised (Appleton 1997). The physiologic determinants of this pulsatility had been attributed to various factors, including transmission of the pulse from right ventricular contraction, the combination of left atrial and ventricular events creating a 'suction' effect, and to changes in the left atrial pressure. It has been demonstrated that events affecting the right side of the heart have little influence on these flow patterns which are governed primarily by changes in left atrial pressure, and this in turn is determined by relaxation and contraction of the left atrium and ventricle (Nishimura, et al 1990, Hoit, et al 1992, Appleton 1997). With the growing interest in Doppler derived indexes of diastolic function, pulmonary venous flow patterns have been studied extensively and variables affecting these flow patterns described.

Normal pulmonary venous flow can be divided into one or two systolic peaks of forward flow, followed by a diastolic component, also demonstrating forward flow, and a negative peak representing atrial reversal flow (Smiseth, et al 1999, Appleton, et al 2000).

Measurement of pulmonary venous flow is not easy and can vary greatly with sampling site. The apical four-chamber view is used. In human beings, it is recommended that a small sample size (2- 3mm) is used, with slight anterior angulation and that this is placed 1-2cm into the pulmonary vein (Appleton, et al 1997). Positioning of the cursor too close to the left atrium leads to a flow pattern resembling that of the left atrial pressures and is subject to wall motion artefact, positioning further into the pulmonary bed is resemblant of pulmonary arterial pressures (Appleton, et al 1997).

Like mitral flow, pulmonary venous flow is influenced by numerous factors. For example, it is an age-dependant measurement. As an individual ages, the pulmonary venous flow patterns show a greater systolic than diastolic flow velocity, and an increase in the velocity of the atrial reversal wave (Klein and Tajik 1991, Schober and Luis Fuentes 2001a). This may be due to prolonged relaxation or relaxation abnormalities in older patients. However, this alteration with age has also been demonstrated in a paediatric population, where relaxation abnormalities are unlikely (Abdurrahman 1998). In the same study it was found that the pulmonary venous flow diastolic component was also affected by heart rate, although the systolic and atrial reversal flows were unaffected (Abdurrahman 1998). This is in contrast to the other studies, which have reported a positive correlation between early, or peak, S

velocity and heart rate, and a negative correlation between heart rate and pulmonary venous atrial reversal flow (Appleton 1997, Schober and Luis Fuentes 2001a). It is because of the variation in the peak systolic velocity, that the pulmonary venous systolic to diastolic ratio increases during sinus tachycardia (Klein and Tajik 1991). At very high heart rates the systolic and diastolic waves may fuse.

Loading conditions can also affect pulmonary venous flow velocities. A decrease in preload has been shown to decrease the height and the duration of the atrial reversal flow, and increase the deceleration time of diastolic forward flow. In addition, in some individuals, the systolic signal may become biphasic (Nishimura, et al 1990, Hoit, et al 1992, Appleton 1997). An increase in preload has the opposite effect on the atrial reversal flow; both systolic and diastolic flow velocities increase and their deceleration times shorten. An increase in afterload has been shown to have the same effects as an increase in preload (Nishimura, et al 1990). Importantly, pulmonary venous flow is altered by respiration. Measurements should therefore be averaged over several cardiac cycles and preferably recorded during apnoea (Appleton, et al 1997).

It has been demonstrated that in patients with atrial fibrillation, forward systolic flow is still present, although it is of lower amplitude. Therefore, it has been established that the downward motion of the mitral annulus contributes towards the systolic flow (Nishimura, et al 1990). Since this apical motion of the mitral valve is related to ventricular pressures, a direct correlation can be seen between ventricular output and the velocity of systolic flow. When the systolic flow is seen as a biphasic component, which occurs with lower filling pressures, it has been hypothesised that

the first peak is caused by the atrial relaxation and the second is dependant upon the mitral valve motion (Keren, et al 1985).

Diastolic forward flow reflects the early transmitral flow. The peak pulmonary venous diastolic flow occurs approximately 50msec after peak E wave velocity In human beings. Once the mitral valve has opened the left atrium acts as 'an open conduit' and blood from the pulmonary veins flows directly into the left ventricle. Therefore, peak E wave velocity and duration are dependent upon the same factors as the pulmonary venous flow diastolic component (Keren, et al 1985, Klein and Tajik 1991, Schober, et al 1998).

Atrial contraction increases the pressure in the left atrium and in doing so reverses the pulmonary-atrial pressure gradient, the result of which is flow from the left atrium into the pulmonary circulation; termed the atrial reversal flow. This is not directly comparable to the forward atrial flow (A wave) since there is a discrepancy in the orifice sizes (Nishimura, et al 1990). However, if left ventricular pressure is raised the pressure in the left atrium needs to be greater to achieve the same velocity of forward flow. This is reflected in the pulmonary venous flow and the atrial reversal is relatively more pronounced. An increase in ventricular compliance has the opposite effect. If there is an increase in preload both pulmonary atrial reversal wave and mitral A wave are increased (Nishimura, et al 1990, Rossvoll and Hatle 1993). The duration of the pulmonary venous atrial reversal wave has been compared with the duration of mitral A wave flow. It has been found that if the atrial reversal wave exceeds the duration of the mitral A wave then left ventricular diastolic pressure is increased (Keren, et al 1985, Rossvoll and Hatle 1993). Since a

significant decrease in ventricular compliance is not believed to occur with aging this ratio may be less age dependent than other indexes of pulmonary or mitral flow (Appleton 1993, Klein, et al 1998). The ratio of transmitral A wave to pulmonary venous atrial reversal duration has been used to assess the severity of certain forms of cardiac disease (Abdalla, et al 1998).

Isovolumic Relaxation Time (IVRT)

An estimate of the IVRT can be measured from the left ventricular five chamber apical view (Appleton, et al 1997). Since this is the time between aortic valve closure and mitral valve opening it is necessary to simultaneously record both events. This is achieved by placing a Doppler sampling gate in the left ventricle between the transmitral inflow and aortic outflow. The transducer is angled toward the aortic area until the aortic valve 'click' is recorded. The IVRT is seen as the delay between the aortic valve click and the beginning of mitral flow (Appleton, et al 1997). Doppler recordings of this are ten to 25msecs longer than phonocardiogram measurements when the end and beginning of flow are measured, because mitral flow occurs after initial valve separation. Since the IVRT is determined primarily by the timing of the mitral valve opening and therefore, the atrioventricular pressure gradient, its duration is influenced by both left ventricular relaxation and left atrial pressure (Appleton, et al 1988, Nishimura, et al 1989b). It has been demonstrated that IVRT is a good reflection of τ during changes in contractility, but this correlation is lost when there are alterations in preload (Myreng and Smiseth 1990). Furthermore, IVRT is heart rate dependant (Schmitz, et al 2003). Notably, it has

been seen that by correcting for heart rate in normal children, the IVRT is constant (63 ± 7 msec) (Schmitz, et al 2003).

Occasionally, flow may be recorded during IVRT (Sasson, et al 1987). This is seen in individuals with increased systolic function, and is most common in cases of HCM when there is near cavity obliteration. This is thought to be caused by asynchronous wall motion, leading to the formation of intraventricular flow gradients (Sasson, et al 1987). The movement of these flow gradients could be mistaken for the mitral E wave leading to the recording of an erroneously short IVRT. For this reason it is advantageous to record both mitral and aortic valve clicks, so as to be sure the IVRT is truly measuring the period between the two (Appleton, et al 2000).

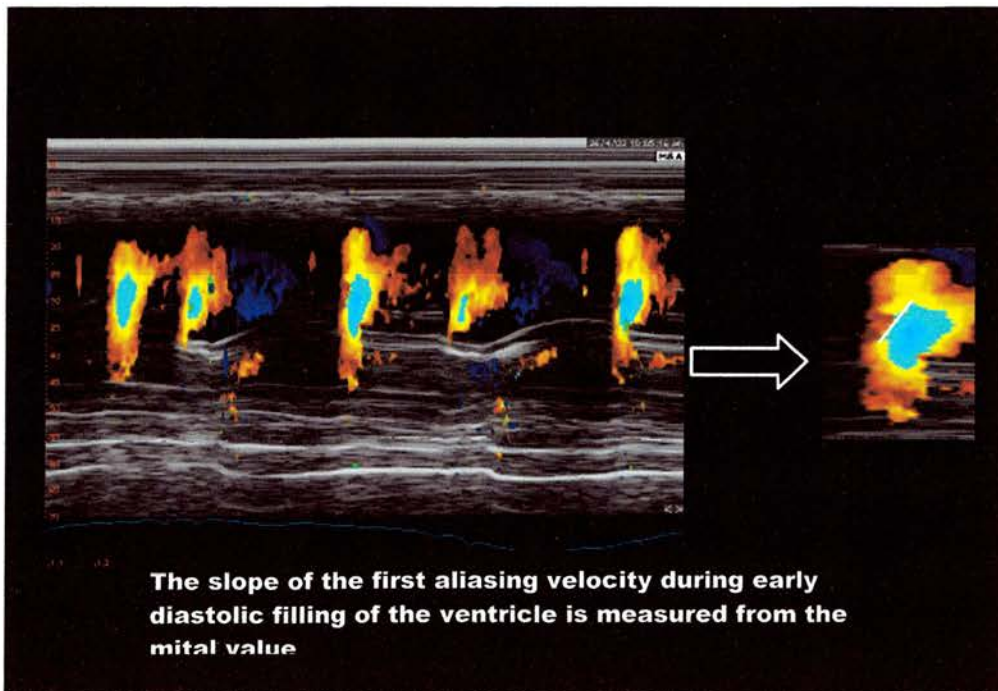
Although these non-invasive measures can give us an estimate of ventricular relaxation and compliance, the number of factors that can affect them has made it difficult to make diagnoses based on these results and investigators have attempted to identify alternative techniques that will give a better estimate of τ and dV/dP under variable conditions.

Colour M-mode Flow Propagation

In 1992, Brun first described the use of colour M-mode flow propagation as an alternative measure of left ventricular relaxation (Brun, et al 1992). This method records the propagation of flow through the mitral valve orifice. It is measured from the apical four chamber view; a colour-flow Doppler sector is positioned over the mitral valve and into the left ventricle, then a cursor is placed through the centre of

the mitral valve and a colour M-mode recording taken. Early papers describing this technique then measured the gradient of the E wave front and compared this to mitral E wave analysis and cardiac catheterisation measurements (Brun, et al 1992). The slope measured by Brun is not uniformly seen in all cases. Today, there are three different techniques used to measure colour M-mode propagation velocity (V_p) (Stoddard, et al 1994, Takatsuji, et al 1996, Garcia, et al 1998). However, a recent paper comparing these techniques recommended the method of Garcia and colleagues (Garcia, et al 1998). This technique has been refined so that the slope of the first aliasing velocity during early filling from the mitral valve plane to four centimetres distally into the left ventricular cavity is now measured (Garcia, et al 1997, Garcia, et al 1998) (Figure 2). The advantages of using colour M-mode analysis is that it is able to provide both good temporal and spatial resolution.

Figure 2: Colour M-mode Propagation Velocity



It has been found that colour M-mode flow propagation generally demonstrates a good correlation with transmitral E wave velocities in normal patients, but in patients with heart disease and pseudonormal flow patterns the V_p is decreased (Takatsuji, et al 1996). It has also been noticed that in these patients the early flow did not reach the apex, but flow from atrial contraction did, with the exception of patients with DCM (Vanoverschelde, et al 1990, Stugaard, et al 1994), in whom flow was not recorded past the mid-ventricular level (Brun, et al 1992).

In catheterised patients, it has been found that V_p is inversely related to τ . During both beta-blockade and asynchronous contraction (engendered by large acute myocardial ischaemia) this correlation remains; suggesting that V_p is independent of cardiac geometry but is in fact responding to changes in wall motion (Stugaard, et al 1993). The asynchronous wall motion observed in many disease states, including myocardial infarction, DCM and HCM, reduces V_p , independent of mitral inflow (Brun, et al 1992, Stugaard, et al 1993, Møller, et al 2000).

The correlation between V_p and τ during dobutamine infusion, led Brun to the conclusion that V_p was independent of preload (Brun, et al 1992). This independence has since been demonstrated in both animal and human models and it has been found that ventricular relaxation is the main determinant of V_p in a variety of conditions (Garcia, et al 1999, Garcia, et al 2000, Møller, et al 2000).

The V_p is therefore not the equivalent of the transmitral E velocity. The difference between these two variables is thought to be due to the formation of vortices during the acceleration of flow through the mitral annulus. It is the propagation of these vortices that play a major role in determining V_p (Vierendeels, et al 2002).

Since V_p does not undergo pseudonormalisation, the ratio of these variables (E/V_p) corrects for the effect of left ventricular relaxation. Therefore, E/V_p can be used as an estimation of capillary wedge pressure (Garcia, et al 1997). Gonzalez-Vilchez and colleagues suggested an alternative method for the estimation of capillary wedge pressure using V_p , $10^3/([2 \cdot IVRT] + V_p)$ (Gonzalez-Vilchez, et al 1999). However, this has yet to be tested in a group other than the study group from which it was derived.

The results of studies to date indicate that V_p shows excellent correlation to τ and as such is the most accurate non-invasive indicator of left ventricular relaxation that can be established using conventional echocardiography. Knowledge of the differences between this variable and other diastolic indexes can enable us to draw inferences about both atrial pressure, and loading conditions, giving a better overview into the diastolic function of the left heart.

1.3.2 Techniques used to assess myocardial excursion

1.3.2.1 Measurement of Myocardial Excursion and Displacement

It has been demonstrated that, while analyses of conventional ultrasound techniques are able to provide us with an assessment of diastolic filling, the affect of various physiological and haemodynamic variables can lead to discrepancies between diastolic filling and diastolic function. Several techniques have been developed to try and better assess myocardial function and advance our understanding of different diseases. One such modality is Doppler tissue imaging (DTI), a range of techniques

that can be used to assess global and regional myocardial velocity and as such, give us new insights into myocardial function and disease processes.

1.3.2.2 Myocardial Fibre Orientation

When the heart contracts the myocardial mass remains constant. Thickening in one direction must therefore be accompanied by shortening in another direction. Since an ultrasound image has at best only two dimensions, DTI analysis of myocardial exertion requires knowledge of both the myocardial structure and the morphology of contraction.

The myocardium is a form of striated muscle only found in the heart (Pederson 1984). The external surface forms the epicardium and the internal surface forms the endocardium. The ventricular walls are comprised of muscle fibres, which are divided into longitudinal and circumferential layers. It is suggested that these are not separate layers per se but a continuum of fibres running from the heart base to the apex (Streeter, et al 1969). The endocardium and epicardium are composed of longitudinal fibres, while at the mid-wall level the fibres display a circumferential orientation. Early experiments alluding to this relationship were performed on canine hearts (Rushmer, et al 1953, Streeter, et al 1969). It has since been demonstrated that the fibre orientation within the feline heart is essentially similar to that found both within the canine and human hearts (Matre, et al 1986). While fibre angles show little interspecies variation, there is a slightly wider variation between the angles of alignment within the feline heart (Matre, et al 1986).

It is well recognised that the contraction of the cardiac muscle layers is asynchronous, with a wave of contraction extending from the level of the mitral annulus toward the apex (Ling, et al 1979). The circumferential fibres contribute approximately two thirds of the force responsible for ejection, while the longitudinal fibres shorten prior to circumferential contraction, giving the ventricle a more spherical form (Gallagher, et al 1985). It is thought that in certain disease states the sequence and timing of these events may become altered leading to the asynchrony of global contraction and a decrease in ejection fraction per unit shortening (Simone, et al 1997). Notably, it has been shown that as an individual ages, the degree of longitudinal fibre shortening decreases whilst the circumferential component increases, demonstrating a change in myocardial synchrony with age (Wandt, et al 1998).

1.3.2.3 Rate of Change of Wall Thickness

The potential benefit of measuring myocardial excursion has long been recognised. Traditionally, this was performed using an M-mode recording to trace the left ventricular endocardial and epicardial borders from end diastole to end systole. This gives a measurement of the rate of change of wall thickness (RCWT) (Hatle and Sutherland 2000). Although this technique has a good temporal resolution, perpendicular alignment could only be achieved for the free wall and septum, therefore only allowing radial thickening and thinning to be assessed. Recent developments in post-processing M-mode applications have improved the ability of

this technique by introducing sectors which can be placed anywhere within the myocardium.

1.3.2.4 Mitral Annulus Motion

A similar principle is used in the assessment of mitral annulus motion (MAM). Again, this technique is based upon M-mode imaging, but this time from a four chamber apical view. This allows assessment of the mitral annulus displacement and therefore the overall longitudinal function of the heart. It has been shown that this relates well to global systolic function, being positively correlated with the ejection fraction (Gulati, et al 1996, Schober and Luis Fuentes 2001b). The major limitations of these techniques are the relatively poor signal to 'noise' ratio when compared to DTI modalities.

1.3.2.5 Doppler Tissue Imaging

The idea of using pulsed-wave Doppler to assess myocardial motion was first suggested in 1961 (Yoshida, et al 1961). However, it was not until 1989 that Issaz and colleagues published the first paper describing the pattern of left ventricular myocardial excursion (Isaaz, et al 1989). The principle behind this technique is the Doppler shift phenomenon.

Conventional Doppler ultrasound uses this principle to assess the velocity of blood as it flows through the heart and vessels. However, the same concept can also be used

to assess the velocity of myocardial excursion. The movement of the ventricular walls generate Doppler shift frequencies of low velocity and high amplitude, whereas the blood-pool generates signals of high velocity and low amplitude (approximately 40dB lower) (Sutherland, et al 1999). Therefore, reflected ultrasound signals can be divided into these two components, which have minimal overlap.

Traditionally, ultrasound machines have filtered out the low velocity signals in order to decrease 'noise'. There are now machines available, which are able to alter the threshold and filtering algorithms, and therefore filter out the signals originating from the blood-pool, allowing the velocities generated by myocardial motion to be depicted (Sutherland, et al 1999). With such refinements, more and more detailed patterns of left ventricular wall motion have become apparent.

There are many ways in which DTI can be used to assess myocardial motion. Some of these, such as pulsed wave DTI (pw-DTI), provide a regional analysis and, as such, are useful at investigating abnormal areas of wall motion within the myocardium, whereas others, such as colour DTI (c-DTI), are able to provide an assessment of global function.

Pulsed-wave Doppler Tissue Imaging

This technique measures the instantaneous peak myocardial velocity as it moves through a pre-selected sample volume. Although this technique has no spatial resolution within a selected sample volume, it has excellent temporal resolution (over 300Hz), normally equivalent to three or four milliseconds (Sutherland and Hatle

2002). The data collected typically demonstrate three dominant waveforms, two of which occur during diastole and one, which occurs during systole. By comparing the timing of the waveforms seen to the mitral inflow profiles, ECG and phonocardiogram recordings, investigators have determined that the principle velocity during systole corresponds to the aortic ejection time (Hatle and Sutherland 2000). This can sometimes be divided into S'_1 and S'_2 . It is thought that S'_1 may represent the peak aortic flow velocity (Hatle and Sutherland 2000). The first of the diastolic peaks is the E' , the second the A' . In normal people E' has been found to precede or coincide with early mitral flow and mitral valve opening (Sohn, et al 1997); as such this velocity is related to the rate of relaxation (Yamanda, et al 1999). The A' peak correlates with the mitral A wave and is therefore the result of the myocardial motion resulting from atrial systole (Hatle and Sutherland 2000).

In young, healthy, individuals the predominant diastolic force is myocardial relaxation and therefore, the E' wave has a greater amplitude than the A' wave (Rychik and Tian 1996, Yamanda, et al 1999, Kapusta, et al 2000). As a person ages, the myocardial relaxation velocity decreases. Therefore, as with the conventional methods of assessing diastolic function, there is a progressive decrease in E' with age, and an increase in A' (Yamanda, et al 1999). The age at which the ratio of E'/A' becomes greater than one depends upon which site is being interrogated (Munagala, et al 2003).

In addition to the three main velocities (S' , E' and A'), there are short peaks, sometimes bi-directional, occurring at the start of systole and diastole that correspond to the regional isovolumic contraction and relaxation velocities,

respectively. These velocities are of short duration, and their timing varies at different locations within the ventricle (Garcia, et al 1996, Trambaiolo, et al 2001). For these reasons they are believed to represent regional changes in the ventricular shape during the isovolumic periods and as such are termed isovolumic contraction' (IVC'), and isovolumic relaxation' (IVR') (it is thought that peak IVC' may be associated with the opening of the aortic valve) (Garcia, et al 1996).

Different echocardiographic views show different velocity profiles, even if the sample is placed at the same level within the myocardium. Velocities which occur at 90 degrees to the Doppler beam are measured as zero. Therefore, the different fibre types are analysed from different angles; the longitudinal fibres from the four or five-chamber apical view and circumferential fibres from parasternal short and long axis views (Oki, et al 1997, Oki, et al 1999).

It has been found that the amplitude, duration and timing of myocardial velocities vary depending on which wall is being studied and at which point in the wall the sample volume is placed (Pai and Gill 1998a). The onset of diastolic motion is reported to occur earlier in the longitudinal fibres than in the circumferential, and earlier in the lateral wall than in the septum (Oki, et al 1997, Galiuto, et al 1998). A base to apex velocity gradient has also been noted, with the highest and earliest velocities occurring at the mitral annulus and decreasing towards the apex (Oki, et al 1997, Oki, et al 1999). These findings are in agreement with the early invasive studies of wall motion (Rushmer, et al 1953, Streeter, et al 1969).

Mitral Annulus Velocities: pw-DTI Analysis

The longitudinal epicardial and endocardial fibres have a common insertion at the mitral annulus (Streeter, et al 1969). Alterations in the dynamics of these fibres determine the longitudinal motion of the mitral annulus (MAM). The MAM has been described as being less dependent upon regional abnormalities, reflecting global left ventricular relaxation (Gulati, et al 1996). The velocities recorded by pw-DTI are relatively load independent, at least within physiological thresholds (Nagueh, et al 1997, Sohn, et al 1997, Agmon, et al 1999, Farias, et al 1999). Peak E' represents myocardial distension during early diastole (E' demonstrates a good correlation with τ) (Oki, et al 1997, Sohn, et al 1997, Ommen, et al 2000). Therefore, pw-DTI patterns can be used to differentiate normal individuals from those with pseudonormal filling patterns (Nagueh, et al 1997, Farias, et al 1999).

It is known that both E and E' are positively correlated with τ , and as such indicate myocardial relaxation (Appleton, et al 1988, Oki, et al 1997, Sohn, et al 1997, Ommen, et al 2000). This correlation is much stronger for E', because E is also affected by left atrial pressure (Choong, et al 1987, Choong, et al 1988, Stoddard, et al 1989, Thomas and Weyman 1991). It therefore follows that, by removing the effect of relaxation from the transmitral E wave velocity, I are left with a measure of left atrial pressure. This has been demonstrated by several groups; a strong correlation between E/E' and left atrial pressure having been determined (Nagueh, et al 1999b, Fristenburg, et al 2000, Ommen, et al 2000). Notably, it has been shown that E/E' is strongly related to pulmonary capillary wedge pressure even when the mitral flow patterns are partially summated (Nagueh, et al 1998). Overall, it has

been found that, in human beings, an E/E' ratio of less than eight accurately estimates a normal atrial pressure, and a ratio greater than fifteen indicates an increased filling pressure, but values between eight and fifteen show some overlap and it is not possible to ascertain whether or not the atrial pressure is raised (Nagueh, et al 1997, Nagueh, et al 1999b, Ommen, et al 2000). It has also been demonstrated that these values are of less diagnostic use if there is preserved systolic function, as can occur in HCM. In such cases, E' no longer acts as a load insensitive variable (Nagueh, et al 2001b) and E wave velocities are less sensitive, thus decreasing the value of both variables (Nagueh, et al 1999b, Friskenburg, et al 2000). However, in one study of patients with HCM, E/E' yielded an r-value of 0.76, compared to 0.53 for A duration to pulmonary venous atrial reversal duration, and 0.33 for E/A (Nagueh, et al 1999b).

In normal patients and patients with left ventricular dysfunction, subendocardial longitudinal systolic pw-DTI velocities at the level of the mitral annulus have been shown to correlate well with peak dp/dt (Yamanda, et al 1998, Sohn, et al 2001).

The Effects of Disease on pw-DTI Patterns

Changes occurring in the velocity profile are generally not disease specific, but merely result from alterations in the velocity and timing of myocardial motion. However, in ischaemic heart disease, specific alterations can be seen. The systolic velocity can be severely depressed, late in onset, and there may be a phenomenon known as post-systolic shortening or thickening (PSS or PST, respectively); in which

a deflection, in the same orientation as the S' peak, is seen during the isovolumic relaxation period (Edvardsen, et al 2000, Rambaldi, et al 2003). This can be detected within five seconds of the onset of ischaemia (Derumeaux, et al 1998). In an experimental study, PST was induced in cats and ischaemia maintained until the disappearance of PST. The myocardium was then allowed to reperfuse, and as this happened the PST returned. The time taken for 'reperfusion-PST' to disappear was correlated to the duration of occlusion and the extent of myocardial necrosis (Song, et al 2003). However, identification of PST relies upon the sample volume being placed on or near to the ischaemic segment and can therefore be problematic (Hatle and Sutherland 2000).

In the presence of chronic myocardial infarction, very small excursions may be present, bearing little resemblance to the normal velocity profile; this is due to scar formation (Hatle and Sutherland 2000). In sub-acute infarction, velocities of a shorter duration than normal may be seen. These are likely to be due to tethering of the infarcted area to surrounding areas and not actually due to velocities being initiated by the infarcted area (Hatle and Sutherland 2000). Diastolic velocities may be decreased, and E'/A' reversal may occur; even when the systolic velocities are preserved (Trambaiolo, et al 2001). These changes are seen earliest by placing the sample volume within the subendocardium, since this layer is the first to be affected by ischaemic episodes (Rahimtoola 2001). There is a normal velocity gradient that exists between the endocardium and epicardium with the endocardium moving the fastest and contributing to 75% of wall thickening and thus having a greater effect on the ejection fraction (Rahimtoola 2001). At rest each myocyte within this layer is supplied by two capillaries within the capillary network and at increased stress,

exercise or on exposure to dobutamine, more capillaries open and each myocyte has an increased blood supply (Kaul 2001). If this increase in perfusion does not occur the myocyte will hibernate; if there is a decrease in perfusion to less than 25% of normal the myocyte will die, and this in turn will affect all myocytes supplied by affected capillaries. It has been demonstrated that E' is dependent upon myocyte numbers, as well as the β -receptor density (Shan, et al 2000). Both necrosis and hibernation can therefore be observed by the use of DTI. If the cause of the ischaemia is removed before necrosis occurs then the myocytes will return to normal, often after an initial hypermotile phase (Bach, et al 1996, Garot, et al 1999). The ejection fraction (EF) will increase and there is a corresponding increase in peak systolic velocity (Bach, et al 1996).

Pulsed-wave Doppler techniques have also proven successful at differentiating human restrictive pericardial disease from RCM. Analysis of the velocity profile of the lateral mitral annulus taken from the apical four-chamber view, has shown that an $E' \geq 8.0$ cm/s is 100% specific and 89% sensitive at differentiating patients with constrictive pericarditis from those with RCM (Rajagopalan, et al 2001).

It has also been demonstrated that both systolic and diastolic components of the Doppler profile are altered in the presence of hypertrophy (Oki, et al 1998, Severino, et al 1998, Mishiro, et al 2000) even when global systolic function is preserved. To date, studies have demonstrated a decrease in E' or both E' and S' velocities in HCM as well as prolongation of E' deceleration, isovolumic relaxation and the time from the second heart sound to E' (Severino, et al 1998). A correlation between τ and the time delay between the second heart sound and E' has been reported. In addition, it

has been found that the standard deviation of this delay is not only increased in people with HCM, it too is correlated to τ , suggesting that DTI can detect asynchrony of relaxation in patients with HCM (Pai and Gill 1998b, Oki, et al 2000).

The transmitral E/lateral annular E' has been shown to be correlated inversely with peak oxygen consumption during exercise testing of patients with HCM (Matsumura, et al 2002). In addition, this ratio has been shown to be correlated with the New York Heart Association (NYHA) class designation (Matsumura, et al 2002).

Another study has demonstrated a significant correlation between pw-DTI from the mitral annulus and MAM in people with HCM. However, in that study, this correlation was poor in the un-diseased state (Rodriguez, et al 1996). Furthermore, in people with HCM, a decrease in myocardial systolic velocity along the longitudinal axis, prior to a corresponding decrease in the radial axis, has been alluded to, demonstrating asynchrony of contraction in patients with HCM (Mishiro, et al 2000, Cardim, et al 2003). In addition, these studies, amongst others, have demonstrated impaired systolic function in non-hypertrophied segments of myocardium (Oki, et al 2000, Tabata, et al 2000, Cardim, et al 2003).

A reduction in E' and S' has been demonstrated to occur prior to the onset of hypertrophy in a transgenic model and more recently in people with mutations encoding for familial HCM. Notably, 13 of these 43 people had no phenotypic expression of hypertrophy (Nagueh, et al 2000, Nagueh, et al 2001a). Even though the decrease in pw-DTI velocity was more marked in individuals with phenotypic expression of HCM, the technique still demonstrated a high sensitivity and specificity in its ability to differentiate mutation carriers from controls (sensitivity

90%, specificity 100%). These studies have demonstrated that familial HCM is in fact primarily a disease of myocardial dysfunction and that the hypertrophy occurs secondary to this (Nagueh, et al 2001a). Furthermore, low S' and E' velocities have been reported in a familial study of myosin binding protein C gene (Arg 502 Gln) mutations, responsible for HCM, even in the absence of hypertrophy (Cardim, et al 2002).

In human beings, HCM is the most common cause of sudden death in competitive athletes under 35 years of age (Cardim, et al 2003). The adaptive cardiac changes which occur with endurance training can mimic HCM. It has been demonstrated that pw-DTI E' velocity is normal or increased in 'athletic hearts' whereas this velocity is decreased in HCM (Caso, et al 2000, Vinereanu, et al 2001, Cardim, et al 2003). Furthermore, S' has been shown to decrease with pathological forms of hypertrophy, whereas it remains normal in athleticism (Vinereanu, et al 2001, Cardim, et al 2003).

In people with hypertension changes are, similar to those reported in HCM. An increase in left ventricular mass has been correlated to the elevation in blood pressure (Olsen, et al 2002). Studies investigating the myocardial velocities in hypertension have demonstrated a decrease in S' in people thought to have isolated diastolic dysfunction (Poulsen, et al 2003). The E' velocity has been shown to be decreased and the A' increased compared to normal subjects (Oki, et al 1998). Furthermore, the time from the second heart sound to peak E' was increased in the hypertensive group (Oki, et al 1998). In people with hypertension the E' has been shown to be negatively correlated with τ , whereas the time from the second heart sound to peak E' was positively correlated with τ , and the A' correlated well with left ventricular

end-diastolic pressure in the absence of transmitral pseudonormalisation (Oki, et al 1998).

Pulsed-wave DTI is of use when local areas of myocardial excursion are of interest. It can also be used to assess mitral annulus velocity and thus provide a measure of mitral annulus motion, which has also been shown to correlate well with left ventricular ejection fraction (Rodriguez, et al 1996). It cannot be used to assess overall myocardial motion (Oki, et al 1997). These profiles have the disadvantage of being altered by bundle branch blocks (Brodin, et al 1999). They are also age specific (Yamanda, et al 1999), as are all myocardial imaging modalities; since there is a natural alteration in the way the myocardium contracts with age and a concurrent reduction in τ . They are also heart rate dependant; the A' to E' ratio increases at high heart rates (Mori, et al 2000). This is due to a decrease in E'; unlike transmitral flow velocities when a similar change in the A to E ratio is brought about by an increase in the A wave amplitude (Mori, et al 2000). It is because of these limitations that age and heart rate must be corrected for when analysing pw-DTI tracings.

Right Ventricular pw-DTI

Recently, the velocity of the tricuspid annulus also has been investigated. It has been determined that, in people without cardiac abnormalities, the S' and A' velocities are far greater than those at the mitral annulus (Alam, et al 1999). When heart failure is present, S' has been found to decrease and a good correlation between right ventricular ejection fraction and S' has been determined (Meluzín, et al 2001). In

addition, in people with or without systolic dysfunction, it has been demonstrated that mean right atrial pressure can be estimated by the ratio of tricuspid E to tricuspid E' (Nagueh, et al 1999a). Furthermore, tricuspid annulus motion has been shown to provide an accurate assessment of both right ventricular systolic and diastolic function in chronic pulmonary hypertension (Moustapha, et al 2001) and inferior myocardial infarction (Alam, et al 2000).

Overall, the power of DTI techniques in the assessment of left ventricular function in a variety of normal and diseased states is obvious, and would support its application in the investigation of cardiac disease in veterinary species.

Although, pw-DTI is the only DTI technique that will be investigated in this thesis, there are some pertinent studies which have utilised other DTI techniques to investigate both HCM and disease states linked to specific cardiomyopathies in human beings. Therefore, a brief description of these modalities will follow. This is by no means an extensive review of these techniques, or all of the available applications of DTI.

Colour Doppler Tissue Imaging

In 1992, McDicken and colleagues (McDicken, et al 1992) first described the use of colour velocity imaging as a means of calculating the velocities within a rotating tissue-mimicking phantom. These results have since been validated in the dog and in human beings (Fleming, et al 1994a, Fleming, et al 1994b, Miyatake, et al 1995, Gorscan, et al 1997). The technique applies the colour Doppler principle to the

myocardium allowing analysis of the velocity of each group of 3x3 pixels, and colour codes the resulting velocity in accordance with the direction and velocity of motion (Uematsu, et al 1995). Motion towards the transmitter is red, away from it blue; the faster the tissue velocity, the brighter the hue.

The colour Doppler images can be assessed visually in order to assess myocardial motion (Drozd, et al 2000). However, visual assessment is relatively inaccurate even with suitable frame rates. Therefore, different techniques have been developed in order to aid analysis of the information in these images. These include post-processing of the colour M-mode or analysis of the motion at a single point, similar to pulsed-wave Doppler analyses. It should be remembered that c-DTI is a technique that analyses the mean velocities, whereas pw-DTI analyses peak myocardial velocities. This decreases the accuracy of myocardial velocity imaging with comparison to pw-DTI. However, c-DTI is particularly useful during stress echocardiography, since a DTI cine loop can be stored from either the apical four chamber, or parasternal long axis view, and the “real time” image subsequently used for post-processing extraction of velocity profiles from different points within the myocardium (Sutherland and Hatle 2002). This allows analysis of both the systolic and diastolic velocities of both the circumferential and longitudinal fibres from the long axis and four chamber apical view, respectively (Trambaiolo, et al 2001). Using this technique it is possible to extract velocity information from approximately 90% of wall segments, with the exclusion of the apex and anterior septum from the free long-axis view (Bach, et al 1996, Uematsu and Miyatake 1999). Reproducibility is excellent; however, velocities are subject to age, heart rate and gender variations, all of which act as independent variables (Palka, et al 1996, Fraser, et al 2001,

Wilkenshoff, et al 2001). The gender variation is not understood but it has been noticed that, whilst the same at baseline, men have a higher response to dobutamine stress under DTI than women (Fraser, et al 2001).

Both pw-DTI and c-DTI can be used to assess myocardial velocities. The principle differences between the techniques being that pw-DTI measures instantaneous velocities whereas, c-DTI measures the mean velocity at a selected point within the myocardium; pw-DTI has a superior frame rate, and c-DTI data can be collected for large areas of myocardium, and the points analysed post-collection, making this modality more suited to stress echocardiography. However, during pw-DTI and c-DTI sampling the velocity of any selected point is affected by the velocity of the surrounding myocardium (termed tagging). By analysing the displacement between two selected points within the myocardium, the effects of tagging and overall cardiac displacement are avoided (Sutherland and Hatle 2002).

Section 4 Echocardiography in the Cat

1.4 Introduction

It is obvious from the previous section that a great deal of information is available on DTI techniques in the assessment of ventricular dysfunction in human beings. It is only recently that such techniques have been used to any great extent in veterinary species, therefore in comparison to what is known in human beings, there remains a gap in our knowledge and understanding.

1.4.1 The Feline Echocardiogram

The first reported use of echocardiography in the cat was in 1979 (Pipers, et al 1979). This was followed by a series of papers in the early 1980s describing the use of echocardiography to produce both two-dimensional and M-mode studies of the feline myocardium (DeMadron, et al 1985, Jacobs and Knight 1985, Fox, et al 1995). Many of these, and later, studies have used anaesthetised or sedated cats. However, there are reports of echocardiographic variables in unsedated cats (Jacobs and Knight 1985, Sisson, et al 1991).

It has become evident that whilst hypertrophy is common in feline myocardial disease, the degree of hypertrophy does not always correlate with the clinical signs or disease course (Bright, et al 1999). Echocardiographic data does however, correlate well with pathological studies; usually finding that the interventricular septum and free wall are both hypertrophied, but also recognising isolated areas of septal or segmental hypertrophy (Fox 1999). In some cases, concurrent, dynamic outflow tract turbulence is also recognised. This can be either left or right ventricular outflow

tract turbulence (LVOT, or RVOT respectively) (Fox 1999, Rishniw and Thomas 2002).

When present, RVOT obstruction appears to be more common in an aged feline population. An increased incidence has been reported with concurrent non-cardiac disease, such as CRF, with or without hypertension, hyperthyroidism, anaemia and neoplasia (Rishniw and Thomas 2002).

Dynamic LVOT is sometimes associated with mitral regurgitation and SAM (Fox 1999). The cause of this phenomenon has evoked great controversy. Proposed mechanisms include; a narrowing of the subaortic outflow tract, abnormally long anterior and posterior mitral valve leaflets, anteriorly displaced papillary muscles, and increased outflow tract velocities giving rise to a Venturi effect causing the septal mitral valve leaflet to be dragged towards the interventricular septum during systole (Fox 1999). Whatever the cause of SAM, the presence of this phenomenon is thought to correlate with pathological identification of an interventricular mural plaque and fibrosis of the septal leaflet of the mitral valve apparatus (Liu, et al 1981). Notably, cats with SAM have been reported to have an improved prognosis compared to those without (Atkins, et al 1992).

In addition, turbulence at the mid-ventricular level has been identified in some cats with hypertrophy. This can also be associated with SAM. It has been suggested that this may be caused by hypertrophy of the papillary muscles and hyperdynamic myocardial contractility (Fox 1999).

It is recognised that cardiac hypertrophy, and with this diastolic dysfunction, are common in the cat. In 1989, Doppler echocardiography was used to investigate many indices of diastolic function in healthy cats (Santilli and Bussadori 1998). These investigators reported that, as in human beings, many of these indices were age dependant; age was positively correlated with A wave velocity, peak pulmonary venous S wave velocity and systolic fraction, and inversely correlated with the transmitral E to A ratio, the diastolic filling time and the velocity time interval of the E wave (Santilli and Bussadori 1998). Notably, pulmonary venous atrial reversal was not correlated with age; this is in contrast to findings in dogs (Schober, et al 1998). The R-R interval (measured from the electrocardiogram) was found to be positively correlated with IVRT and diastolic filling time of transmitral flow, and negatively correlated with the peak A wave velocity, peak atrial reversal velocity, and the atrial reversal velocity time integral of pulmonary venous flow (Santilli and Bussadori 1998). These findings reflect the same changes with age and heart rate that have been reported in human beings (Appleton, et al 1991, Klein and Tajik 1991, Schirmer, et al 2000). Furthermore, comparisons between the non-invasive indices of diastolic relaxation and invasive measurements in young, healthy, cats, have demonstrated significant correlations between τ , and IVRT, V_p , peak A velocity and peak pulmonary venous S velocity (Schober, et al 2003). Peak E and pulmonary venous D were both found to be affected by relaxation, but both of these indices were preload sensitive. Left ventricular end diastolic pressure was related to peak E velocity and the ratio of E to V_p , under a variety of loading conditions (Schober, et al 2003). In that study it was found that there was only a weak correlation between E' and τ . In addition, there was a moderate correlation between τ and pulmonary

venous S, S' and transmitral A (Schober, et al 2003). These investigators found no significant relationship between E' to E or A duration to pulmonary venous atrial reversal duration, and left ventricular end diastolic pressure (Schober, et al 2003). The load sensitivity of E and E' has also been reported in human beings, where it has been demonstrated that when systolic function is preserved, both E and E' are sensitive to loading conditions (Nagueh, et al 1999b, Fristenburg, et al 2000, Nagueh, et al 2001a).

The transmitral flow patterns and the IVRTs have also been studied in cats with HCM. It was reported that affected cats showed significantly lower E velocities, a reduced E deceleration, an increased A velocity and prolonged IVRT compared to normal cats (Bright, et al 1999).

It has been found that, as in human beings, pw-DTI indices can be used to assess the velocity within the feline myocardium. The pw-DTI velocities have been reported in cats with HCM and compared to unaffected cats. These investigators reported a decrease in both peak systolic and peak diastolic velocities recorded from the mitral annulus of affected cats (Gavaghan, et al 1999).

Recently, MVG and mean myocardial velocity (MMV) data have been published, using colour M-mode DTI, in normal cats (Koffas, et al 2003). In that study we demonstrated that the early diastolic myocardial motion is biphasic and can be divided into E1 and E2. In addition, we found that E2 of the MVG and A of the MMV were correlated positively with age, and that there was a negative correlation between age and the MMV, E2 and S phases (Koffas, et al 2003).

While there is some information available assessing the echocardiographic changes in feline myocardial disease, this information is somewhat limited. With the advent of more sophisticated echocardiographic techniques and greater accumulative power for data collection and post collection analysis, the opportunity is available to use these techniques to elucidate the pathophysiological mechanisms of feline myocardial disease.

Hypothesis

Diastolic dysfunction is thought to be a common abnormality in cats with cardiac disease. Typically, this dysfunction is recognised in association with hypertrophic cardiomyopathy (HCM). However, it is also known that many non-cardiac diseases can impart affects on the myocardium via a combination of direct, neuroendocrine and loading alterations and that diastolic impairment can occur as a result of these disorders. To date, little is known about the affects of these diseases on the myocardial dynamics. However, the recent advent of pulsed-wave Doppler tissue imaging (pw-DTI) techniques offers a new non-invasive tool for the investigation of many different aspects of myocardial motion.

I hypothesised that with different forms of naturally occurring hypertrophic and specific feline cardiomyopathies, the myocardial dynamics would be altered and that pw-DTI techniques would be able to differentiate between these disease processes.

Aim

The aim of this study was to assess the pw-DTI velocities in a range of primary cardiomyopathies and disease states linked to specific cardiomyopathies in human beings in order to ascertain whether or not there are any disease specific abnormalities in myocardial function. In doing so I hoped to gain a greater incite into the main functional derangements in a range of feline disorders.

Chapter 2

Measurement of variability in feline echocardiography: An assessment of traditional and pulse-wave Doppler tissue imaging techniques

In order to comprehend the clinical significance of changes within the feline echocardiogram, it is first necessary to understand the repeatability and reproducibility of the measured variables.

The aim of this study was to assess the repeatability and reproducibility of both standard (2-dimensional, M-mode and spectral Doppler) and more advanced (pulsed-wave Doppler tissue imaging, and colour M-mode propagation velocity) feline echocardiographic measurements in order to further validate the use of this new methodology for the investigation of myocardial function (and dysfunction) in cats.

Abstract

The objective of this study was to determine the intraoperator, interobserver, and intraobserver variability in both a series of conventional echocardiographic variables and in some of the newer measurements of diastolic function, including colour M-mode flow propagation velocity, isovolumic relaxation time and pulsed-wave Doppler tissue imaging (pw-DTI) velocities. Four cats were each scanned five times over a three-day period. The repeatability of these echocardiographic analyses was compared (intraoperator repeatability). One scan from each cat was then randomly selected and two observers, with similar levels of experience, measured each of these scans (interobserver repeatability). After a minimum of five weeks, one scan was randomly selected from each cat, and was re-measured by the original observer (intraobserver variation).

The standard echocardiographic measurements were relatively repeatable in both their acquisition and measurement by a single investigator; there was a greater degree of variation between the two observers. The predominant (S', E' and A') pw-DTI velocities from the left apical four-chambered view, generally demonstrated a coefficient of variation ~20%. However, with pw-DTI, velocities recorded during the isovolumic phases, the velocity of the tricuspid annulus, and the radial fibre velocity within the interventricular septum, are poorly repeatable and should therefore be interpreted with caution.

Introduction

Echocardiography is widely used for the diagnosis and assessment of many cardiac conditions (Moise and Fox 1999). Both two-dimensional and Doppler techniques are routinely applied to assess sequential cardiac changes. Furthermore, advances in sonographics (Isaaz, et al 1989, McDicken, et al 1992) have lead to an increase in the information that can be gained by the use of tissue Doppler techniques.

Doppler tissue imaging (DTI) modalities are a range of relatively new techniques, which can be applied to record myocardial velocity (Sutherland, et al 1999). All of these techniques exploit the principle of the Doppler shift phenomenon. While conventional ultrasound uses this principle to assess the velocity of blood as it travels through the heart and vessels, the same concept can also be used to assess the velocity of myocardial excursion. Using these techniques detailed patterns of left ventricular wall motion have become apparent (Figure 3).

Pulsed-wave Doppler tissue imaging (pw-DTI) has received recent attention from veterinary cardiologists (Gavaghan, et al 1999, Schober, et al 2003). It is a technique that measures the instantaneous peak myocardial velocity as it moves through a pre-selected sample volume. This technique has excellent temporal resolution (over 300Hz) (Sutherland and Hatle 2002) and has therefore been used to assess the velocities within the feline myocardium (Gavaghan, et al 1999).

In order to comprehend the clinical significance of changes within the feline echocardiogram, it is first necessary to understand the repeatability and reproducibility of the measured variables. Whilst the reproducibility of conventional

M-mode echocardiographic variables have been reported in the cat (DeMadron, et al 1985, Chetboul, et al 2003a), these reports have not investigated the repeatability of spectral Doppler analyses. In addition, whilst there have been reports of the reproducibility of other forms of Doppler tissue analysis in the cat (Koffas, et al 2003, Chetboul, et al 2004), these studies have not investigated pw-DTI. Furthermore, studies within the human literature, reporting the variability of various pw-DTI variables, have only assessed a limited number of measurements (Vinereanu, et al 1999, Khan, et al 2004). A study of a large number of pw-DTI variables is necessary to validate this technique. Therefore, the aim of this study was to assess the repeatability and reproducibility of both standard and more advanced feline echocardiographic measurements in order to further validate the use of this new methodology for the investigation of myocardial function (and dysfunction) in cats.

Materials and Methods

Population Characteristics

Four domestic short-haired (DSH) cats were studied. All the cats were presented to the University of Edinburgh, Small Animal Hospital for routine health assessment. The group comprised two male and two female cats; both females and one male were neutered. The ages of the cats were one year, five years, eight years and 14 years. The weights ranged from 3.2kg to 4.6kg. Each cat underwent five full Doppler echocardiographic examinations. These were divided over three days with each cat undergoing three examinations on one of these days, and one examination on each of the other two days. A total of 20 echocardiographic examinations were performed.

Echocardiographic procedure

Echocardiographic examination was performed using a Vingmed Vivid FiVe ultrasound machine with built-in DTI capacity (GE Medical Systems-Horten, Norway) equipped with a five MegaHertz flat phased array (FPA) probe (GE Medical Systems-Horten, Norway). All images were stored digitally on optical discs (Verbatim Optical-Japan) and analysed retrospectively. Whilst scanning, an electrocardiogram trace (lead II) was recorded simultaneously. All cats were in sinus rhythm. The sector width and depth were adjusted to maximise the cardiac image. The gain settings were optimised for each individual case. The focus was adjusted to the depth of interest. All pulsed Doppler tracings were made using the high pulsed-repetition frequency (HPRF) Doppler modality. For each variable the mean

of five measurements was recorded. These measurements were made from adequate, consecutive waveforms, which were all recorded from the same trace.

All of the cats were examined in lateral recumbency. No sedation was administered; instead one assistant gently restrained each of the cats in lateral recumbency. The same assistant was present for all examinations.

In order to assess the reproducibility of both standard and pw-DTI techniques, a wide range of echocardiographic variables were measured (Table 1). Images were analysed using the 'Echopac' software (GE Medical Systems for Mackintosh). Diastolic events were analysed at end-diastole, which was identified by the start of the QRS complex (Moise and Fox 1999). Atrial systole was identified by its proximity to the P wave (Appleton, et al 1997). Systolic events were measured at end-systole, this was defined by the end of the T wave (Moise and Fox 1999). For each measurement (other than the 2-dimensional measurements) the R-R interval was recorded and the mean R-R interval for the complexes, which were measured, was calculated. The horizontal axis of the tracings was magnified to increase the accuracy of the timing and duration measurements.

Two-Dimensional and M-mode Evaluation

From the right parasternal long-axis view the interventricular septal diameter was measured just below the level of the mitral valve. This measurement was made perpendicular to the long axis of the heart. It was measured at end-diastole using the leading edge-to-leading edge technique (Henry, et al 1980, Peterson, et al 1993).

The M-mode recording taken from the right parasternal short-axis, at chordae level, was used to measure the left ventricular chamber dimensions. The leading edge-to-leading edge technique was used (Sahn, et al 1978). End-diastole was identified by the beginning of the Q wave on the ECG; systole was measured at the point of maximal septal excursion (Moise and Fox 1999).

A two-dimensional, short-axis right-sided parasternal image of the aorta and left atrium was used to measure the aortic and left atrial diameters at end diastole (Thomas, et al 1993). These were measured using an inner-edge, to inner-edge technique. The aortic diameter was measured from the mid-part of the right coronary cusp to the commissures of the left and non-coronary cusps. The left atrial diameter was measured in the same frame, by extending the line used to measure the aorta; care being taken to avoid the pulmonary vein (Häggström, et al 1994).

Spectral Doppler Evaluation

The pulmonary artery velocity was recorded from the short axis right parasternal heart base view. A sampling gate of 1.9 mm was used.

The left apical five-chamber view was used to record the aortic velocity. Again a sampling gate of 1.9 mm was used.

The left apical four-chamber view was used to assess the transmitral and trans-tricuspid flow patterns. Colour flow Doppler was used to aid the placement of a cursor in line with the mitral inflow. A sampling gate of 1.9mm was placed in line

with this flow, at the level of the mitral valve tips (Appleton, et al 1997). A pulsed Doppler trace of transmitral flow was recorded. Every effort was made to record tracings that demonstrated minimal summation. The transducer was then angled cranially until a cursor could be placed in line with trans-tricuspid flow, and the procedure was repeated. The peak velocity of the E and A waves were measured. If there was complete summation of the E and A waves the peak E+A velocity was recorded.

The duration of the mitral A wave was measured. In order to optimise this, the frozen image was magnified along the x-axis. The A wave duration was measured from either the start of the A wave, or from a perpendicular line dropped from the point where E and A summated to baseline, to the end of the A wave (Appleton, et al 1997).

In order to measure the pulmonary venous flow a colour flow sector was positioned over the pulmonary veins. The left apical four-chamber view was then rotated slightly until alignment with flow from the lateral pulmonary vein was achieved. A Doppler cursor, with a sampling gate of 1.9mm, was placed approximately two to three millimetres into the pulmonary vein, and the spectral trace was recorded. This technique was modified from the human guidelines, in which it is recommended that a larger sample volume is placed approximately one centimetre into the pulmonary vein (Appleton, et al 1997).

From the pulmonary venous flow recordings the velocity of systolic flow (S), diastolic flow (D) and atrial reversal flow (Ar) were measured. The x-axis (time) was magnified and the duration of Ar was measured.

The isovolumic relaxation time was measured as the interval between aortic valve closure (identified by the aortic valve click) or cessation of aortic flow and mitral valve opening or, commencement of transmitral flow (Appleton, et al 1997). This was imaged by simultaneously positioning a colour Doppler sector over both the mitral inflow and the left ventricular outflow tract of the left apical five-chamber view. A pulsed Doppler sampling gate of 1.9mm was placed between the two colour flow maps and a trace recorded. Every effort was made to ensure the aortic valve clicks were evident on this trace (Appleton, et al 1997).

Colour M-mode Evaluation

The propagation velocity (V_p) was measured from the apical four-chamber view, by positioning a colour Doppler sample over the mitral inflow. A cursor was placed through the centre of the mitral inflow and a colour M-mode was recorded. The image was frozen and the colour baseline shifted until an aliasing core was evident as the blood flowed through the mitral valve (Garcia, et al 1998). The V_p was calculated from the colour M-mode tracing. The image was magnified. The gradient of the first aliasing core within the E wave was measured from mitral valve opening to approximately one centimetre into the left ventricle (adapted from Garcia, et al 1998).

Pulsed-wave Doppler Tissue Imaging

The radial myocardial velocity was measured from both the free wall and interventricular septum of the right parasternal long and short axis views. A pw-DTI sample gate was placed over the free wall at the mid-ventricular level (Figure 4). The right parasternal long axis four-chamber view was optimised to ensure that the longitudinal axis was at approximately 90° to the cursor. The sampling gate was set at 3.9mm. This was considered to be the largest possible sampling gate that could accurately be placed over the selected area of myocardium, as is recommended (Sutherland and Hatle 2002). This procedure was then repeated, sampling an area at the level of the mid-interventricular septum. From the right parasternal short axis view tracings were obtained from the free wall and the interventricular septum at the level of the chordae tendinae; the same procedure was used as had been applied to the long-axis view.

Longitudinal myocardial motion was assessed from the left apical four-chamber view. Velocities from the septal and lateral aspects of the mitral annulus, mid-septal and mid-lateral wall level were recorded in a similar manner to those recorded from the right parasternal views (Figure 4). Every effort was made to ensure that the angle of incidence was minimised when recording any Doppler variable.

For all the pw-DTI recordings the velocities of S', A', E', IVR', and IVC' (for definitions, see Figure 3) were measured. The biphasic IVR' and IVC' waveforms were measured as IVRr and IVRb, IVCr and IVCb, the suffix r representing flow towards the transducer and b representing flow away from the transducer.

Occasionally the E' and A' waves were fused; in these cases E'+A' was measured (Sutherland and Hatle 2002).

Statistical Analysis

The results of the 20 scans recorded by one echocardiographer on five different occasions, in each of the four cats (intraoperator variability), were compared. In order to assess the interobserver variability, one scan from each of the four cats, was selected. Two different observers, with similar levels of experience, measured each of these scans. Each observer was unaware of the previous results. The intraobserver variability was calculated by re-analysing one of these scans from each cat after a period of at least five weeks and the results compared to the original analysis. The scans selected for the intraobserver repeatability were chosen by random number generation. All scans were measured without reference to the previous results.

For the intraobserver variability the statistical analysis was performed using the raw data since the same complexes could be measured. The first set of measurements was compared to a second set of measurements and a standard paired t-test was performed to analyse the data for statistically significant differences. A p value of ≤ 0.01 was taken as demonstrating statistical significance. This level was chosen to reduce the chances of a Type I error; since the p values were often related, a Bonferroni correction was not suitable (Bland 2000).

In order to compare the results for intraoperator variability, the mean of the five measurements was calculated for each of the 20 scans. From day to day and examination to examination, the heart rate can vary; the intraoperator data were heart rate corrected using the $\sqrt{\text{RR}}$ method. For the interobserver analysis, the statistical analysis was performed using the raw data. For both the intraoperator data and the interobserver data, a one-way analysis of variance (ANOVA) was performed. From the analysis of variance table the square root of the residual mean square was calculated (s_w) and from this the coefficient of variation was calculated and quoted as a percentage (Bland 2000). The 95% confidence intervals were calculated using the equation:

$$S \cdot E_v \approx \frac{V}{\sqrt{2 \cdot n}} \cdot t$$

Where $S \cdot E_v$ is the sample variance, V is the coefficient of variation, n is the number of observations and t the t -value for $(n-1)$ degrees of freedom at the $p=0.05$ level (Sokal and Rohlf 1995). For both analyses, when summation of diastolic flow or velocity patterns occurred, the summated data were excluded from the analysis. Although every effort was made to capture adequate images on every occasion, occasionally the data were un-interpretable or rapid movements (such as isovolumic waveforms) were not visible, therefore these were not measured in the analysis. The frequency of acquisition (λ) is reported in each of the results tables. Traces (such as those for the interventricular septum from the short axis view) in which too few results were obtained to fulfil the criteria for statistical analysis were excluded.

Results

Intraoperator Repeatability-see Table 1.

All cats were scanned on five occasions over a three-day period (n=20). However, the majority of the data from one study was corrupted, by a computer malfunction, and therefore, only four scans were analysed for this cat (with the exception of the 2-D measurements which were not affected).

The coefficient of variation was less than 20% for all conventional variables, with the 2-dimensional variables demonstrating coefficients of variation under 10% and many of the M-mode and spectral Doppler variables demonstrating a variation of less than 15%.

The DTI results generally demonstrated higher coefficients of variation for the velocity of IVC' and IVR', particularly IVCb. In addition, the pw-DTI measurements recorded from the long axis, both at the level of the interventricular septum and free wall were highly variable, as were those recorded from the tricuspid annulus (Table 1). The remaining systolic and diastolic excursions demonstrated a coefficient of variation of less than 20%, with the exception of the A' measured from the apical lateral wall and the S' at the apical mid septum. There were insufficient numbers of measurable complexes recorded from the short axis to allow analysis of the repeatability of measuring radial fibre excursion within the interventricular septum.

Intraobserver Repeatability-see Table 2

The intraobserver repeatability demonstrated significant differences in the measurement of the pulmonary venous flow diastolic wave ($p=0.007$) and atrial reversal velocity ($p<0.001$). In addition, the velocity of the IVCr wave recorded from the long axis interventricular septum demonstrated significant variation ($p=0.004$). None of the remaining variables demonstrated a significant difference between the first and second set of measurements. The observational frequency for each measurement is reported in Table 2: Unfortunately, the selected scans did not demonstrate measurable IVCb from either the short axis interventricular septum or the lateral aspect of the tricuspid annulus and therefore, the variability of this variable was not investigated.

Interobserver Repeatability-see Table 3

The data from one scan of each of the four cats was analysed by two different observers blinded to the any previous results. It was found that the coefficient of variation was generally less than 20% for the measurements obtained from the M-mode analysis, with the exception of the colour M-mode propagation velocity, demonstrated a variability of $45.69\pm15.12\%$. The spectral Doppler analysis demonstrated high coefficient of variability for measurements of pulmonic velocity, $22.41\pm7.42\%$, transmitral A wave, $29.52\pm9.77\%$, isovolumic relaxation time, $32.34\pm10.70\%$, and pulmonary venous S wave velocity, $37.70\pm12.48\%$.

The repeatability of the pw-DTI velocities was lower for the long and short axis views, as was the acquisitional frequency (see Table 3). The coefficients of variation of the principle pw-DTI velocities recorded from the longitudinal fibres within the left ventricular wall were generally less than 20%, with the exception of the A' velocity from the apical lateral wall, $22.90 \pm 8.97\%$, and at the level of the mid-interventricular septum, $22.89 \pm 7.57\%$, and the E' measured at the lateral aspect of the mitral annulus, $28.24 \pm 9.35\%$. The velocities recorded during the isovolumic contraction phases were poorly repeatable at multiple sites. Both the A' and isovolumic relaxation velocity toward the transducer were poorly repeatable when measured from right ventricular lateral wall at the level of the tricuspid annulus ($36.17 \pm 11.97\%$ and $25.29 \pm 12.79\%$, respectively).

Discussion

To my knowledge, this is the first study to examine the variability and repeatability of such an extensive range of echocardiographic measurements in the cat. Previously there have been studies addressing the repeatability of echocardiographic variables in both dogs and cats (Santilli and Bussadori 1998, Dukes McEwan, et al 2002, Chetboul, et al 2003a, Koffas, et al 2003, Chetboul, et al 2004). However, in these papers either a limited number of variables were investigated or, in the wider studies, pw-DTI was not investigated (Santilli and Bussadori 1998, Dukes McEwan, et al 2002). The repeatability of a range of colour Doppler tissue imaging (c-DTI) variables have been reported previously (Koffas, et al 2003, Chetboul, et al 2004). However, the c-DTI technique allows analysis of the velocity of each group of 3x3 pixels by colour coding the resulting velocity in accordance with the direction and velocity of motion (Uematsu, et al 1995). Therefore, c-DTI is a technique that analyses mean velocity, whereas pw-DTI analyses peak myocardial velocity. In addition, the c-DTI samples myocardial velocities at a lower frame rate than pw-DTI, thereby increasing the accuracy of pw-DTI (Sutherland, et al 1999). For this reason I chose to assess the variability in a wide range of echocardiographic variables, including pw-DTI variables. The repeatability of a number of pw-DTI variables has been investigated in humans (Vinereanu, et al 1999), where it was found that the reproducibility of measurements from the long axis was greater than that from the short axis, and that the highest repeatability could be obtained from the lateral aspect of the mitral annulus. The tricuspid annulus produced reproducible results, whereas the right ventricular lateral wall demonstrated a high degree of variability. In that study, there was no analysis of isovolumic velocities. The reported coefficients of

variation were generally between ten and 20%, with poor reproducibility being reported when the coefficient of variation exceeded 20% (Vinereanu, et al 1999).

In the current study the acquisition of isovolumic complexes was variable (reported as the frequency of acquisition), as were the velocities measured from these complexes, particularly the velocity of isovolumic contractile motion. These velocities are typically of a very short duration and seen as sharp spikes on the pw-DTI traces. It is possible that the event resolution of pw-DTI (typically six to eight milliseconds) (Sutherland and Hatle 2002) is inadequate to accurately measure these short duration 'spikes'.

Intraoperator Variability

The intraoperator analysis demonstrated that, with one investigator performing the ultrasound examination and analysing the results, the standard echocardiographic variables are relatively repeatable, even when the scans are performed on different days. The analysis demonstrated that the velocities recorded from the long axis free wall and interventricular septum demonstrated a high degree of variability. However, in contrast to previous reports in human beings, the repeatability of the free wall velocities was better from the short axis. Since both the long and short axis views interrogate radial motion, these views should provide comparable results. In human beings and cats, the velocities recorded by DTI analysis have been shown to vary throughout the ventricle, with the apical velocities being lower than those recorded at the level of the mitral annulus (Oki, et al 1997, Oki, et al 1999, Chetboul,

et al 2004). Therefore, variations in the level at which the sample volume was placed may have resulted in a poor repeatability. From the long axis view the cursor was placed at the mid-ventricular level; which was assessed manually. In contrast, in the short axis plane the chordae tendinae were used as landmarks to ease cursor placement. This may have resulted in more repeatable measurements being acquired from the short axis views.

Insufficient data were collected from the interventricular septum of the short axis view to allow evaluation of these results. Acquisition of data from this area was highly inconsistent with uninterpretable traces often being attained. A total of six traces were measured from this area. However, as five of them were from the same cat, they were not suitable for analysis by the described method. The long axis view also demonstrated poor attainability from this area. The underlying reason for this problem is unknown. However, there were no problems with two-dimensional image acquisition or alignment with the interventricular septum and it was thought that the difficulties in interpreting the traces might result from the super-imposition of right ventricular circumferential fibre motion on the traces (Sutherland and Hatle 2002).

The longitudinal fibre E' and A' waveforms (assessed from the apical four-chamber view) were summated in all five tracings obtained from one of the cats, and were therefore excluded from the analysis. This cat also demonstrated summation of the transmitral E and A waveforms, but not the radial fibre waveforms. It is known that in human beings, early longitudinal diastolic motion precedes motion within the radial fibres (Oki, et al 1997, Galiuto, et al 1998). Whether or not this difference in the timing of events is adequate to allow separation of the radial traces, or whether

this was a phenomenon common to only this one cat cannot be assessed by this study.

The A' velocity recorded from the lateral wall of an apical four chamber view and the velocities recorded from the tricuspid annulus demonstrated a wide degree of variability. This may have been in part due to an increased angle of incidence at these sites. In addition, variations in the site of measurement may have contributed to the variability of the apical lateral wall A' and mid-septal S' velocities.

Intraobserver Analysis

The intraobserver data reported in this study represent the variability of the measuring technique, and the clinical significance of this was assessed as part of the intraoperator analysis. Therefore, a t-test was performed to investigate if there was a statistically significant difference. Overall, the measurements were found to be highly repeatable. However, there was a significant variation in the measurements recorded from the atrial reversal and diastolic components of the pulmonary venous flow traces. This difference could only be corrected for by excluding the results of 50% of the traces. Whilst these traces were not of optimal quality, they were typical of those obtained from normal cats, and therefore, I believe that the measurement of pulmonary venous flow velocities may be problematic in normal cats. Subjectively, it is my experience that the pulmonary venous flow traces are of superior quality in cats with cardiac disease. Typically, acquisition of a pulmonary venous flow trace is easier in cats with an enlarged left atrium, probably due to dilation of the pulmonary

veins. Therefore, these results should be interpreted with caution, and not applied to the entire feline population. Furthermore, the IVCr phase recorded from the long axis view of the interventricular septum demonstrated a high degree of variability. Again, the traces analysing the radial motion of the interventricular septum are frequently suboptimal and interpretation of the waveforms can be problematic. The significant variation of this measurement could be corrected by removing the results from one cat, in which the tracing was particularly unclear.

The intraobserver repeatability should be considered when interpreting the intraoperator variability. In order to analyse each of the echocardiographic analyses, it is necessary to measure the stored images. Therefore, when comparing the data sets from different echocardiographic analyses, the results encompass not only the inherent variability of data acquisition, but also measurement and inter-day physiological variations. In this study the intraobserver variability was minimal. Therefore, the intraoperator variability reported, is in the main, a result of the variability in data acquisition. This in turn will be affected not only by the operator, but also by physiological variation.

Interobserver Analysis

I have demonstrated that, between the two observers used, there was an acceptable level of variation (<20%) in the majority of two-dimensional and M-mode measurements. The IVSd demonstrated slightly more than 20% variability, but the colour-M-mode velocity was highly variable. The spectral Doppler analyses

demonstrated sub-optimal variation in the measurement of pulmonic velocity, transmitral A wave velocity, pulmonary venous S wave velocity and IVRT. The repeatability of pw-DTI measurements obtained from the long and short axis walls was poor, as was the acquisitional frequency, with comparisons of measurements within the radial fibres of the interventricular septum, consisting of only the S' and E' from the short axis views. Generally there was good agreement between the observers for the results obtained from the longitudinal fibre analysis. There was slightly more than 20% variation in some of the measurements of A' velocity, and in the E' velocity recorded from the lateral aspect of the mitral annulus. The isovolumic contraction phases recorded from the longitudinal fibre velocities frequently demonstrated an unacceptable degree of variation between the two observers, as did the A' velocity and IVRr recorded from the right ventricular lateral wall at the level of the mitral annulus. Some of the variation reported in the analysis of interobserver repeatability may have occurred from measuring of different spectral traces. Whilst it was decided that the first five, adequate, consecutive traces would be measured, the subjective assessment of an adequate trace may have negatively affected the repeatability results. The increased variability demonstrated between different observers should be considered when longitudinal analysis of feline echocardiographic changes is performed, and where possible to same observer should repeat the analysis.

The logistics of storing measurements within the 'Echo-pac' biased the results of this study. Unfortunately, measurements are stored to only two decimal places. Many of the variables measured in this study produce very low measurements and therefore recording these to only two decimal places increases measurement error and with this

decreases the repeatability. It was primarily for this reason that a variability of up to 20% was felt to be acceptable, as has been reported previously in human beings (Vinereanu, et al 1999).

These results demonstrate that whilst the conventional echocardiographic variables and the majority of pw-DTI variables demonstrate an acceptable degree of variation; pw-DTI measures of tricuspid annular motion, and movement during the isovolumic phases are relatively unreliable in the cat. Furthermore, data acquisition interrogating the radial movement of the free wall appears more repeatable when measured from a right parasternal short axis view. Analysis of the velocity of circumferential fibre motion within the interventricular septum is problematic. While it appears relatively unreliable from the right parasternal long axis view, the frequency of acquisition is poor from the short axis view. The poor repeatability of these measurements may be a result of the circumferential fibre orientation within the septum, since approximately a third of these fibres are continuous with those from the right ventricle. Therefore, if the pw-DTI sampling gate does not remain within the two-thirds of the interventricular septum nearest the left ventricle, the effects of these fibres are superimposed on the velocity trace.

Conclusion

In conclusion, the standard echocardiographic measurements were relatively repeatable in both their acquisition and measurement by a single investigator, although there was a greater degree of variation between the two observers. The pw-

DTI velocities recorded during the isovolumic phases, the velocity of the tricuspid annulus, and radial fibre velocity within the interventricular septum, are poorly repeatable and should therefore be interpreted with caution. However, the predominant (S', E' and A') pw-DTI velocities from the left apical four-chambered view, generally demonstrated a coefficient of variation ~20%, which I felt to represent an acceptable level of repeatability. The predominant pw-DTI velocities recorded from the left ventricular longitudinal fibres were therefore found to be relatively repeatable. The significance of clinical and biological alterations in the pw-DTI velocities in cats can now be interpreted in light of the repeatability of this technique.

2D Heart Variables	λ	Coefficient of Variation (%)	S.Ev
Ao Diameter	20	5.08	± 1.68
Left Atrial Diameter	20	5.52	± 1.83
Basilar Septal Bulge	20	3.19	± 1.06
M-mode Variables			
LVDd	19	8.16	± 2.78
LVPFWd	19	16.68	± 5.68
LVDs	19	8.97	± 3.06
LVPFWs	19	14.92	± 5.08
IVSd	19	9.45	± 3.22
IVSs	19	12.02	± 4.09
pct FS	19	11.03	± 3.76
LVEF	19	7.56	± 2.58
Vp	19	18.52	± 6.31
Spectral Doppler Variables			
AV	19	9.77	± 3.33
PV	19	14.35	± 4.89
ME	13	6.36	± 2.17
MA	13	11.00	± 3.75
TE	14	15.70	± 5.35
TA	14	19.34	± 6.59
IVRT	19	13.85	± 4.72
PVD	19	11.40	± 3.88
PVS	19	15.05	± 5.13
PAV	19	17.43	± 5.94
ArDur	19	10.05	± 3.42
MaDur	19	9.16	± 3.12

Tissue Doppler Variables Long Axis Septum	λ	Coefficient of Variation (%)	S.Ev
S'	9	14.93	± 8.09
E'	9	26.08	± 14.20
A'	9	50.2	± 27.33
IVRb	-	-	-
IVRr	-	-	-
IVCr	-	-	-
IVCb	8	33.73	± 19.90
Short Axis Free Wall			
S'	19	16.39	± 5.58
E'	19	18.45	± 6.29
A'	19	13.85	± 4.72
IVRb	15	22.75	± 8.91
IVRr	15	12.06	± 4.54
IVCr	7	52.27	± 34.18
IVCb	17	22.48	± 8.17
Long Axis Free Wall			
S'	19	21.00	± 7.15
E'	19	25.55	± 8.70
A'	19	16.53	± 5.63
IVRb	17	11.60	± 4.22
IVRr	-	-	-
IVCr	-	-	-
IVCb	10	28.48	± 14.41
Apical Free Wall			
S'	12	13.20	± 5.93
E'	13	12.94	± 5.53
A'	13	34.08	± 14.56
IVRb	7	19.17	± 12.54
IVRr	8	13.28	± 7.85
IVCr	13	25.43	± 10.87
IVCb	13	19.75	± 8.44

Apical Mid-Septum	λ	Coefficient of Variation (%)	S.Ev
S'	19	20.67	± 7.04
E'	14	9.62	± 3.93
A'	14	16.79	± 6.86
IVRb	18	13.63	± 4.79
IVRr	11	25.28	± 12.01
IVCr	16	22.19	± 8.36
IVCb	12	29.67	± 13.33
Apical Septal Mitral Annulus			
S'	19	17.35	± 5.91
E'	14	18.25	± 7.45
A'	14	18.62	± 7.60
IVRb	18	19.82	± 6.97
IVRr	16	16.35	± 6.16
IVCr	17	22.38	± 8.14
IVCb	19	30.49	± 10.39
Apical Lateral Mitral Annulus			
S'	19	19.15	± 6.52
E'	14	17.71	± 7.23
A'	14	18.49	± 7.55
IVRb	13	15.05	± 6.43
IVRr	13	20.21	± 8.64
IVCr	13	27.13	± 11.59
IVCb	16	21.86	± 8.24
Lateral Tricuspid Annulus			
S'	19	22.96	± 7.82
E'	14	26.46	± 10.80
A'	14	27.70	± 11.31
IVRb	16	23.83	± 8.98
IVRr	12	23.14	± 10.40
IVCr	18	36.49	± 12.83
IVCb	-	-	-

Where: λ represents the frequency of acquisition; S.Ev, the 95% confidence intervals; Ao, aorta; LVD, left ventricular diameter; IVS, interventricular septum; LVPFW, left ventricular free wall; d, diastole; s, systole; pct FS, percentage fractional shortening; LVEF, left ventricular ejection fraction; Vp, propagation velocity; AV, aortic velocity; PV, pulmonary velocity; ME and MA, transmitral early and late diastolic flow, respectively; TE and TA, trans-tricuspid early and late diastolic flow, respectively; IVRT, isovolumic relaxation time; PV, pertaining to pulmonary venous flow; S, systolic flow; D, diastolic flow; Ar, atrial reversal; V, velocity; Dur, duration; S', systolic velocity; E', early diastolic velocity; A', late diastolic velocity; IVRb, velocity of movement occurring during the isovolumic relaxation time, (directed away from the transducer); IVRr, the velocity of movement within the isovolumic relaxation phase (directed toward the transducer); IVCb and IVCr, velocity of movement during the isovolumic contraction phase (directed away from and toward the transducer, respectively). Bold type-face represents a coefficient of variation greater than 20%.

2D Heart Variables	λ	T-Statistic	P value
Ao Diameter	20	-0.459	0.650
Left Atrial Diameter	20	-0.337	0.739
Basilar Septal Bulge	20	-1.753	0.096
M-mode Variables			
LVDd	20	-0.949	0.355
LVFWd	20	0.740	0.468
LVDs	20	-2.103	0.049
LVFWs	20	1.027	0.318
IVSd	20	1.851	0.080
IVSs	20	-0.791	0.439
Vp	20	1.629	0.120
Spectral Doppler Variables			
AV	20	-0.685	0.502
PV	20	0.064	0.950
ME	15	<0.001	1.000
MA	15	-0.666	0.517
TE	20	0.050	0.961
TA	20	-0.107	0.916
IVRT	20	1.552	0.137
PVD	20	3.005	0.007
PVS2	20	-1.447	0.164
PAV	20	5.037	<0.001
ArDur	20	-2.305	0.349
MaDur	20	-2.305	0.033

Tissue Doppler Variables	λ	T-Statistic	P value
Long Axis Septum			
S'	15	1.000	0.334
E'	15	2.432	0.029
A'	15	2.567	0.022
IVRb	5	-0.535	0.621
IVRr	5	-1.000	0.374
IVCr	5	-6.000	0.004
IVCb	10	0.802	0.443
Short Axis Septum			
S'	15	-1.964	0.070
E'	15	-0.564	0.581
A'	15	<0.001	1.000
IVRb	10	1.964	0.081
IVRr	5	-1.000	0.374
IVCr	15	-1.169	0.262
IVCb	0	-	-
Short Axis Free Wall			
S'	20	-1.371	0.186
E'	20	2.027	0.057
A'	20	0.719	0.481
IVRb	20	2.666	0.015
IVRr	20	-0.438	0.666
IVCr	15	1.000	0.334
IVCb	20	0.370	0.716
Long Axis Lateral Wall			
S'	20	1.000	0.330
E'	20	0.721	0.479
A'	20	1.000	0.330
IVRb	15	0.250	0.806
IVRr	15	1.740	0.104
IVCr	10	<0.001	1.000
IVCb	15	-1.146	0.271

Tissue Doppler Variables	λ	T-Statistic	P value
Apical Free Wall			
S'	10	0.000	1.000
E'	10	0.349	0.735
A'	10	-1.000	0.343
IVRb	5	<0.001	1.000
IVRr	10	-0.429	0.678
IVCr	10	-1.000	0.343
IVCb	10	0.514	0.619
Apical Mid-Septum			
S'	20	-1.000	-1.000
E'	15	0.323	0.323
A'	15	-1.871	-1.871
IVRb	15	2.646	2.646
IVRr	5	1.000	1.000
IVCr	10	1.000	1.000
IVCb	15	-0.807	-0.807
Apical Septal Mitral Annulus			
S'	20	-0.370	0.716
E'	15	0.000	1.000
A'	15	-1.382	0.189
IVRb	15	1.075	0.301
IVRr	20	-1.000	0.330
IVCr	20	0.295	0.772
IVCb	20	0.567	0.577
Apical Lateral Mitral Annulus			
S'	20	1.552	0.137
E'	15	0.521	0.610
A'	15	-1.468	0.164
IVRb	5	1.000	0.374
IVRr	15	-0.250	0.806
IVCr	20	-0.252	0.804
IVCb	20	-0.370	0.716
Apical Lateral Tricuspid Annulus			
S'	20	0.89	0.385
E'	15	0.000	1.000
A'	15	-0.793	0.475
IVRb	15	<0.001	1.000
IVRr	15	<0.001	1.000
IVCr	20	0.252	0.804
IVCb	0	-	-

Where: λ , Frequency of Acquisition; T-Statistic, value from T-test; P value, probability value; Ao, aorta; LVD, left ventricular diameter; IVS, interventricular septum; LVFW, left ventricular free wall; d, diastole; s, systole; Vp, propagation velocity; AV, aortic velocity; PV, pulmonary velocity; ME and MA, transmitral early and late diastolic flow, respectively; TE and TA, trans-tricuspid early and late diastolic flow, respectively; IVRT, isovolumic relaxation time; PV, pertaining to pulmonary venous; S, systolic flow; D, diastolic flow; Ar, atrial reversal flow; V, velocity; Dur, duration; S', systolic velocity; E', early diastolic velocity; A', late diastolic velocity; IVRb, velocity of movement occurring during the isovolumic relaxation time, (directed away from the transducer); IVRr, the velocity of movement within the isovolumic relaxation phase (directed toward the transducer); IVCb and IVCr, velocity of movement during the isovolumic contraction phase (directed away from and toward the transducer, respectively). Bold type-face represents a coefficient of variation greater than 20%.

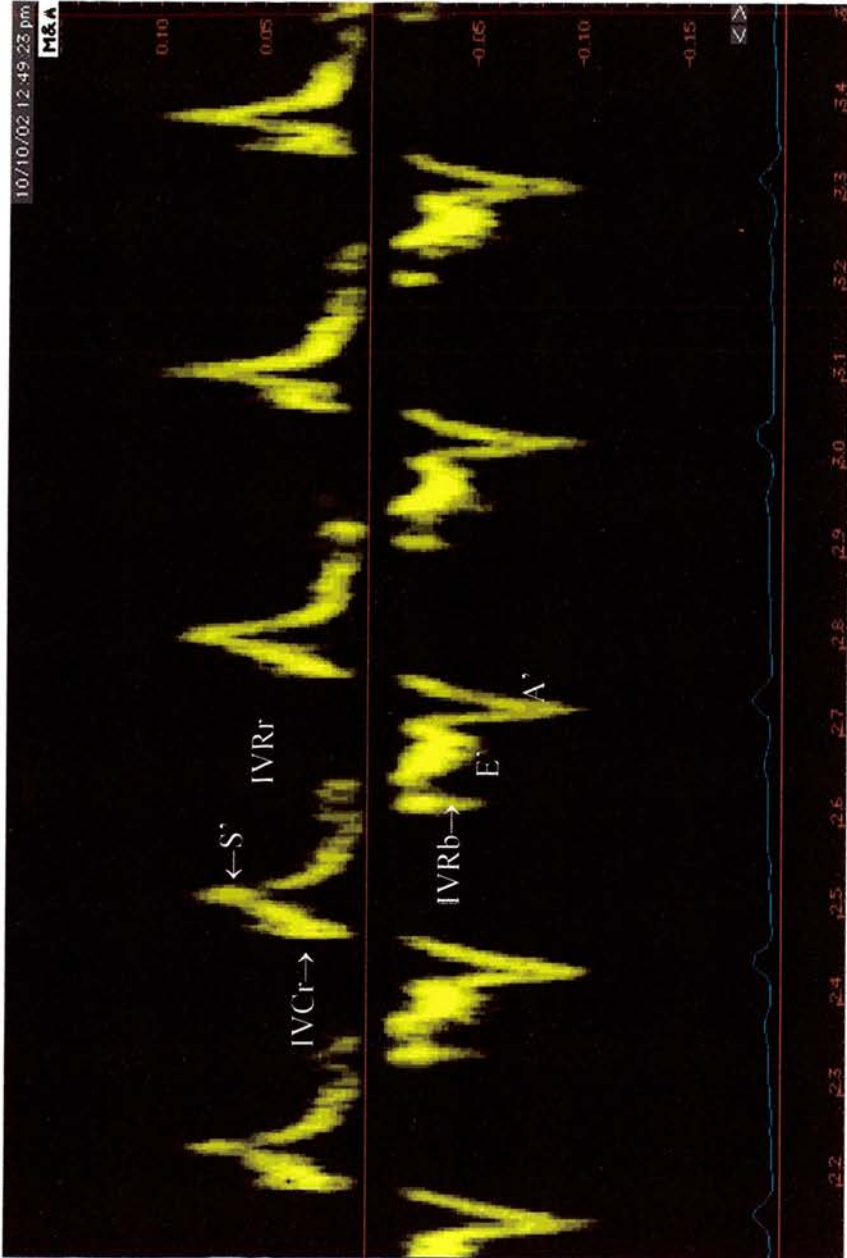
2D Heart Variables	λ	Coefficient of Variation (%)	S.Ev
Ao Diameter	20	12.12	± 4.01
Left Atrial Diameter	20	19.17	± 6.34
Basilar Septal Bulge	20	13.66	± 4.52
M-mode Variables			
LVDd	20	10.06	± 3.32
LVPWd	20	15.22	± 5.04
LVDs	20	13.85	± 4.58
LVPWs	20	12.58	± 4.16
IVSd	20	20.77	± 6.87
IVSs	20	14.91	± 4.93
pct FS	20	18.14	± 6.00
Vp	20	45.69	± 15.12
Spectral Doppler Variables			
AV	20	15.67	± 5.19
PV	20	22.41	± 7.42
ME	20	9.07	± 3.00
MA	20	29.52	± 9.77
TE	20	18.84	± 6.23
TA	20	19.72	± 6.53
IVRT	20	32.34	± 10.70
PVD	20	10.02	± 3.32
PVS	20	37.70	± 12.48
PAV	20	11.74	± 3.89
ArDur	20	18.07	± 5.98
MaDur	20	20.11	± 6.66

Tissue Doppler Variables	λ	Coefficient of Variation (%)	S.Ev
Short Axis Septum			
S'	5	18.43	± 16.18
E'	5	9.26	± 8.13
A'	-	-	-
IVRb	-	-	-
IVRr	-	-	-
IVCr	-	-	-
IVCb	-	-	-
Short Axis Free Wall			
S'	20	20.57	± 6.81
E'	20	25.21	± 8.34
A'	20	26.70	± 8.84
IVRb	15	20.11	± 7.76
IVRr	20	18.31	± 6.06
IVCr	10	61.79	± 31.26
IVCb	15	19.39	± 7.48
Long Axis Free Wall			
S'	20	21.68	± 7.17
E'	20	24.62	± 8.15
A'	20	25.21	± 8.34
IVRb	20	17.64	± 5.84
IVRr	20	17.71	± 5.86
IVCr	5	8.59	± 7.54
IVCb	20	31.24	± 10.34
Apical Free Wall			
S'	15	17.30	± 6.77
E'	15	18.67	± 7.31
A'	15	22.90	± 8.97
IVRb	5	15.82	± 13.89
IVRr	5	14.92	± 13.10
IVCr	15	11.39	± 4.46
IVCb	15	26.22	± 8.68

Apical Mid-Septum	λ	Coefficient of Variation (%)	S.Ev
S'	20	16.15	± 5.34
E'	20	14.94	± 4.94
A'	20	22.89	± 7.57
IVRb	20	16.49	± 5.46
IVRr	-	-	-
IVCr	20	11.83	± 10.39
IVCb	20	17.11	± 6.70
Apical Septal Mitral Annulus			
S'	20	18.43	± 6.10
E'	20	17.28	± 5.72
A'	20	11.70	± 3.87
IVRb	20	21.60	± 8.46
IVRr	20	15.02	± 5.88
IVCr	20	23.92	± 7.92
IVCb	20	20.21	± 6.69
Apical Lateral Mitral Annulus			
S'	20	12.36	± 4.09
E'	20	28.24	± 9.35
A'	20	12.63	± 4.18
IVRb	20	12.67	± 4.96
IVRr	20	12.05	± 4.72
IVCr	20	13.90	± 5.44
IVCb	20	31.13	± 9.97
Lateral Tricuspid Annulus			
S'	20	8.35	± 2.76
E'	20	17.00	± 5.62
A'	20	36.17	± 11.97
IVRb	20	18.15	± 7.25
IVRr	20	25.29	± 12.79
IVCr	20	10.17	± 5.14
IVCb	20	-	-

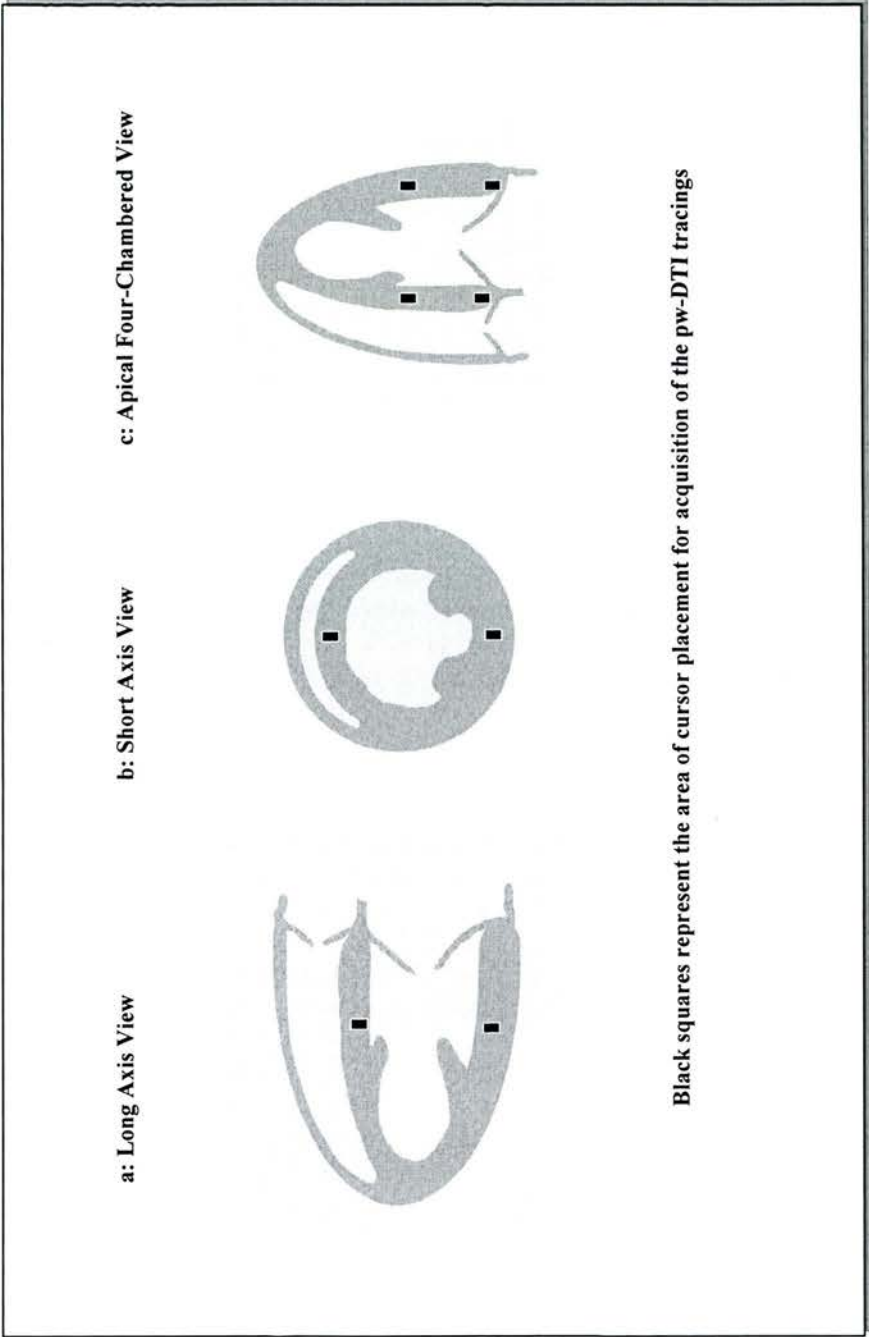
Where: λ represents the frequency of acquisition; S.Ev, the 95% confidence intervals; Ao, aorta; LVD, left ventricular diameter; IVS, interventricular septum; LVPW, left ventricular free wall; d, diastole; s, systole; pct FS, percentage fractional shortening; LVEF, left ventricular ejection fraction; Vp, propagation velocity; AV, aortic velocity; PV, pulmonary velocity; ME and MA, transmitral early and late diastolic flow, respectively; TE and TA; trans-tricuspid early and late diastolic flow, respectively; IVRT, isovolumic relaxation time; PV, pertaining to pulmonary venous flow; S, systolic flow; D, diastolic flow; Ar, atrial reversal; V, velocity; Dur, duration; S', systolic velocity; E', early diastolic velocity; A', late diastolic velocity; IVRb, velocity of movement occurring during the isovolumic relaxation time, (directed away from the transducer); IVRr, the velocity of movement within the isovolumic relaxation phase (directed toward the transducer); IVCb and IVCr, velocity of movement during the isovolumic contraction phase (directed away from and toward the transducer, respectively). Bold type-face represents a coefficient of variation greater than 20%.

Figure 3: A typical pulsed-wave Doppler tissue imaging (pw-DTI) tracing



A typical pulse-wave Doppler tissue imaging (pw-DTI) tracing showing the systolic velocity (S'), early diastolic velocity (E'), late diastolic velocity (A'), the velocity of movement during isovolumic relaxation (IVR'), directed away from the probe (IVRb), directed toward the probe (IVRr), and the velocity of movement during isovolumic contraction (IVC'), directed toward the probe (IVCr). This tracing demonstrates no obvious motion during the isovolumic contraction period, which is directed away from the transducer (IVCb).

Figure 4: Placement of sampling gate for acquisition of pulsed-wave Doppler tissue imaging (pw-DTI) velocities



Chapter 3: Age related variation in pulsed-wave Doppler tissue imaging velocities in normal geriatric cats and geriatric cats with primary cardiomyopathies or disease states linked to specific cardiomyopathies in human beings

In human beings, it has been demonstrated that these DTI derived variables correlate well with invasive measures of systolic and diastolic function (Yamanda, et al 1998), although there appears to be an age-related affect, with diastolic function deteriorating as an individual ages (Yamanda, et al 1999, Munagala, et al 2003).

The aim of this study was to determine whether or not age has a significant affect upon pw-DTI velocities in aged cats, and whether or not any of the primary cardiomyopathies or disease states linked to specific cardiomyopathies in human beings identified in the cat, alter the relationship between pw-DTI velocities and age.

Abstract

Doppler tissue imaging (DTI) techniques can provide an alternative tool for the non-invasive quantification of regional and global myocardial function. In human beings, it has been demonstrated that DTI variables correlate well with invasive measures of systolic and diastolic function, although there appears to be an age related affect, with diastolic dysfunction occurring as a person ages. Similar findings have also been reported in the cats from 10 months to twelve years of age.

The aim of this study was to determine whether or not age has a significant confounding affect on pulsed-wave DTI velocities recorded from normal geriatric cats or geriatric cats with primary cardiomyopathies or disease states linked to specific cardiomyopathies in human beings.

Ninety cats over eight years of age were included in this study. These cats were classified as being unaffected, or having a basilar septal bulge (BSB), hypertrophic cardiomyopathy (HCM), hyperthyroidism, chronic renal failure (CRF), or hypertension. The age of the cats varied from eight to eighteen years (mean 11.8 years, s.d 2.7 years). Pulsed-wave DTI S', E' and A' velocities were assessed from various sites within the myocardium.

No found evidence that pw-DTI velocities are affected by age in a normal geriatric cat population was found. Furthermore, I was unable to demonstrate any significant difference in the relationship between pw-DTI velocities and age in the cats with any of the diseases studied.

When all of the cats were analysed (both unaffected and diseased), it was found that only the A' velocity recorded from the interventricular septum, at the level of the mitral annulus, was significantly associated with the age of the cat. However, age was found to account for only 3.5% of the variation in this velocity. None of the other seventeen velocities examined demonstrated a significant relationship with age.

This study suggests that, in geriatric cats, it is not necessary to correct for age when using pulsed-wave DTI to study myocardial function.

Introduction

Cardiac hypertrophy is not infrequently identified in cats (Atkins, et al 1992, Fox 1999). It may be seen as a manifestation of primary myocardial disease (hypertrophic cardiomyopathy [HCM]) or be secondary to various systemic disorders, such as hyperthyroidism, acromegaly or hypertension (Fox 1999). Diastolic dysfunction is believed to be the principle functional abnormality in cats with HCM, and is also documented in other causes of cardiac hypertrophy (Moise and Dietze 1986, Bond, et al 1988, Bright, et al 1999, Fox 1999, Kittleson, et al 1999).

Doppler Tissue Imaging (DTI) techniques have recently been developed to provide an alternative tool for the non-invasive quantification of regional and global myocardial function (McDicken, et al 1992, Yamanda, et al 1998). In human beings, it has been demonstrated that these DTI derived variables correlate well with invasive measures of systolic and diastolic function (Yamanda, et al 1998), although there appears to be an age-related affect, with diastolic function deteriorating as an individual ages (Yamanda, et al 1999, Munagala, et al 2003). Pulsed-wave DTI (pw-DTI) variables have been shown to demonstrate a significant correlation with invasive measures of diastolic function in normal anaesthetised cats (Schober, et al 2003). Furthermore, it has been demonstrated that cats with HCM demonstrate decreased indices of diastolic function, as assessed by pw-DTI (Gavaghan, et al 1999). Previously, it has been reported that there is a weak, but significant,

relationship between pw-DTI velocities and age in a group of 25 normal cats, the mean age of which was 6 ± 3.5 years of age, range 10 months to 14 years (Koffas, et al 2001, Koffas 2003). This relationship was lost in cats with HCM (n=23), the mean age of which was 6.9 ± 3 years, range one to 12 years (Koffas, et al 2001, Koffas 2003). However, since that study included, in the normal group, three cats under the age of one year, it is unclear whether or not the relationship between DTI velocities and age is continuous throughout life, or if this is a developmental change with little clinical relevance in the mature feline. Therefore, the aim of this study was to determine whether or not age has a significant affect upon pw-DTI velocities in aged cats, and whether or not any of the primary cardiomyopathies or disease states linked to specific cardiomyopathies in human beings identified in the cat, alter the relationship between pw-DTI velocities and age.

Materials and Methods

Selection of cases

A total of 248 cats were assessed over a three-year period for possible inclusion in the study. All of the cats were privately owned animals, selected from cases seen at either the first opinion or referral clinics of the University of Edinburgh, Hospital for Small Animals, and they lived within the Edinburgh area. All cats examined in this study were of eight years of age or older; there was no upper age limit.

All owners gave informed written consent. In addition, a full history was taken. Particular attention was paid to any history of cardiac disease, duration of illness, and current or previous medications.

Measurement of blood pressure

Once admitted to the hospital, the cats were allowed approximately one hour to acclimatise. They were then taken to a quiet room and their systolic blood pressure was recorded using an indirect Doppler flow-meter (Parks Electronic; model B-811, Perimed, Bury St Edmunds, UK). The systemic blood pressure was then measured using a technique consistent with the guidelines set out by the hypertension consensus panel (Stepien 2004).

Once the blood pressure had been recorded, a full physical examination was performed. Particular attention was paid to the hydration status of the cats, the presence of thyroid nodules, renal size and shape, the presence of hepatomegaly and the pulse quality. The respiratory and heart rate were recorded, as were any auscultatory abnormalities.

Identification of Systemic Disease

Routine serum biochemistry and haematology profiles (Appendix 1), including total thyroxine (tT4), were assessed for all cats (unless they had already been performed in the preceding fortnight). Cats with a blood glucose concentration of 8 mmol/l, or greater, had a serum fructosamine level measured. Routine laboratory analysis was performed at The Royal (Dick) School of Veterinary Studies (R(D)SVS) Laboratory.

Any cats that were found to be azotaemic at the time of sampling and had not previously been diagnosed with renal insufficiency, had a repeat blood sample taken approximately two weeks later for re-assessment of serum urea and creatinine concentrations.

The cats were placed in right lateral recumbency and a six-lead electrocardiogram (ECG) (Cardiovit AT-60, Schiller AG, Switzerland) was recorded. The amplitude, duration and timing of complexes was measured, and compared with reference values (Tilley 1992). A note was made of any rhythm or conduction abnormalities. Any cat found to be in atrial fibrillation was excluded from the study, as these cats have abnormal diastolic function due to the absence of atrial systole.

Echocardiographic Examination

Echocardiographic examination was performed using a Vingmed Vivid FiVe ultrasound machine with built-in DTI capacity (GE Medical Systems-Horten, Norway) equipped with a five MegaHertz flat phased array (FPA) probe (GE Medical Systems-Horten, Norway). All images were stored digitally on optical discs (Verbatim Optical-Japan) and analysed retrospectively. Whilst scanning, an electrocardiogram trace (lead II) was recorded simultaneously. The sector width and depth were adjusted to maximise the cardiac image. The gain settings were optimised for each individual case. The focus was adjusted to the depth of interest. All pulsed Doppler tracings were made using the high pulsed-repetition frequency (HPRF) Doppler modality. For each variable the mean of five measurements was recorded. These measurements were made from adequate, consecutive, waveforms which were all recorded on a single trace.

All images were acquired with the cats in lateral recumbency, scanning through the dependent chest wall. All cats were scanned un-sedated.

Long-axis Radial Myocardial Velocity

A pw-DTI sample gate was placed over the free wall at the mid-ventricular level (Figure 4a). The right parasternal long axis four-chamber view was optimised to ensure that the longitudinal axis was at approximately 90° ($\pm 5^\circ$) to the cursor. The

sampling gate was set at 3.9mm. This was considered to be the largest possible sampling gate that could accurately be placed over the selected area of myocardium, as is advised (Sutherland and Hatle 2002).

Short-axis Radial Myocardial Velocities

The DTI mode was used to obtain tracings from the free wall at the level of the chordae tendinae (Figure 4b); the same procedure was used as had been applied to the long-axis view.

Longitudinal Myocardial Velocities

The apical four-chamber view was optimised. The positioning was manipulated so that the interventricular septum bisected the centre of the scanning vector. The pw-DTI cursor, with a sampling gate of 3.9mm, was then placed within the left two-thirds of the interventricular septum, at the level of the mitral annulus (Figure 4c); again this was felt to be the largest sampling gate that could accurately be placed at this site, as is advised by those who developed these techniques (Sutherland and Hatle 2002). The baseline and velocity scales were adjusted to optimise the tracing. The corresponding trace was recorded and the cursor was then moved to record the pw-DTI velocities from the mid-septal level (Figure 4c). When imaging the septum attempts were made to ensure the cursor was placed over the two-thirds of the septum closest to the left ventricle. This was done in order to minimise any effect of

the right ventricle on these tracings (Sutherland and Hatle 2002). The cardiac image was then rotated until the left ventricular lateral wall was in line with the cursor and the procedure repeated at the level of the mitral annulus and a point midway between the apex and mitral annulus (Figure 4c).

Echocardiographic Post-Processing and Data Analysis

Images were analysed using the Echopac software (GE Medical Systems for Macintosh). Diastolic events were analysed at end-diastole, which was identified by the start of the QRS complex (Moise and Fox 1999). Atrial systole was identified by its association with the P wave (Appleton, et al 1997). Systolic events were measured at end-systole, which was defined by the end of the T wave (Moise and Fox 1999). For the M-mode measurements systole was taken as the nadir of septal motion (Moise and Fox 1999). Events associated with any premature or ectopic beats were not measured; the complexes immediately prior to, and after, any ectopic complexes were also ignored. For each measurement, the associated R-R interval was measured and the mean R-R interval was calculated. The horizontal axis of the tracings was magnified to increase the accuracy of the timing and duration measurements.

Myocardial Excursion Patterns

For all the pw-DTI recordings the principle velocity during systole (S'), and the two principle velocities during diastole (E' and A') were measured. Occasionally the E' and A' waves were fused; in these cases the E'+A' velocity was measured.

Grouping of the Cats

Cats were classified as unaffected cats if they were clinically healthy and were normal on physical examination, including auscultation. In addition, routine blood sampling revealed no significant abnormalities and the systolic blood pressure was between 120 and 160 mmHg. Auscultation, a six-lead ECG and standard two-dimensional and M-mode echocardiographic examinations revealed no abnormalities.

Cats were grouped according to their systolic blood pressure, haematology and serum biochemistry results, and echocardiography findings. Cats were classified as hyperthyroid if their serum tT4 was equal to or exceeded 48 nmol/l (reference range 13-48nmol/l). A diagnosis of CRF was made if the serum creatinine exceeded 177 µmol/l (reference range 30-177 µmol/l) on two separate occasions approximately 14 days apart. Diabetes mellitus was diagnosed in cats with a blood glucose exceeding 8mmol/l (reference range 3.3-5.0mmol/l) and a serum fructosamine above 3.5 mmol/l (reference range 1.0-3.5mmol/l). Systemic hypertension was diagnosed if the systolic blood pressure exceeded 200 mmHg, was between 170 mmHg and 200

mmHg with concomitant ocular lesions, or was over 170 mmHg on two or more subsequent visits. Cats were diagnosed with HCM if they did not fall into any of the above groups, the packed cell volume was within normal limits (PCV 0.24-0.45 l/l), and they had M-mode evidence of concentric hypertrophy (either the left ventricular free wall or interventricular septum measuring six millimetres or greater at end-diastole, on standard M-mode (Sisson, et al 1991)). Cats were excluded if they demonstrated chamber dilation or evidence of other forms of acquired or congenital cardiac disease. A separate group of cats demonstrating a localised area of hypertrophy affecting only the basilar septum, with no other cardiac signs, was also identified: These cats were classified as having a lone basilar septal bulge (BSB). For a cat to be classified as having a BSB, the serum biochemistry results could not demonstrate any of the above changes, the PCV had to be within the normal range, the systolic blood pressure had to be below 170 mmHg, and the M-mode measurements had to be within normal limits (Sisson, et al 1991). However, the two-dimensional measurement of the basilar interventricular septal thickness, from the right parasternal long axis view, was six millimetres or greater. Cats with more than one of the diseases outlined above (ie: hypertension and CRF), or any other severe systemic disease were excluded from the analysis.

Statistical Analysis

The statistical analysis was carried out using S-Plus (version 6.2.1, 1988, 2003 Insightful Corp. S: Copyright Lucent Technologies Inc.). The mean and standard deviation of the ages in each of the disease groups was calculated. The age

distribution between groups was compared using a one-way ANOVA. Multiple analysis techniques were then applied (Tukey).

Multiple linear regression analysis was performed to determine whether or not the various pw-DTI variables correlated with age in normal geriatric cats or in diseased cats. In addition, multiple linear regression techniques were performed to assess whether there was a difference in the relationship between pw-DTI velocities and age in the normal and diseased groups and whether or not the pw-DTI velocities recorded from any particular disease group demonstrated a significant variation with age. In the event that the data were normally distributed, a logarithmic transformation (\log_{10}) was applied, and the distribution of the data reassessed for normality. A p-value of <0.05 was taken as demonstrating statistical significance.

Results

Overall, ninety cats were included in the study. Cats were excluded for a multitude of reasons, including the presence of atrial fibrillation, anaemia, myocardial masses, poor data acquisition, poor compliance, or severe arrhythmias. Only four cats with DM were identified, and therefore, this group was excluded from the analysis. In addition, any cat with more than one disease identified was excluded from the study.

Of these cats included, eight were judged to be free of disease (unaffected), nineteen were classified as having a BSB, sixteen had HCM, twenty-two were hyperthyroid (HiT4), nineteen had CRF and six were hypertensive (HiBP).

The mean age of the included cats was 11.8 yrs, standard deviation 2.7 yrs (range 8-18 years), with the age of the unaffected cats ranging from 8-14 years, mean 10.0 yrs. All the cats were neutered; there were 40 female cats and 50 males, and there was no gender bias in any of the groups. Overall, there was a significant difference in the age of the cats between disease groups ($p=0.02$). However, multivariate analyses failed to demonstrate a significantly different age in any of the groups when compared to each group individually.

The myocardial velocities measured in the unaffected cats demonstrated no significant relationship with age at any of the sites measured (Tables 4-5 & Figures 5-8). When all of the cats were studied, only the A' velocity measured from the apical view (at the septal aspect of the mitral annulus) demonstrated a significant

relationship with age ($p=0.042$, $R^2=0.0348$). Of the cats with diseases, only the E' velocity measured from the apical view (at the septal aspect of the mitral annulus) demonstrated a relationship with age ($p=0.0117$, $R^2=0.6807$), but none of the other seventeen sites investigated demonstrated a significant relationship with age. The comparison between the diseased and unaffected cats demonstrated no significant differences, whilst the different disease groups did not vary in their association with age, with the exception of the S' velocity from the free wall, measured from the short axis view (SFWSV) ($p=0.0044$, $R^2=0.270$), and the S' velocity at the same location but measured from the long-axis view (LFWSV) ($p=0.016$, $R^2=0.213$). Within the diseased groups the SFWSV only demonstrated a significant association with age in the cats with hyperthyroidism, ($p=0.023$, $R^2=0.232$), whereas the LFWSV was influenced by the hypertensive group of cats ($p=0.008$, $R^2=0.854$).

Discussion

The current study generally found no evidence that pw-DTI velocities are affected by age in either a normal or diseased geriatric cat population. Although there were relatively few unaffected cats within the sample population, there was no evidence that pw-DTI velocities varied with age in this group, aged 8-14 years. Furthermore, I demonstrated no significant difference in the relationship between pw-DTI velocities and age in any of the disease groups studied.

When all of the cats were analysed (both unaffected and diseased), it was found that only the A' velocity recorded from the interventricular septum, at the level of the mitral annulus, was significantly associated with the age of the cat. However, age was found to account for only 3.5% of the variation in this velocity. None of the other seventeen velocities examined demonstrated a significant relationship with age.

Analysis of the diseased groups of cats demonstrated a significant relationship between age and pw-DTI velocities recorded from the free wall of the long and short-axis four-chamber view. Both of these imaging planes can be used to assess the velocity of the circumferential myocardial fibres. Therefore, it is perhaps not surprising that the S' velocity from both of these views demonstrated a similar relationship with age. However, sub-group analysis demonstrated that there was a significant relationship between the long-axis S' velocity and age in the hypertensive cats and the short-axis S' velocity and age in the hyperthyroid cats. Whilst the S' from the short-axis view did demonstrate a trend toward an age association in the

hypertensive cats, this failed to reach statistical significance ($p=0.08$). Since these views should both be measuring the same fibres and therefore, should be related, the sub-group analysis raises concerns over the accuracy of this aspect of the technique. Indeed, I have previously demonstrated that the repeatability of measurements recorded from the short axis view are highly variable (Chapter 2). Such variations may therefore result from this poor repeatability and may be compounded by the small sample size, particularly in the hypertensive group of cats, which included only six cases.

In human beings, it has been shown that as individuals age left ventricular diastolic function is impaired (Yamanda, et al 1999). It is believed that this occurs in part, due to impaired myocardial relaxation and in part due to increased myocardial stiffness (myocardial fibrosis and collagen deposition increasing with age) (Yamanda, et al 1999). In this species, it has been demonstrated that there is a significant negative correlation between E' and age and a positive correlation between A' and age (Yamanda, et al 1999, Munagala, et al 2003). However, in children, the relationship between pulse-wave DTI velocities and age appears to differ from that within the adult population, with studies suggesting an increase in early diastolic velocities in the first few years of life, followed by a positive correlation with age (Kapusta, et al 2000, Eidem, et al 2004).

In cats, we have previously reported a significant association between pw-DTI E' velocities and age in a group of 25 normal cats aged 10 months to 14 years (mean 6 ± 3.5 years) (Koffas, et al 2001, Koffas, et al 2005). In that study we reported that there was no such relationship between age and pw-DTI E' velocities in cats with

HCM. The HCM group of cats comprised 23 cats aged 1-12 years (mean 6.9 ± 3 years). Notably, the current study identified no significant association between the pw-DTI E' velocity and age at most sites in either the unaffected geriatric cats, or the diseased cats. Whilst the previous study was performed on cats of any age, it predominantly included cats of young to middle age (three cats were aged one year, or less, and only three cats were over nine years of age). The current study investigated the effect of age on pw-DTI velocities in cats over eight (8-18) years. Therefore, there was minimal overlap between the age distributions studied.

The current study was limited primarily by the small sample size; this was especially true for the unaffected group of cats, which comprised only eight individuals. Unfortunately, geriatric cats without systemic or cardiac disease were not readily identified within the population seen at the Hospital for Small Animals. Furthermore, there were only six hypertensive cats included in the study. Primary or 'essential' hypertension is rare in the cat and hypertensive cats are frequently found to have other concomitant diseases (such as CRF or hyperthyroidism). To negate any confusion generated by the presence of interacting disease processes, I excluded any cats with multiple diseases from the analysis. This led to a very small group of cats with hypertension. However, even in light of these limitations, the reported findings suggest that in geriatric cats, irrespective of disease status, pw-DTI velocities are generally not related to age, with the exception of the longitudinal fibre velocity at the septal aspect of the mitral annulus during atrial systole; where only 3% of the variability could be attributed to the age of the cat. This study suggests that, in geriatric cats, it is not necessary to correct for age when using pulsed-wave

DTI to study myocardial function, and it allows normal values to be established without the inclusion of age as a possible confounding factor.

Table 4: Linear regression analysis assessing the relationship between age and pulsed-wave Doppler tissue imaging (pw-DTI) velocities

		All	Unaffected	Diseased	Dis. vs. Unaff	Dis. diff	CRF	BSB	HCM	HiT4	HiBP
log10 SFWSV	Int/num.df	-1.2490	-1.2247	-1.5341	1	4	-1.3370	-1.0098	-1.2399	-1.4436	-0.8703
	Slope/den.df	0.0031	0.0014	0.0264	121	69	0.0118	-0.0164	-0.0006	0.0214	-0.0277
	t/F	0.9156	0.4085	1.4268	1.3005	4.1685	1.6989	-1.8511	-0.0611	2.4570	-2.5413
	pval	0.3617	0.6837	0.2035	0.2564	0.0044	0.1076	0.0839	0.9521	0.0233	0.0846
	Rsqu	0.0068	0.0014	0.2533	0.0329	0.2704	0.1451	0.1860	0.0003	0.2319	0.6828
log10 SFWEV	Int/num.df	-1.2607	-1.2844	-1.3140	1	4	-1.2510	-1.2646	-1.2680	-1.2320	-0.8552
	Slope/den.df	0.0026	0.0040	0.0180	115	65	0.0058	-0.0015	-0.0032	0.0001	-0.0312
	t/F	0.5594	0.8302	0.5976	0.1828	0.5844	0.6593	-0.1211	-0.1949	0.0135	-1.3227
	pval	0.5769	0.4082	0.5761	0.6698	0.6750	0.5185	0.9052	0.8487	0.9894	0.2777
	Rsqu	0.0027	0.0062	0.0667	0.0356	0.1404	0.0249	0.0010	0.0032	0.000	0.3684
log10 SFWAV	Int/num.df	-1.2126	-1.1956	-1.3851	1	4	-1.3230	-1.2634	-1.1299	-1.2494	-1.1728
	Slope/den.df	0.0059	0.0048	0.0177	115	65	0.0173	0.0108	-0.0016	0.0122	-0.0027
	t/F	1.6247	1.2828	0.6987	0.2607	0.5111	1.8546	1.2353	-0.1177	1.3103	-0.2604
	pval	0.1069	0.2023	0.5159	0.6106	0.7277	0.0811	0.2357	0.9082	0.2066	0.8114
	Rsqu	0.0221	0.0147	0.0890	0.0370	0.1493	0.1683	0.0923	0.0012	0.0871	0.0221
log10 LFWSV	Int/num.df	-1.1774	-1.1628	-1.2253	1	4	-1.2860	-1.0015	-1.0757	-1.2978	-0.6700
	Slope/den.df	-0.0032	-0.0042	-0.0030	126	70	0.0064	-0.0169	-0.0124	0.0087	-0.0410
	t/F	-0.9866	-1.2054	-0.1963	0.0025	3.6934	0.7546	-1.7992	-1.5074	1.1890	-4.8925
	pval	0.3257	0.2304	0.8508	0.9598	0.0087	0.4608	0.0921	0.1539	0.2484	0.0081
	Rsqu	0.0075	0.0120	0.0064	0.0196	0.2311	0.0324	0.1775	0.1396	0.0660	0.8568
log10 LFWEV	Int/num.df	-1.1855	-1.2140	-1.0934	1	4	-1.4409	-1.2415	-0.9693	-1.2776	-0.9050
	Slope/den.df	-0.0035	-0.0017	-0.0013	122	67	0.0229	-0.0003	-0.0258	0.0012	-0.0200
	t/F	-0.8105	-0.3965	-0.0570	0.0002	1.6980	1.4430	-0.0292	-1.7710	0.1304	-0.8714
	pval	0.4192	0.6925	0.9567	0.9895	0.1608	0.1672	0.9771	0.1000	0.8977	0.4327
	Rsqu	0.0053	0.0013	0.0006	0.0456	0.1431	0.1091	0.0001	0.1944	0.0009	0.1595
log10 LFWAV	Int/num.df	-1.1203	-1.1131	-1.1690	1	4	-1.0634	-1.2102	-0.9718	-1.2190	-0.8351
	Slope/den.df	-0.0012	-0.0016	0.0010	122	67	-0.0085	0.0099	-0.0173	0.0118	-0.0206
	t/F	-0.3106	-0.4169	0.0353	0.0092	2.2496	-0.7500	1.3724	-2.3589	1.1737	-1.3044
	pval	0.7567	0.6775	0.9732	0.9238	0.0729	0.4635	0.1901	0.0346	0.2558	0.2621
	Rsqu	0.0008	0.0015	0.0002	0.0036	0.2384	0.0320	0.1116	0.2997	0.0711	0.2984
log10 ALWSV	Int/num.df	-1.3809	-1.4014	-1.1796	1	4	-1.1451	-1.5050	-1.4623	-1.4053	-1.0909
	Slope/den.df	0.0013	0.0028	-0.0154	100	57	-0.0186	0.0098	0.0027	0.0085	-0.0128
	t/F	0.2431	0.4635	-1.1519	0.2908	0.3353	-0.7716	0.8439	0.1703	0.4328	-0.3333
	pval	0.8084	0.6440	0.3014	0.5909	0.8531	0.4523	0.4140	0.8676	0.6713	0.7706
	Rsqu	0.0006	0.0023	0.2097	0.0073	0.1179	0.0382	0.0519	0.0024	0.0123	0.0526
log10 ALWEV	Int/num.df	-1.1890	-1.2341	-1.0573	1	4	-1.0752	-1.4263	-1.6050	-0.9778	-0.8955
	Slope/den.df	-0.0054	-0.0025	-0.0060	95	55	-0.0118	0.0110	0.0256	-0.0216	-0.0283
	t/F	-1.0039	-0.4471	-0.2556	0.0120	1.4078	-0.4738	0.7160	1.6037	-1.6962	-8.7407
	pval	0.3179	0.6559	0.8108	0.9130	0.2435	0.6424	0.4866	0.1399	0.1105	0.0128
	Rsqu	0.0103	0.0022	0.0161	0.0558	0.1491	0.0147	0.0379	0.2046	0.1609	0.9745
log10 ALWAV	Int/num.df	-1.2821	-1.2889	-1.2337	1	4	-0.9388	-1.3770	-1.0254	-1.3560	-0.8653
	Slope/den.df	0.0045	0.0049	0.0008	96	55	-0.0267	0.0086	-0.0187	0.0102	-0.0176
	t/F	0.9662	0.9831	0.0643	0.0219	1.1483	-1.2343	1.1442	-1.1989	0.7046	-0.4089
	pval	0.3363	0.3281	0.9512	0.8827	0.3437	0.2361	0.2732	0.2582	0.4919	0.7223
	Rsqu	0.0094	0.0105	0.0008	0.0104	0.1365	0.0922	0.0915	0.1257	0.0320	0.0771

(Continued overleaf)

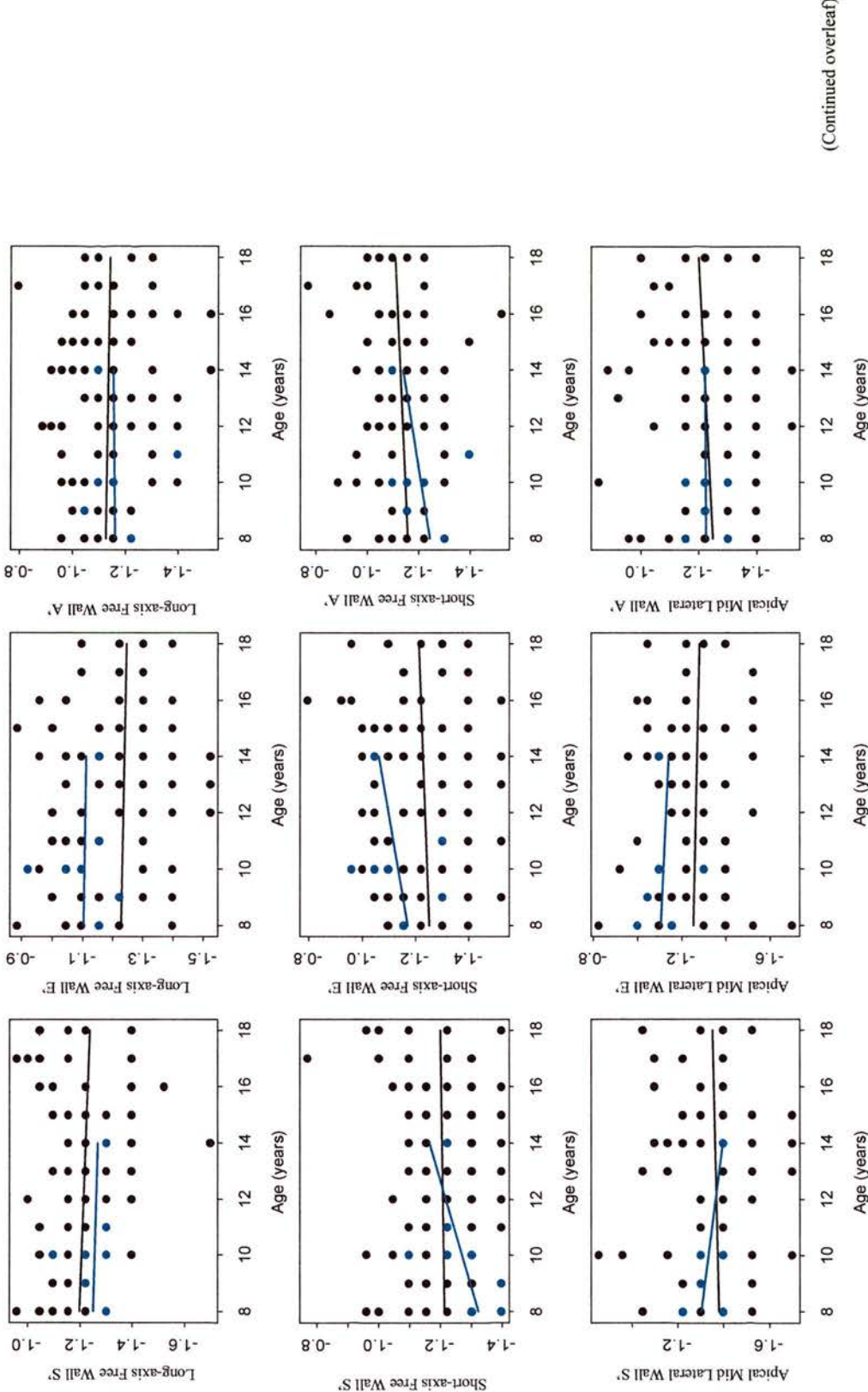
Where SFW, free wall imaged from the right parasternal short-axis view; SV, systolic velocity; EV, early diastolic velocity; AV, atrial systolic velocity; LFW, free wall imaged from the right parasternal long-axis view; ALW, mid-lateral wall imaged from the left apical four chamber view; Dis, diseased; Unaff, unaffected; Diff, different; CRF, chronic renal failure; HCM, hypertrophic cardiomyopathy; BSB, basilar septal bulge; HiT4, hyperthyroid; HiBP, hypertensive; Int, intercept; num df, numerator degrees of freedom; den df, denominator degrees of freedom; t, t-statistic; F, F-statistic; pval, p-value; Rsqu, R squared value; red-type face, significant data points ($p < 0.05$).

Table 5: Linear regression analysis assessing the relationship between age and pulsed-wave Doppler tissue imaging (pw-DTI) velocities (continued)

		All	Unaffected	Diseased	Dis.vs.Unaff	Dis.diff	CRF	BSB	HCM	HiT4	HiBP
log10 AMaSV	Int/num.df	-1.1824	-1.1879	-1.2097	1	4	-1.4538	-0.9562	-1.1918	-1.1417	-1.1300
	Slope/den.df	-0.0099	-0.0096	-0.0052	117	64	0.0156	-0.0281	-0.0122	-0.0119	-0.0171
	t/F	-1.9685	-1.7906	-0.2279	0.0184	0.9537	0.8388	-2.7939	-0.6734	-0.7630	-1.5000
	pval	0.0513	0.0761	0.8273	0.8924	0.4391	0.4132	0.0136	0.5117	0.4566	0.2724
	Rsqu	0.0315	0.0281	0.0086	0.0328	0.1186	0.0397	0.3423	0.0314	0.0351	0.5294
log10 AMaEV	Int/num.df	-1.1471	-1.1820	-1.0239	1	4	-0.9508	-0.9903	-1.4295	-1.0476	-1.5041
	Slope/den.df	-0.0053	-0.0031	-0.0084	110	60	-0.0253	-0.0215	0.0111	-0.0099	0.0179
	t/F	-1.1370	-0.6295	-0.6335	0.0329	1.1353	-1.5093	-1.3482	1.0439	-0.8437	0.5359
	pval	0.2580	0.5304	0.5498	0.8564	0.3486	0.1520	0.1990	0.3155	0.4113	0.6457
	Rsqu	0.0114	0.0038	0.0627	0.0434	0.1767	0.1318	0.1149	0.0773	0.0426	0.1255
log10 AMaAV	Int/num.df	-1.2213	-1.2119	-1.4733	1	4	-1.3556	-1.2718	-0.9707	-0.9789	-1.3592
	Slope/den.df	0.0042	0.0035	0.0293	110	60	0.0175	0.0061	-0.0156	-0.0147	0.0197
	t/F	1.1179	0.8685	1.8493	1.1798	1.4372	0.9757	0.6032	-1.9527	-1.4177	0.6677
	pval	0.2660	0.3871	0.1139	0.2798	0.2328	0.3447	0.5560	0.0727	0.1755	0.5730
	Rsqu	0.0110	0.0072	0.3630	0.0215	0.1522	0.0597	0.0253	0.2268	0.1116	0.1823
ASepSV	Int/num.df	0.0800	0.0801	0.0597	1	4	0.0554	0.1057	0.0886	0.1035	0.0825
	Slope/den.df	-0.0011	-0.0011	0.0012	121	66	0.0002	-0.0035	-0.0017	-0.0019	-0.0008
	t/F	-1.6125	-1.5328	0.4441	0.2718	0.4308	0.0885	-1.6551	-1.1010	-0.9066	-0.2526
	pval	0.1094	0.1281	0.6725	0.6031	0.7859	0.9305	0.1187	0.2895	0.3773	0.8169
	Rsqu	0.0207	0.0200	0.0318	0.0236	0.1863	0.0005	0.1544	0.0797	0.0461	0.0208
ASepEV	Int/num.df	0.0653	0.0587	0.0802	1	4	0.0586	0.0750	0.0384	0.0843	0.1453
	Slope/den.df	-0.0010	-0.0005	-0.0008	111	59	-0.0002	-0.0023	0.0004	-0.0019	-0.0061
	t/F	-1.8292	-1.0226	-0.2453	0.0060	1.1010	-0.1313	-1.9679	0.3694	-1.0819	-2.7892
	pval	0.0700	0.3089	0.8144	0.9386	0.3646	0.8971	0.0726	0.7183	0.2953	0.1081
	Rsqu	0.0288	0.0099	0.0099	0.1164	0.2554	0.0010	0.2440	0.0112	0.0682	0.7955
ASepAV	Int/num.df	0.0666	0.0681	0.0662	1	4	0.0467	0.0502	0.0731	0.0996	0.2005
	Slope/den.df	0.0008	0.0007	0.0004	111	59	0.0027	0.0020	0.0007	-0.0018	-0.0071
	t/F	1.2201	0.9879	0.3430	0.0054	1.8937	1.3286	1.1453	0.3787	-1.3968	-1.2075
	pval	0.2250	0.3255	0.7433	0.9415	0.1235	0.2015	0.2744	0.7115	0.1815	0.3507
	Rsqu	0.0130	0.0092	0.0192	0.0170	0.2014	0.0941	0.0985	0.0118	0.1087	0.4216
log10 ASepASV	Int/num.df	-1.1494	-1.1513	-1.1882	1	4	-1.3211	-0.9352	-1.3268	-1.0475	-0.7916
	Slope/den.df	-0.0027	-0.0026	0.0022	124	67	0.0120	-0.0237	0.0114	-0.0038	-0.0269
	t/F	-0.6194	-0.5602	0.1813	0.0273	2.2211	0.9208	-2.0141	0.9466	-0.4372	-6.0124
	pval	0.5368	0.5764	0.8621	0.8690	0.0760	0.3700	0.0623	0.3599	0.6675	0.0039
	Rsqu	0.0030	0.0027	0.0054	0.0036	0.2261	0.0475	0.2129	0.0602	0.0111	0.9004
log10 ASepAEV	Int/num.df	-1.2608	-1.3068	-0.9216	1	4	-1.5102	-1.2669	-1.2351	-1.0682	-0.7151
	Slope/den.df	-0.0034	-0.0004	-0.0269	116	62	0.0200	-0.0056	-0.0103	-0.0166	-0.0395
	t/F	-0.8216	-0.0841	-3.5769	1.0494	1.3385	1.2328	-0.5196	-0.7882	-1.6863	-0.9409
	pval	0.4130	0.9332	0.0117	0.3078	0.2658	0.2344	0.6115	0.4472	0.1100	0.4162
	Rsqu	0.0057	0.0001	0.6807	0.0604	0.1260	0.0821	0.0189	0.0535	0.1433	0.2279
log10 ASepAA	Int/num.df	-1.2272	-1.2101	-1.1801	1	4	-1.1358	-1.2702	-1.2255	-1.0462	-0.6897
	Slope/den.df	0.0075	0.0064	-0.0029	116	62	-0.0025	0.0097	0.0098	-0.0044	-0.0243
	t/F	2.0627	1.6837	-0.1932	0.1626	0.9769	-0.3234	1.0034	0.8926	-0.4988	-1.4439
	pval	0.0413	0.0951	0.8532	0.6875	0.4267	0.7503	0.3327	0.3912	0.6243	0.2445
	Rsqu	0.0348	0.0251	0.0062	0.0536	0.1623	0.0061	0.0671	0.0675	0.0144	0.4100

Where AMa, Posterior wall at the level of the mitral annulus (imaged from the left apical four-chamber view); SV, systolic velocity; EV, early diastolic velocity; AV, atrial systolic velocity; ASep, mid-interventricular septum (imaged from the left apical four chamber view); ASepA, interventricular septum at the level of the mitral annulus (imaged from the left apical four chamber view); Dis, diseased; Unaff, unaffected; Diff, different; CRF, chronic renal failure; HCM, hypertrophic cardiomyopathy; BSB, basilar septal bulge; HiT4, hyperthyroid; HiBP, hypertensive; Int, intercept; num df, numerator degrees of freedom; den df, denominator degrees of freedom; t, t-statistic; F, F-statistic; pval, p-value; Rsqu, R²; squared value; red-type face, significant data points (p<0.05).

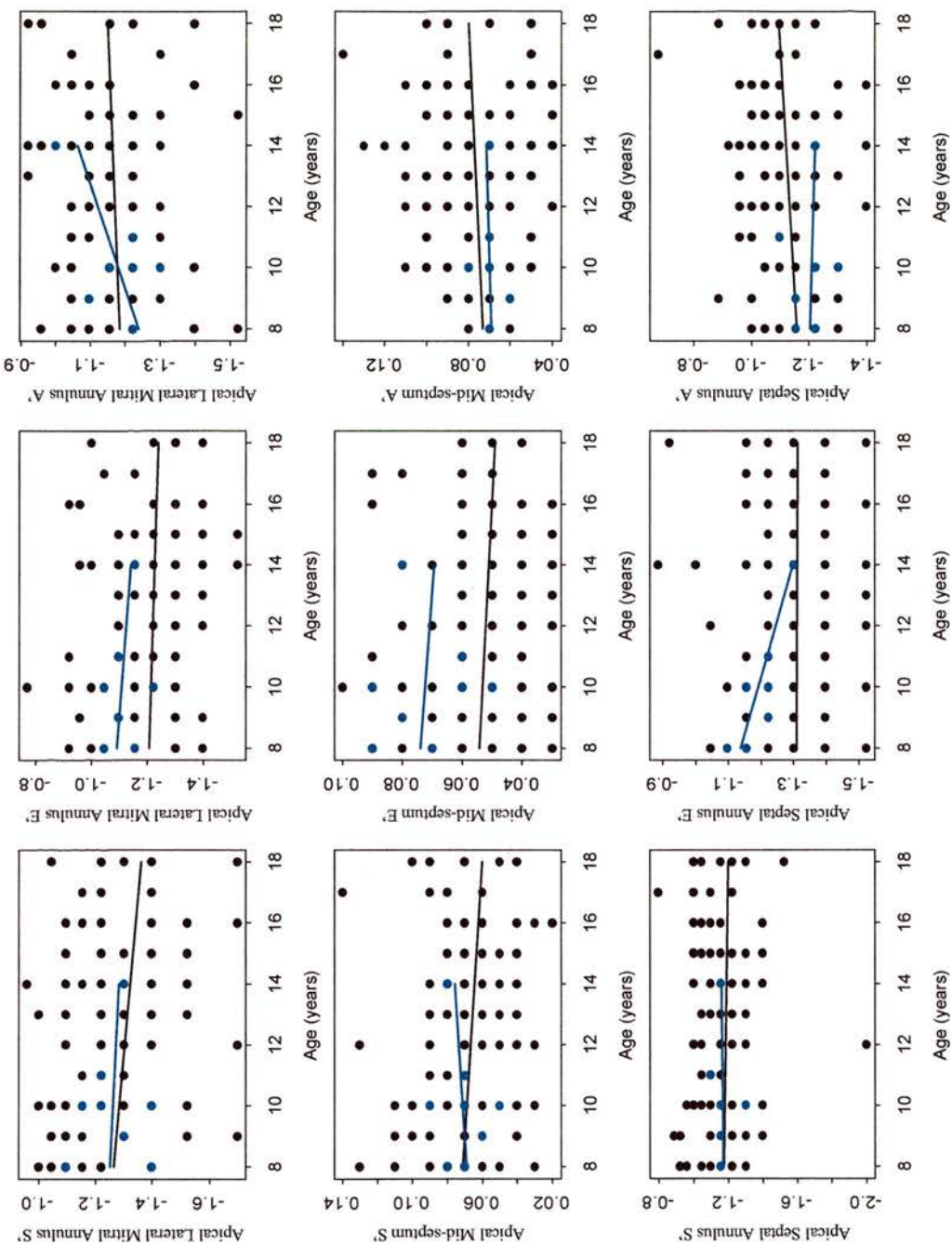
Figure 5: Linear regression analysis of unaffected and diseased cats



(Continued overleaf)

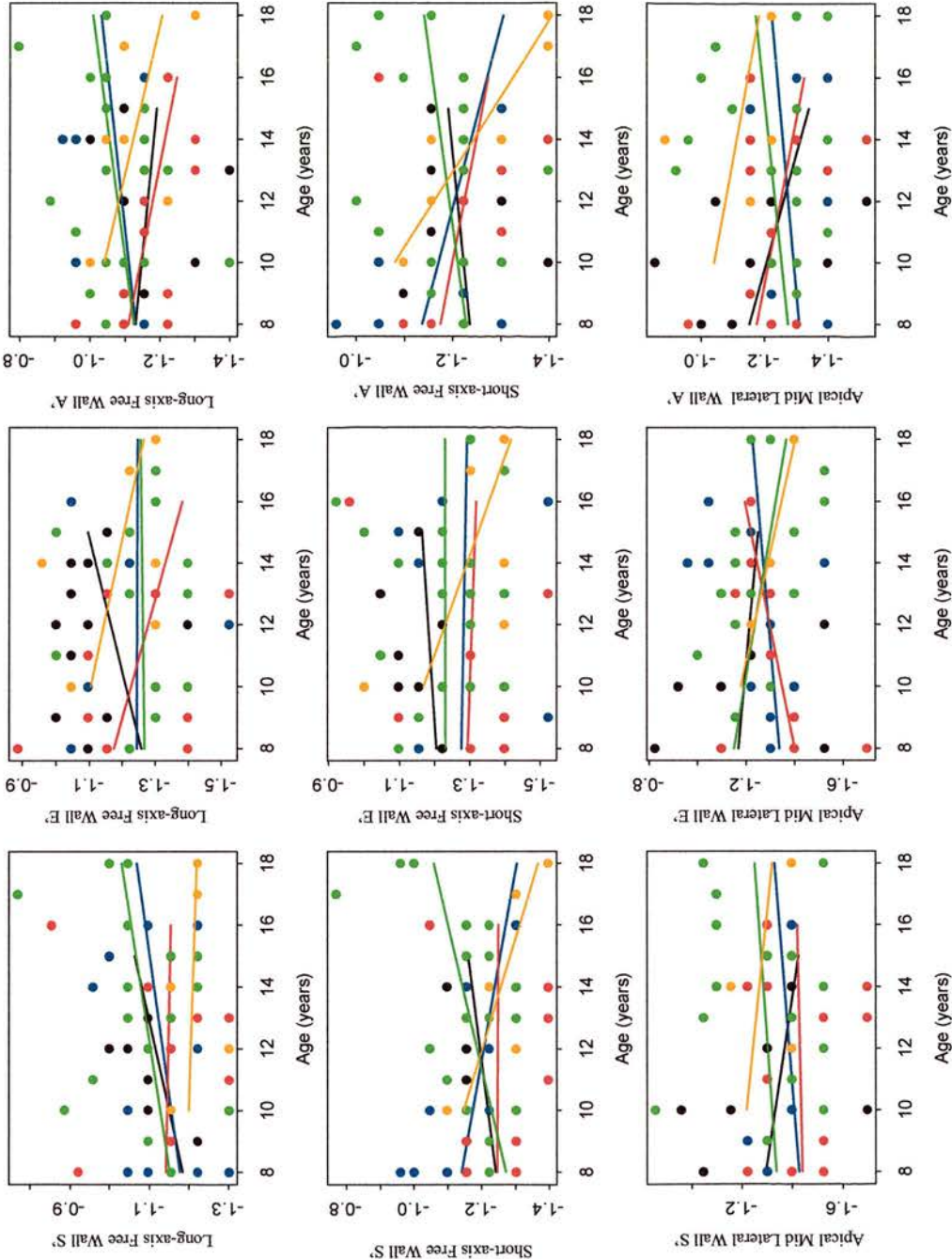
Blue, unaffected; black, diseased cats; FW, measurement of the velocity of the free wall; LW, measurement of the velocity of the lateral wall; L, imaged from the right parasternal long-axis view; S, imaged from the right parasternal short-axis view; A, imaged from the left apical four-chamber view; SV, log₁₀ systolic velocity (m/sec); EV, log₁₀ early diastolic velocity (m/sec); AV, log₁₀ late diastolic velocity (m/sec).

Figure 6: Linear regression analysis of unaffected and diseased cats (continued)



Blue, unaffected; black, diseased cats; Ma, measurement of the velocity of the posterior wall motion (at the level of the mitral annulus); A, imaged from the left apical four-chamber view; Sep, measurement of the velocity of interventricular septal motion (at the mid-septal level); SepA, measurement of the velocity of the interventricular septal motion (at the level of the mitral annulus); SV, \log^{10} systolic velocity (m/sec); EV, \log^{10} early diastolic velocity (m/sec); AV, \log^{10} late diastolic velocity (m/sec).

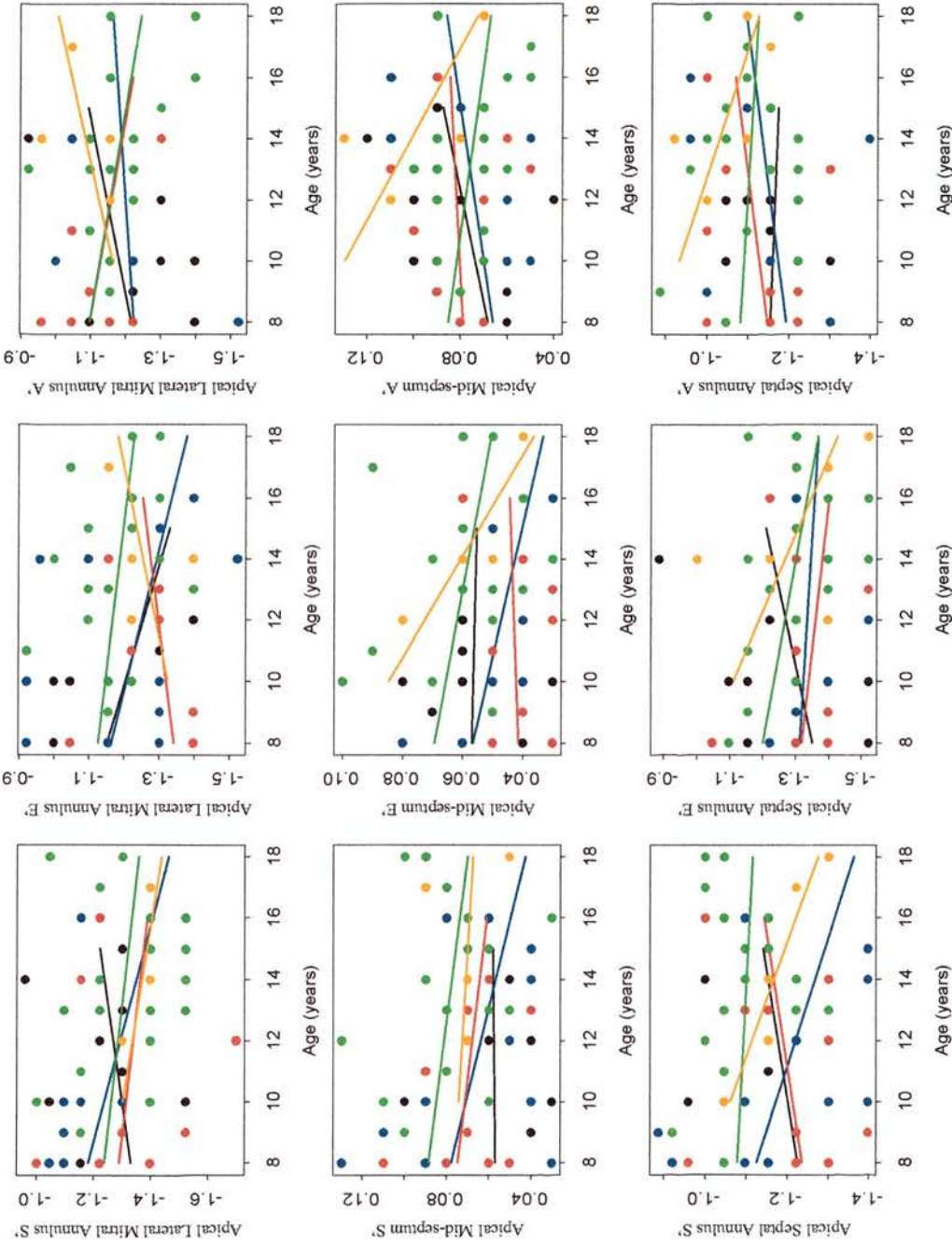
Figure 7: Linear regression analysis of different diseased groups



(Continued overleaf)

Black, BSB; red, HCM; green, CRF; orange, hypertension; blue, log¹⁰ systolic velocity (m/sec); EV, log¹⁰ early diastolic velocity (m/sec); AV, log¹⁰ late diastolic velocity (m/sec).
the lateral wall; L, imaged from the right parasternal long-axis view; S, imaged from the right parasternal short-axis view; A, imaged from the left apical four-chamber view; SV, log¹⁰ systolic velocity (m/sec); EV, log¹⁰ early diastolic velocity (m/sec); AV, log¹⁰ late diastolic velocity (m/sec).

Figure 8: Linear regression analysis of different diseased groups (continued)



Black, BSB; red, HCM; green, hyperthyroidism; blue, CRF; orange, hypertension; Ma, measurement of the velocity of the lateral wall motion (at the level of the mitral annulus); A, imaged from the left apical four-chamber view; Sep, measurement of the velocity of interventricular septal motion (at the mid-septal level); SepA, measurement of the velocity of the interventricular septal motion (at the level of the mitral annulus); SV, \log^{10} systolic velocity (m/sec); EV, \log^{10} early diastolic velocity (m/sec); AV, \log^{10} late diastolic velocity (m/sec)

Chapter 4: Heart rate-related variation in pulsed-wave

Doppler tissue imaging velocities in normal geriatric cats and geriatric cats with primary cardiomyopathies or disease states linked to specific cardiomyopathies in human beings

Pulsed-wave DTI (pw-DTI) variables have been shown to demonstrate a significant correlation with invasive measures of diastolic function in normal anaesthetised cats (Schober, et al 2003). However, it is reported that these velocities are influenced by heart rate.

To date, no studies have assessed the affect of R-R interval (as measured on the electrocardiogram) on pw-DTI indices recorded in cats with various forms of specific cardiomyopathy. The objective of this study was to further investigate the relationship between heart rate (assessed by R-R interval) and pw-DTI velocities within the feline myocardium, and to assess the affect of heart rate in various primary and specific forms of cardiomyopathy.

Abstract

Doppler tissue imaging (DTI) techniques provide an alternative tool for the non-invasive quantification of regional and global myocardial function. Assessment of pulsed-wave (pw)-DTI variables in cats with hypertrophic cardiomyopathy (HCM) has previously shown that there is a significant decrease in the velocity of myocardial movement during diastole. However, it has been suggested that these velocities may not truly represent diastolic function, and that they may be influenced by confounding factors such as age and heart rate.

The aim of this study was to determine whether or not heart rate has a significant confounding affect on pw-DTI velocities recorded from normal geriatric cats or geriatric cats with primary cardiomyopathies or disease states linked to specific cardiomyopathies in human beings.

Ninety cats of eight years of age or above were included in this study. These cats were classified as being unaffected, or having a lone basilar septal bulge (BSB), HCM, hyperthyroidism, chronic renal failure, or hypertension. The heart rate at initial presentation did not vary between the groups of cats. Pulsed-wave DTI S', E' and A' velocities were assessed from various sites within the myocardium.

Overall, it was demonstrated that, in healthy animals, heart rate significantly influenced the S', E' and A' velocities of radial motion and the A' velocities of longitudinal motion. In light of these findings, in healthy animals, the influence of heart rate upon pw-DTI velocities should always be considered in the interpretation of these velocities.

Introduction

Diastolic dysfunction is believed to be the principle functional abnormality in cats with hypertrophic cardiomyopathy (HCM) (Bright, et al 1999, Fox 1999, Kittleson, et al 1999). It is also documented in other causes of cardiac hypertrophy in cats (Moise and Dietze 1986, Bond, et al 1988). Whilst invasive measurements can provide an accurate assessment of diastolic function, these techniques are not widely available, nor are they applicable to clinical cases.

Doppler tissue imaging (DTI) techniques have been developed to provide an alternative tool for the non-invasive quantification of regional and global myocardial function (McDicken, et al 1992, Yamanda, et al 1998). In human beings, it has been demonstrated that DTI derived variables correlate well with invasive measures of systolic and diastolic function (Yamanda, et al 1998). However, in this species, these variables are affected by several factors, including heart rate; as the heart rate increases, so does the A' to E' ratio (Mori, et al 2000).

Pulsed-wave DTI (pw-DTI) variables have previously been shown to demonstrate a significant correlation with invasive measures of diastolic function in normal anaesthetised cats (Schober, et al 2003). In that study it was reported that heart rate acted as an independent variable, affecting the pulmonary venous flow patterns, the isovolumetric relaxation time, the pw-DTI derived A' velocities and with this the ratio of E':A' derived from these velocities. However, in a recent study by Chetboul and colleagues, assessing colour DTI velocities in a group of healthy cats, the investigators reported a positive correlation between S' and E' (or summated E'+A')

velocities and heart rate, at the basal and mid-lateral wall (assessed from the apical four-chamber view) and within the free wall (assessed from the right parasternal short-axis view) (Chetboul, et al 2004). These somewhat conflicting results may have arisen as a result of the different techniques used. This is because pw-DTI has the advantage of a high frame rate, and E' and A' summation is therefore less likely. Summation of images at high heart rate may have been responsible for the increased velocities seen by Chetboul and colleagues (Chetboul, et al 2004).

To date, no studies have assessed the affect of R-R interval (as measured on the simultaneously recorded electrocardiogram) on pw-DTI indices recorded in cats with various forms of specific cardiomyopathy. The objective of this study was to further investigate the relationship between heart rate (assessed by R-R interval) and pw-DTI velocities within the feline myocardium, and to assess the affect of heart rate in various primary and specific forms of cardiomyopathy. Since many of the disease states linked to specific cardiomyopathies in human beings, affect primarily geriatric cats, the cats studied ranged in age from 8-18 years and had a variety of primary conditions, including hyperthyroidism, hypertension, primary HCM, or a localised area of septal hypertrophy (lone basilar septal bulge [BSB]).

Materials and Methods

The selection of cases, identification of systemic disease, grouping of cats and echocardiographic examination protocol used in this study were identical to the procedures outlined in Chapter 3.

Statistical Analysis

The statistical analysis was carried out using S-Plus (version 6.2.1, 1988, 2003 Insightful Corp. S: Copyright Lucent Technologies Inc.). The mean and standard deviation of the R-R interval in each of the disease groups was calculated. The difference in heart rate at initial presentation was compared using a one-way ANOVA. In addition, the R-R interval of each of the variables studied was compared for differences between groups using a one-way analysis of variance (ANOVA). When a significant difference was identified multiple analysis comparisons were performed (Tukey).

Multiple linear regression techniques were performed to assess whether there was a difference in the relationship between pw-DTI velocities and R-R interval in the normal and diseased groups and whether or not the pw-DTI velocities recorded from any particular disease group demonstrated a significant variation with heart rate. In the event that the data were not normally distributed, a logarithmic transformation (\log_{10}) was applied, and the distribution of the data reassessed for normality. A p-value of <0.05 was taken as demonstrating statistical significance.

Results

Overall, ninety cats were included in the study. Cats were excluded for a multitude of reasons, including the presence of atrial fibrillation, anaemia, myocardial masses, poor data acquisition, poor compliance, or severe arrhythmias. Only four cats with DM were identified, and therefore, this group was excluded from the analysis.

Of the cats included, eight were judged to be free of disease (unaffected), nineteen were classified as having a BSB, sixteen had HCM, twenty-two were hyperthyroid (HiT4), nineteen had CRF, and six were hypertensive (HiBP).

The mean heart rate at initial presentation was 183 ± 26 bpm. The heart rate at initial presentation was not significantly different between groups. The mean heart rate of the unaffected cats at initial presentation was 165 ± 22.2 bpm. When the R-R intervals measured for each of the variables during the echocardiographic examination were compared, there was a significant difference in the R-R interval between groups. This was evident in the measurements recorded from the interventricular septum (assessed from the right parasternal long-axis view) ($F=3.27$, $P=0.02$). At this point the R-R interval was significantly longer in the cats with CRF than in the cats with hyperthyroidism.

Multiple linear regression analysis was performed (Tables 6-7 & Figures 9-11). This analysis demonstrated a significant relationship between all of the measurements recorded from the radial fibres (right parasternal long and short axis views, S', E' and A') and the R-R interval. When the relationship between R-R interval and the radial variables was assessed in only the unaffected cats, there remained a significant variation with heart rate (Table 6). However, if only the diseased cats were assessed

the relationship between R-R interval and radial velocity was no longer significant. Furthermore, the disease being studied did not affect the relationship.

The analysis of longitudinal fibre velocity (assessed from the left apical four-chamber view) demonstrated a significant relationship between R-R interval and A' velocity at each of the points studied. At each of these points the unaffected cats demonstrated a significant relationship with R-R interval, whilst the diseased cats did not. There was no significant difference in the relationship between A' velocity and R-R interval between disease groups. In addition to the relationship with A', the S' measured at the mid-lateral wall (from the left apical four-chambered view) demonstrated a significant variation with R-R interval. Whilst there was no significant relationship between the R-R interval and S' velocity in the diseased cats, this velocity varied significantly with R-R interval in the unaffected cats, and when all cats were analysed together. The E' velocity at the septal aspect of the mitral annulus (assessed from the left apical four-chambered view) was also significantly affected by R-R interval in the diseased cats, but not when all cats were analysed together, nor when just the unaffected cats were assessed. However, there was a significant difference in the relationship between R-R interval and disease, with the hypertensive cats demonstrating a significant relationship with R-R interval.

Discussion

A significant relationship between many pw-DTI variables and R-R interval was observed. The strongest association was observed in the measurements obtained from the right parasternal long and short axis views (assessing the radial myocardial velocities). All of the variables measured from these views demonstrated a significant variation with R-R interval, although the R^2 values were relatively low, with heart rate accounting for a maximum of 20% of the variability in the E' velocity recorded from the right parasternal long-axis view. This relationship was observed when either all the cats or only the unaffected cats were assessed. However, when only the diseased cats were studied, there was no evidence of a relationship between heart rate and pw-DTI velocity. In comparison, when assessing the longitudinal function only the A' velocities were consistently affected by heart rate. Again, this relationship was evident when all the cats were assessed or when only the unaffected cats were assessed, but did not hold true when only the diseased cats were assessed.

When all the diseased cats were assessed as a single group, there was no relationship between any of the pw-DTI variables and heart rate (assessed by R-R interval). The affect of heart rate on pw-DTI variables in cats with primary cardiomyopathy has been assessed previously (Gavaghan, et al 1999). In agreement with the current study, the authors of that study reported no significant association between heart rate and pw-DTI velocities in the diseased state.

The S' at the mid-lateral wall (assessed from the left apical four chamber view) was significantly influenced by heart rate, when either all of the cats were analysed, or when only the unaffected cats were analysed (but not when the diseased cats were

assessed). In addition, the E' velocity at the septal aspect of the mitral annulus (assessed from the left apical four chamber view) was significantly related to heart rate in only the unaffected cats. However, the relationship did differ with disease state at this site, when only the hypertensive cats were assessed the pw-DTI variables were significantly affected by R-R interval. It is unclear why these variables might be heart rate dependent when the S' and E' velocities at the remaining sites assessing longitudinal fibre motion were not significantly related to heart rate. These variations may represent regional variations in beta-receptor activity, or may be spurious results.

Previously, the affect of heart rate upon DTI variables has been assessed in a small number of healthy cats (Gavaghan, et al 1999, Schober, et al 2003, Chetboul, et al 2004) (n=20, n=7 and n=6, respectively). Invasive studies have demonstrated that the A' velocity of longitudinal motion was related to heart rate (Schober, et al 2003). In the current study I report a similar finding when all cats are assessed. In contrast, to other studies, a study using colour DTI techniques in healthy cats reported a significant relationship between heart rate and both S' and E' along the longitudinal axis (Chetboul, et al 2004). However, in that study 67% of the diastolic velocities (assessed from the apical four chamber view) were summated and therefore A' was not assessed. Instead, the summated E' and A' were measured as E'. This may have affected the results of their E' analysis. Furthermore, that study assessed the myocardial velocities in six cats, each cat being scanned on six occasions. From the results it appears that only one cat had a heart rate below 170bpm. Since that cat appears to have shown much lower DTI velocities than the other five cats it may have influenced the results of that study (Chetboul, et al 2004).

The relationship between radial fibre velocity and heart rate was previously assessed using both colour and pw-DTI (Gavaghan, et al 1999, Chetboul, et al 2004). Using colour DTI, it was reported that (when assessed from the right parasternal short axis view) both the S' and E' velocities were related to heart rate, at least when the endocardial segments were assessed. Once again, the high number of fused E' and A' complexes in that study precluded the relationship between A' and heart rate from being studied (Chetboul, et al 2004). In the other study, pw-DTI was used to assess the peak diastolic velocity (PDV) (either E' or E'+A') from both the right parasternal short axis view and left apical long-axis view in normal cats and cats with HCM (Gavaghan, et al 1999). These investigators reported that there was a positive correlation between heart rate and PDV in the normal cats, but that the correlation was not as strong for cats with HCM (Gavaghan, et al 1999). The results of the current study are generally in agreement with the cumulative results of these previous studies. Overall, a significant relationship was identified between R-R interval and all of the measurements of radial fibre velocity in the unaffected cats. In addition, there was a significant relationship between many of the longitudinal velocities and the R-R interval in the unaffected group of cats.

The current study was limited primarily by the small sample size; this was especially true for the unaffected group of cats, which comprised only eight individuals. Unfortunately, geriatric cats without systemic or cardiac disease were not readily identified within the population studied. Furthermore, there were only six hypertensive cats included in the study. Primary or 'essential' hypertension is rare in cats and hypertensive cats are frequently found to have other concomitant diseases (such as CRF or hyperthyroidism). To negate any confusion generated by the

presence of interacting disease processes, I excluded any cats with multiple diseases from the analysis. This led to a very small group of cats with hypertension.

Overall, I was able to demonstrate that, in cats, heart rate significantly influenced several of the pw-DTI velocities, especially those assessing radial motion. In light of these findings, in healthy animals, the influence of heart rate upon Doppler variables should always be considered in the interpretation of pw-DTI variables. One correction technique widely used is the root RR method, by which variables are divided by the square root of the R-R interval (Yoshikawa, et al 1993, Akasaka, et al 1994, Dukes McEwan, et al 2002). The heart rate dependence of pw-DTI in cats suggests that when pw-DTI variables are being compared that a correction term is included in the analysis.

Table 6: Linear regression analysis assessing the relationship between R-R interval and pulsed-wave Doppler tissue imaging (pw-DTI) velocities

		All	Unaffected	Diseased	Dis.vs.Unaff	Dis.diff	CRF	BSB	HCM	HiT4	HiBP
log10 SFWSV	Int/num.df	-1.0367	-1.0458	-1.0996	1	4	-1.1268	-1.1351	-0.9346	-0.8762	-0.7761
	Slope/den.df	-0.5077	-0.4738	-0.4387	121	69	-0.2391	-0.1673	-0.9001	-0.8667	-1.5297
	t/F	-3.0491	-2.7113	-0.5346	0.0017	1.0146	-0.5521	-0.4472	-1.7185	-1.8836	-2.7056
	pval	0.0028	0.0077	0.6121	0.9670	0.4060	0.5881	0.6611	0.1077	0.0742	0.0734
	Rsqu	0.0703	0.0601	0.0455	0.0779	0.2198	0.0176	0.0132	0.1742	0.1507	0.7093
log10 SFWEV	Int/num.df	-1.0473	-1.0245	-0.4822	1	4	-0.9412	-1.1378	-0.8622	-1.3111	-0.8814
	Slope/den.df	-0.5245	-0.6145	-1.6324	115	65	-0.7288	-0.3922	-1.2685	0.2434	-1.3098
	t/F	-2.2669	-2.5719	-1.6401	0.6491	0.9536	-1.5176	-0.8201	-1.5867	0.4454	-0.9214
	pval	0.0252	0.0114	0.1619	0.4221	0.4390	0.1475	0.4250	0.1386	0.6613	0.4248
	Rsqu	0.0421	0.0567	0.3498	0.0938	0.1856	0.1193	0.0429	0.1734	0.0109	0.2206
log10 SFWAV	Int/num.df	-0.9289	-0.9333	-1.1171	1	4	-1.1850	-0.8758	-0.7370	-0.7620	-0.9695
	Slope/den.df	-0.6120	-0.5932	-0.2179	115	65	0.1476	-0.7172	-1.1791	-0.9882	-0.7571
	t/F	-3.5198	-3.2652	-0.2084	0.1488	0.7095	0.2502	-2.3848	-1.8184	-2.3202	-2.1129
	pval	0.0006	0.0015	0.8431	0.7004	0.5884	0.8054	0.0307	0.0940	0.0323	0.1250
	Rsqu	0.0957	0.0884	0.0086	0.1020	0.2648	0.0037	0.2749	0.2160	0.2302	0.5981
log10 LFWSV	Int/num.df	-1.0449	-1.0376	-1.3422	1	4	-1.0675	-1.0376	-0.9544	-1.0771	-0.7763
	Slope/den.df	-0.5051	-0.5233	0.2252	126	70	-0.4397	-0.4263	-0.7460	-0.3238	-1.5072
	t/F	-3.3708	-3.3197	0.4056	0.9395	0.3890	-0.9917	-1.0299	-1.5769	-0.8019	-1.2364
	pval	0.0010	0.0012	0.6991	0.3343	0.8158	0.3352	0.3194	0.1371	0.4321	0.2839
	Rsqu	0.0815	0.0841	0.0267	0.0899	0.1276	0.0547	0.0660	0.1508	0.0311	0.2765
log10 LFWEV	Int/num.df	-0.9245	-0.8967	-0.5555	1	4	-0.6022	-0.8459	-0.4545	-1.2277	-0.4244
	Slope/den.df	-0.8865	-0.9968	-1.4077	122	67	-1.7372	-1.0894	-2.2871	-0.1048	-2.4272
	t/F	-4.8284	-5.4078	-2.4990	0.1752	2.2915	-2.2035	-2.9111	-3.3290	-0.2239	-2.2617
	pval	0	0	0.0546	0.6763	0.0686	0.0416	0.0108	0.0054	0.8254	0.0865
	Rsqu	0.1583	0.2000	0.5554	0.2439	0.3426	0.2222	0.3610	0.4602	0.0028	0.5612
log10 LFWAV	Int/num.df	-1.0100	-1.0022	-1.3082	1	4	-1.0495	-0.9221	-0.8220	-0.9186	-0.4691
	Slope/den.df	-0.3644	-0.3862	0.3813	122	67	-0.3139	-0.4766	-0.9787	-0.4488	-2.0909
	t/F	-2.0906	-2.1306	0.3791	0.6122	0.8330	-0.5178	-1.6233	-2.3077	-0.8537	-3.3131
	pval	0.0386	0.0352	0.7202	0.4355	0.5090	0.6113	0.1253	0.0381	0.4045	0.0296
	Rsqu	0.0340	0.0374	0.0279	0.0390	0.2596	0.0155	0.1494	0.2906	0.0389	0.7329
log10 ALWSV	Int/num.df	-1.1495	-1.1185	-1.2916	1	4	-1.3014	-1.1922	-1.2159	-0.7270	-0.6290
	Slope/den.df	-0.6227	-0.7281	-0.0989	100	57	-0.1283	-0.5381	-0.6094	-1.8077	-2.0028
	t/F	-2.7128	-2.9259	-0.2305	0.4430	0.5591	-0.1173	-1.3514	-0.7839	-1.6960	-1.2984
	pval	0.0078	0.0043	0.8268	0.5072	0.6933	0.9082	0.1996	0.4483	0.1105	0.3237
	Rsqu	0.0673	0.0827	0.0105	0.0846	0.1850	0.0009	0.1232	0.0487	0.1609	0.4574
log10 ALWEV	Int/num.df	-1.1799	-1.1337	-1.1047	1	4	-1.0540	-0.9033	-1.3094	-1.6089	-0.9522
	Slope/den.df	-0.2232	-0.3877	-0.0274	95	55	-0.4300	-1.0709	0.0157	1.0867	-1.0928
	t/F	-0.9772	-1.6260	-0.0388	0.1440	1.2539	-0.3888	-2.2600	0.0191	1.4214	-1.4605
	pval	0.3309	0.1074	0.9709	0.7052	0.2992	0.7029	0.0416	0.9852	0.1756	0.2816
	Rsqu	0.0097	0.0282	0.0004	0.0795	0.1628	0.0100	0.2821	0	0.1187	0.5161
log10 ALWAV	Int/num.df	-0.9744	-0.9510	-1.1345	1	4	-1.1550	-1.0892	-0.9177	-0.6981	-0.3557
	Slope/den.df	-0.7277	-0.8050	-0.2267	96	55	-0.2069	-0.5080	-0.9256	-1.6676	-2.3680
	t/F	-3.9816	-4.0533	-0.6244	0.5994	0.7920	-0.2053	-2.0824	-1.3001	-2.2194	-1.3930
	pval	0.0001	0.0001	0.5598	0.4407	0.5354	0.8401	0.0576	0.2227	0.0423	0.2983
	Rsqu	0.1392	0.1529	0.0723	0.1520	0.2055	0.0028	0.2501	0.1446	0.2472	0.4924

(Continued overleaf)

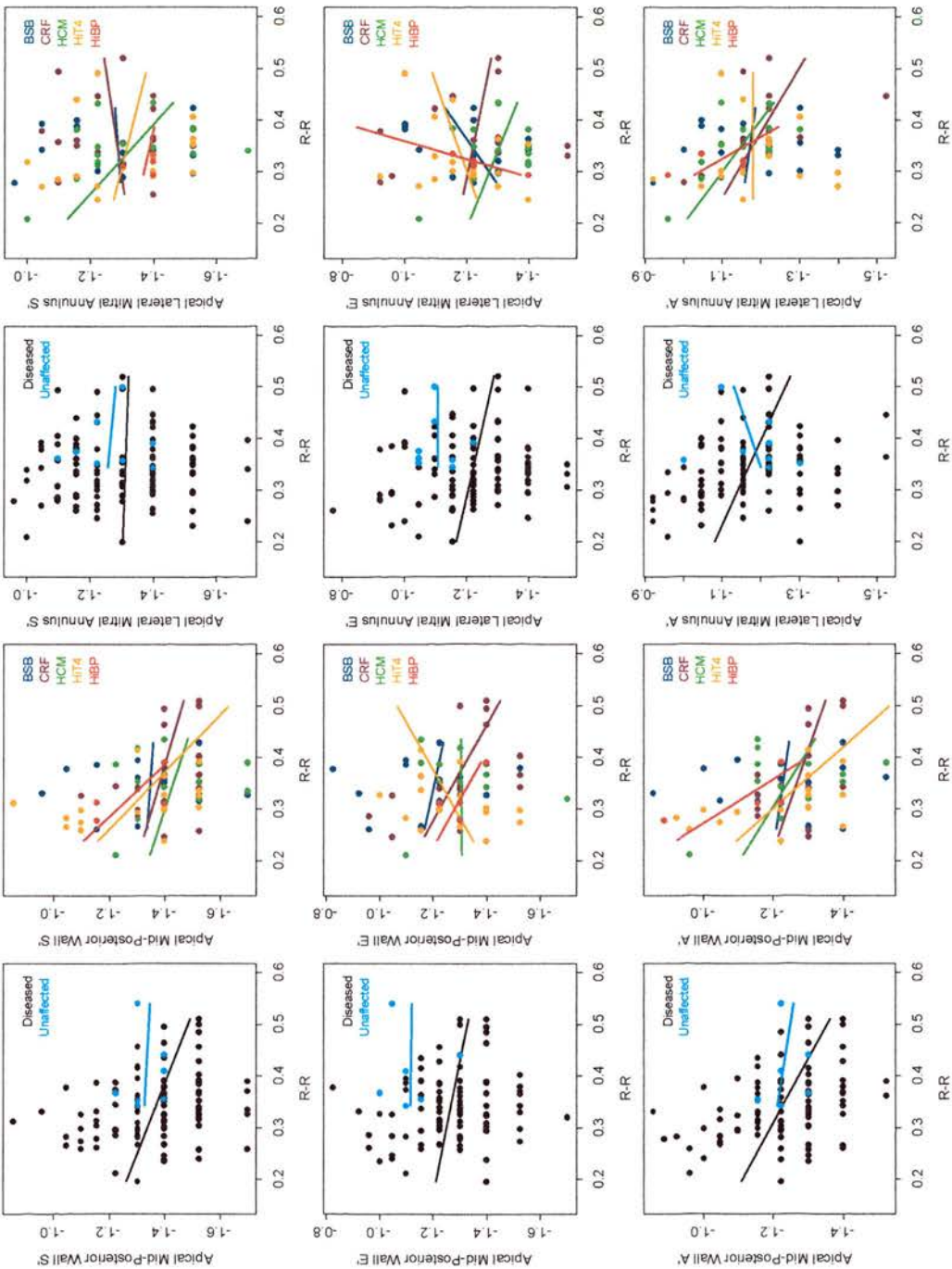
Where SFW, free wall imaged from the right parasternal short-axis view; SV, systolic velocity; EV, early diastolic velocity; AV, atrial systolic velocity; LFW, free wall imaged from the right parasternal long-axis view; ALW, mid-lateral wall imaged from the left apical four chamber view; Dis, diseased; Unaff, unaffected; Diff, different; CRF, chronic renal failure; HCM, hypertrophic cardiomyopathy; BSB, basilar septal bulge; HiT4, hyperthyroid; HiBP, hypertensive; Int, intercept; num df, numerator degrees of freedom; den df, denominator degrees of freedom; t, t-statistic; F, F-statistic; pval, p-value; Rsqu, R squared value; red-type face, significant data points ($p < 0.05$).

Table 7: Linear regression analysis assessing the relationship between R-R interval and pulsed-wave Doppler tissue imaging (pw-DTI) velocities (continued)

		All	Unaffected	Diseased	Dis. vs. Unaff	Dis. diff	CRF	BSB	HCM	HiT4	HiBP
log10 AMaSV	Int/num.df	-1.3012	-1.2921	-1.2018	1	4	-1.3254	-1.3671	-0.8152	-1.1730	-1.2528
	Slope/den.df	-0.0165	-0.0528	-0.1539	117	64	0.1198	0.2426	-1.4880	-0.4056	-0.3833
	t/F	-0.0679	-0.2045	-0.1847	0.0069	0.8339	0.1211	0.4605	-1.7818	-0.6024	-0.1939
	pval	0.9460	0.8383	0.8595	0.9338	0.5086	0.9051	0.6518	0.0965	0.5554	0.8641
	Rsqu	0	0.0004	0.0057	0.0059	0.0855	0.0009	0.0139	0.1849	0.0222	0.0185
log10 AMaEV	Int/num.df	-1.1249	-1.0927	-1.1118	1	4	-1.6052	-1.1020	-1.0724	-1.3759	-3.0642
	Slope/den.df	-0.2555	-0.3752	0.0102	110	60	1.1202	-0.3358	-0.6646	0.5876	5.7530
	t/F	-1.1507	-1.6127	0.0205	0.1324	1.4187	1.4558	-0.4567	-1.2832	1.1938	4.2648
	pval	0.2523	0.1098	0.9843	0.7167	0.2387	0.1661	0.6549	0.2218	0.2499	0.0508
	Rsqu	0.0117	0.0244	0.0001	0.0622	0.1680	0.1238	0.0147	0.1124	0.0818	0.9009
log10 AMaAV	Int/num.df	-0.9782	-0.9585	-1.3576	1	4	-1.1057	-0.9034	-0.8022	-1.1810	-0.3327
	Slope/den.df	-0.5499	-0.6098	0.4561	110	60	-0.1890	-0.7888	-0.9929	0.0015	-2.3639
	t/F	-3.1785	-3.3489	0.6516	1.6077	0.7514	-0.2237	-2.0069	-2.7727	0.0031	-0.6678
	pval	0.0019	0.0011	0.5388	0.2075	0.5610	0.8260	0.0645	0.0158	0.9975	0.5730
	Rsqu	0.0827	0.0973	0.0661	0.0968	0.1637	0.0033	0.2234	0.3716	0	0.1823
log10 ASepSV	Int/num.df	-1.1069	-1.0804	-0.9794	1	4	-1.5250	-1.2832	-0.7430	-1.3153	-0.6827
	Slope/den.df	-0.2766	-0.3697	-0.4105	121	66	0.7773	0.1928	-1.2559	0.5940	-1.4526
	t/F	-1.4132	-1.6340	-1.4431	0.0046	1.8234	1.1012	0.3604	-3.6747	1.0594	-0.9463
	pval	0.1601	0.1050	0.1991	0.9461	0.1348	0.2861	0.7236	0.0025	0.3042	0.4138
	Rsqu	0.0160	0.0227	0.2576	0.0338	0.2078	0.0666	0.0086	0.4910	0.0619	0.2299
log10 ASepEV	Int/num.df	-1.2666	-1.1881	-1.1320	1	4	-1.3012	-1.2787	-1.2686	-1.3328	-0.6236
	Slope/den.df	-0.0713	-0.3334	-0.0381	111	59	0.1089	-0.1365	-0.3114	0.2595	-1.9262
	t/F	-0.3885	-1.6562	-0.0989	0.3330	0.3325	0.1632	-0.3071	-0.4789	0.4572	-0.8450
	pval	0.6984	0.1007	0.9244	0.5651	0.8550	0.8723	0.7641	0.6406	0.6537	0.4871
	Rsqu	0.0013	0.0255	0.0016	0.1155	0.1733	0.0016	0.0078	0.0188	0.0129	0.2631
log10 ASepAV	Int/num.df	-0.9370	-0.9058	-1.0678	1	4	-0.6966	-0.9450	-0.7341	-1.1864	0.0474
	Slope/den.df	-0.5606	-0.6556	-0.2081	111	59	-1.2733	-0.5484	-1.0253	0.1679	-3.2719
	t/F	-3.8493	-3.8235	-1.9005	1.0886	2.3119	-2.4457	-1.5380	-1.9132	0.4581	-2.8916
	pval	0.0002	0.0002	0.1061	0.2991	0.0681	0.0256	0.1500	0.0799	0.6530	0.1017
	Rsqu	0.1159	0.1222	0.3758	0.1269	0.2863	0.2603	0.1647	0.2337	0.0129	0.8070
log10 ASepAS	Int/num.df	-1.0783	-1.0439	-1.2147	1	4	-1.2259	-1.1189	-0.8444	-1.2510	-0.5966
	Slope/den.df	-0.3067	-0.4158	0.1188	124	67	0.1070	-0.2444	-1.0443	0.4787	-1.7876
	t/F	-1.6446	-1.9655	0.5292	0.8760	1.4726	0.1784	-0.4141	-2.1081	1.2152	-2.5818
	pval	0.1025	0.0517	0.6157	0.3511	0.2203	0.8605	0.6847	0.0535	0.2409	0.0612
	Rsqu	0.0210	0.0317	0.0446	0.0327	0.1887	0.0019	0.0113	0.2409	0.0799	0.6250
log10 ASepAE	Int/num.df	-1.2187	-1.1687	-1.1412	1	4	-1.1743	-1.2101	-1.0122	-1.5663	0.2205
	Slope/den.df	-0.2441	-0.4171	-0.1214	116	62	-0.3531	-0.3342	-0.9720	0.8567	-4.6717
	t/F	-1.3866	-2.1506	-0.4991	0.3413	3.1943	-0.4688	-0.6384	-1.4005	1.8847	-3.7526
	pval	0.1682	0.0337	0.6355	0.5602	0.0189	0.6452	0.5335	0.1889	0.0767	0.0331
	Rsqu	0.0160	0.0403	0.0399	0.0897	0.2016	0.0128	0.0283	0.1513	0.1728	0.8244
log10 ASepAA	Int/num.df	-0.9761	-0.9504	-1.3269	1	4	-1.0493	-0.9577	-0.5970	-1.2294	-0.5106
	Slope/den.df	-0.4537	-0.5191	0.2866	116	62	-0.3404	-0.5534	-1.4655	0.3903	-1.6605
	t/F	-2.9770	-3.0447	1.1160	3.2580	2.4853	-0.9931	-1.1907	-3.2102	0.9671	-1.7209
	pval	0.0035	0.0029	0.3071	0.0737	0.0526	0.3346	0.2536	0.0083	0.3470	0.1837
	Rsqu	0.0699	0.0777	0.1719	0.1070	0.2655	0.0548	0.0920	0.4837	0.0522	0.4968

Where AMa, Posterior wall at the level of the mitral annulus (imaged from the left apical four-chamber view); SV, systolic velocity; EV, early diastolic velocity; AV, atrial systolic velocity; ASep, mid-interventricular septum (imaged from the left apical four chamber view); ASepA, interventricular septum at the level of the mitral annulus (imaged from the left apical four chamber view); Dis, diseased; Unaff, unaffected; Diff, different; CRF, chronic renal failure; HCM, hypertrophic cardiomyopathy; BSB, basilar septal bulge; HiT4, hyperthyroid; HiBP, hypertensive; Int, intercept; num df, numerator degrees of freedom; den df, denominator degrees of freedom; t, t-statistic; F, F-statistic; pval, p-value; Rsqu, R; squared value; red-type face, significant data points ($p < 0.05$).

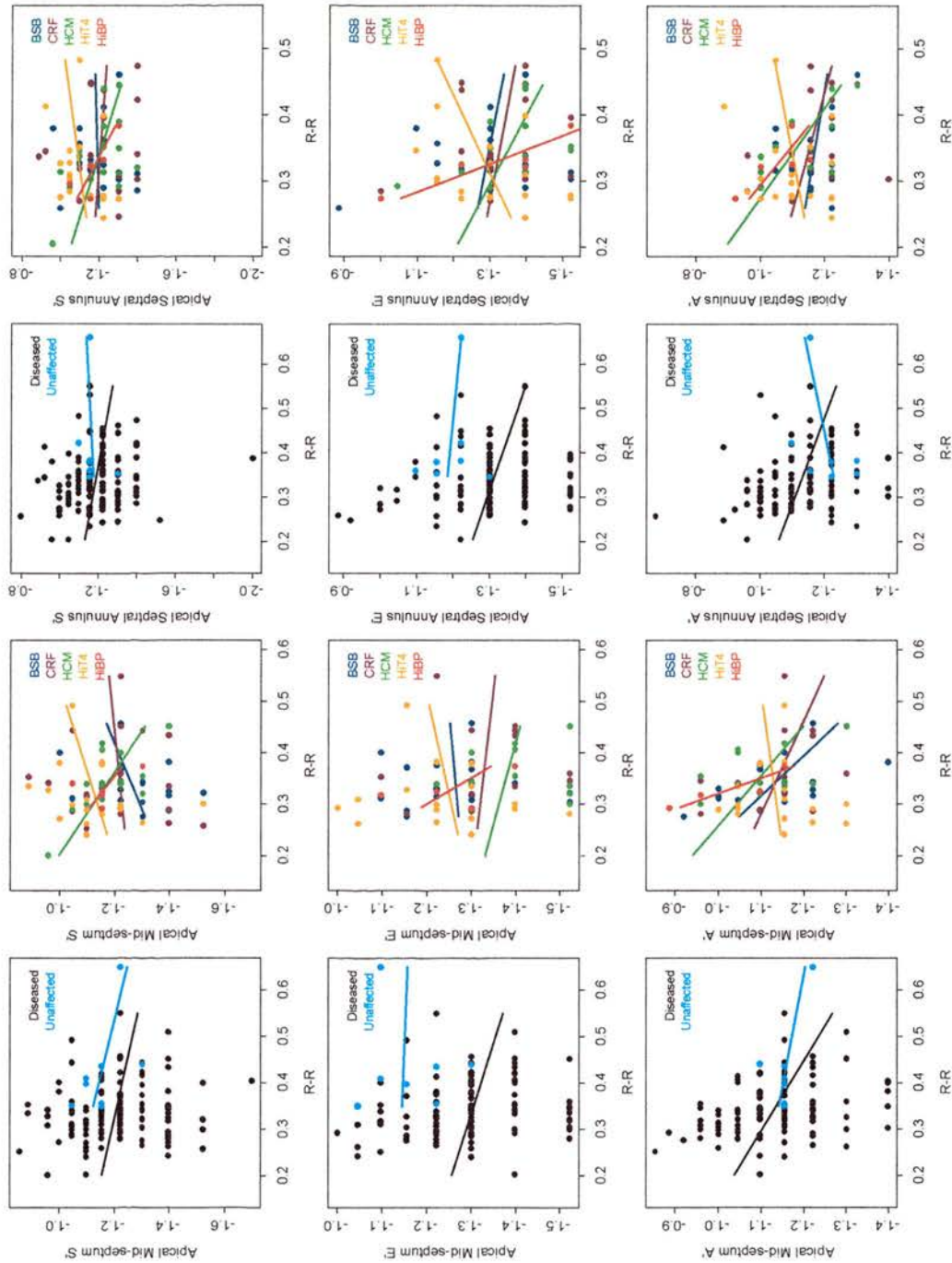
Figure 10: Linear regression analysis of different diseased groups



(Continued Overlay)

Diseased, Cats which are not unaffected; BSB, Basilar spetal bulge; CRF, Chronic renal failure; HCM, Hypertrophic cardiomyopathy; HIT4, Hypertension; HiBP, Hypertension; R-R; R-R interval of the corresponding variable; Apical, imaged from the left apical four-chamber view; S', \log_{10} systolic velocity (m/sec); E', \log_{10} early diastolic velocity (m/sec); A', \log_{10} late diastolic velocity (m/sec); R-R, R-R interval in seconds.

Figure 11: Linear regression analysis of different diseased groups (continued)



Diseased, Cats which are not unaffected; BSB, Basilar septal bulge; CRF, Chronic renal failure; HCM, Hypertrophic cardiomyopathy; HT4, Hyperthyroidism; HBP, Hypertension; R-R, R-R interval of the corresponding variable; SV, \log^{10} systolic velocity (m/sec); EV, \log^{10} early diastolic velocity (m/sec); AV, \log^{10} late diastolic velocity (m/sec); Apical, imaged from the left apical four-chamber view; S, systolic velocity; E, early diastolic velocity; A, late diastolic velocity; R-R, R-R interval in seconds.

Chapter 5

The application of pulsed wave Doppler tissue imaging and conventional echocardiographic techniques, in the evaluation of cardiac function in normal geriatric cats and aged cats with primary cardiomyopathies or disease states linked to specific cardiomyopathies in human beings.

In human beings with myocardial disease, pw-DTI techniques can be applied to determine a non-invasive estimation of diastolic function. For example, the early diastolic velocity is decreased in people with HCM. These techniques can also be used to assess the velocity of myocardial motion in the cat. It has previously been demonstrated that the peak systolic and peak diastolic velocities recorded from the mitral annulus are decreased in cats with HCM, when compared to normal cats. However, to date, the velocity of myocardial motion has not been reported in any of the specific cardiomyopathies in cats, nor have there been any comparisons between the echocardiographic features demonstrated in the disease states linked to specific cardiomyopathies in human beings.

The aim of this study was to compare the echocardiographic measurements from normal geriatric cats, aged cats with BSB or with HCM, to one another and to

measurements from geriatric cats with various forms of specific cardiomyopathy (hyperthyroidism and CRF) in order to determine whether or not there are group-specific abnormalities in the velocity of myocardial motion.

Abstract

Cardiac dysfunction is commonly identified in geriatric cats. Disease may be primary, typically hypertrophic cardiomyopathy (HCM), or may occur in association with a specific disease.

Doppler tissue imaging (DTI) techniques allow for the non-invasive assessment of myocardial dynamics. These techniques have demonstrated regional and global diastolic impairment in various forms of human cardiomyopathy and in cats with HCM.

The aim of this study was to compare the echocardiographic measurements recorded from normal cats, cats with basilar septal bulge (BSB) and cats with HCM to one another and to cats with various forms of specific cardiomyopathy, in order to determine whether or not any of these groups demonstrate abnormalities in the velocity of myocardial motion.

According to the inclusion criteria, a total of 66 cats were compared using conventional echocardiographic (2-dimensional, M-mode and Spectral Doppler measurements) and pw-DTI techniques. The cats were divided into the following groups: Unaffected (n=8), BSB (n=17), HCM (n=14), hyperthyroid (HiT4)(n=12) and chronic renal failure (CRF)(n=15).

In this group of geriatric cats, hypertrophy of the basilar septum was frequently identified as the sole abnormality. The lack of dynamic impairment in these cats

might suggest that this is in fact a form of normal senile remodelling rather than a localised form of HCM.

In the cats with HCM, I demonstrated a decrease in the E' velocity recorded by pw-DTI at the interventricular septum, and a tendency towards a decrease at the lateral aspect of the mitral annulus, recorded from the left apical four-chamber view.

The hyperthyroid cats demonstrated increased S' velocities, suggesting an increased inotropic state. In addition, the hyperthyroid cats demonstrated increased A' velocities, the cause of which is undetermined, but which may suggest mild diastolic dysfunction or increased atrial systolic function.

The cats with CRF demonstrated an increased thickness of the basilar interventricular septum (as was found in the majority of cats studied) and some mild spectral Doppler abnormalities. The pw-DTI analysis did not reveal any abnormalities in this group. Since pw-DTI is relatively load independent whilst loading conditions are known to influence spectral Doppler measurements, these findings may suggest that the abnormalities witnessed in the cats with CRF were due to an alteration in the loading conditions rather than as a result of myocardial dysfunction. In such cases pw-DTI may be useful in differentiating between loading alterations and diastolic dysfunction.

This study demonstrates that pw-DTI techniques can be used to assess wall motion abnormalities in a variety of diseases and that whilst in HCM these techniques can detect a decrease in the velocity of the early diastolic wall motion, there is no such decrease detectable in cats with BSB, CRF or hyperthyroidism.

Introduction

The World Health Organisation defines cardiomyopathies as diseases of the myocardium associated with cardiac dysfunction (Richardson, et al 1996). In addition, it states that hypertrophic cardiomyopathy (HCM) is characterized by left and/or right ventricular hypertrophy, which is usually asymmetric and involves the interventricular septum and that the left ventricular volume is typically normal or reduced (Richardson, et al 1996). In human beings, HCM is predominantly a familial disease, transmitted as an autosomal dominant trait, typically caused by mutations within the genes encoding for the sarcomeric proteins (Richardson, et al 1996). Pathological changes include myocyte hypertrophy and disarray, with areas of increased loose connective tissue (Richardson, et al 1996). However, this classification system also distinguishes between ‘primary’ cardiac hypertrophy (HCM) and cardiac dysfunction occurring secondary to systemic disease, for which the term ‘specific cardiomyopathy’ is ascribed. The specific cardiomyopathies are further divided according to the underlying aetiology, giving rise to terms such as hypertensive cardiomyopathy, thyrotoxic cardiomyopathy and ureamic cardiomyopathy (Richardson, et al 1996).

Whilst the exact mechanisms by which the various specific cardiomyopathies result in myocardial dysfunction is still subject to debate, it appears that the signalling pathways (Bahouth 1991, Kent, et al 1991), neurohumoral activity (Slatopolsky, et al 1980, Dillmann 1983, Yamazaki, et al 1999b) and therefore, myocardial alterations are, to some extent disease specific.

This human classification system has been broadly applied to the feline cardiomyopathies, with all of the principle 'primary' cardiomyopathies that have been seen in humans having been demonstrated in cats (Fox 1999). Furthermore, some of the specific cardiomyopathies that have been reported in human beings, are also documented in cats, namely thyrotoxic cardiomyopathy and hypertensive cardiomyopathy (Moise and Dietze 1986, Bond, et al 1988, Nelson, et al 2002, Chetboul, et al 2003b). To date, in the cat, the existence of a specific uraemic cardiomyopathy has not been reported. However, there have been a number of reports of specific cardiac abnormalities occurring in cats with chronic renal failure (CRF) (Rush, et al 1990, Taugner, et al 1996, Adin, et al 2000, Rishniw and Thomas 2002, Rishniw, et al 2004).

In addition to the classical hypertrophy seen in primary myocardial disease, there exists a group of aged cats with neither generalised hypertrophy, nor identifiable causes of secondary hypertrophy; in these cats, a thickening is identified at the base of the septum, with the end diastolic thickness being greater than 0.6cm, when viewed from the right parasternal long axis view (Figure 12). It is recognised that as cats age the position of the heart may alter (as is typically identified as increasing sternal contact identified on lateral thoracic radiography (Burk and Ackerman 1996). It could therefore be hypothesised that this alteration in the cardiac axis may lead to a deviation in the aortic angulation, consequent alteration in the geometry of the aortic root, and with this the interventricular septum. However, the significance of this localised pattern of hypertrophy has not yet been determined. Notably, in human beings, a localised form of cardiac hypertrophy, affecting only the basilar septum has also been identified (Lewis and Maron 1994). This occurs in an aged population,

and can be seen as the sole abnormality. This pattern of hypertrophy was initially thought to be a normal aging change (Lewis and Maron 1994). However, diastolic dysfunction has now been identified in some affected individuals either at rest or when stress echocardiography was performed (Henein, et al 1997). In addition, in some people mutations of the cardiac sarcomeric proteins (beta-myosin heavy chain) have been identified, with other family members often being affected by HCM (Solomon, et al 1993). Therefore, at present, it is unclear whether or not basilar septal bulge (BSB) is a form of senile remodelling or a localised form of HCM.

Doppler tissue imaging

The use of pulsed-wave Doppler to assess myocardial motion was first suggested in 1961 (Yoshida, et al 1961). However, it was not until 1989 that Issaz and colleagues published the first paper describing the pattern of left ventricular myocardial excursion (Isaaz, et al 1989). The principle behind this technique is the Doppler shift phenomenon.

Whilst conventional ultrasound uses this principle to assess the velocity of blood as it travels through the heart and vessels, the same concept can also be used to assess the velocity of myocardial excursion. The movement of the ventricular walls generate Doppler shift frequencies of low velocity and high amplitude, whereas the blood-pool generates signals of high velocity and low amplitude (approximately 40dB lower) (Sutherland, et al 1999). Therefore, reflected ultrasound signals can be divided into these two components, which have minimal overlap.

Traditionally, ultrasound machines have filtered out the low velocity signals in order to decrease 'noise'. There are now machines available, which are able to alter the threshold and filtering algorithms, and therefore filter out the signals originating from the blood-pool, allowing the velocities generated by myocardial motion to be depicted (Sutherland, et al 1999). With such refinements, more and more detailed patterns of left ventricular wall motion have become apparent.

There are many ways in which DTI can be used to assess myocardial motion. Some of these, such as pulsed-wave DTI (pw-DTI), provide a regional analysis and, as such, are useful at investigating localised myocardial abnormalities, whereas others, such as colour DTI (c-DTI), are able to provide an assessment of global function.

Pulsed-wave DTI is a technique that measures the instantaneous peak myocardial velocity as it moves through a pre-selected sampling gate. In people with myocardial disease, it has been shown to be a relatively load insensitive technique (Nagueh, et al 1997, Sohn, et al 1997, Agmon, et al 1999, Farias, et al 1999). Previously, it has been demonstrated that the early diastolic velocity is decreased in people with HCM (Matsumura, et al 2002). In addition, it has been shown in human beings and in genetically altered rabbits (with a genotype discriminating for HCM) that pw-DTI can detect diastolic dysfunction prior to the onset of hypertrophy (Nagueh, et al 2000, Nagueh, et al 2001a). Furthermore, it has been found that, as in humans, pw-DTI indices can be used to assess the velocity of myocardial motion in the cat (Gavaghan, et al 1999, Schober, et al 2003). This technique has already been used to show that the peak systolic and peak diastolic velocities recorded from the mitral annulus are decreased in cats with HCM, when compared to normal cats (Gavaghan,

et al 1999). However, to date, the velocity of myocardial motion has not been reported in any of the feline specific cardiomyopathies, nor have there been any comparisons between the echocardiographic features demonstrated in the disease states linked to specific cardiomyopathies in human beings.

I hypothesised that if BSB is a form of localised HCM, then the segmental hypertrophy should be accompanied by diastolic dysfunction. Based on the evidence that pw-DTI can detect myocardial dysfunction prior to the onset of hypertrophy, one would expect that if BSB truly represents a form of cardiomyopathy, pw-DTI should detect myocardial dysfunction, even in non-hypertrophied segments.

The aim of this study was to compare normal geriatric cats, aged cats with BSB, and cats with HCM, to one another and to geriatric cats with various forms of specific cardiomyopathy (hyperthyroidism and CRF) in order to determine whether or not there were any group specific abnormalities in the velocity of myocardial motion.

Materials and Methods

The selection of cases, identification of systemic disease and echocardiographic examination protocol used in this study were identical to the procedures outlined in Chapter 3.

Grouping of the Cats

Cats were classified as unaffected cats if they were clinically healthy and were normal on physical examination, including auscultation. In addition, routine blood sampling revealed no significant abnormalities and the systolic blood pressure was between 120 and 160 mmHg. Auscultation, a six-lead ECG and standard two-dimensional and M-mode echocardiographic examinations revealed no abnormalities.

Cats were grouped according to their systolic blood pressure, haematology and serum biochemistry results, and echocardiography findings. Cats were classified as hyperthyroid if their serum tT4 was equal to or exceeded 48 nmol/l (reference range 13-48nmol/l). A diagnosis of CRF was made if the serum creatinine exceeded 177 μ mol/l (reference range 30-177 μ mol/l) on two separate occasions approximately 14 days apart. Diabetes mellitus was diagnosed in cats with a blood glucose exceeding 8mmol/l (reference range 3.3-5.0mmol/l) and a serum fructosamine above 3.5 mmol/l (reference range 1.0-3.5mmol/l). Systemic hypertension was diagnosed if the systolic blood pressure exceeded 200 mmHg, was between 170 mmHg and 200 mmHg with concomitant ocular lesions, or was over 170 mmHg on two or more

subsequent visits. Cats were diagnosed with HCM if they did not fall into any of the above groups, the packed cell volume was within normal limits (PCV 0.24-0.45 l/l), and they had M-mode evidence of concentric hypertrophy (either the left ventricular free wall or interventricular septum measuring six millimetres or greater at end-diastole, on standard M-mode (Sisson, et al 1991)). Cats were excluded if they demonstrated chamber dilation or evidence of other forms of acquired or congenital cardiac disease. A separate group of cats demonstrating a localised area of hypertrophy affecting only the basilar septum, with no other cardiac signs, was also identified: These cats were classified as having a lone basilar septal bulge (BSB). For a cat to be classified as having a BSB, the serum biochemistry results could not demonstrate any of the above changes, the PCV had to be within the normal range, the systolic blood pressure had to be below 170 mmHg, and the M-mode measurements had to be within normal limits (Sisson, et al 1991). However, the two-dimensional measurement of the basilar interventricular septal thickness, from the right parasternal long axis view, was six millimetres or greater. Cats with more than one of the diseases outlined above (ie: hypertension and CRF), cats receiving any medication or cats with any severe systemic disease were excluded from the analysis.

Statistical Analysis

The statistical analysis was carried out using S-Plus (version 6.2.1, 1988, 2003 Insightful Corp. S: Copyright Lucent Technologies Inc.). The population characteristics were analysed using a one-way analysis of variance (ANOVA), or for the binomial data, a Fishers exact test. The results of the echocardiographic analysis

were adjusted to account for heart rate, using the square root R-R method, then the measurements were compared using a one-way analysis of variance with multiple comparisons being performed using a Tukey analysis. The distribution of the means and the homoscedasticity of the residuals were tested. When either the distribution of the residuals or the variance was unsatisfactory, standard transformation techniques (\log_{10}) were applied to normalise the distributions. A p value of ≤ 0.05 was taken as demonstrating statistical significance.

Results

A total of sixty-six cats were included in the study. Cats were excluded for a multitude of reasons, including the presence of atrial fibrillation, multiple diseases, anaemia, myocardial masses, poor data acquisition, poor compliance, or severe arrhythmias.

Of the 66 cats included, there were eight 'unaffected', seventeen with BSB, fourteen with HCM, twelve with hyperthyroidism (HiT4) and fifteen with CRF. Whilst there were six cats with 'essential' hypertension, and a further four cats with diabetes mellitus identified, all but one of these cats were receiving medication and therefore these groups were excluded from the current study. All of the cats were neutered. There were 30 female cats and 36 male cats. The age, gender, systolic blood pressure (BP), heart rate at initial examination, serum tT4 and creatinine concentration were recorded in all of the cats. In addition, the weight was recorded in all but two of the cats, and the respiratory rate at initial examination was recorded in 49 of the cats. The median age of the cats was 11.7 years (range 8-18 years). The mean systolic blood pressure of the cats was 145mmHg (range 101-160mmHg). The heart rate at initial examination was recorded; this ranged from 140 bpm to 220 bpm (mean 177bpm). The respiratory rate at initial examination was recorded in 49 of the cats; this ranged from 20-80 bpm, mean 36bpm. The mean weight of 64 of the cats was 4.75kg (range 2.15-6.60 kg).

Analysis of the population characteristics demonstrated that there was no significant difference between the groups with regard to the gender, BP, heart rate at initial examination, or respiratory rate at initial examination. The tT4 concentration

demonstrated a significant difference between the groups of cats ($F=41.379$, $P<0.001$). However, multiple comparisons established that it was only in the cats with hyperthyroidism that the tT4 was significantly higher than in any of the other groups of cats (as had been dictated by the inclusion criteria). A similar finding was demonstrated in the analysis of serum creatinine concentration ($F=14.350$, $P<0.001$) with only the cats diagnosed as having CRF demonstrating a significantly higher creatinine concentration than all the other groups of cats (as had also been dictated by the inclusion criteria). The age of the cats varied significantly between groups ($F=4.279$, $P=0.004$); multiple comparison techniques (Tukey) demonstrated that the cats with hyperthyroidism were older than the unaffected cats, the cats with BSB, or the cats with HCM.

Similarly, the weight of the cats demonstrated a significant difference between groups ($F=3.079$, $P=0.023$), with the hyperthyroid cats being significantly lighter than the cats with HCM.

The results of the analysis of variance in the echocardiographic measurements are presented in Table 8. Multiple comparisons were performed on any variable that demonstrated a significant difference between groups (Figure 13).

2-Dimensional Analysis

The aortic and left atrial diameter demonstrated no significant difference between the groups. However, the thickness of the interventricular septum, assessed from the two-dimensional image, demonstrated a significant variation ($F=12.92$, $P<0.001$).

Multiple comparisons demonstrated that the cats with HCM had a thicker interventricular septum than those with BSB, CRF or the unaffected cats, whereas the unaffected cats demonstrated a decreased interventricular septal thickness compared to the cats with BSB (as dictated by the inclusion criteria), the cats with CRF and the cats with hyperthyroidism.

M-mode measurements

The M-mode measurements demonstrated significant variation between groups, in the measurement of left ventricular free wall thickness, in both systole ($F=5.324$, $P<0.001$) and diastole ($F=7.809$, $P<0.001$), and in the thickness of the interventricular septum, in both systole ($F=3.740$, $P=0.009$) and diastole ($F=5.219$, $P=0.001$). Multiple comparisons demonstrated that, in all cases, the cats with HCM had higher values than the groups of cats with either BSB or the unaffected cats. The HCM cats also demonstrated an increased thickness in the free wall (both during systole and diastole), than the cats with CRF.

Spectral Doppler Analysis

The velocities of aortic and pulmonic flow demonstrated significant differences between the groups ($F=13.728$, $P<0.001$ and $F=7.077$, $P<0.001$, respectively). Inter-group analysis demonstrated that these variations were produced by increased

velocities in the cats with HCM or hyperthyroidism, when compared to either the unaffected or BSB groups, and in the case of the aortic velocity, the CRF group.

The transmitral velocity demonstrated significant variations in the E velocity ($F=2.699$, $P=0.042$), the A velocity ($F=4.616$, $P=0.003$) and the ratio of E:A ($F=3.108$, $P=0.011$). However, multiple comparisons failed to demonstrate any significant variation in the E velocity between any two groups, whilst the A velocity was increased in cats with HCM and hyperthyroidism, when compared to unaffected cats, and the E:A ratio was decreased in the cats with HCM compared to the unaffected cats.

The trans-tricuspid flow demonstrated a significant variation in only the E velocity ($F=2.777$, $P=0.038$); this arose from a lower E velocity in the cats with CRF compared to those with hyperthyroidism.

When the pulmonary venous flow patterns were compared, it was demonstrated that there were significant variations in both the duration of the atrial reversal wave ($F=2.881$, $P=0.030$) and the ratio of transmitral A wave duration to atrial reversal duration ($F=3.468$, $P=0.013$). However, inter-group analysis demonstrated no significant variations between groups.

Pulsed-wave Doppler tissue imaging (pw-DTI) measurements

The pw-DTI analysis demonstrated significant variations in the S' velocities measured from the right parasternal long and short axis views ($F=2.560$, $P=0.048$ and

$F=3.499$, $P=0.012$, respectively). Multiple comparisons demonstrated, in both cases, that this effect was caused by a higher S' velocity in the hyperthyroid cats compared to the unaffected cats. In addition, the S' measured from the short axis view was higher in the hyperthyroid cats than in the cats with BSB. The A' velocity measured from the right parasternal long axis view also demonstrated significant variations ($F=4.662$, $P=0.002$). Multiple comparisons demonstrated that the velocity was increased in hyperthyroid cats when compared to unaffected cats, cats with BSB or cats with HCM.

The velocities measured from the left apical view at the level of the mid-lateral wall demonstrated no significant variation between groups. Whereas those measured at the level of the mitral annulus demonstrated a significant variation in the E' velocity ($F=2.658$, $P=0.042$): Although there was a trend toward a decreased E' velocity in cats with HCM when compared to either unaffected cats, or cats with hyperthyroidism, this failed to reach significance. The E' velocity also demonstrated significant variation between groups when it was assessed from the left apical view at the mid-interventricular septal sight. Tukey analysis demonstrated that there was a significant decrease in the cats with HCM compared to those with either BSB or the unaffected cats. In addition, at this sight, comparisons of the summated E'+A' velocity (when present) demonstrated a significant variation between groups, which was brought about by an increased velocity in the cats with HCM compared to cats with either CRF or hyperthyroidism. The velocities recorded from the interventricular septum at the level of the mitral annulus demonstrated significant differences in the S' ($F=3.348$, $P=0.015$) and A' ($F=3.289$, $P=0.017$) velocities. Multiple comparison analysis demonstrated that the S' velocity was increased in

hyperthyroid cats when compared to cats with CRF or HCM and tended to be higher in unaffected cats and cats with BSB, although this was not significant. Furthermore, at this site, the A' velocity was increased in cats with hyperthyroidism when compared to the unaffected cats.

Discussion

This is the first study to assess the myocardial dynamics in a range of feline disease states linked to specific cardiomyopathies in human beings, and compared these findings to normal cats and cats with HCM.

This study demonstrates no significant variation between cats with BSB and cats that were classed as unaffected; other than the thickness of the interventricular septum at its basilar aspect (as dictated by the classification criteria). Furthermore, significant variations between these groups of cats and the cats with HCM were demonstrated. These observations lend credence to the hypothesis that, in the cat BSB may be a form of senile remodelling, rather than a form of localised HCM.

An increase in the systolic and late diastolic velocities in cats with hyperthyroidism was demonstrated. The increase in S' wave velocity is suggestive of an increase in systolic function in this disease, whereas the increase in A' wave velocity may be associated with either loading alterations or impairment of relaxation during diastole.

In addition, in cats with HCM I demonstrated a decrease in the E' velocity recorded by pw-DTI at the interventricular septum, and tendency towards a decrease at the lateral aspect of the mitral annulus, recorded from the left apical four-chamber view.

Population Characteristics

In this study there were significant differences in the age and weight distribution of the cats; with the hyperthyroid cats being both older and weighing less than the other

groups of cats. Whilst these findings may be of some concern, I have demonstrated previously that within a population of cats over eight, age does not have a significant affect on any of the variables measured, with the exception of the left apical A' velocity recorded from the interventricular septum (at the level of the mitral annulus); where age was found to account for 3.5% of the variation in this variable (Chapter 3). However, in the current study, there was no significant difference in the A' velocity at this point. The weight of the hyperthyroid group of cats was lower than the weights of the other groups of cats. However, since one of the salient features of hyperthyroidism is weight loss, this is perhaps not surprising. Furthermore, the lower body weight in this group is not reflective of the size of these cats, since it is reasonable to presume that these cats had poor body condition scores. Had body condition scores been recorded, a comparison of body weight corrected for condition score would have been more appropriate.

Two-Dimensional Analysis

There were no significant differences in either the left atrial diameter, or the aortic diameter between any of the groups in this study. The inclusion criteria allowed recruitment of only those cats that were not receiving medication. Therefore, many cats in congestive heart failure were excluded, making, the HCM group in particular, a relatively mild disease group; with only one cat demonstrating a left atrial diameter greater than 1.5cm (reference range, 1.17 ± 0.17 cm (Sisson, et al 1991)).

The thickness of the basilar interventricular septum was increased in cats with HCM to a greater extent than it was increased in the BSB group. However, I demonstrated an increase in the thickness of this area of the interventricular septum in all the diseased groups, compared to the unaffected cats. Interestingly, of the 66 cats included in the study only 13 failed to demonstrate hypertrophy of the basilar septum (data not shown). This finding would suggest that BSB, with or without concurrent disease, is a common finding in aged cats.

M-mode Analysis

The comparison of M-mode variables demonstrated an increase in the thickness of the interventricular septum and free wall in cats with HCM compared to unaffected cats and to cats with BSB. The mean measurements obtained from the interventricular septum in both systole and diastole were outside of the published reference range, as were those obtained during diastole, from the free wall. This would suggest that the majority of cats in the HCM group demonstrated symmetric myocardial hypertrophy. The diastolic thicknesses recorded from the free wall were increased in the hyperthyroid cats compared to the unaffected cats. The M-mode variables measured from the interventricular septum, were not significantly different in the cats with CRF or hyperthyroidism compared to the cats with HCM, nor were they significantly different to the measurements obtained from the unaffected groups of cats. However, compared to the unaffected cats, they did tend to demonstrate mild increases in these M-mode variables; this was particularly true of the cats with hyperthyroidism. This would suggest that the cats with hyperthyroidism tend to

demonstrate predominantly asymmetric hypertrophy affecting mainly the free wall. This agrees other reports of M-mode changes in hyperthyroid cats, where it has previously been reported that free wall hypertrophy was identified in 30-71.9% of cases whereas hypertrophy of the interventricular septum was identified in only 10-39.8% of cases (Moise and Dietze 1986, Bond, et al 1988).

Spectral Doppler Analysis

The velocity of aortic and pulmonic outflow was increased in the cats with hyperthyroidism and HCM compared to either the unaffected or BSB groups of cats. Increased outflow velocities can be caused by either an increase in systolic function or outflow tract obstruction. Both the hyperthyroid group of cats and the cats with HCM demonstrated an increased thickness at the basilar interventricular septum, which could conceivably lead to outflow tract obstruction. However, it has been suggested that cats with hyperthyroidism may demonstrate an increased systolic function (Bond, et al 1988), which could in turn increase outflow velocities.

The transmitral early diastolic velocity tended to be higher in cats with hyperthyroidism compared to any of the other groups of cats. Whilst there was a significant difference between groups, the wide range of values measured meant that this finding was not significant when the Tukey analysis was performed. This non-significant increase in the E velocity within the hyperthyroid cats may occur due to an alteration in the diastolic function, alteration in loading conditions or a reduction in the duration of diastole in this group. Notably, the hyperthyroid cats demonstrated

a significantly higher transmitral A wave velocity, when compared to the unaffected cats. An increased A wave velocity is normally associated with a decrease in the E wave velocity, this change resulting from impaired relaxation (Appleton, et al 1988). However, in the hyperthyroid cats, there was no alteration in the E:A ratio, and a concomitant (non-significant) increase in the E velocity. This group of cats demonstrated a shorter R-R interval, whilst the transmitral flow was being assessed, than any of the other groups of cats (data not shown). Whilst the variables were corrected for heart rate using standard methods, it has previously been demonstrated that, at high heart rates, diastole is shortened to a greater extent than systole (Hamlin 1999). Shortening the duration of diastole, and therefore, the time for ventricular filling, in theory, could result in more rapid ventricular filling, as was demonstrated in the hyperthyroid cats. However, the equation applied does not differentiate systolic from diastolic events, and therefore this correction may not have been ideal. Similarly, in humans, a decrease in R-R interval has been shown to reduce the increase in the A wave amplitude, but not the E wave amplitude (Mori, et al 2000). It has also been reported previously that, in the cat, the R-R interval is negatively correlated with the peak A wave velocity (Santilli and Bussadori 1998). Therefore, the increase in the A wave velocity in the hyperthyroid cats, may have been caused by the increased heart rate within this group. Alternatively the increased A wave velocity might merely represent increased atrial systolic function (Appleton, et al 1988).

The transmitral atrial systolic velocity was also increased in cats with CRF or HCM compared to the unaffected cats; however, the R-R interval was not significantly different in these groups of cats. In addition, the ratio of early transmitral flow, to

atrial systolic flow, was decreased in all of the diseased groups compared to the unaffected cats, although, this only reached significance in the cats with HCM. The alteration in the transmitral E:A ratio suggests that as a group, these cats demonstrate impaired relaxation.

Whilst the pulmonary venous flow patterns demonstrated some variation in the duration of atrial reversal flow and the ratio of the duration of transmitral A to the duration of the atrial reversal flow (A:Ar), there was no significant inter-group variation. However, the duration of pulmonary venous atrial reversal flow tended to be increased in cats with CRF when they were compared to normal cats, and the ratio of A:Ar tended to be decreased in either cats with HCM or CRF when compared to the other groups of cats. A decreased A:Ar ratio is suggestive of an increase in left atrial pressure (Keren 1986, Rossvoll and Hatle 1993). Notably, the mean left atrial size was higher in these two groups compared with the other groups of cats, although this was not statistically significant. This may suggest that some of the cats with HCM or CRF displayed pseudonormal relaxation.

Doppler Tissue Imaging

The pulsed-wave DTI analysis demonstrated an increase in both the S' and A' velocities in the hyperthyroid cats. These velocities were significantly higher within this group (compared to unaffected cats) at multiple sites, including the free wall assessed from the right parasternal short and long axis views and the septal aspect of the mitral annulus, assessed from the left apical four-chamber view. Whilst the right

parasternal views assess radial fibre velocities, the apical views assess longitudinal fibre velocities (Sutherland, et al 1999). These findings would therefore suggest that in hyperthyroid cats there are localised areas demonstrating increased systolic function in both the radial and longitudinal fibres. Previously, it has been demonstrated that hyperthyroid cats have an increased fractional shortening and it has been suggested that this may be caused by an increased inotropic state (Bond, et al 1988). There was no increase in the fractional shortening of the hyperthyroid cats in the current study, although relatively few cats were included. However, the pw-DTI analysis provided evidence for a similar increase in systolic function. There are several reasons why hyperthyroid cats might demonstrate an increase in inotropic state, these include upregulation of the sympathetic nervous system, as has been demonstrated by increased numbers of beta-1 adrenoceptors in hyperthyroidism (Bahouth 1991), or an increased metabolic demand (Dillmann 1983). In human beings, it has previously been reported that pw-DTI S' and E' velocities are positively correlated with the beta-adrenoceptor density, and negatively correlated with the percentage of interstitial fibrosis (Shan, et al 2000). Therefore, one could hypothesise that the increased S' velocities in the hyperthyroid cats, may be related to the increased beta-receptor density in the hyperthyroid state. The increase in A' velocity at the same sites normally suggests diastolic dysfunction (Oki, et al 1997, Oki, et al 1998). However, in such an event one would normally expect the E' to be decreased, unless, as in human beings, this variable is also increased due to the increased number of beta-receptors (Shan, et al 2000), thereby negating the expected decrease in E' velocity.

The E' velocity was significantly lower in the HCM cats (compared to either the unaffected cats or the cats with BSB) when assessed from the left apical four-chamber view at the level of the mid-interventricular septal, and tended to be decreased in cats with HCM (when compared to either unaffected cats or cats with hyperthyroidism) at the lateral aspect of the mitral annulus. Previously, a decreased peak diastolic pw-DTI velocity has been demonstrated in cats with HCM compared to normal cats (Gavaghan, et al 1999). Whilst my findings are in agreement with this previous study, it was perhaps surprising that E' was not found to be decreased at more sites. The relationship between E' and tau has been assessed and been shown to be relatively poor in the normal cat (Schober, et al 2003). Coupled with the relatively mild disease (only one of the HCM group demonstrating left atrial enlargement), it is perhaps not surprising that the pw-DTI analysis did not clearly demonstrate diastolic dysfunction at more sites. Furthermore, previously I have demonstrated that the variability in measurement of pw-DTI velocities is approximately 20%, making interpretation of results problematic (Chapter 2).

Cats with CRF were assessed in the current study. There has previously been some suggestion that cats with CRF may demonstrate cardiac abnormalities (Rush, et al 1990, Taugner, et al 1996, Adin, et al 2000, Rishniw and Thomas 2002, Rishniw, et al 2004). I found that, compared to unaffected cats, cats with CRF demonstrate an increased thickness of the basilar interventricular septum, an increased transmitral A wave velocity, and a tendency toward increased duration of the pulmonary venous flow atrial duration. However, I identified no significant alterations in the pulsed-wave DTI velocities recorded within this group of cats. These variables are relatively load insensitive when compared to the spectral Doppler methods of

assessing diastolic function (Nagueh, et al 1997). Therefore, my findings might suggest that, other than the hypertrophy of the basilar interventricular septum, the changes identified in cats with CRF are the result of alterations in loading.

Study Limitations

This study was limited by the small sample size. This was particularly true of the unaffected cats, which comprise the minority of cats that were studied. Many of the cats with BSB were originally presented as apparently normal cats. Whilst, it is possible that BSB may be a normal aging change, at present, it was felt that as the aetiology remains unknown, cats with BSB should be designated as a separate group. I have previously demonstrated that in a group of cats over eight, age does not significantly affect pw-DTI velocities (Chapter 3). However, my inclusion criteria dictated that cats entering the study must be eight years of age or above. This stipulation was made in an attempt to age match the unaffected and diseased groups (since many of the diseases associated with linked to specific cardiomyopathies in human beings, occur in aged populations), and as good scientific practice dictates. Unfortunately, due to the clinical nature of this study, completely age matched groups were not achieved, with the hyperthyroid group of cats being older than unaffected cats, or the cats with BSB or HCM.

Initially, I had also intended to include groups of cats with hypertension and diabetes mellitus. However, I was unable to identify a sufficient number of cats with either of these conditions, and no significant concurrent diseases, that were not already

receiving medication. Therefore, these groups of cats were excluded from the analysis.

This study was performed on clinical cases, many of which were, at least from a cardiovascular standpoint, asymptomatic. Had these not been clinical cases, this study would have benefited from the histopathological assessment of myocardial tissue, which would be necessary to investigate correlations between beta-receptor density, the amount of interstitial fibrosis and the pw-DTI measurements.

Summary

In summary, I found no evidence that BSB is a form of disease. In the aged cat population studied, the basilar interventricular septum was frequently greater than six millimetres. The lack of dynamic impairment in these cats might suggest that this is in fact a form of normal senile remodelling.

Even in a group of cats without advanced HCM, I was able to demonstrate a decrease in the E' velocity recorded by pw-DTI at the interventricular septum, and a tendency towards a decrease at the lateral aspect of the mitral annulus, recorded from the left apical four-chamber view.

The hyperthyroid cats had a tendency towards decreased E' and demonstrated increased A' velocities; these changes providing some evidence that these cats demonstrate diastolic dysfunction. In addition, the increased S' velocity within this group suggests increased inotropy.

The cats with CRF demonstrated an increased basilar septal thickness, and some alteration in their spectral Doppler velocities. However, these cats lacked changes in their pw-DTI analysis; a finding that may suggest that, as in human beings (Ommen, et al 2000), pw-DTI can be used to differentiate between alterations in myocardial function and altered loading conditions.

Table 8: Investigation into echocardiographic differences between groups (quoting the associated test statistic (F), the probability that the difference in variation was due to chance (P) and the degrees of freedom(subscript)).

Tissue Doppler Variables	Disease	
	F	P
Long Axis Free Wall		
S'	60,4= 2.560	0.048
E'	59,4=0.763	0.554
A'	59,4= 4.662	0.002
E'+A'	-	-
Short Axis Free Wall		
S'	60,4= 3.499	0.012
E'	57,4=2.035	0.102
A'	57,4=2.214	0.079
E'+A'	-	-
Apical Free Wall		
S'	51,4=2.104	0.094
E'	49,4=1.241	0.306
A'	49,4=0.519	0.722
E'+A'	-	-
Apical View Mid-Septum		
S'	59,4=2.038	0.101
E'	57,4= 4.580	0.003
A'	57,4=1.066	0.382
E'+A'	2,1= 762.900	0.026
Apical Septal Mitral Annulus		
S'	60,4= 3.348	0.015
E'	57,4=1.226	0.310
A'	57,4= 3.289	0.017
E'+A'	-	-
Apical Lateral Mitral Annulus		
S'	59,4=0.485	0.747
E'	57,4= 2.658	0.042
A'	57,4=1.132	0.351
E'+A'	-	-

Spectral Doppler Variables	Disease	
	F	P
2D Heart Variables		
Ao Diameter*	60,4=0.927	0.454
Left Atrial Diameter*	60,4=1.620	0.182
Septal Thickness*	61,4= 12.192	<0.001
M-mode Variables		
LVDd	61,4=0.710	0.588
LVFWd	61,4= 7.809	<0.001
LVDs	61,4=1.171	0.333
LVFWs	61,4= 5.324	<0.001
IVSd	61,4= 5.219	0.001
IVSs	61,4= 3.740	0.009
FS	61,4=2.098	0.092
EF	61,4=2.195	0.080
Vp	60,4=1.012	0.408
Spectral Doppler Variables		
AV	61,4= 13.728	<0.001
PV	61,4= 7.077	<0.001
ME	47,4= 2.699	0.042
MA	47,4= 4.616	0.003
ME:MA	47,4= 2.745	0.039
ME+A	11,3=1.769	0.211
TE	45,4= 2.777	0.038
TA	45,4=2.302	0.073
TE:TA	45,4=1.507	0.217
TE+A	11,3=1.746	0.215
IVRT	58,3=0.161	0.957
PVD	57,4=0.468	0.759
PVS	57,4=0.614	0.654
PVS:D	57,4=0.840	0.506
PVAr	57,4=2.455	0.056
ArDur	57,4= 2.881	0.030
MADur	59,4=0.680	0.608
MA:Ar Dur	57,4= 3.468	0.013

Where: F, F-value, subscript is the degrees of freedom between the groups and the residuals; P, P-value; Ao, aorta; LVD, left ventricular diameter; IVS, interventricular septum; LVPw, left ventricular posterior wall; d, diastole; s, systole; Vp, propagation velocity; FS, percentage fractional shortening; EF, ejection fraction; AV, aortic velocity; PV, pulmonary velocity; ME and MA, transmitral early and late diastolic flow, respectively; ME+A, the velocity of the summated transmitral flow; TE and TA, trans-tricuspid early and late diastolic flow, respectively; TE+A, summated trans-tricuspid flow; IVRT, isovolumic relaxation time; PV, pertaining to pulmonary venous; S, systolic flow; D, diastolic flow; Ar, atrial reversal flow; V, velocity; Dur, duration; S', systolic velocity; E', early diastolic velocity; A', late diastolic velocity; E'+A', summated diastolic flow. Bold type-face represents a P <0.05.

Figure 12: Right parasternal long-axis view demonstrating a localised basilar septal bulge in a cat.

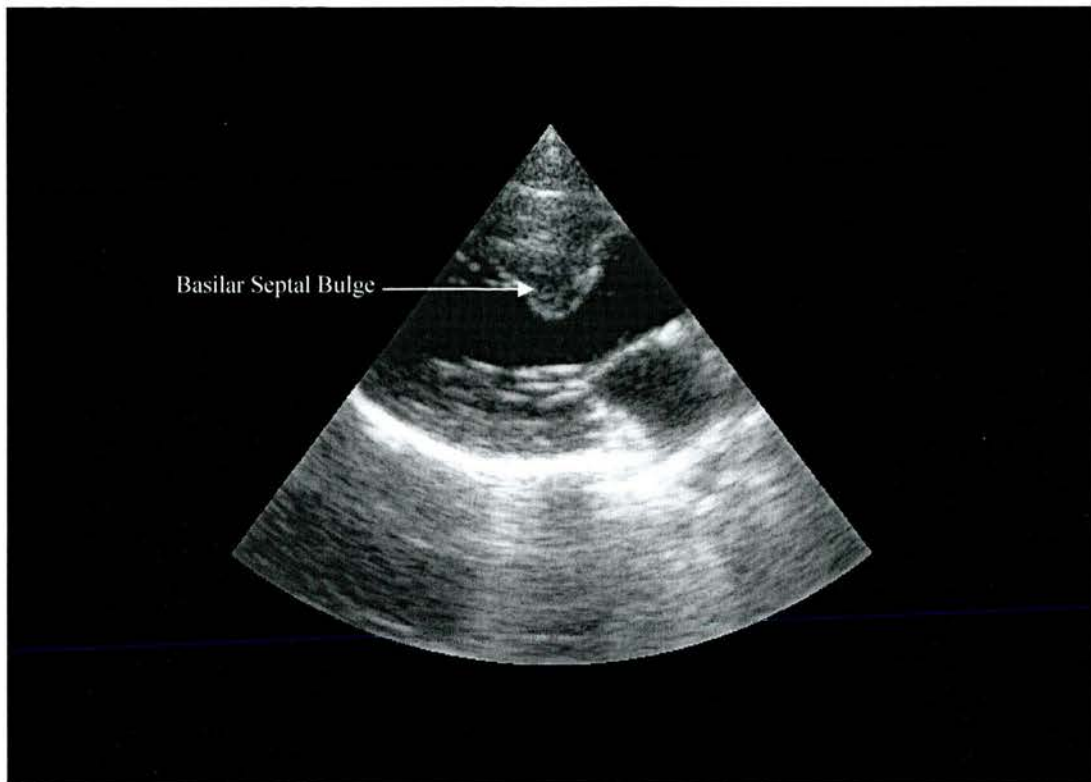
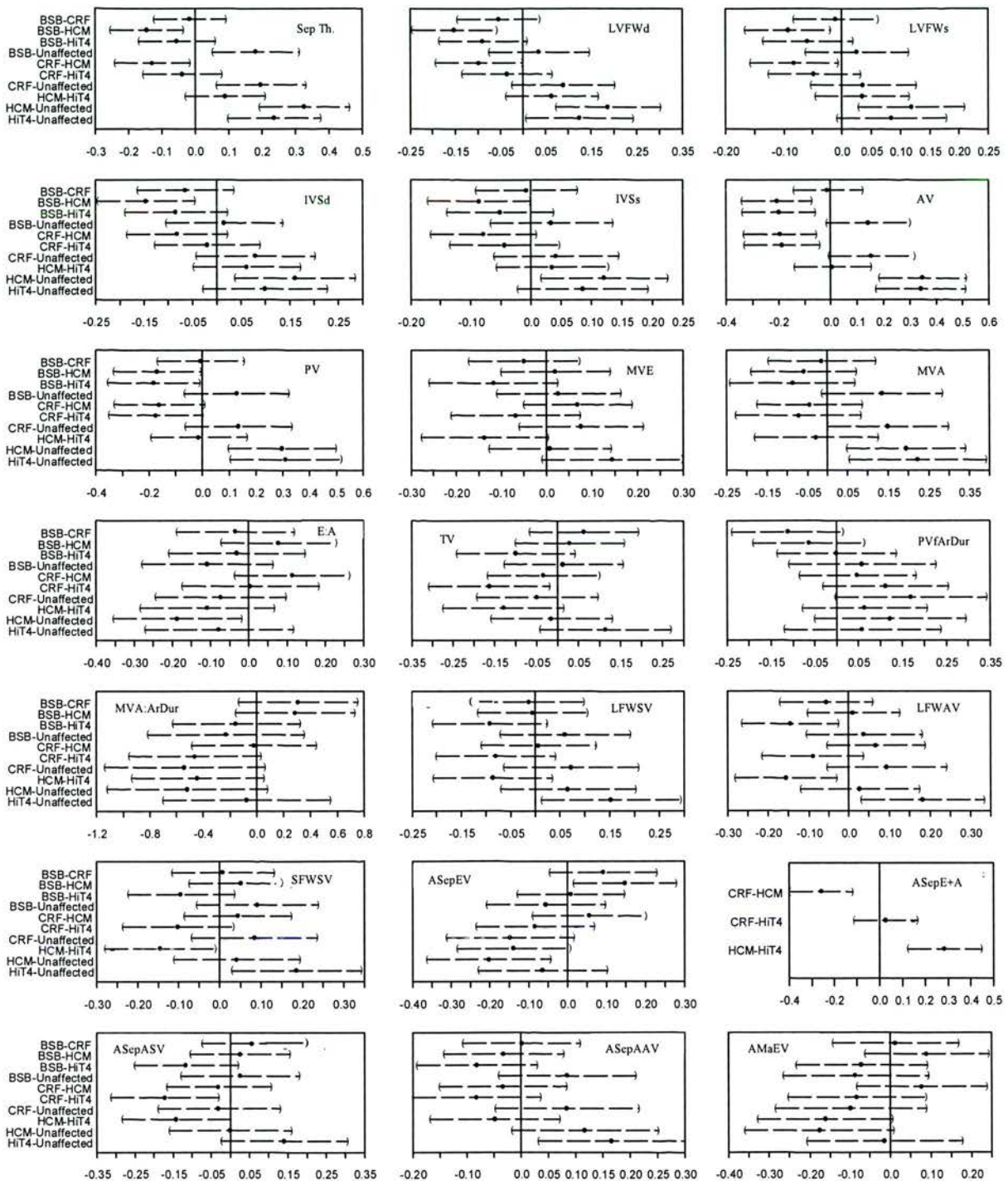


Figure 13: Multiple comparisons by the Tukey method

Plots represent the outcomes of the Tukey analysis. Bars represent 95% confidence intervals, significant differences do not cross 0. Where, BSB, basilar septal bulge; CRF, chronic renal failure; HCM, hypertrophic cardiomyopathy; HiT4, hyperthyroid cats; Sep Th., thickness of the interventricular septum (assessed from the right parasternal long-axis view); LVFW, left ventricular free wall; d, diastole; s, systole; IVS, interventricular septum; AV, aortic velocity; PV, pulmonic velocity; MVE, transmitral E wave velocity; MVA, transmitral A wave velocity; E:A, ratio of transmitral E to A; TE, trans-tricuspid E wave velocity; PVfArDur, pulmonary venous flow atrial reversal duration; MVA:ArDur, ratio of the duration of MVA to pulmonary venous flow Ar duration; LFW, the free wall (imaged from the right parasternal long-axis); SV, systolic velocity; AV, late diastolic velocity; EV, early diastolic velocity; E+A, summated E' and A' velocity, SPW, the posterior wall (imaged from the right parasternal short-axis); ASep, mid-interventricular septum (imaged from the left apical four chamber view); ASepA, septal aspect of the mitral annulus (imaged from the left apical four-chamber view), AMa, lateral aspect of the mitral annulus (imaged from the left apical four-chamber view).

Chapter 6

The application of pulsed wave Doppler tissue imaging, and conventional echocardiographic techniques, in the evaluation of cardiac function in treated and untreated hyperthyroid cats

Previously, I have reported an increase in both pw-DTI S' and A' velocities in untreated hyperthyroid cats (Chapter 5). Whilst echocardiographic abnormalities have been described in hyperthyroid cats before and after treatment, to date, there have been few studies, in either the human or veterinary literature, evaluating the affects of medical treatment on pw-DTI variables in thyrotoxic cardiomyopathy.

The aim of this study was to investigate the effect of carbimazole upon thyrotoxic feline myocardium by comparing conventional echocardiographic measurements (two-dimensional, spectral Doppler, and M-mode) and more advanced measurements of diastolic function (pw-DTI, colour M-mode propagation velocity and isovolumetric relaxation time) in normal cats, to those recorded from treated and untreated hyperthyroid cats.

Abstract

The aim of this study was to investigate the effect of carbimazole upon thyrotoxic feline myocardium by comparing the conventional echocardiographic measurements (two-dimensional, spectral Doppler, and M-mode) and more advanced measurements of diastolic function (pulsed-wave Doppler tissue imaging [pw-DTI], colour M-mode propagation velocity and isovolumetric relaxation time) in normal cats, to those recorded from treated and untreated hyperthyroid cats.

Twenty-eight cats underwent echocardiographic evaluation; of these, eight were classified as normal geriatric cats, twelve were untreated hyperthyroid cats, and eight were treated hyperthyroid cats. The results of these examinations were compared, to investigate any association.

Specific findings included a decrease in the colour M-mode propagation velocity in untreated hyperthyroid cats when compared to normal cats; which may suggest that ventricular asynchrony exists in untreated hyperthyroid cats.

Overall, the echocardiographic variables that demonstrated a difference between the normal cats and the treated hyperthyroid cats, also demonstrated a trend towards a similar relationship between the normal cats and the untreated hyperthyroid cats (with the exception of the A' velocity within the longitudinal fibres at the mid-interventricular septum), the velocity of which was increased in the treated hyperthyroid cats, but not in the untreated cats.

In eight of the hyperthyroid cats, I observed a pattern similar to post systolic thickening (PST), as has previously been documented in human beings. The velocity

of the PST was decreased at the mid-lateral wall within the longitudinal fibres of cats with treated hyperthyroidism compared to untreated cats. If PST represents changes in cats similar to those described in human beings, this would imply that with treatment the feline myocardium is less prone to hypoxic changes.

The treated hyperthyroid cats generally demonstrated less variation from the normal cats, compared to the untreated hyperthyroid cats, suggesting that the use of carbimazole improves the function of the feline myocardium in thyrotoxic cardiomyopathy.

Introduction

Hyperthyroidism is recognised as the most commonly occurring endocrine disorder in the domestic cat; the incidence of which is approximately 1-2% (Fox, et al 1999). It is a disorder of the thyroid gland leading to overproduction of thyroid hormones; thyroxine (T4) and tri-iodothyronine (T3). This is usually caused by a functional thyroid adenoma involving one (30%) or both (70%) thyroid lobes, with less than 2% of cases being caused by a follicular or papillary carcinoma (Feldman and Nelson 2004).

Clinical Features of Feline Hyperthyroidism

Hyperthyroidism is a disease that can affect cats between the ages of four and 23 years (mean age, 13 yrs) (Thoday and Mooney 1992, Gunn-Moore 2005). There are no breed or sex predilections reported, although the Siamese breed may be protected (Kass, et al 1999). Hyperthyroidism affects many body systems and for this reason clinical signs can be diverse. It has been reported that abnormalities of the cardiovascular system can be found on physical examination in 95% of hyperthyroid cats (Santilli, et al 2000), and that most cats show changes similar to those seen in hypertrophic cardiomyopathy (HCM), with only occasional cases demonstrating myocardial failure, or changes similar to those seen in dilated cardiomyopathy (DCM). The most common alterations within the cardiovascular system are; hyperkinetic femoral pulses (91%), systolic murmurs (45%), gallop sounds (32%) and sinus tachycardia (26%) (Santilli, et al 2000).

In an attempt to find an accurate non-invasive diagnostic method to evaluate the cardiovascular status of these patients many studies have been performed to look at the electrocardiographic, echocardiographic and radiographic changes of affected individuals.

Electrocardiographic studies have reported a sinus tachycardia in 20-34% of hyperthyroid cats (Moise and Dietze 1986, Fox, et al 1993, Santilli, et al 2000) and a left ventricular enlargement pattern is noticed in 7-22% of these cats (Moise and Dietze 1986, Fox, et al 1993, Santilli, et al 2000). Various arrhythmias and conduction disturbances have also been reported, such as left anterior fascicular block and right bundle branch block (Fox, et al 1993).

Cardiac enlargement is frequently apparent on thoracic radiography (in approximately 60% of cases) (Moise and Dietze 1986, Santilli, et al 2000). In addition, changes suggestive of pulmonary oedema or pleural effusion may also be evident.

Echocardiographic examinations have revealed that a proportion of cats with hyperthyroidism demonstrate left ventricular wall hypertrophy, interventricular septal hypertrophy, left atrial dilatation, and an increase in the ratio of the diameter of the left atrium to the aortic diameter (Moise and Dietze 1986). In addition to these changes, other authors have also reported an increase in left ventricular end diastolic diameter (but not left ventricular end systolic diameter), and an increase in the indices of contraction such as the percentage change in the ventricular diameter

(Bond, et al 1988). This indicates that, in patients not in congestive heart failure, hyperthyroidism is associated with an increased inotropic state (Bond, et al 1988).

Hyperthyroidism is largely a treatable disorder. Options for treatment include; oral anti-thyroidal medication (such as methimazole, or carbimazole), uni- or bilateral thyroidectomy, or radioactive iodine therapy. Some cats also require concurrent medications, most frequently to address the associated heart disease (Feldman and Nelson 2004).

The majority of actions elicited by T₃ appear to take place in the nucleus, where T₃ receptor proteins are located. By binding to these receptors, the transcription of specific genes is affected. The type and number of genes affected is widespread, perhaps explaining the multiple changes seen in organs systems under the influence of thyroid stimulation. One of the principle genetic alterations is seen in the expression of the cardiac myosin heavy chain (MHC) isoforms. These are products of two genes which encode for α and β -MHC. Thyroid hormone (T₃) has been shown to up-regulate the production of α -MHC and down-regulate β -MHC (Tiska, et al 1990). One of the effects of which is to increase the level of myosin V₁ isoenzyme and to decrease the level of myosin V₃, thereby leading to an increased velocity of contraction and diastolic relaxation. Other genes which T₃ has been shown to upregulate include the gene encoding cardiac Troponin (Tn) (Averyhart-Fullard, et al 1994). In hyperthyroid rats TnI is upregulated at a transcriptional level; thus increasing cardiac cross-bridge cycling, and thereby enhancing the force of contraction (Dieckman and Solaro 1990).

In addition to these genetic changes, the activity of Ca^{2+} -ATPase is increased (Suko 1973, Dillmann 1990). This causes a greater build up of calcium in the sarcoplasmic reticulum during diastole, resulting in an enhanced relaxation. When, during systole, this calcium is released, the increased availability results in more cross-bridge formation and therefore, an enhanced force of contraction (Suko 1973).

In addition, increased levels of T3 are responsible for the upregulation of Na^+ , K^+ -ATPase α_2 , α_3 , and β -isoforms resulting in an increase in the concentration of sarcolemmal Na^+ , K^+ -ATPase isozymes (although, to date, this has only been demonstrated in neonates) (Orlowski and Lingrel 1990). One of the actions of this is to maintain Na^+ and K^+ gradients across the plasma membrane, playing an essential role in the electroactivity of muscle. It is thought that alterations in the expression of these isoforms may play a role in modulating myocardial function and ionotropy (Dieckman and Solaro 1990).

Exposure of ventricular myocytes to T3 has also been shown to increase the number of β_1 -adrenergic receptors per cell (Bahouth 1991). Interestingly, the number of β_2 receptors remain unaltered (Bahouth 1991). This increase in β_1 -receptors may result in tachycardia and an increase in inotropic response.

Hyperthyroidism results in an increase in tissue oxygen consumption, which leads to peripheral vasodilation; and together these demand an increase in circulatory dynamics (Dillmann 1983). The overall effect of T3 upon the heart, peripheral circulation and sympathetic nervous system, is to cause an increase in the force and rate of contraction and an increase in the speed of relaxation; giving rise to the syndrome of 'thyrotoxic cardiomyopathy' (Richardson, et al 1996).

Doppler Tissue Imaging

Pulsed-wave DTI (pw-DTI) has received a lot of recent attention from cardiologists (Garcia, et al 1996, Gavaghan, et al 1999, Schober, et al 2003). It is a technique that measures the instantaneous peak myocardial velocity as it moves through a pre-selected sample volume. The technique has excellent temporal resolution (over 300Hz) (Sutherland and Hatle 2002) and has therefore been used to assess the velocities within the feline myocardium (Gavaghan, et al 1999, Schober, et al 2003). Different echocardiographic views show different velocity profiles, even if the sample is aligned in a similar position; velocities occurring at 90° to the Doppler beam are measured as zero.

It is recognised that the endocardium and epicardium are composed of longitudinal fibres, while at the mid-wall level the fibres display a circumferential orientation (Streeter, et al 1969). Early experiments alluding to this relationship were performed on canine hearts (Rushmer, et al 1953, Streeter, et al 1969). It has since been demonstrated that the fibre orientation within the feline heart is essentially similar to that found both within the canine and the human heart (Matre, et al 1986). While fibre angles show little interspecies variation, there is a slightly wider variation between the angles of alignment within the feline heart (Matre, et al 1986). Therefore, the different fibre types are analysed from different angles; the longitudinal fibres from the four or five-chamber apical view and circumferential fibres from parasternal short and long axis views (Oki, et al 1997, Oki, et al 1999).

Previously, pw-DTI techniques have been used to assess regional myocardial dynamics in both people and cats with HCM (Pai and Gill 1998b, Severino, et al 1998, Gavaghan, et al 1999, Mishiro, et al 2000, Oki, et al 2000, Koffas 2003, Koffas, et al 2005), and in people with hypertension (Oki, et al 1998, Poulsen, et al 2003) and ischaemic heart disease (Edwardsen, et al 2000, Rambaldi, et al 2003). The systolic velocity can be severely depressed and late in onset, and there may be a phenomenon known as post-systolic thickening (PST). In PST, a deflection (in the same orientation as the S' peak) is seen during the isovolumic relaxation period (Edwardsen, et al 2000, Rambaldi, et al 2003). In human beings, these changes are seen earliest by placing the sampling gate within the subendocardium, since this layer is the first to be affected by ischaemic episodes (Rahimtoola 2001). We have previously reported a pw-DTI pattern resembling PST in cats with HCM (Koffas, et al 2005).

Previously, I have reported an increase in both pw-DTI S' and A' velocities in untreated hyperthyroid cats (Chapter 5). Whilst echocardiographic abnormalities have been described in hyperthyroid cats before and after treatment (Moise and Dietze 1986, Bond, et al 1988, Santilli, et al 2000); to date, there have been few studies, in either the human or veterinary literature, evaluating the affects of medical treatment on pw-DTI variables in thyrotoxic cardiomyopathy.

The aim of this study was to investigate the effect of carbimazole upon thyrotoxic feline myocardium by comparing conventional echocardiographic measurements (two-dimensional, spectral Doppler, and M-mode) and more advanced measurements of diastolic function (pw-DTI, colour M-mode propagation velocity and

isovolumetric relaxation time) in normal cats, to those recorded from treated and untreated hyperthyroid cats and in doing so to ascertain whether or not cats being treated with carbimazole demonstrate any alteration in the myocardial dynamics when compared to either unaffected cats or to untreated hyperthyroid cats.

Materials and Methods

The selection of cases, identification of systemic disease and echocardiographic examination protocol used in this study were identical to the procedures outlined in Chapter 3.

Grouping of the Cats

The normal cats were selected from first opinion cases presenting for geriatric health checks. All of these cats were clinically healthy and were normal on physical examination, including auscultation. Routine blood sampling was used to determine that the urea, creatinine and tT4 concentrations, and the packed cell volume (PCV) were within the reference ranges. The systolic blood pressure was measured and found to be between 120 and 170 mmHg. Auscultation, a six-lead ECG and standard two-dimensional and M-mode echocardiographic examinations revealed no abnormalities.

Cats were classified as hyperthyroid if their serum tT4 was equal to or exceeded 48 nmol/l (reference range 13-48 nmol/l) or they had previously been shown to have a tT4>48nmol/l, but were now receiving anti-thyroid medication. Cats found to be hyperthyroid, or with a history of hyperthyroidism, were then divided into those receiving medication (carbimazole) and those that were untreated. Any cats found to have concomitant disease(s), were excluded from the study.

Statistical Analysis

The statistical analysis was carried out using S-Plus (version 6.2.1, 1988, 2003 Insightful Corp. S: Copyright Lucent Technologies Inc.). The population characteristics were analysed using a one-way analysis of variance (ANOVA), or for the binomial data, a Fishers exact test. The results of the echocardiographic analysis were adjusted to account for heart rate, using the root RR method, then the measurements were compared using a one-way analysis of variance with multiple comparisons being performed using a Tukey analysis. The distribution of the means and the homoscedasticity of the residuals were tested. When either the distribution of the residuals or the variance was unsatisfactory, standard transformation techniques (\log_{10}) were applied to normalise the distributions. A p value of ≤ 0.05 was taken as demonstrating statistical significance.

Results

A total of 30 cats were selected. Of these eight were classified as normal, 12 were hyperthyroid, but had never received medication, and 10 were hyperthyroid but receiving medication. However, two of the medicated hyperthyroid cats were excluded from the study because they had not received medication for two and five days, respectively. All the treated cats were receiving carbimazole. There were no other medications prescribed.

Population Studied

The population characteristics are shown in Table 9. There was no significant difference between the weight of the cats, or systolic blood pressure, in the different groups studied. The age differed in that the cats with untreated hyperthyroidism were older than the normal cats, but not significantly different to the treated cats; the treated cats were not significantly older than the normal cats. The respiratory rate at initial presentation was higher in all the hyperthyroid cats when compared to the normal cats. However, there was no difference between the respiratory rate of the treated and untreated hyperthyroid cats. The heart rate varied significantly between groups; the treated hyperthyroid cats demonstrating a significantly higher heart rate than the normal cats. However, there was no significant difference between the treated and untreated hyperthyroid cats, and the untreated hyperthyroid cats demonstrated a statistically similar heart rate to the normal group of cats. The thyroid hormone concentration was significantly higher in the cats with hyperthyroidism (both the treated and untreated groups). There was no significant

difference between the serum tT4 concentration in the treated versus the untreated hyperthyroid groups. The creatinine concentration was significantly lower in the hyperthyroid cats (both the treated and untreated cases) than in the normal cats. The electrocardiogram revealed no abnormalities in the normal cats (as dictated by the inclusion criteria), however, the cats with hyperthyroidism demonstrated several ECG abnormalities (Table 9); these included an increase in the amplitude of the R wave (n=9), a left anterior fascicular block pattern (n=4), and various arrhythmias (n=2).

Echocardiographic Examination

The results of the analysis of variance in the echocardiographic measurements are presented in Table 10. Multiple comparisons were performed on each variable that demonstrated a significant difference between groups (Figure 14).

The two-dimensional echocardiographic analysis revealed no differences in the left atrial diameter, or the aortic diameter. However, the thickness of the basilar interventricular septum was increased in both the treated and untreated hyperthyroid groups of cats, when compared to the normal group of cats.

The M-mode measurements demonstrated an increase in the thickness of the free wall in the untreated hyperthyroid cats compared to the normal cats, during both systole and diastole, and an increase in the thickness of the interventricular septum during systole in the same group. Whilst the treated hyperthyroid cats demonstrated no significant difference from the untreated hyperthyroid cats, this group only

demonstrated a significant increase in the thickness of the free wall during systole when compared to normal cats. The colour M-mode propagation velocity was decreased in all the hyperthyroid cats compared to the normal group of cats, however, this only reached significance in the untreated cats.

The spectral Doppler analysis demonstrated significant differences in the velocity of flow within the aorta. Multiple comparisons demonstrated that the untreated hyperthyroid cats had a higher aortic velocity than either the normal or treated hyperthyroid cats, and that the treated hyperthyroid cats demonstrated a higher aortic velocity than the normal cats. A similar relationship was evident in the analysis of the pulmonic flow. However, the velocities recorded from the untreated hyperthyroid cats were not significantly higher than those recorded from the treated hyperthyroid cats.

The transmitral flow demonstrated significant variation in both the early diastolic (E) and late diastolic (A) flow velocities. In both cases this was associated with a significantly higher velocity in the untreated hyperthyroid cats when compared to the normal cats. The trans-tricuspid A wave demonstrated a similar increase in the untreated hyperthyroid cats compared to the normal cats.

The only pulmonary venous flow variable to demonstrate a significant variation between groups was the velocity of the atrial reversal wave. This was increased in all the hyperthyroid cats (both treated and untreated groups) when compared to the normal group of cats. However, there was no significant difference in the atrial reversal velocity between the two hyperthyroid groups.

When compared with the normal group of cats, the untreated hyperthyroid cats demonstrated significantly higher velocities within the radial myocardial fibres of the free wall (assessed from both the right parasternal long and short axis views) during systole (S') and late diastole (A'). There were no significant differences between the treated hyperthyroid cats and the normal cats, although the A' velocity assessed from the right parasternal long axis view, was significantly higher in the untreated hyperthyroid cats than it was in the treated hyperthyroid cats.

The untreated hyperthyroid cats demonstrated significantly elevated S' and A' velocities in the longitudinal fibres of the interventricular septum, at the level of the mitral annulus (when assessed from the apical four chamber view) compared to the normal group of cats. The treated and untreated hyperthyroid groups were not significantly different from one another at either of these points. However, the treated hyperthyroid cats demonstrated a significantly elevated A' velocity at this site, when compared to the normal cats. The A' velocity, assessed from the same view, but at the level of the mid-interventricular septum, demonstrated a significant decrease in the untreated hyperthyroid cats compared with the treated hyperthyroid cats, and a significant increase in the treated hyperthyroid cats compared to the normal cats. The velocities recorded in the untreated hyperthyroid cats were not significantly different from those recorded in the normal cats.

Four cats demonstrated PST within the longitudinal fibres, at the mid lateral wall level (when assessed from the left apical four chamber view). All four of these cats were hyperthyroid, two were receiving medication and two were untreated. The mean velocity of PST in the treated hyperthyroid cats was 0.05m/s, whereas in the

untreated hyperthyroid cats the mean velocity was 0.085m/s. However, because there were only four cats, no statistical analysis was performed in these results.

Discussion

I found no evidence that carbimazole negatively affects thyrotoxic feline myocardium. All of the echocardiographic variables that demonstrated a difference between the normal cats and the treated hyperthyroid cats, also demonstrated a trend towards a similar variation in the untreated hyperthyroid cats; with the exception of the A' velocity within the longitudinal fibres at the mid-interventricular septum. The variation at this point was thought to have occurred due to abnormally low velocities in some of the untreated hyperthyroid cats, rather than as a result of toxic changes within the myocardium. These results suggest that with a decrease in tT4 concentration following carbimazole administration there is restoration of myocardial function, with echocardiographic variables approaching those in normal cats, even before a euthyroid state is achieved.

Population Characteristics

The group characteristics demonstrated some variation. The normal group of cats was significantly younger than the untreated hyperthyroid group. Whilst, in human beings, it has been shown that there is a correlation between pw-DTI velocities and age (Yamanda, et al 1999, Munagala, et al 2003); I have previously demonstrated that in normal geriatric cats, age does not significantly affect any of the echocardiographic variables measured (Chapter 3). Furthermore, in hyperthyroid cats I found that only the S' velocity recorded from the right parasternal short axis view demonstrated a significant variation with age (Chapter 3). Therefore, the

discrepancy in age between the normal and untreated hyperthyroid cats should have had minimal impact on the results of this study.

The respiratory rate at initial presentation was significantly higher in the hyperthyroid cats, compared to the normal cats. It did not differ between the two groups of hyperthyroid cats. Respiratory abnormalities (including tachypnoea) have previously been reported in hyperthyroid cats (Thoday and Mooney 1992). Hyperthyroidism is known to increase sympathetic stimulation (Dillmann 1983, Hammond 1987, Bahouth 1991, Burggraaf, et al 2001), and the increased respiratory rate is likely to be a result of this.

The heart rate was significantly higher in the treated hyperthyroid cats, than it was in the normal cats. Interestingly, the untreated hyperthyroid cats demonstrated no significant difference in the heart rate compared to the normal cats. However, the heart rate of the treated hyperthyroid cats was not significantly higher than that of the untreated group of hyperthyroid cats. The treated cats had previously been diagnosed as hyperthyroid and placed on medication prior to taking part in the study. It may therefore have been, in part, the presence of a relative tachycardia which alerted the referring veterinarians to the underlying thyroid problem; whereas the untreated hyperthyroid cats were diagnosed as suffering from hyperthyroidism at the time of presentation for the study. Tachycardia is reported in 26-62% of hyperthyroid cats (Thoday and Mooney 1992, Santilli, et al 2000), however, according to the criteria used in these studies, none of the cats included in the current study were actually tachycardiac (heart rate > 240bpm).

Surprisingly, the serum concentration of tT4 was not significantly different between the treated and untreated hyperthyroid groups of cats. This would imply that, generally, the treated group of cats were not being medicated adequately. There was a slightly lower serum tT4 concentration within the treated group of hyperthyroid cats, but the mean tT4 was still well outside of the reference range (97.8 nmol/l, reference range 13-48 nmol/l). Whilst this discrepancy means that I was unable to fully evaluate the affect of (successful) treatment upon the feline echocardiographic variables that I assessed, it is perhaps serendipitous, as it allows us to assess the affect of medication (carbimazole [5mg given every 8-12hrs]) upon the feline myocardium without full resolution of the thyrotoxic state.

The serum creatinine concentration was decreased in both the hyperthyroid groups of cats compared to the normal group of cats. I had excluded any hyperthyroid cats with biochemical evidence of CRF. It has previously been reported that hyperthyroid cats are prone to weight loss and an increased catabolic state (Feldman and Nelson 2004), which causes muscle wastage, decreasing the total body creatinine concentration (Barber and Elliott 1996). In addition, a decreased serum creatinine concentration has previously been described in human beings and cats with thyrotoxicosis (Barber and Elliott 1996, Verhelst, et al 1997, Jayagopal, et al 2003). This is thought to result from an increased glomerular filtration rate in these patients (Barber and Elliott 1996, Verhelst, et al 1997). Either, or both, of these mechanisms may be responsible for the decreased serum creatinine concentrations in the hyperthyroid cats in the current study.

Electrocardiographic Analysis

Electrocardiographic changes were seen frequently in the hyperthyroid cats, with 75% of the cats demonstrating abnormalities on their ECG. Previous reports suggest that a left ventricular hypertrophy pattern is present in 7-49% of hyperthyroid cats (Peterson, et al 1982, Moise and Dietze 1986, Fox, et al 1993, Santilli, et al 2000) and a LAFB has been reported in approximately 2-8% of cases (Peterson, et al 1982, Fox, et al 1993). I identified a pattern consistent with left ventricular hypertrophy (R-wave elevation) in 45% of cases and a LAFB in 20% of cases. Arrhythmias are also recognised in hyperthyroidism, with atrial premature complexes (APCs) being reported in 2-11% of cases, and ventricular premature complexes (VPCs) being reported in 2-4% of cases (Peterson, et al 1982, Fox, et al 1993). Similarly, I recognised APCs in 5% of cases, and VPCs in a further 5% of cases. The conduction abnormalities recognised in hyperthyroidism are hypothesised to be the result of myocardial fibrosis (Liu, et al 1984).

Variations between Normal and Hyperthyroid Cats

I have previously reported echocardiographic abnormalities in untreated hyperthyroid cats (Chapter 5). In that study I compared several groups of untreated cats with different forms of cardiomyopathy. I demonstrated a significant increase in the thickness of the basilar interventricular septum (assessed from the right parasternal long-axis view) and the left ventricular free wall (assessed by M-mode). The velocity of flow within the aorta and pulmonary artery was significantly

increased in hyperthyroid cats compared to normal cats, as was the atrial component of the transmitral flow (A wave). The pw-DTI analysis revealed increases in the S' velocity within the free wall (assessed from both the long and short axis views), the A' velocity within the free wall (assessed from the right parasternal long axis view) and within the interventricular septum, at the level of the mitral annulus (assessed from the left apical four chamber view). Whilst the same groups of normal and untreated cats were assessed in this study, there were some additional variations between the untreated hyperthyroid cats and normal cats. This apparent discrepancy arose from the inclusion of fewer groups of cats, and with this less data spread. Therefore, in addition to the changes reported previously, the current study demonstrated significant increases in the M-mode measurement of systolic wall thicknesses, with both the free wall and interventricular septum being increased in the untreated hyperthyroid cats compared to the normal cats. These changes are consistent with those reported previously and suggest that there are both systolic and diastolic abnormalities in hyperthyroid cats (Moise and Dietze 1986, Bond, et al 1988).

Colour M-mode Propagation Velocity

In addition to conventional M-mode analysis, I assessed the colour M-mode propagation velocity (Vp). I was able to demonstrate a significant decrease in the Vp in the untreated hyperthyroid cats compared to the normal cats. In healthy catheterised cats, it has previously been found that Vp is inversely related to τ (Schober, et al 2003). In human beings, it has been demonstrated that during both

beta-blockade and asynchronous contraction (engendered by acute myocardial ischaemia) this correlation remains; suggesting that V_p is independent of cardiac geometry but is in fact responding to changes in wall motion (Stugaard, et al 1993). The asynchronous wall motion observed in many disease states, reduces V_p , independent of mitral inflow (Brun, et al 1992, Stugaard, et al 1993, Møller, et al 2000). In the current study, the significant decrease in V_p in the untreated hyperthyroid cats may therefore suggest that ventricular asynchrony is present.

Pulsed-wave Doppler Tissue Imaging

The untreated hyperthyroid cats demonstrated increased S' and A' velocities within the radial fibres of the free wall (assessed from both the right parasternal long and short axis views), and in the longitudinal fibres (assessed from the left apical four chamber view) within the interventricular septum (at the level of the mitral annulus). These findings are similar to those reported previously (Chapter 5), when I hypothesised that the increase in S' velocity may reflect an increase in the beta-receptor density; a strong relationship between S' and β -receptor density having been reported previously (Shan, et al 2000). However, E' velocity is also reported to increase with β -receptor density (Shan, et al 2000). It is known that, in human beings, E' decreases with worsening diastolic function (Oki, et al 1997, Sohn, et al 1997, Ommen, et al 2000) and that E' is decreased in cats with HCM (Gavaghan, et al 1999, Koffas, et al 2005). However, I demonstrated no significant difference between the E' velocities in the normal and hyperthyroid cats. The increase in A' velocity at multiple sites normally suggests diastolic dysfunction (Oki, et al 1997,

Oki, et al 1998). However, in such an event one would normally expect the E' to be decreased, unless, as in human beings, this variable is also increased due to the increased number of beta-receptors (Shan, et al 2000), thereby negating the expected decrease in E' velocity. Alternatively, it has been hypothesised that in the hyperthyroid heart, the activity of Ca^{2+} -ATPase is increased. This causes a greater build up of calcium in the sarcoplasmic reticulum during diastole, resulting in an enhanced relaxation. When, during systole this calcium is released, the increased availability results in more cross-bridge formation and therefore, an enhanced force of contraction (Suko 1973).

The radial fibre S' and A' velocities within the free wall were significantly elevated, whereas only the velocity of fibre motion within the interventricular septum at the level of the mitral annulus was affected when longitudinal fibre motion was assessed. The increases in S' and A' demonstrated in hyperthyroid cats support the occurrence of asynchronous contraction in this group. Asynchronous contraction is reported in people and cats with HCM (Pai and Gill 1998b, Mishiro, et al 2000, Oki, et al 2000, Cardim, et al 2003, Koffas, et al 2005) but has not previously been demonstrated in hyperthyroidism.

Variations Between the Treated and Untreated Hyperthyroid Cats

The treated hyperthyroid cats demonstrated no significant lowering of the serum tT4 concentration compared to the untreated group of cats; however, the serum tT4 did tend to be lower in this group, which included two euthyroid cats. This group of cats

generally demonstrated similar findings to those reported in the untreated hyperthyroid cats, although, frequently the measurements from this group demonstrated wide confidence intervals and failed to demonstrate significant differences from the normal group. The only significant variations between the treated and untreated hyperthyroid cats were the velocity of flow within the aorta, the A' velocities measured within the radial fibres of the free wall (assessed from the right parasternal long axis view only) and within the mid-interventricular septum (assessed from the left apical four-chamber view). In addition, the velocity of PST within the longitudinal fibres of the apical lateral wall was lower in treated cats than in the untreated cats.

The aortic velocity was significantly higher in both the treated and untreated hyperthyroid cats, compared to the normal cats, as well as being significantly higher in the untreated hyperthyroid cats than in the treated cats. The basilar interventricular septum was significantly thicker in both the untreated and treated hyperthyroid cats when compared to normal cats. Increased aortic velocity is usually the result of either outflow tract obstruction, increased systolic function (Fox, et al 1999), or, as may be the case in the current study, a combination of both of these factors.

The A' velocity recorded from the right parasternal long axis free wall was significantly lower in the treated hyperthyroid cats than in the untreated hyperthyroid cats. At this site, the treated hyperthyroid cats demonstrated an A' velocity similar to the normal cats. In addition, none of the radial fibre velocities recorded from the treated hyperthyroid cats were significantly different to those recorded in the normal

cats. This may suggest that, with treatment, circumferential function is restored prior to longitudinal function.

It is perhaps notable that the A' velocity within the longitudinal fibres, at the mid-interventricular septum, was not increased in untreated cats compared to normal cats, whilst it was increased in treated cats compared to both normal cats and untreated hyperthyroid cats. Since the A' velocity at the other sites was typically increased in the hyperthyroid cats compared to the normal cats, it is surprising that at this particular site, the untreated cats demonstrated a decreased A' velocity.

Within the hyperthyroid groups of cats there were some cats identified which demonstrated a decreased S' velocity followed by a late systolic excursion. This pattern is thought to resemble PST, a phenomenon reported in human beings and associated with myocardial infarction (Edvardsen, et al 2001, Rambaldi, et al 2003). Notably, this pattern was not present in any of the normal cats, and occurred only within the longitudinal fibres of the lateral wall in the hyperthyroid cats. It is known that in human beings the sub-endocardium, and therefore the longitudinal fibre velocities, is more sensitive to hypoxia than other areas of myocardium (Edvardsen, et al 2000, Rahimtoola 2001, Rambaldi, et al 2003). The velocity of PST thickening at the apical lateral wall appeared to be decreased in treated hyperthyroid cats compared to untreated hyperthyroid cats. In an experimental study, PST was induced in (previously normal) cats and ischaemia maintained until the disappearance of PST. The myocardium was then allowed to reperfuse, and as this happened the PST returned. The time taken for 'reperfusion-PST' to disappear was correlated to the duration of occlusion and the extent of myocardial necrosis (Song,

et al 2003). The reduction in the velocity of PST in treated hyperthyroid cats may therefore infer that there was increased perfusion of affected myocardial segments in this group.

Limitations

I was able to demonstrate an improvement in many echocardiographic variables with the treatment of hyperthyroidism. However, the treated cats rarely demonstrated a return to completely normal function. This is probably because, as a group, the treated cats remained hyperthyroid. Therefore, from the current study, I cannot determine whether or not cardiac function is normalised with a return to the euthyroid state.

The untreated group of hyperthyroid cats were significantly older than the normal cats. Previously, I have demonstrated that in normal geriatric cats there is no significant relationship between age and any of the pw-DTI velocities studied (Chapter 3). However, in hyperthyroid cats, there is a significant relationship between age and the S' velocity within the free wall assessed from the right parasternal short axis view (Chapter 3). Therefore, it would be expected that at this point the S' velocity would be increased in the hyperthyroid group if age had been acting as a significant confounding factor. In the current study, the S' within the radial fibres of the free wall was increased in the untreated hyperthyroid cats. However, the S' was also increased at other sites within the myocardium, at which

there was no significant relationship with the age of the cat demonstrated previously (Chapter 3).

This study was limited by the small sample size. The normal and treated hyperthyroid groups each comprised only eight cats. Demonstrating significant variations between such small groups can be problematic. Furthermore, I have previously demonstrated that the variability in measurement of pw-DTI velocities is approximately 20% (Chapter 2). Poorly repeatable variables will demonstrate wide confidence intervals and therefore, the differences must be marked in order to demonstrate significant variations. However, in light of these limitations, I demonstrated several significant variations, suggesting that there are marked changes in feline thyrotoxicosis.

In the future a longitudinal study assessing the alteration in pw-DTI velocities in hyperthyroid cats, treated until a euthyroid state is achieved, is warranted. Unfortunately, of the cats in the current study, at the time of writing, eight cats had been euthanised, three were lost to follow-up, three were not receiving any medication, two had undergone thyroidectomy and four had developed other significant disease(s). Of the two cats that underwent thyroidectomy, one was reassessed four months post-surgery. It is perhaps interesting to note, that in this case the V_p had increased from 17.73cm/s to 30.82cm/s, and the S' velocities recorded from the lateral wall (imaged from the left apical four chamber view) demonstrated a decrease from 0.14m/s to 0.05m/s and from the lateral aspect of the mitral annulus (also imaged from the left apical four chamber view) demonstrated a decrease from 0.1m/s to 0.04m/s. All of the other pw-DTI S' and A' velocities which

were assessed, demonstrated either mild decreases or remained unchanged. However, in order to fully assess the affects of medication upon thyrotoxic myocardium, a follow-up study is required, where the myocardial velocities in a group of adequately treated hyperthyroid cats will be assessed.

Conclusions

I found no evidence that carbimazole imposes toxic effects upon the thyrotoxic feline myocardium. All of the echocardiographic variables that demonstrated a difference between the normal cats and the treated hyperthyroid cats also demonstrated a similar variation in the untreated hyperthyroid cats (with the exception of the A' velocity within the longitudinal fibres at the mid-interventricular septum). The variation at this point was thought to have occurred due to abnormally low velocities in some of the untreated hyperthyroid cats, rather than as a result of toxic changes within the treated hyperthyroid cats. These results suggest that with a decrease in tT4 concentration following carbimazole administration, there is restoration of myocardial function, with echocardiographic variables approaching those in normal cats, even before a euthyroid state is achieved.

In addition, I documented a decrease in the colour M-mode propagation velocity in the hyperthyroid left ventricle. This finding is thought to represent asynchronous relaxation in humans (Stugaard, et al 1993, Møller, et al 2000) and may suggest that ventricular asynchrony exists in the hyperthyroid cat.

I observed a pattern similar to PST in eight of the twenty hyperthyroid cats. There were four cats that demonstrated PST at the mid-lateral wall within the longitudinal fibres. The velocity of this PST was decreased in the two cats with treated hyperthyroidism compared to the two untreated cats. If PST represents similar changes in cats, as have been described in human beings, this would imply that with carbimazole treatment the feline myocardium is less prone to hypoxic changes.

Generally, the treated hyperthyroid cats demonstrated less variation from the normal cats, compared to the untreated hyperthyroid cats. Hence, this study suggests that the use of carbimazole alone improves the function of the feline myocardium in thyrotoxic cardiomyopathy.

Table 9: Population characteristics

Disease	Age (yrs)	Weight (kg)	Breed	BP (mmHg)	ECG	RR (bpm)	HR (bpm)	Treatment (prior to study)	Sex	T4 (nmol/l)	Crea (μmol/l)	Notes
Normal	10	5.2	DSH	140.0	NAD	24	160	None	MN	24.5	139	
Normal	10	5.7	DLH	126.4	NAD	32	156	None	FN	19.6	133	
Normal	8	4.6	BSH	121.6	NAD	24	160	None	FN	25.6	156	
Normal	10	4.6	DSH	145.0	NAD	30	190	None	FN	23.2	159	
Normal	11	5.6	DSH	148.0	NAD	28	180	None	MN	27.6	150	
Normal	9	4.4	DSH	144.4	NAD	20	140	None	MN	24.0	110	
Normal	8	6.2	DLH	144.8	NAD	-	200	None	MN	25.7	155	
Normal	14	5.4	DSH	131.6	NAD	30	140	None	MN	26.3	197*	*Crea @10 days - 161μmol/l
HiT4	15	3.9	DLH	136.4	NAD	28	156	None	FN	52.0	154	
HiT4	14	3.4	DSH	128.0	R-1mV	35	170	None	FN	83.7	89	
HiT4	9	6.1	DSH	160.0	NAD	-	160	None	MN	111.0	137	
HiT4	18	2.2	DSH	100.8	R-1.6mV	30	220	None	FN	224.0	108	
HiT4	13	3.4	DSH	122.0	R-1mV	-	160	None	FN	137.0	86	
HiT4	11	-	DSH	153.2	R-1.5mV	40	220	None	FN	77.8	114	
HiT4	15	3.2	DSH	141.6	LAFB	50	160	None	FN	112.0	106	
HiT4	14	3.8	DLH	149.6	VPCs	44	200	None	FN	72.0	112	
HiT4	12	5.5	DSH	156.0	R-2.6mV	-	200	None	MN	148.0	138	
HiT4	17	6.1	DSH	150.4	LAFB	60	192	None	MN	268.0	103	
HiT4	16	2.8	DSH	136.4	LAFB	-	200	None	FN	108.0	60	
HiT4	16	4.4	DLH	145.6	R-1.7mV	-	180	None	FN	102.0	89	
HiT4	13	-	DSH	142.8	SPCs	44	200	CBZ 5mg q12hrs 30 days	FN	71.3	118	
HiT4	10	5.4	DSH	130.4	NAD	24	180	CBZ 5mg q8hrs 42 days	FN	223.0	89	
HiT4	10	5.7	DSH	160.0	NAD	60	220	CBZ 5mg q8hrs 12 days	MN	105.0	100	
HiT4	10	2.9	DSH	136.0	R-1mV	48	180	CBZ 5mg q12hrs 14 days	FN	200.0	63	
HiT4	18	2.4	DSH	145.2	R-1.5mV	-	186	CBZ 5mg q12hrs 395 days	FN	15.2	121	
HiT4	14	4.2	DSH	160.0	NAD	-	220	CBZ 5mg q8hrs 14 days	MN	96.0	123	
HiT4	13	4.1	DSH	160.0	LAFB	60	240	CBZ 5mg q12hrs 30 days	FN	55.5	103	
HiT4	8	3.9	DSH	147.2	R-2mV	-	200	CBZ 5mg q8hrs 15 days	MN	16.1	158	

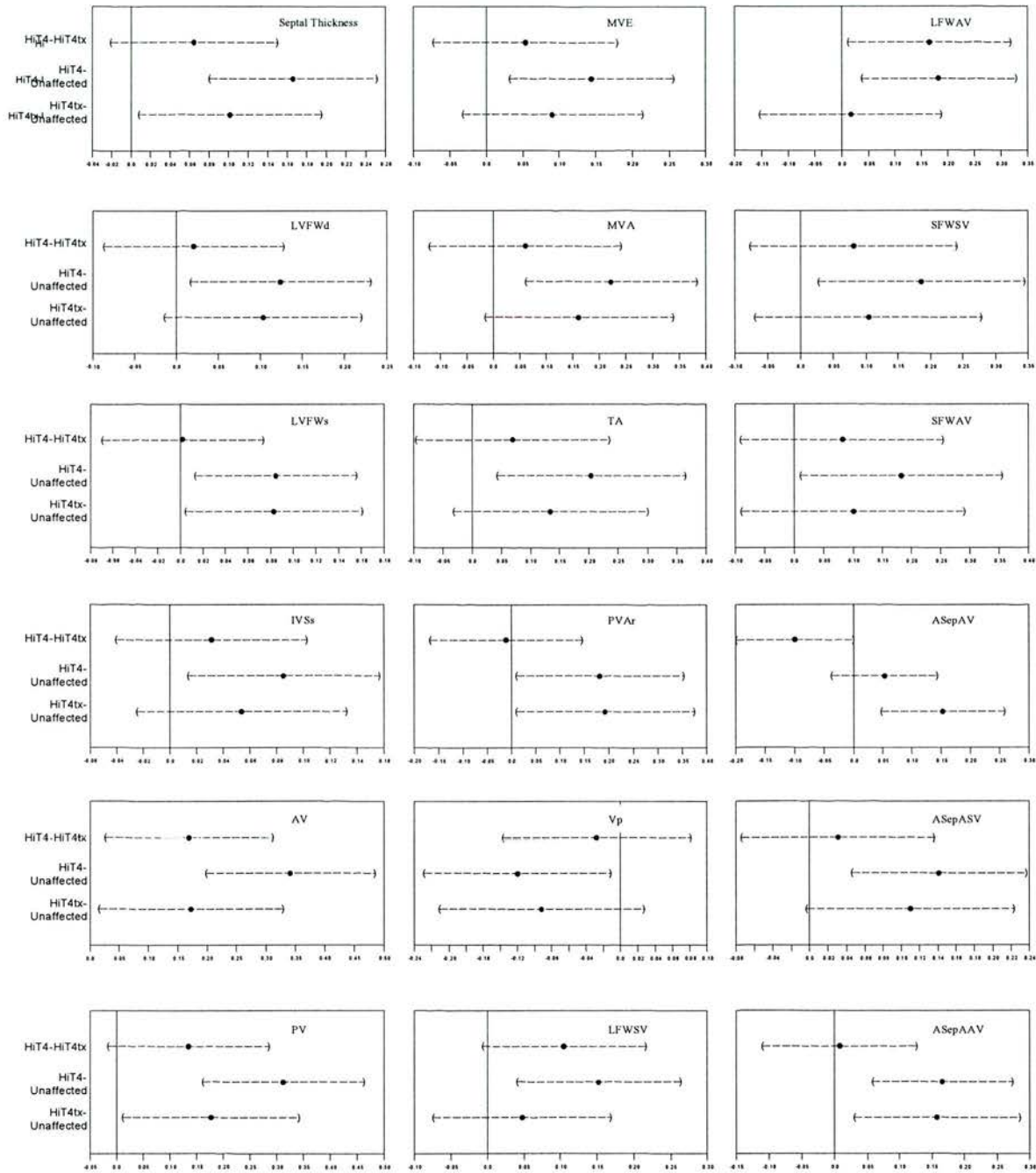
Where: BP, Systolic Blood Pressure; ECG, Electrocardiographic Changes; RR, Respiratory Rate; HR, Heart Rate; T4, Serum Thyroxine Concentration; Crea, Serum Creatinine Concentration; HiT4, Hyperthyroidism; DSH, Domestic Short Haired Cat; DLH, Domestic Long Haired Cat; NAD, No Abnormalities Detected; LAFB, Left Anterior Fascicular Block; R, R wave; VPCs, Ventricular Premature Complexes; SPCs, Supraventricular Premature Complexes; CBZ, Carbimazole; mg, milligrams, q, every; hrs, hours; MN, Male Neutered; FN, Female Neutered

Table 10: One-way analysis of variance (ANOVA) assessing the variation between groups (quoting the associated test statistic (F), the probability that the difference in variation was due to chance (P) and the degrees of freedom(subscript)).

Tissue Doppler Variables	Inter-Group	
	F	P
Long Axis Free Wall		
S'	(2,25)= 6.380	0.006
E'	(2,22)=2.358	0.118
A'	(2,22)= 6.423	0.006
Short Axis Free Wall		
S'	(2,25)= 4.296	0.025
E'	(2,22)=1.679	0.210
A'	(2,22)= 3.598	0.044
Apical Lateral Wall		
S'	(2,20)=0.777	0.473
E'	(2,20)=1.121	0.346
A'	(2,19)=0.557	0.581
Apical Mid-Septum		
S'	(2,23)=1.490	0.246
E'	(2,22)=0.663	0.525
A'	(2,22)= 6.730	0.005
Apical Septal Mitral Annulus		
S'	(2,23)= 6.682	0.005
E'	(2,23)=1.176	0.326
A'	(2,23)= 8.268	0.002
Apical Lateral Mitral Annulus		
S'	(2,22)=0.008	0.992
E'	(2,22)=1.154	0.334
A'	(2,22)=0.987	0.389

2D Heart Variables	Inter-Group	
	F	P
Ao Diameter*	(2,25)=0.493	0.617
Left Atrial Diameter*	(2,25)=0.585	0.565
Septal Thickness*	(2,25)= 11.757	<0.001
M-mode Variables		
LVDd	(2,25)=0.082	0.921
LVFWd	(2,25)= 4.430	0.023
LVDs	(2,25)=0.616	0.548
LVFWs	(2,25)= 5.106	0.014
IVSd	(2,25)=2.493	0.103
IVSs	(2,25)= 4.403	0.023
FS	(2,25)=2.040	0.151
EF	(2,25)=2.065	0.148
Vp	(2,25)= 3.904	0.033
Spectral Doppler Variables		
AV	(2,25)= 17.956	<0.001
PV	(2,25)= 13.331	<0.001
ME	(2,17)= 5.610	0.013
MA	(2,17)= 6.782	0.007
ME:MA	(2,17)=1.063	0.367
ME+A	(2,6)=0.177	0.688
TE	(2,20)=1.777	0.195
TA	(2,20)= 5.336	0.014
TE:TA	(2,20)=2.812	0.084
TE+A	(2,2)=0.387	0.597
IVRT	(2,23)=0.203	0.817
PVD	(2,22)=0.593	0.561
PVS	(2,22)=2.422	0.112
PVS:D	(2,22)=0.597	0.559
PVAr	(2,22)= 4.405	0.025
ArDur	(2,22)=3.336	0.054
MADur	(2,24)=0.026	0.974
MA:Ar Dur	(2,22)=2.695	0.089

Where: F, F-value, subscript shows the degrees of freedom between groups and residuals; P, P-value for comparisons between all three groups; Ao, aorta; LVD, left ventricular diameter; IVS, interventricular septum; LVPw, left ventricular posterior wall; d, diastole; s, systole; Vp, propagation velocity; FS, percentage fractional shortening; EF, ejection fraction; AV, aortic velocity; PV, pulmonic velocity; ME and MA, transmitral early and late diastolic flow, respectively; ME+A, the velocity of the summated transmitral flow; TE and TA; trans-tricuspid early and late diastolic flow, respectively; TE+A, summated trans-tricuspid flow; IVRT, isovolumic relaxation time; PV, pertaining to pulmonary venous; S, systolic flow; D, diastolic flow; Ar, atrial reversal flow; V, velocity; Dur, duration; S', systolic velocity; E', early diastolic velocity; A', late diastolic velocity; E'+A', summated diastolic flow. Bold type-face represents a P <0.05.

Figure 14: Multiple comparisons by the Tukey method

Plots represent the outcomes of the Tukey analysis: Bars represent the 95% confidence intervals, significant differences do not cross 0. Where: HiT4, untreated hyperthyroid cats; HiT4tx, treated hyperthyroid cats; Unaffected, normal cats; LVPW, left ventricular posterior wall; s, systole; d, diastole; IVS, interventricular septum; AV, aortic velocity; PV, pulmonary artery velocity; MVE, transmitral E wave velocity; MVA, transmitral A wave velocity; TA, trans-tricuspid A wave velocity; PVAr, pulmonary venous flow, atrial reversal velocity; LFW, long-axis free wall; S, peak motion during systole; A, peak motion during late diastole; V, velocity; SFW, short-axis free wall; ASep, apical four chamber view, at the mid-septal level; ASepA, apical four chamber view

Chapter 7

The clinical application of pulsed-wave Doppler tissue imaging and colour M-mode propagation velocity for the assessment of left ventricular relaxation

In human beings it has been shown that while conventional echocardiographic estimates of diastolic function (transmitral and pulmonary venous flow patterns) can give an estimate of ventricular relaxation and compliance, a number of confounding factors that can affect them. This has made it difficult to make diagnoses based on the analysis of these flow patterns. Therefore, investigators have attempted to identify alternative techniques that will give a better estimate of τ and dV/dP under variable conditions. These techniques include the measurements of isovolumic relaxation time, colour M-mode propagation velocity, and pw-DTI estimates of diastolic velocities.

The aim of this study was to compare pw-DTI velocities to conventional echocardiographic assessment of diastolic filling in various disease states in geriatric cats, in order to further validate the use of pw-DTI as an investigative modality for use in the approximation of diastolic function (and dysfunction) in the cat. This will then provide a reference for the clinical investigation of myocardial disease in this species.

Abstract

Diastolic dysfunction has been shown to play an important role in myocardial disease in human beings. While Doppler assessments of left ventricular filling variables have been used to estimate diastolic function, these methods are load sensitive and as such differentiation between the normal and pseudonormal state can be problematic. Therefore, Doppler tissue imaging (DTI) techniques have also been used in human beings to assess diastolic function since, at least in the diseased state, these measurements appear relatively load insensitive.

The aim of this study was to compare pulsed-wave DTI velocities to conventional echocardiographic assessment of diastolic filling (transmitral and pulmonary venous flow patterns) in geriatric cats with normal cardiac function, and those with various degrees of diastolic dysfunction.

A total of 80 cats were included in the analysis. All of the cats were aged eight years or older and had presented for a variety of problems including hypertrophic cardiomyopathy, hyperthyroidism, hypertension, diabetes mellitus, chronic renal failure, or for routine health checks. The cats were grouped on the basis of their transmitral E:A ratio and the ratio of transmitral A to pulmonary venous atrial reversal flow, according to the following criteria: Cats with a transmitral E:A and an A:Ar ratio of greater than one were classified as normal; cats with an E:A ratio of less than one and an A:Ar of greater than one were classified as having impaired relaxation; cats with a transmitral E:A of greater than one and an A:Ar of less than one were classified as pseudonormal or restrictive. Of these 80 cats, 21 demonstrated a normal relaxation pattern, 51 demonstrated a pattern consistent with impaired

relaxation and eight demonstrated either a pseudonormal (n=4) or restrictive filling pattern (n=4), these last eight cats were analysed as one group.

I demonstrated that cats display all of the diastolic patterns seen in human beings, and that the changes observed using the different methods demonstrated concurrence. In addition, I was able to describe a variety of methods of assessing diastolic function in the cat, and the suitability of these methods of assessment in a group of aged felines.

This study provides evidence that the human classification system and the previously described methods of determining diastolic function can be used to assess myocardial function in the cat and thereby provides an extra tool for the diagnosis of myocardial disease in this species.

Introduction

In the last two decades, diastolic dysfunction has been recognised as playing a major role in producing the symptoms of heart failure (Nishimura, et al 1989a). Approximately one third of people with congestive heart failure have normal systolic function, and it is thought that their symptoms are due to diastolic dysfunction (Nishimura, et al 1989b). Furthermore, in many disease states diastolic abnormalities have been shown to precede systolic dysfunction (Nishimura, et al 1989b). Diastolic dysfunction acts to increase left ventricular pressure per unit of blood entering the ventricle. In turn, this increases the pressure in the left atrium and ultimately in the pulmonary circulation, leading to signs of left-sided congestive heart failure (Nishimura, et al 1989a). Compensatory mechanisms may decrease the volume of blood filling the heart, leading to a decreased cardiac output and signs of forward failure, even in the presence of normal systolic function (Nishimura, et al 1989a).

Traditionally, assessment of diastolic function was performed in a catheterisation laboratory. However, in 1982, Kitabatake speculated that Doppler echocardiography could be used for the non-invasive assessment of left ventricular diastolic filling (Kitabatake, et al 1982). When investigators first began to describe echocardiographic methods of assessing the interventricular pressure-volume relationship, they studied the velocity of blood flow across the mitral valve. However, the measurements obtained represent global ventricular filling where the rate of flow through the mitral valve is altered by both changes in ventricular compliance and the rate of ventricular relaxation (Nishimura and Appleton 1996).

With the realisation that transmitral flow represented a non-invasive method of assessing diastolic function, numerous studies have investigated the effects that different physiological conditions and disease states can have on these variables. They found that although transmitral flow generally demonstrated a fair correlation with invasive measurements, these patterns are subject to alteration under a variety of conditions (Choong, et al 1987, Smith, et al 1989, Stoddard, et al 1989, Nishimura, et al 1990, Appleton, et al 1991, Schober and Luis Fuentes 2001a).

Studies have been performed in which left ventricular pressure and transmitral flow patterns were recorded simultaneously. These demonstrated that a reduction in preload results in a decreased E velocity and prolongation of the E wave deceleration time, without corresponding changes in the A wave (Choong, et al 1987, Stoddard, et al 1989, Nishimura, et al 1990); whereas, an increase in preload results in an increased E velocity, an increased A velocity, and a decrease in the E wave deceleration time (Stoddard, et al 1989, Nishimura, et al 1990). A decrease in preload is able to alter the E:A ratio without corresponding alterations in τ (Choong, et al 1987, Stoddard, et al 1989).

Attaining tracings that are a valid representation of transmitral flow has its own inherent difficulties. Initially, flow through the mitral valve is directed centrally but then changes to a posterolateral orientation. This angle of alteration becomes more obtuse with ventricular enlargement, making accurate alignment even harder. This is best corrected by looking for smooth sharp envelopes with a near linear downward slope, and listening for the best flow signal (Appleton, et al 1997). Additionally, at

high heart rates the two waveforms may become summated, making interpretation impossible.

These diastolic filling patterns are not a direct measure of diastolic function. Since mitral velocity and its respective gradients are determined by the complex interplay between multiple factors, assumptions made with respect to compliance and relaxation should be interpreted with caution. For this reason, other diastolic modalities are now considered alongside mitral inflow in order to gain a better oversight into cardiac dynamics.

With the growing interest in Doppler derived indexes of diastolic function, pulmonary venous flow patterns have been studied extensively and variables affecting these flow patterns have been described. Normal pulmonary venous flow can be divided into one or two systolic peaks of forward flow, followed by a diastolic component, also demonstrating forward flow, and a negative peak representing atrial reversal flow (Smiseth, et al 1999, Appleton, et al 2000). Measurement of pulmonary venous flow is not easy and can vary greatly with sampling site. Like mitral flow, pulmonary venous flow is influenced by numerous criteria. Perhaps most importantly, it is an age dependant measurement: As an individual ages, the pulmonary venous flow patterns show a greater systolic than diastolic flow velocity, and an increase in the velocity of the atrial reversal wave (Klein and Tajik 1991, Schober and Luis Fuentes 2001a). It has been suggested that this may be due to prolonged relaxation or relaxation abnormalities in older patients (Klein and Tajik 1991).

Loading conditions can also affect pulmonary venous flow velocities. A decrease in preload has been shown to decrease the height and duration of the atrial reversal flow, and increase the deceleration time of diastolic forward flow. In addition, in some individuals, the systolic signal may become biphasic (Nishimura, et al 1990, Hoit, et al 1992, Appleton 1997). An increase in preload has the opposite effect on the atrial reversal flow; both systolic and diastolic flow velocities increase and their deceleration times shorten. An increase in afterload has been shown to have the same effects as an increase in preload (Nishimura, et al 1990). Importantly, pulmonary venous flow is altered by respiration. Measurements should therefore be averaged over several cardiac cycles and preferably recorded during apnoea (Appleton, et al 1997).

Diastolic forward flow reflects the early transmitral flow. The peak pulmonary venous diastolic flow occurs approximately 50msec after peak E wave velocity in human beings. Once the mitral valve has opened, the left atrium acts as 'an open conduit' and blood from the pulmonary veins flows directly into the left ventricle. Therefore, peak E wave velocity and duration are dependent upon the same factors as the pulmonary venous flow diastolic component (Keren, et al 1985, Klein and Tajik 1991, Schober, et al 1998).

Atrial contraction increases the pressure in the left atrium and in doing so reverses the pulmonary-atrial pressure gradient, the result of which is flow from the left atrium into the pulmonary circulation; termed the atrial reversal flow. This is not directly comparable to the forward atrial flow (A wave) since there is a discrepancy in the orifice sizes (Nishimura, et al 1990). However, if the left ventricular pressure

is raised the pressure in the left atrium needs to be greater to achieve the same velocity of forward flow. This is reflected in the pulmonary venous flow and the atrial reversal is relatively more pronounced. An increase in ventricular compliance has the opposite effect. If there is an increase in preload both pulmonary atrial reversal wave and mitral A wave are increased (Nishimura, et al 1990, Rossvoll and Hatle 1993). The duration of the pulmonary venous atrial reversal wave has been compared with the duration of mitral A wave flow. It has been found that if the atrial reversal wave exceeds the duration of the mitral A wave then left ventricular diastolic pressure is increased (Keren, et al 1985, Rossvoll and Hatle 1993). Since a significant decrease in ventricular compliance is not believed to occur with aging this ratio may be less age dependent than other indexes of pulmonary or mitral flow (Appleton 1993, Klein, et al 1998). Furthermore, the ratio of transmitral A wave to pulmonary venous atrial reversal duration has previously been shown to be useful in assessing the severity cardiac disease (Abdalla, et al 1998).

Isovolumic Relaxation Time (IVRT)

An estimate of IVRT can be measured from the left ventricular five chamber apical view (Appleton, et al 1997). Since this is the time between aortic valve closure and mitral valve opening it is necessary to simultaneously record both events. Since the IVRT is determined primarily by the timing of the mitral valve opening and, therefore, the atrioventricular pressure gradient, its duration is influenced by both left ventricular relaxation and left atrial pressure (Appleton, et al 1988, Nishimura, et al 1989b). It has been demonstrated that IVRT is a good reflection of τ during changes

in contractility, but this correlation is lost when there are alterations in preload (Myreng and Smiseth 1990). Furthermore, IVRT is heart rate dependant (Schmitz, et al 2003).

Although these non-invasive indexes can give us an estimate of ventricular relaxation and compliance, the number of confounding factors that can affect them has made it difficult to make diagnoses based on these results and investigators have attempted to identify alternative techniques that will give a better estimate of τ and dV/dP under variable conditions.

Colour M-mode Flow Propagation

In 1992, Brun first described the use of colour M-mode flow propagation as an alternative measure of left ventricular relaxation in human beings (Brun, et al 1992). This method records the propagation of flow through the mitral valve orifice. It is measured from the apical four-chamber view; a colour Doppler sector is positioned over the mitral valve and into the left ventricle, then a cursor is placed through the centre of the mitral valve and a colour M-mode recording taken. Early papers describing this technique then measured the gradient of the E wave front and compared this to mitral E wave analysis and cardiac catheterisation measurements (Brun, et al 1992). The slope measured by Brun is not uniformly seen in all cases. Today, there are three different techniques used to measure colour M-mode propagation velocity (V_p) (Stoddard, et al 1994, Takatsuji, et al 1996, Garcia, et al 1998). However, a recent paper comparing these techniques recommended the

method of Garcia and colleagues (Garcia, et al 1998, Sessoms, et al 2002). This technique has been refined so that the slope of the first aliasing velocity of the early filling wave is measured from the mitral valve plane, four centimetres distally into the left ventricular cavity (Garcia, et al 1997, Garcia, et al 1998). The advantages of using colour M-mode analysis is that it provides both good temporal and spatial resolution.

In human beings, colour M-mode flow propagation generally demonstrates a good correlation with transmitral results in normal patients. However, in patients with heart disease and pseudonormal flow patterns the V_p was decreased, suggesting that it is a relatively pre-load insensitive measure of diastolic function (Takatsuji, et al 1996). In addition, in catheterised patients, it has been shown that V_p is inversely related to τ . During both beta-blockade and asynchronous contraction (engendered by large acute myocardial ischaemia) this correlation remains; suggesting that V_p is independent of cardiac geometry but is in fact responding to changes in wall motion (Stugaard, et al 1993). The asynchronous wall motion observed in many disease states, including myocardial infarction, dilated cardiomyopathy (DCM) and hypertrophic cardiomyopathy (HCM), reduces V_p , independent of mitral inflow (Brun, et al 1992, Stugaard, et al 1993, Møller, et al 2000).

The correlation between V_p and τ during dobutamine infusion, led Brun to the conclusion that V_p was independent of preload (Brun, et al 1992). This independence has since been demonstrated in both animal and human models and it has been found that ventricular relaxation is the main determinant of V_p in a variety of loading conditions (Garcia, et al 1999, Garcia, et al 2000, Møller, et al 2000). The

V_p is therefore not the equivalent of the transmitral E velocity. The difference between these two variables is thought to be due to the formation of vortices during the acceleration of flow through the mitral annulus. It is the propagation of these vortices that play a major role in determining V_p (Vierendeels, et al 2002).

Since V_p does not undergo pseudonormalisation, the ratio of these variables (E/V_p) corrects for the effect of left ventricular relaxation. Therefore, E/V_p can be used as an estimation of capillary wedge pressure (Garcia, et al 1997). The results of studies in human beings indicate that V_p shows excellent correlation to τ and as such is the most accurate non-invasive indicator of left ventricular relaxation that can be established using conventional echocardiography (Garcia, et al 1997). Knowledge of the differences between this variable and other diastolic indexes enables us to draw inferences about both atrial pressure, and loading conditions, giving a better overview of the diastolic function of the left heart.

It has been demonstrated that, while analyses of conventional ultrasound techniques are able to provide an assessment of diastolic filling, the effect of various physiological and haemodynamic variables can lead to discrepancies between diastolic filling and diastolic function. Several techniques have been developed to try to assess myocardial function more accurately and to advance our understanding of different diseases. One such modality is Doppler tissue imaging (DTI); this includes a range of techniques that can be used to assess global and regional myocardial velocity and as such, give new insights into myocardial function and disease processes.

Pulsed-wave DTI (pw-DTI) is a technique that measures the instantaneous peak myocardial velocity as it moves through a pre-selected sampling gate. In people with myocardial disease, it has been shown to be a relatively load insensitive technique (Nagueh, et al 1997, Sohn, et al 1997, Agmon, et al 1999, Farias, et al 1999).

Peak E' represents myocardial distension during early diastole (E' demonstrates a good correlation with τ) (Oki, et al 1997, Sohn, et al 1997, Ommen, et al 2000). Therefore, pw-DTI patterns can be used to differentiate normal individuals from those with pseudonormal filling patterns (Nagueh, et al 1997, Farias, et al 1999) (Figure 15). It is known that both E and E' are positively correlated with τ , and as such indicate myocardial relaxation (Appleton, et al 1988, Oki, et al 1997, Sohn, et al 1997, Ommen, et al 2000). This correlation is much stronger for E' , because E is also affected by left atrial pressure (Choong, et al 1987, Choong, et al 1988, Stoddard, et al 1989, Thomas and Weyman 1991). It therefore follows that, by removing the effect of relaxation from the transmitral E wave velocity, I are left with a measure of left atrial pressure. This has been demonstrated by several groups, who have shown a strong correlation between E/E' and left atrial pressure (Nagueh, et al 1999b, Fristenburg, et al 2000, Ommen, et al 2000). In fact, E/E' is strongly related to pulmonary capillary wedge pressure even when the mitral flow patterns are partially summated (Nagueh, et al 1998). Overall, it has been found that, in human beings, an E/E' ratio of less than eight accurately estimates a normal atrial pressure, and a ratio of greater than fifteen indicates an increased filling pressure; values between eight and fifteen show some overlap and it is not possible to ascertain whether or not the atrial pressure is raised (Nagueh, et al 1997, Nagueh, et al 1999b, Ommen, et al 2000).

Doppler echocardiography has previously been used to investigate some of the indices of diastolic function in healthy cats, and the same transmitral and pulmonary venous flow patterns described in normal human beings have been demonstrated in this species (Santilli and Bussadori 1998). Furthermore, comparisons between the non-invasive indices of diastolic relaxation and invasive measurements in young healthy cats have demonstrated significant correlations between τ , and IVRT, V_p , peak A velocity and peak pulmonary venous S velocity (Schober, et al 2003). Peak E and pulmonary venous D were both found to be affected by relaxation, but both of these indices were preload sensitive. There was only a weak correlation between E' and τ (Schober, et al 2003). In addition, there was a moderate correlation between τ and pulmonary venous S, S' and transmitral A (Schober, et al 2003). There was no significant relationship between E' to E, or A duration to pulmonary venous atrial reversal duration and left ventricular end diastolic pressure (Schober, et al 2003). The load sensitivity of E and E' has also been reported in normal human beings, where it has been demonstrated that when systolic function is preserved, both E and E' are sensitive to loading conditions (Nagueh, et al 1999b, Friskenburg, et al 2000, Nagueh, et al 2001a). However, in diseased states it appears that E' becomes a relatively load insensitive variable and as such E' and $E:E'$ can be used to estimate τ (Choong, et al 1987, Choong, et al 1988, Stoddard, et al 1989, Thomas and Weyman 1991).

These diastolic variables have also been studied in cats with HCM. It has previously been reported that affected cats showed significantly lower E velocities, a reduced E deceleration, an increased A velocity and prolonged IVRT compared to normal cats (Bright, et al 1999). It has also been found that, as in human beings; pw-DTI indices

can be used to assess the velocity within the feline myocardium. The pw-DTI velocities have been reported in cats with HCM and compared to unaffected cats: A decrease was reported in both peak systolic and peak diastolic velocities, when recorded from the mitral annulus of affected cats (Gavaghan, et al 1999).

Aim

The aim of this study was to compare pw-DTI velocities to conventional echocardiographic assessment of diastolic filling in various disease states in geriatric cats, in order to further validate the use of pw-DTI as an investigative modality for use in the approximation of diastolic function in this species. This will then provide a reference for the clinical investigation of myocardial disease in the cat.

Materials and Methods

The selection of cases, identification of systemic disease, grouping of cats and echocardiographic examination protocol used in this study were identical to the procedures outlined in Chapter 3.

Grouping of the Cats

The cats were grouped on the basis of their transmitral E:A ratio and the ratio of transmitral A to pulmonary venous atrial reversal flow, according to the following criteria (Figure 15): Cats with a transmitral E:A and an A:Ar ratio of greater than one were classified as normal; cats with an E:A ratio of less than one and an A:Ar of greater than one were classified as having impaired relaxation; cats with a transmitral E:A of greater than one and an A:Ar of less than one were classified as pseudonormal or restrictive.

Statistical Analysis

The statistical analysis was carried out using S-Plus (version 6.2.1, 1988, 2003 Insightful Corp. S: Copyright Lucent Technologies Inc.). The population characteristics were analysed using a one-way analysis of variance (ANOVA), or for the binomial data (gender), a Fisher's exact test. The distribution of disease was assessed using a Chi squared analysis. The results of the echocardiographic analysis were adjusted to account for heart rate, using the square root R-R method. The

measurements were then compared using a one-way analysis of variance with multiple comparisons being performed using a Tukey analysis. The distribution of the means and the homoscedasticity of the residuals were tested. When either the distribution of the residuals or the variance was unsatisfactory, standard transformation techniques (\log_{10}) were applied to normalise the distributions. A p value of ≤ 0.05 was taken as demonstrating statistical significance.

Results

A total of 134 cats were considered for inclusion. However, 44 of these were excluded because they demonstrated summated transmitral flow patterns ($n=40$), or because the acquisition of pulmonary venous flow was not possible ($n=4$). In addition, a further ten cats were excluded because they could not be grouped accurately; eight of these had either an E:A ratio or an A:Ar ratio equal to one, and a further two failed to meet the grouping criteria (ie: both the E:A and A:Ar ratios were less than one). Therefore, a total of 80 cats were included in the analysis. Of these, 21 demonstrated normal relaxation flow patterns, 51 demonstrated flow patterns consistent with impaired relaxation and eight demonstrated either a pseudonormal ($n=4$) or restrictive filling pattern ($n=4$); due to the small sample size and a continuum of dysfunction, the latter two groups were analysed as one.

Population Characteristics

The weight, systolic blood pressure, heart rate at initial presentation, tT4, and serum creatinine concentrations, were not significantly different between any of the groups. However, there was a significant variation in the age of the cats ($p=0.01$), those with impaired relaxation flow patterns being significantly older than the normal cats. However, there was no significant difference in the age of the normal cats compared to the cats with pseudonormalisation or restrictive flow patterns, nor was there a significant difference in the age of the cats with impaired relaxation flow patterns, compared to the cats with pseudonormalisation or restrictive flow patterns. The

respiratory rate of the cats at initial presentation also differed ($p=0.05$), with the cats with pseudonormalised or restrictive flow patterns demonstrating a significantly higher respiratory rate than the cats with impaired relaxation flow patterns.

The distribution of different diseases was assessed (Table 11). There was no association between disease and diastolic function (other than the unaffected cats, which were all classified as normal).

Two-dimensional Analysis (Table 12 & Figure 16)

The left atrial diameter demonstrated a significant variation between the groups. Multiple comparisons demonstrated that this was due to a significant enlargement in the cats with pseudonormal or restrictive flow patterns, when compared to either the normal cats or the cats with impaired relaxation flow patterns. The thickness of the basilar interventricular septum (assessed from the right parasternal long-axis view) was significantly greater in the cats with impaired relaxation flow patterns compared to the normal cats.

M-mode Echocardiographic Analysis (Table 12 & Figure 16)

The diameter of the left ventricle during diastole was significantly different between the three groups, with the left ventricular diameter being significantly greater during diastole in the cats with pseudonormal or restrictive flow patterns, compared to the

cats with impaired relaxation flow patterns. The thickness of the interventricular septum during diastole was significantly greater in the cats with impaired relaxation flow patterns compared to the normal cats. The left ventricular free wall was thicker during diastole in the cats with pseudonormal or restrictive flow patterns compared to the normal cats. Whilst both the left ventricular ejection fraction and percentage fractional shortening demonstrated significant differences when all three groups were compared; multiple comparison analysis was unable to demonstrate significant differences between any two of the groups.

The colour M-mode Vp was not significantly different between any of the groups studied. The ratio of transmitral E wave velocity to Vp was calculated, this also failed to demonstrate any significant difference between the groups.

Spectral Doppler Analysis (Table 12 and Figures 16-17)

Both the aortic and pulmonary artery velocities demonstrated significant variations between the groups. Multiple comparisons demonstrated that in both cases this was due to a decreased velocity in the normal cats compared to the cats with impaired relaxation flow patterns, however, this trend failed to reach statistical significance with regard to the aortic velocity.

The transmitral E wave velocity (MVE) was significantly different between groups, with the cats with impaired relaxation flow patterns demonstrating a significantly lower MVE than the cats with pseudonormalised or restrictive flow patterns. The

transmitral A wave velocity (MVA) was significantly lower in the normal cats and in the cats with pseudonormalisation or restrictive flow patterns, compared to the cats with impaired relaxation flow patterns. As might be expected from the grouping criteria, the E:A ratio was significantly different between any two of the groups studied. The duration of the transmitral A wave was significantly shorter in the cats with pseudonormal or restrictive flow patterns compared to either the normal cats or the cats with impaired relaxation flow patterns.

The trans-tricuspid E wave was significantly higher in the cats with normal flow patterns compared to those with impaired relaxation patterns. There were no differences between the velocities recorded from either the normal cats or the cats with impaired relaxation flow patterns and those with pseudonormal or restrictive flow patterns. There was no significant variation in the A wave between groups. However, the ratio of trans-tricuspid E to A velocity was significantly lower in the cats with impaired relaxation or pseudonormal or restrictive flow patterns compared to the normal cats.

The pulmonary venous flow patterns demonstrated a significant variation in the velocity of the diastolic component; being lower in the cats with impaired relaxation flow patterns compared to the cats with pseudonormal or restrictive flow patterns. There was no significant difference in the velocity of the pulmonary venous flow S component, although the ratio of peak S to peak D was significantly lower in the cats with pseudonormal or restrictive flow patterns, when compared to either the normal cats or cats with impaired relaxation flow patterns. The atrial reversal velocity of the pulmonary venous flow was significantly higher in the cats with pseudonormal or

restrictive flow patterns compared to either those with normal or impaired relaxation flow patterns. The duration of the pulmonary venous atrial reversal wave was significantly prolonged in the cats with pseudonormal or restrictive flow patterns compared to either the normal cats or the cats with impaired relaxation flow patterns. The ratio of transmitral A duration to pulmonary venous Ar duration was likewise significantly lower in cats with pseudonormal or restrictive flow patterns compared to the cats with either normal or impaired relaxation flow patterns.

The spectral Doppler assessment of isovolumetric relaxation time (IVRT) demonstrated a significant prolongation in the cats with impaired relaxation flow patterns compared to the cats with pseudonormal or restrictive flow patterns.

Pulsed-wave Doppler Tissue Imaging (Table 12 and Figure 18)

The S' and A' velocities demonstrated no significant differences between the groups, at any of the sites studied. However, the E' velocities were significantly different between the groups at all of the sites studied, with the exception of the E' measured at the free wall from the right parasternal short axis view and the E' measured at the mid-interventricular septal level (from the left apical four chambered view). At each site the E' was higher in the normal cats than in the cats with impaired relaxation flow patterns. In addition, at the lateral aspect of the mitral annulus (assessed from the left apical four chamber view), the peak E' velocity was higher in the normal cats than in the cats with pseudonormal or restrictive flow patterns. The ratio of E' to A' was significantly higher in the normal cats than in the cats with impaired relaxation

flow patterns at all of the sites studied. In addition, the velocities recorded from the lateral wall (assessed from the left apical four chamber view) demonstrated a significantly higher ratio of E' to A' in the normal cats compared to the cats with pseudonormal or restrictive flow patterns. The ratio of transmitral E to E' was calculated for the longitudinal velocities recorded from the mitral annulus. At both the septal and the lateral aspect of the annulus, this ratio was significantly increased in the cats with pseudonormal or restrictive flow patterns compared to either the normal cats or the cats with impaired relaxation flow patterns.

Discussion

This study has for the first time demonstrated that when conventional variables are used to group cats according to their diastolic function, there is concurrence between the conventional groupings and the pw-DTI velocities, with cats with pseudonormal or restrictive flow patterns demonstrating significantly lower E' velocities at the majority of sites studied.

In this study all the cats were eight years of age, or older. In human beings, it has been reported that there is a 'natural history of diastolic function', with normal older people (over seventy years of age) demonstrating impaired relaxation (Appleton, et al 2000). It is unclear whether or not such a phenomenon also occurs in the cat, or at what age such a E to A reversal might occur. It has been reported that as cats age the transmitral peak E velocity decreases (Koffas, et al 2001, Koffas 2003, Koffas, et al 2005). However, I have previously demonstrated that, in a cohort of cats eight years of age or over, there is no significant association between age and early diastolic velocities (Chapter 3). In the current study, there was a significant difference between the age of the cats with impaired relaxation flow patterns and the cats in the normal group, with cats demonstrating patterns consistent with impaired diastolic function being older than the normal cats. However, there was no difference between the age of the normal cats and those with pseudonormal or restrictive relaxation flow patterns, or between the age of the cats with impaired relaxation flow patterns and those with pseudonormal or restrictive relaxation flow patterns. Since the aim of this study was to examine the level of agreement between different techniques of assessing diastolic function, not to describe which cats demonstrate

diastolic dysfunction; effects imposed by age would only be relevant if they affected one method of assessment more than another. In human beings, diastolic function is thought to deteriorate as an individual ages and as the left ventricle becomes more fibrotic (Appleton, et al 2000). Since this primarily affects the ventricle, rather than being a loading affect, all of the methods of assessment should, theoretically, be affected to a similar degree.

The respiratory rate of the cats with pseudonormal or restrictive flow patterns was elevated compared to that of the cats with impaired relaxation flow patterns. This is perhaps not surprising, as the cats with pseudonormal or restrictive flow patterns are most likely to be in congestive heart failure (CHF), and would therefore be expected to demonstrate a higher respiratory rate than the other groups of cats. What is perhaps surprising, and may highlight one of the main limitations of this study, is that there was no significant difference between the normal cats and those with pseudonormal or restrictive flow patterns. This may represent the inaccuracy of grouping cats by load sensitive measures of diastolic function, and might suggest that some of the cats in these groups were misclassified. However, without invasive measures, the diastolic function of each of the cats could not be determined conclusively, and although in human beings pw-DTI has been shown to be relatively load insensitive, until now this technique has not been applied to a large number of cats.

Two-dimension Analysis

The left atrial diameter was significantly greater in the cats with pseudonormal or restrictive flow patterns compared to either of the other groups. Although, as it has been previously stated, there may have been some cats which were 'misclassified' as either normal or pseudonormal, the significantly greater atrial diameter in this group suggests that the majority of these cats were grouped correctly. Those with elevated left atrial pressures (ie: the cats with pseudonormal or restrictive flow patterns) would be expected to have left atrial enlargement, whereas those with normal or impaired relaxation should not have elevated left atrial pressures and therefore should have had normal left atrial diameters.

The thickness of the interventricular septum, assessed from the right-parasternal long axis view, was significantly elevated in the cats with impaired relaxation flow patterns compared to the normal cats. I have previously demonstrated that in a group of cats with lone basilar septal bulge (BSB) the diastolic function was not significantly different to a group of normal cats (Chapter 5). In addition, the M-mode measurement of the interventricular septum during diastole, also demonstrated that the cats with impaired relaxation flow patterns had significantly thicker septi than the other groups of cats. The cats with pseudonormal or restrictive flow patterns demonstrated greater diastolic measurements of free wall thickness than the other groups of cats. Together, these findings might suggest that cats with isolated interventricular hypertrophy are more likely to demonstrate impaired relaxation, whereas those with increased free wall thickness, are more likely to have pseudonormal or restrictive flow patterns. Previously, it has been reported that cats

with hypertrophic obstructive cardiomyopathy (HOCM) have an improved prognosis compared to those with HCM (Rush, et al 2002). Since HOCM is usually associated with hypertrophy of the interventricular septum, it may follow that these cats had greater septal thicknesses.

The diameter of the left ventricle during diastole was significantly greater in the cats with pseudonormal or restrictive flow patterns compared to the cats with impaired relaxation flow patterns, but was not significantly different from the normal cats. It is recognised that cats with HCM have a normal or slightly decreased diastolic diameter (Bright, et al 1992, Fox 1999). However, once the disease progresses to CHF (those with pseudonormal or restrictive flow patterns) there is an increase in ventricular loading (Koffas 2003). The significant difference in the left ventricular diastolic diameter between these two groups is likely to be a combination of a slight (non-significant) decreased diameter in the cats with impaired relaxation flow patterns and an increased diameter in the cats with pseudonormal or restrictive flow patterns.

Although there were significant differences in the fractional shortening (FS) and ejection fraction (EF) between groups, these differences were relatively weak and variations between specific groups could not be identified. The systolic M-mode measurements were not significantly different between the groups. Since the groups were divided according to diastolic function this is not entirely unexpected, although one might have hypothesised that the cats with severely abnormal diastolic function might have had some systolic abnormalities.

Neither the Vp nor the ratio of transmitral E wave to Vp were sensitive enough to detect difference between the different groups. I have previously reported that the measurement of Vp is poorly repeatable, with a coefficient of variation of 50% (Chapter 2). Although the measurement of Vp can vary from 0 to infinity and theoretically the poor repeatability may therefore be of little relevance, in reality (in the absence of constrictive pericardial disease) the measurement of Vp tends to vary between 10 and 100 cm/sec and therefore the poor repeatability will confound these results.

Spectral Doppler Analysis

The velocity of flow within the aortic and pulmonary artery was increased in the cats with impaired relaxation flow patterns compared to the normal cats, although this trend failed to reach significance in the case of the aortic velocity. This finding lends further credence to the hypothesis that the cats with dynamic ventricular outflow obstruction and septal hypertrophy are more likely to demonstrate impaired relaxation and therefore, would carry an improved prognosis, as has been reported previously (Rush, et al 2002). Alternatively, cats with pseudonormal or restrictive flow patterns might have decreased velocities of ventricular outflow, although I found no evidence that this group had decreased systolic function.

The differences in the transmitral flow patterns was expected, with cats with impaired relaxation flow patterns demonstrating decreased E wave velocities and increased A wave velocities, and with this an altered E:A ratio. Since the ratio of peak E wave velocity to peak A wave velocity was one of the criteria used to group the cats, little significance should be attributed to these changes. The duration of the transmitral A wave was significantly shorter in cats with pseudonormal or restrictive flow patterns. Whilst the ratio of A:Ar was another of the criteria used to group the cats, it is notable that this duration was decreased in the cats with pseudonormal or restrictive flow patterns (as well as the duration of Ar being prolonged). The A wave duration is likely to be decreased in cats with restrictive physiology as the decreased ventricular compliance will cause the atrioventricular pressure gradient to equalise more quickly (Thomas and Weyman 1991). Further analysis of the data (not shown) demonstrated that three of the four cats with restrictive flow patterns demonstrated the shortest durations of transmitral A wave flow.

The trans-tricuspid flow patterns demonstrated a significantly higher velocity of early diastolic filling in the normal cats compared to the other groups. However, there were no other differences detected between the groups. Whilst the pattern of trans-tricuspid flow is subject to alterations with respiration (Appleton, et al 2000), the apparent lack of right-sided abnormalities may suggest that these cats demonstrated primarily left-sided changes.

The systolic component (S) of the pulmonary venous flow patterns demonstrated no significant variation between the groups. However, the diastolic component (D) was decreased in cats with impaired relaxation flow patterns compared to those cats with

normal or with pseudonormal and restrictive flow patterns. It has previously been reported that in normal cats the S and D waves are approximately equal (ratio of S:D 1.14 ± 0.32 and 0.9 ± 0.29) (Santilli and Bussadori 1998, Schober, et al 2003). In human beings, as diastolic function becomes impaired, the ratio of S to D is reported to reverse, with the D wave becoming smaller (Appleton 1997). Since this is primarily due to diastolic dysfunction, the decrease in D wave peak velocity is not surprising, although it might have been expected that the cats with pseudonormal and restrictive flow patterns would vary from both the cats with a filling pattern suggestive of impaired relaxation and the normal cats.

The ratio of S:D was significantly decreased in cats with pseudonormal or restrictive flow patterns compared to the other groups of cats. This ratio is thought to reflect ventricular compliance and filling pressures (Appleton 1997). It is therefore not surprising that the group of cats containing those with the least compliance (ie: a restrictive flow patterns) demonstrated the lowest S:D ratios.

The velocity of peak atrial reversal flow was elevated in cats with pseudonormal or restrictive flow patterns. This group of cats should represent those with increased left atrial pressures. This assumption is supported by the increased left atrial size in this group of cats, and further supported by the increased atrial reversal velocities. Since there is no valve between the left atrium and the pulmonary veins, an increase in left atrial pressure results in an increased 'back pressure' on the pulmonary circulation and therefore an increased velocity of the pulmonary venous atrial reversal wave (Appleton 1997).

Whilst the duration of transmitral A to pulmonary venous atrial reversal wave was significantly different between groups (being lower in the cats with pseudonormal or restrictive flow patterns), this ratio was one of the criteria used to group the cats and therefore these findings are to be expected.

The IVRT has been reported to increase in people and cats with impaired diastolic function, and, in people, to decrease when there is a restrictive physiology (Nishimura, et al 1989a, Myreng and Smiseth 1990, Bright, et al 1999). In agreement with these reports, my results demonstrated a significant increase in the IVRT of cats with impaired relaxation flow patterns compared to those with restrictive or pseudonormal flow patterns. However, I demonstrated no significant difference between the normal cats and the cats with impaired relaxation flow patterns. This may represent misclassification of cats or inaccuracies of the measuring technique: The latter may result from the logistics of data storage that required the 'echo-pac' software to round-off these very short durations to the closest 0.01 second.

Pulsed-wave Doppler Tissue Imaging

There were no significant difference in the S' or A' velocities at any of the sites studied between any of the groups. It could therefore be inferred that the cats demonstrated no significant systolic dysfunction. This would be supported by the lack of alteration in the conventional measures of systolic function. The A' would be expected to decrease in cats with a restrictive physiology, as it does in human beings

with restrictive cardiomyopathy (Nishimura, et al 1989a, Appleton, et al 2000). However, since there were only four cats with restrictive flow patterns, these cats were analysed with the cats with pseudonormal flow patterns, and therefore, inferences regarding this group alone cannot be made.

The E' velocity was decreased in the normal cats compared to the cats with impaired relaxation flow patterns at all the sites interrogated, although this failed to reach significance at the short axis free wall site (assessed from the right parasternal long-axis view) and at the level of the mid-septum (assessed from the left apical four chamber view). A decrease in E' has been reported previously in cats with HCM (Gavaghan, et al 1999, Koffas 2003, Koffas, et al 2005)(Chapter 5). The measures of pw-DTI are considered to be relatively load insensitive and therefore more representative of diastolic function (Nagueh, et al 1997, Sohn, et al 1997, Agmon, et al 1999, Farias, et al 1999). Peak E' represents myocardial distension during early diastole (E' demonstrates a good correlation with τ) (Oki, et al 1997, Sohn, et al 1997, Ommen, et al 2000). Therefore, pw-DTI patterns can be used to differentiate normal individuals from those with pseudonormal flow patterns (Nagueh, et al 1997, Farias, et al 1999). This study demonstrates such a decrease in the E' velocities, although statistical significance was not always obtained. This was probably due, in part, to the small sample size, particularly in the pseudonormal and restrictive flow patterns group, and possibly due to the potential misclassification of cats. Since I could not obtain any invasive measurements I did not have a 'gold standard' with which to compare my cases; I was therefore reliant upon load dependant estimates of diastolic function. If, in the cat, the assessment of pw-DTI is as load insensitive as

has been suggested in the human field, then the grouping of cats according to load sensitive measurements may have lead to misclassification of cases and with this, spurious results. However, in human beings, it has been shown that pw-DTI is more accurate at identifying diastolic dysfunction than conventional methods (Nagueh, et al 1997, Sohn, et al 1997, Agmon, et al 1999, Farias, et al 1999). Unfortunately, without invasive measurements, I am unable to provide information regarding the sensitivity of these techniques in the cat.

The ratio of E' to A' was decreased in cats with pseudonormal or restrictive flow patterns. This is similar to findings reported in human beings, where it is reported that as diastolic function deteriorates there is a decrease in the E' velocity, with an initial increase in A' amplitude and then a gradual decrease in both E' and A' waves (Nagueh, et al 1997, Farias, et al 1999).

The E to E' ratio was calculated for the mitral annular velocities. Since E is dependant upon both the left atrial pressure and left ventricular relaxation and E' is a more load independent measure, the ratio of E to E' can be used to calculate left atrial pressure (Nagueh, et al 1999b, Fristenburg, et al 2000, Ommen, et al 2000). At both the lateral and septal aspects of the mitral annulus this ratio was increased in cats with pseudonormal or restrictive flow patterns, therefore suggesting that this group of cats demonstrated elevated left atrial pressures. In human beings, it has been found that an E:E' ratio of less than eight accurately estimates a normal atrial pressure, and a ratio greater than 15 indicates an increased filling pressure. However, values between eight and 15 show some overlap and it is not possible to ascertain whether or not the atrial pressure is raised (Nagueh, et al 1997, Nagueh, et

al 1999b, Ommen, et al 2000). It is perhaps notable that at the lateral aspect of the mitral annulus none of the normal cats demonstrated a E:E' greater than 15, furthermore, none of the cats with pseudonormal or restrictive flow patterns demonstrated a ratio of less than eight. There were four cats, classed as normal, which had an E:E' ratio between eight and 15; three of these cats demonstrated a left atrial diameter within the 75th percentile (of the normal group of cats). There were three normal cats with elevated E:E' ratios when the septal aspect of the mitral annulus was assessed, one of which had an enlarged left atrium. There were no cats with pseudonormal or restrictive flow patterns, which demonstrated a ratio below eight at this site. These observations provide some evidence that E:E' may also provide us with a non-invasive estimate of left atrial pressure for use in the cat.

Limitations

As stated previously, the current study grouped the cats according to their conventional echocardiographic measurements of diastolic function. This is not ideal, since it is known that these measurements are subject to affects other than ventricular diastolic function. Ideally, invasive measurements would have been correlated to the diastolic measures. To minimise the inaccuracy of these grouping I relied on both transmitral E:A ratio and the ratio of the duration of transmitral A to pulmonary venous Ar wave, rather than utilising just one measure of diastolic function. The increased left atrial size in the pseudonormal and restrictive flow patterns group would suggest that the grouping criteria used were not completely

inappropriate. However, there were some cats that were judged to be normal, but which demonstrated either areas of hypertrophy ($n=12$), and/or an increased left atrial diameter ($n=1$). By grouping the cats in this manner the study became biased, because altered loading conditions may have led to some cats with pseudonormal function being placed in the normal group, thereby making us less likely to detect differences in the pw-DTI measurements.

Pseudonormal and restrictive flow patterns were not common (there were only four cats with each filling pattern). I therefore decided to place these cats in one group. Whilst it is expected that there may have been some variations between these cats, there is a dynamic continuum from pseudonormal to restrictive flow, so analysing these cats as a single group should not have dramatically altered my results.

Whilst the different groups included cats with a variety of diseases and receiving a variety of medications, these were representative of cases presented to our clinic and are therefore, representative of the clinical situation. Furthermore, this study was designed to assess the agreement between different estimates of diastolic function, not the affect of disease upon the myocardium. Assessment of the distribution of disease amongst the diastolic flow pattern groupings demonstrated that there was no association between filling pattern and disease in any of the groups (other than the unaffected cats which were all classified as normal, $p<0.001$).

Conclusions

I found that the majority (64%) of cats over eight years of age demonstrated a filling pattern consistent with impaired relaxation. This is reported as a normal finding in people over seventy years of age (Schirmer, et al 2000). However, in the current study, which only included cats over eight years of age, there were 21 cats (26%) that were judged to have normal diastolic function on the basis of their transmitral and pulmonary venous flow patterns. Whilst these criteria are not specific at determining diastolic function, this finding may suggest that normal cardiac function is not uncommon in aged cats. Furthermore, this study was performed using clinical cases, some of which were referred to our institution, so it may have been biased toward the inclusion of cats with cardiac abnormalities, and the incidence of diastolic dysfunction in this population cannot truly be assessed.

I was able to demonstrate that cats can show all of the diastolic patterns seen in human beings, and found good agreement between the changes observed using the different methods. Invasive studies performed in normal cats have previously demonstrated that with alterations in load and heart rate the feline myocardium responds in a similar manner to the human myocardium (Schober, et al 2003), and this study would support those findings.

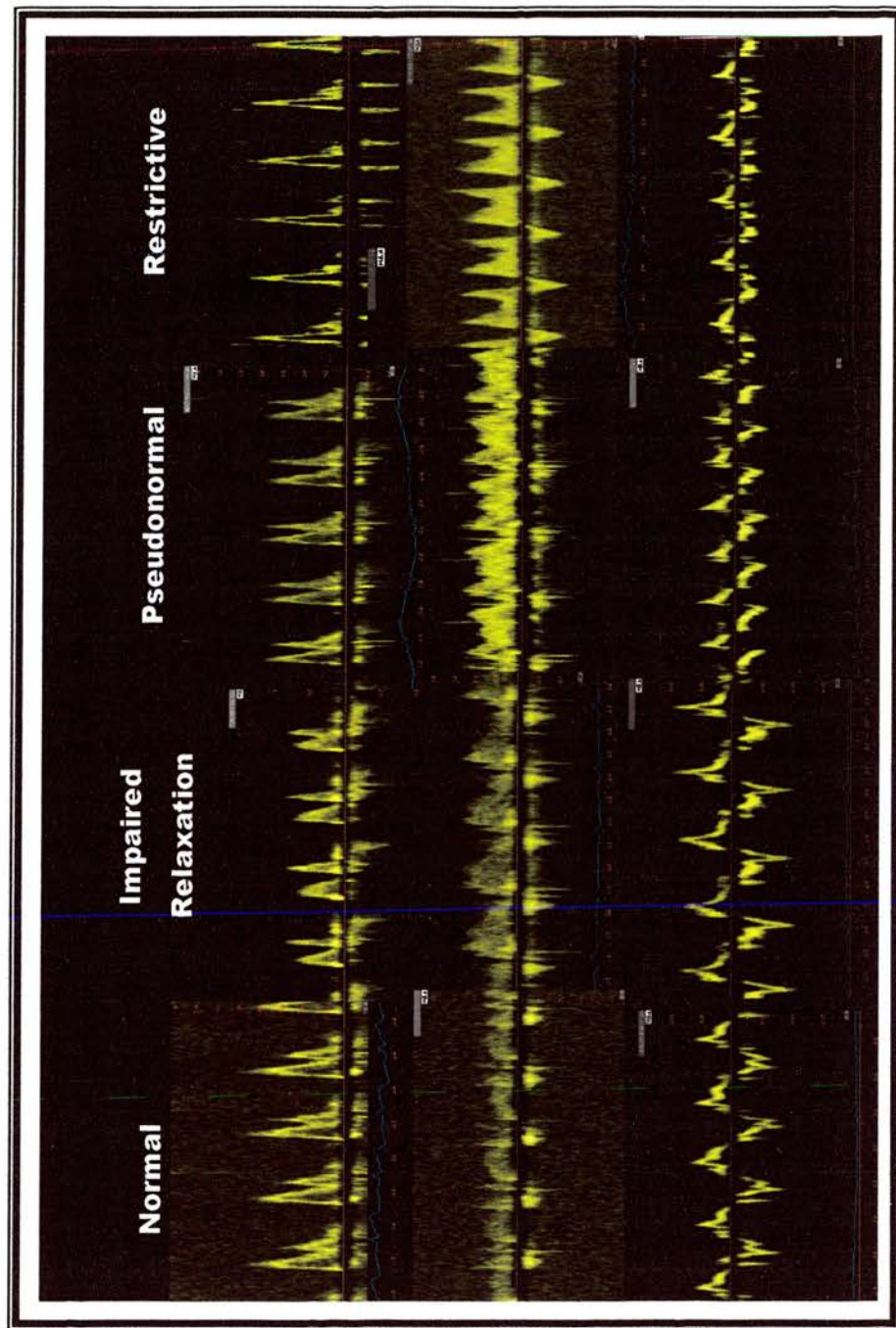
This study enabled us to describe a variety of methods of assessing diastolic function in the cat, and to discuss the suitability of these methods of assessment in a group of aged cats. Whilst the majority of cats fell into a particular functional group, there were a total of forty cats that were not grouped; the majority of these demonstrated

summation of their transmitral or pulmonary venous flow patterns. Pulsed-wave DTI offers a new method of assessment for cases that cannot be classified using the conventional measurements. This is because the E' and A' velocities recorded by pw-DTI rarely demonstrated summation and the technique can therefore be used to help assess cats with summated transmitral or pulmonary venous flow patterns. In support of this, in human beings, it has been shown that the ratio of E to E' provides a good estimate of left atrial pressure even when the transmitral velocities are summated (Nagueh, et al 1998).

It is the authors belief that, since no single non-invasive method of assessing diastolic function is infallible, as many different measures of diastolic function should be assessed as possible to try to identify localised areas of myocardial dysfunction. This will help categorise cats according to their functional abnormalities rather classifying them entirely on ventricular morphology. The combination of DTI and mitral and pulmonary flow dynamics may provide us with a better estimate of left ventricular filling pressures. However, the accurate assessment of an individual patient (rather than a large group of cats) requires a stepwise approach, incorporating all the available data.

This study provides evidence that the human classification system and the described methods of determining diastolic function can be used to assess myocardial function in the cat and thereby provides an extra tool for the diagnosis of myocardial disease. In the future, the use of these techniques might be useful in determining the prognosis of a particular case and in deciding whether or not medical intervention is advocated.

Figure 15: The effect of varying diastolic function of transmitral, pulmonary venous and pulsed wave Doppler tissue imaging (pw-DTI) velocities



Where the first row represents the different stages of diastolic function measured by transmitral flow, the second row, the different pulmonary venous flow patterns which are recognised and the third row, the relatively preload independent assessment by pw-DTI:- note the progressive decrease in E' velocity, compared to the increase that occurs with pseudonormalisation in the conventional techniques.

Table 11: The association between disease and diastolic flow pattern

Disease	Normal (n)	Impaired Relaxation (n)	Pseudo, or Restrictive (n)	Chi-Squared value and P-value
Acromegaly	0	1	0	X^2 2.483, $p=0.289$
BSB	3	10	0	X^2 2.034, $p=0.362$
CRF	3	8	3	X^2 0.375, $p=0.829$
CRFHiBP	1	2	0	X^2 0.375, $p=0.584$
DM	1	2	1	X^2 1.075, $p=0.584$
DMCRF	2	1	0	X^2 2.703, $p=0.259$
HCM	0	9	1	X^2 4.235, $p=0.120$
HiBP	0	3	0	X^2 1.772, $p=0.412$
HiT4	5	7	1	X^2 1.203, $p=0.545$
HiT4CRF	0	5	1	X^2 2.412, $p=0.299$
HiT4HiBP	0	3	1	X^2 2.136, $p=0.344$
Unaffected	6	0	0	X^2 18.22, $p<0.001$

Where: n, number of cats; Pseudo., pseudonormal flow pattern; X^2 , Chi-squared value; BSB, basilar septal bulge; CRF, chronic renal failure; HiBP, hypertension; DM, diabetes mellitus; HCM; hypertrophic cardiomyopathy.

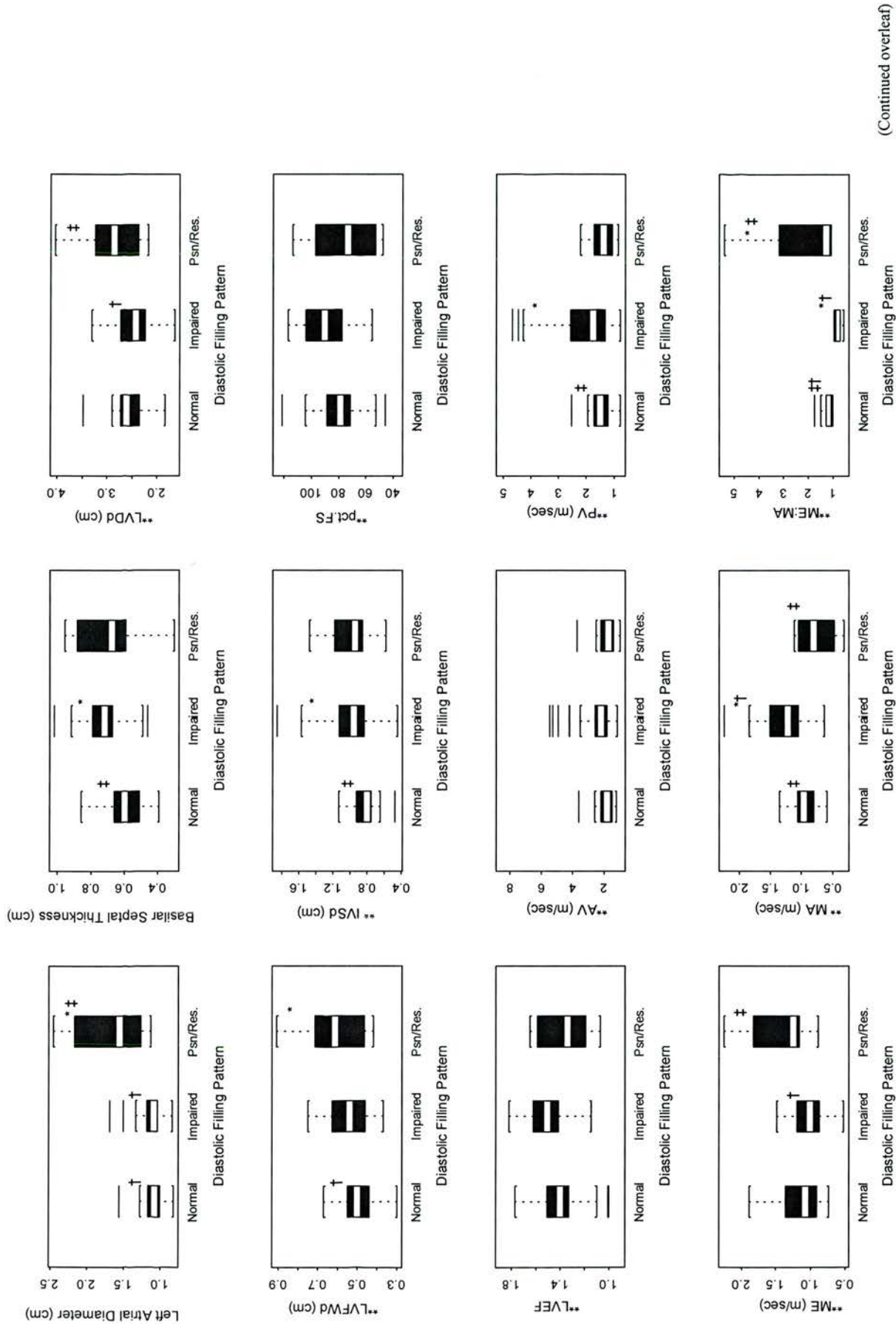
Table 12: Results of the one-way analysis of variance (ANOVA) assessing the differences in echocardiographic measurements between the groups (quoting the associated test statistic (F), the probability that the difference in variation was due to chance (P) and the degrees of freedom(subscript)).

2D Heart Variables	Disease	
	F	P
Ao Diameter*	(2,77)=1.114	0.334
Left Atrial Diameter*	(2,77)= 24.070	<0.001
Septal Thickness*	(2,77)= 8.329	0.001
M-mode Variables		
LVDd	(2,77)= 4.296	0.017
LVPwd	(2,77)= 4.457	0.015
LVDs	(2,77)=3.078	0.052
LVPws	(2,77)=2.358	0.101
IVSd	(2,77)= 4.247	0.018
IVSs	(2,77)=1.107	0.336
FS	(2,77)= 3.615	0.048
EF	(2,77)= 3.883	0.025
Vp	(2,73)=2.102	0.130
E:Vp	(2,73)=0.961	0.387
Spectral Doppler Variables		
AV	(2,75)= 3.788	0.027
PV	(2,77)= 4.288	0.017
ME	(2,77)= 6.707	0.002
MA	(2,77)= 17.850	<0.001
ME:MA	(2,77)= 64.584	<0.001
ME+A	-	-
TE	(2,67)= 3.737	0.029
TA	(2,67)= 2.245	0.114
TE:TA	(2,67)= 19.409	<0.001
TE+A	(2,2)=1.821	0.355
IVRT	(2,74)= 3.494	0.035
PVD	(2,77)= 3.924	0.024
PVS	(2,77)=1.271	0.286
PVS:D	(2,77)= 8.855	<0.001
PVAr	(2,77)= 8.829	<0.001
ArDur	(2,77)= 18.638	<0.001
MADur	(2,77)= 10.877	<0.001
MA:Ar Dur	(2,77)= 50.610	<0.001

Tissue Doppler Variables	Disease	
	F	P
Long Axis Free Wall		
S'	(2,76)=0.705	0.477
E'	(2,74)= 3.473	0.036
A'	(2,74)=0.125	0.882
E':A'	(2,74)= 3.212	0.046
Short Axis Free Wall		
S'	(2,74)=0.892	0.414
E'	(2,72)=2.089	0.131
A'	(2,72)=2.089	0.137
E':A'	(2,72)= 8.226	<0.001
Apical Lateral Wall		
S'	(2,69)=1.350	0.267
E'	(2,61)= 4.806	0.012
A'	(2,61)=1.120	0.333
E':A'	(2,61)= 9.226	<0.001
Apical View Mid-Septum		
S'	(2,72)=1.768	0.178
E'	(2,70)=1.550	0.220
A'	(2,70)=1.342	0.268
E':A'	(2,70)= 5.801	0.005
Apical Septal Mitral Annulus		
S'	(2,73)=0.933	0.397
E'	(2,71)= 6.029	0.004
A'	(2,71)=2.052	0.136
E':A'	(2,71)= 10.003	<0.001
ME:E'	(2,71)= 5.122	0.008
Apical Lateral Mitral Annulus		
S'	(2,70)=2.566	0.084
E'	(2,70)= 6.840	0.002
A'	(2,68)=0.058	0.943
E':A'	(2,68)= 4.770	0.012
ME:E'	(2,68)= 7.099	0.002

Where: F, F-value, subscript numbering is the degrees of freedom of the groups and the residuals; P, P-value; Ao, aorta; LVD, left ventricular diameter; IVS, interventricular septum; LVPw, left ventricular posterior wall; d, diastole; s, systole; Vp, propagation velocity; FS, percentage fractional shortening; EF, ejection fraction; AV, aortic velocity; PV, pulmonary velocity; ME and MA, transmitral early and late diastolic flow, respectively; ME+A, the velocity of the summated transmitral flow; TE and TA; trans-tricuspid early and late diastolic flow, respectively; TE+A, summated trans-tricuspid flow; IVRT, isovolumic relaxation time; PV, pertaining to pulmonary venous; S, systolic flow; D, diastolic flow; Ar, atrial reversal flow; V, velocity; Dur, duration; S', systolic velocity; E', early diastolic velocity; A', late diastolic velocity; E'+A', summated diastolic flow. Bold type-face represents a P<0.05.

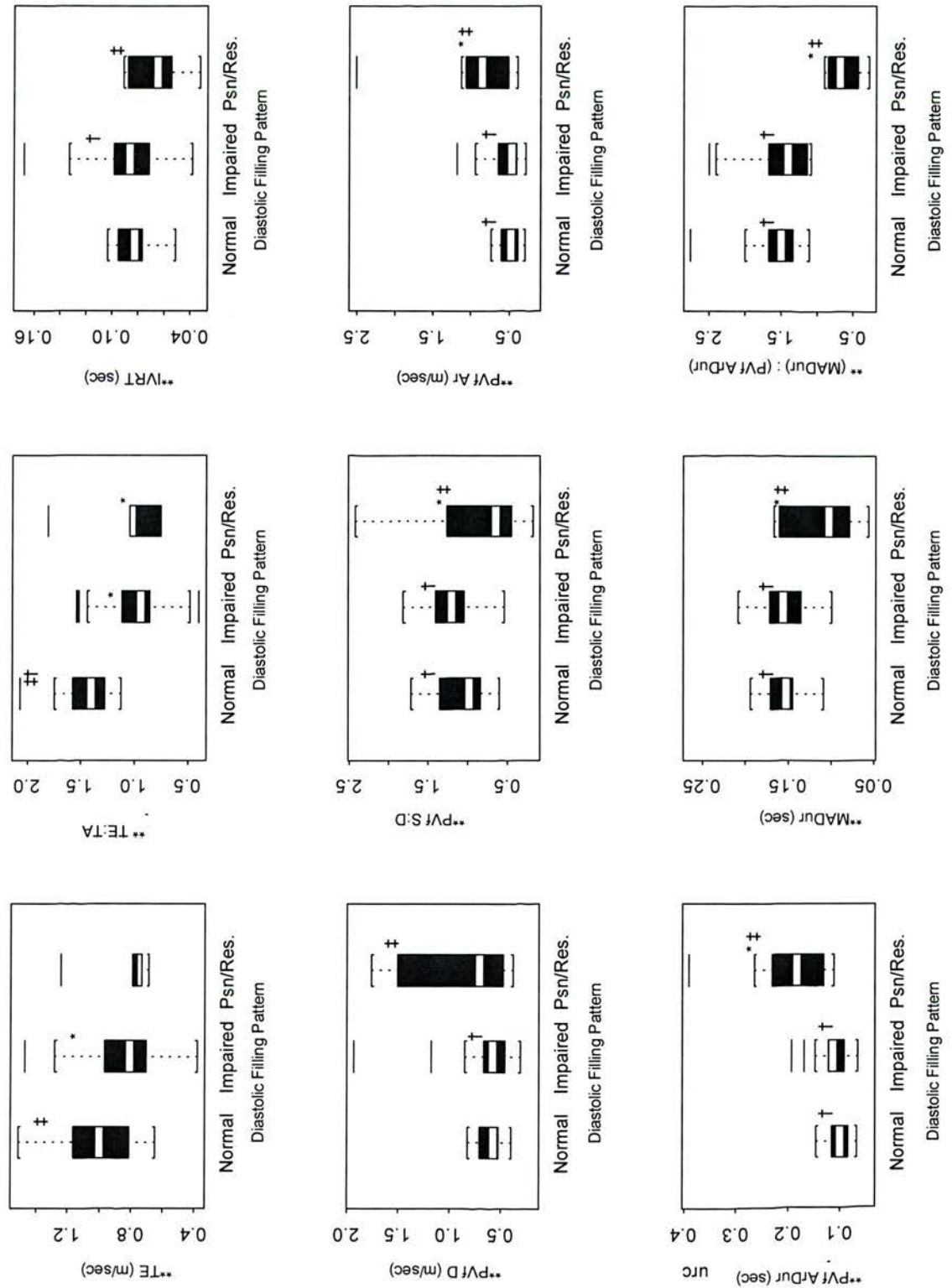
Figure 16: Significant variations between groups



(Continued overleaf)

Where: The limits of the boxes represent the inter-quartile range, the white bar the mean, the whiskers extend to the nearest value not beyond a standard span (1.5) from the quartiles. **Measurements have been corrected for heart rate using the $\sqrt{R-R}$ method. LVD, left ventricular diameter; IVS, interventricular septum; LVFW, left ventricular free wall; d, diastole; pct.FS, percentage fractional shortening; LVEF, left ventricular ejection fraction; AV, aortic velocity; PV, pulmonary velocity; ME and MA, transmitral early and late diastolic flow, respectively; Psn/Res., pseudonormal or restrictive group; *, significantly different from the normal cats ($p < 0.05$); #, significantly different from the impaired relaxation group ($p < 0.05$); +, significantly different from the pseudonormal/restrictive group ($p < 0.05$)

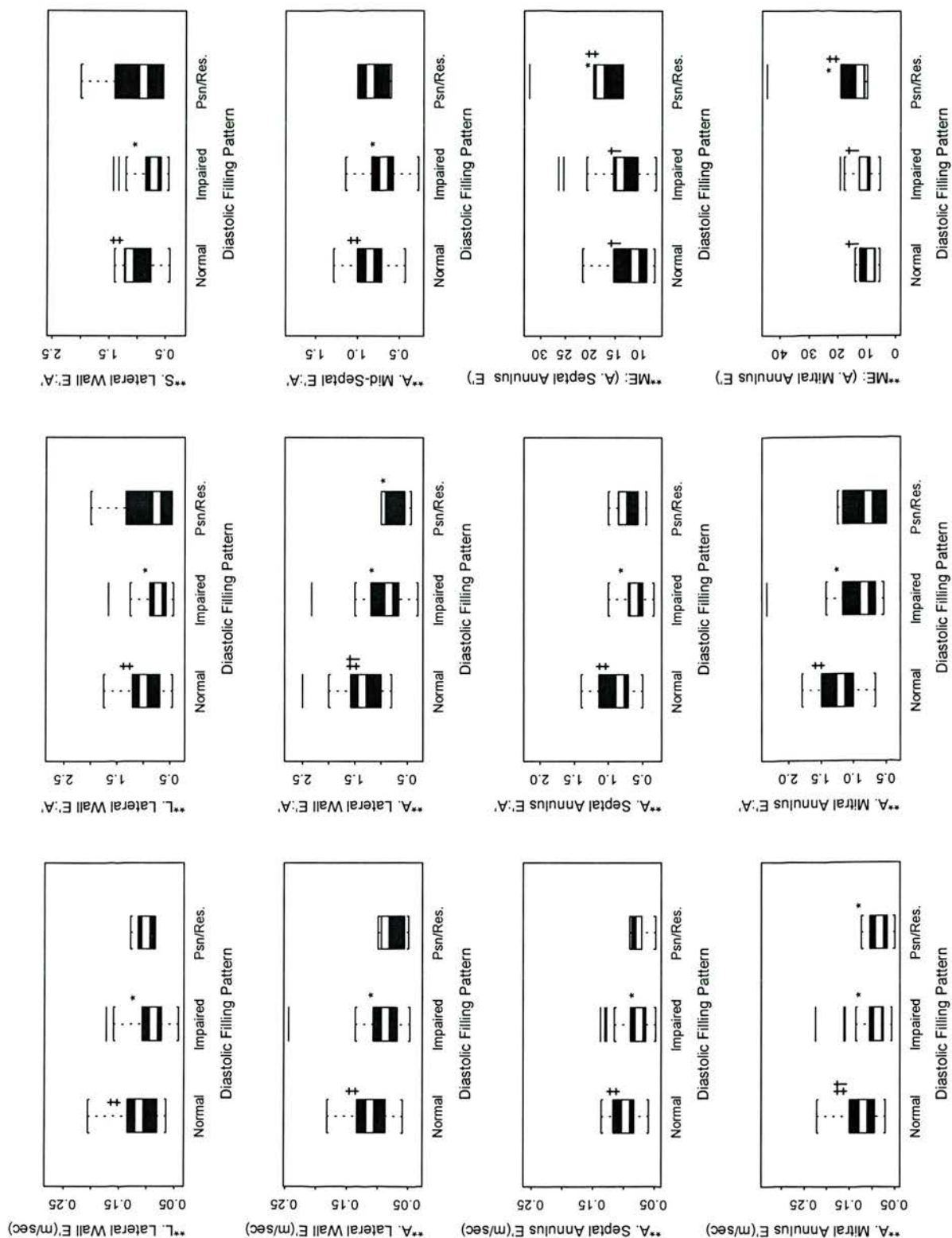
Figure 17: Significant variations between groups (continued)



Where: The limits of the boxes represent the inter-quartile range, the white bar the mean, the whiskers extend to the nearest value not beyond a standard span (1.5) from the quartiles. **Measurements have been corrected for heart rate using the $\sqrt{R-R}$ method. TE and TA, trans-tricuspid early and late diastolic flow, respectively; IVRT, isovolumic relaxation time; PvF, pertaining to pulmonary venous; S, systolic flow; D, diastolic flow; Ar, atrial reversal flow; Dur, duration; MA, transmitral late diastolic flow; Psn/Res., pseudonormal or restrictive group; *, significantly different from the normal cats ($p < 0.05$); †, significantly different from the impaired relaxation group ($p < 0.05$); †, significantly different from the pseudonormal/restrictive group ($p < 0.05$)

(Continued overleaf)

Figure 18: Significant variations between groups (continued)



Where: The limits of the boxes represent the inter-quartile range, the white bar the mean, the whiskers extend to the nearest value not beyond a standard span (1.5) from the quartiles. **Measurements have been corrected for heart rate using the $\sqrt{R-R}$ method. L.; Left apical four-chambered view; E'; early diastolic velocity; E'A'; late diastolic velocity; ME, transmitral early diastolic flow; Psn/Res., pseudonormal or restrictive group.*, significantly different from the normal cats ($p < 0.05$); †, significantly different from the impaired relaxation group ($p < 0.05$); ‡, significantly different from the pseudonormal/restrictive group ($p < 0.05$)

General Discussion

The aim of this study was to assess the pw-DTI velocities in a range of primary and cats with disease states linked to specific cardiomyopathies in human beings, in order to ascertain whether or not there are any disease specific abnormalities in myocardial function. In doing so I hoped to gain a greater insight into the main cardiac derangements in a range of feline disorders.

Initially, the repeatability of a wide range of pw-DTI velocities were assessed. It was demonstrated that the pw-DTI velocities recorded during the isovolumic phases, the velocity of the tricuspid annulus, and radial fibre velocity within the interventricular septum, were poorly repeatable. However, the predominant (S', E' and A') pw-DTI velocities from the left apical four-chambered view, generally demonstrated a coefficient of variation of ~20%, which I felt represented an acceptable level of repeatability. In light of these findings, the radial velocities within the interventricular septum and the velocity of motion during the isovolumic phases and the right ventricular wall motion were excluded from further analyses.

In order to fulfil my aim it was felt necessary to further assess what affects various confounding influences were imposing on the pw-DTI measurements. In order to achieve this multiple linear regression analyses were performed to determine whether or not, in a group of cats eight years of age or above, either age or R-R interval was significantly related to the recorded velocity. I found that, in geriatric cats, irrespective of disease status, pw-DTI velocities were generally not related to the age

of the cat. However, in healthy animals, heart rate (assessed by the R-R interval) significantly influenced several of the pw-DTI velocities, especially those assessing radial motion. In light of these findings, in healthy animals, the influence of heart rate upon Doppler variables should always be considered in the interpretation of pw-DTI variables. The heart rate dependence of pw-DTI velocities in normal cats suggests that when normal cats are included in the analysis, a correction term should be incorporated.

Once the expected variability and the affects of age and R-R interval were established; data were compared from a range of cats with primary cardiomyopathies and disease states linked to specific cardiomyopathies in human beings. It was found that in a group of cats with mild HCM, there was a decrease in the E' velocity recorded by pw-DTI at the interventricular septum, and tendency towards a decrease at the lateral aspect of the mitral annulus, recorded from the left apical four-chamber view.

In the aged cat population studied, the basilar interventricular septum was frequently greater than six millimetres. The lack of dynamic impairment in these cats suggests that BSB is in fact a form of normal senile remodelling rather than a form of disease.

Most cats with CRF demonstrated an increased basilar septal thickness, and the group as a whole revealed some alterations in their spectral Doppler velocities. However, these cats lacked changes in their pw-DTI analysis. Since spectral Doppler measurements are recognised as being load sensitive, whereas pw-DTI velocities are generally considered less sensitive to alterations in loading; this finding that may suggest that, as in human beings (Ommen, et al 2000), pw-DTI can be used

to differentiate between alterations in myocardial function and altered loading conditions and that the alterations witnessed on spectral assessment of cats with CRF were in fact due to alterations in the loading conditions.

The hyperthyroid cats had a tendency towards decreased E' and demonstrated increased A' velocities providing evidence of diastolic dysfunction. In addition, the increased S' velocity within this group suggests increased inotropy. By comparing hyperthyroid cats receiving carbimazole (as a sole therapy) to untreated hyperthyroid cats, it was found that there was no evidence that carbimazole imposes adverse effects upon the myocardial dynamics measured from the thyrotoxic feline myocardium. All of the echocardiographic variables that demonstrated a difference between the normal cats and the treated hyperthyroid cats also demonstrated a similar variation in the untreated hyperthyroid cats (with the exception of the A' velocity within the longitudinal fibres at the mid-interventricular septum). In addition, a decrease in the colour M-mode propagation velocity was documented in the hyperthyroid heart. This finding is thought to represent asynchronous relaxation when it is found in human beings (Stugaard, et al 1993, Møller, et al 2000) and may suggest that ventricular asynchrony exists in hyperthyroid cats. These results suggest that with a decrease in $tT4$ concentration (following carbimazole administration) there is restoration of myocardial function, with echocardiographic variables approaching those in normal cats, even before a euthyroid state is achieved. Whilst the treated hyperthyroid cats generally demonstrated less variation from the normal cats, when compared to the untreated hyperthyroid cats, these cats had not been treated adequately, with the majority remaining hyperthyroid. This study suggests that the use of carbimazole alone improves the function of the feline

myocardium in thyrotoxic cardiomyopathy. However, in order to fully assess the affects of medication upon the thyrotoxic myocardium, a follow-up study is required, where the myocardial velocities in a group of adequately treated hyperthyroid cats, will be assessed.

By estimating the diastolic function using transmitral and pulmonary venous flow patterns, it was found that the majority (64%) of cats over eight years of age demonstrated a filling pattern consistent with impaired relaxation. This is reported as a normal finding in people over seventy years of age (Schirmer, et al 2000). However, in the current study, which only included cats over eight years of age, there were 21 cats (26%) that were judged to have normal diastolic function on the basis of their transmitral and pulmonary venous flow patterns. Whilst these criteria only estimate diastolic function (and they can be influenced by multiple confounding factors), this finding may suggest that normal myocardial function is not uncommon in aged felines (Schober, et al 2003). Furthermore, this study was performed using clinical cases, some of which were referred to our institution, so it may have been biased toward the inclusion of cats with cardiac abnormalities, and the incidence of diastolic dysfunction is likely to have been overestimated.

It was demonstrated that cats show all of the diastolic patterns seen in human beings, and that there was good agreement between the changes observed using the different non-invasive estimates (principally transmitral and pulmonary venous flow and pw-DTI). Invasive studies performed in normal cats have previously demonstrated that with alterations in load and heart rate the feline myocardium responds in a similar

manner to the human myocardium (Schober, et al 2003), and the current study would support those findings.

It is the author's belief that, since no single non-invasive method of assessing diastolic function is infallible, as many as possible different measures of diastolic function should be assessed when trying to identify localised areas of myocardial dysfunction. This will help categorise cats according to their functional abnormalities rather classifying them entirely on ventricular morphology. The combination of DTI and mitral and pulmonary flow dynamics may provide us with a better estimate of left ventricular filling pressures. However, the accurate assessment of an individual patient (rather than a large group of cats) requires a stepwise approach, incorporating all the available data.

The study demonstrated that pw-DTI velocities differ in thyrotoxic myocardium from the other diseases. However, no specific alterations were observed in cats with CRF or BSB. While this might suggest that these cats do not have diastolic impairment it could also mean that the techniques used were not sufficiently sensitive (or repeatable) to detect mild abnormalities within myocardial dynamics. Initially, the inclusion of cats with other forms of specific cardiomyopathy (including hypertension and DM) had been envisaged. However, relatively few cats with these conditions and without concurrent disease(s), or medical intervention, were recruited and therefore, these cats were excluded from the analysis.

Future Studies

In order to assess whether or not myocardial wall motion abnormalities demonstrated by DTI techniques relate to changes within the structure of the myocardium, it is necessary to document histopathological abnormalities in affected segments of the myocardium. A study assessing myocardial dynamics pre-mortem with histopathological follow-up at post mortem examination will therefore be undertaken.

In the future further studies are required to assess the affect of medication upon the alterations observed in the thyrotoxic myocardium and various other forms of specific cardiomyopathy, such as hypertensive cardiomyopathy. In addition, these techniques will be used to try and determine whether or not the myocardial abnormalities resolve with adequate treatment of the disease.

It has been demonstrated that pw-DTI can detect myocardial abnormalities in cats with mild HCM. These techniques could be applied to a cohort of cats with HCM in order to assess the progression of the disease and the response to various forms of medication.

Summary

This study provides evidence that the human classification system and the described methods of determining diastolic function can be used to assess myocardial function in the cat and thereby provides an extra tool for the diagnosis of myocardial disease

in this species. In the future, these techniques might be useful in determining the prognosis of a particular case and in deciding whether or not medical intervention is advocated and in assessing the response to treatment.

Appendix 1: Haematology and Serum Biochemistry Profile

Haematology	Units	Reference range
RBC count	$\times 10^{12}/l$	5.50-10.00
PCV	l/l	0.24-0.45
Haemoglobin	g/dl	8.00-14.00
MCV	fl	39.00-55.00
MCHC	%	30.00-36.00
Platelets (manual)	$\times 10^9/l$	300.00-600.00
Total WBC count	$\times 10^9/l$	7.00-20.00
Neutrophils (seg)	$\times 10^9/l$	2.50-12.80
Neutrophils (band)	$\times 10^9/l$	0.00-0.00
Lymphocytes	$\times 10^9/l$	1.50-7.00
Monocytes	$\times 10^9/l$	0.07-0.85
Eosinophils	$\times 10^9/l$	0.00-1.00
Basophils	$\times 10^9/l$	0.00-0.20

Biochemistry	Units	Reference range
Total protein	g/l	69.00-79.00
Albumin	g/l	28.00-39.00
Globulin	g/l	23.00-50.00
AP	IU/L	10.00-100.00
ALT	IU/L	6.00-83.00
Bile acids	$\mu\text{mol}/l$	0.00-7.00
Cholesterol	mmol/l	2.0-3.4
Glucose	mmol/l	3.30-5.00
Creatinine	$\mu\text{mol}/l$	40.00-177.00
Urea	mmol/l	2.80-9.80
Inorganic phosphate	mmol/l	1.40-2.50
Calcium	mmol/l	2.10-2.90
Creatine Kinase	IU/L	50-200
Potassium	mmol/l	4.00-5.00
Sodium	mmol/l	145.00-156.00
Total Thyroxine	nmol/l	13-48

RBC, Red blood cell; PCV, Packed cell volume; MCV, Mean corpuscle volume; MCHC, Mean corpuscle haemoglobin content; WBC, White blood cell; seg, segmented; AP, Alkaline phosphatase; ALT, Alanine transferase.

Reference List

- Abdalla I, Murray D, Lee J-C, Stewart WJ, Tajik AJ & Klein AL (1998) Duration of pulmonary venous atrial reversal flow velocity and mitral inflow a wave: New measure of severity of cardiac amyloidosis. *Journal of the American Society of Echocardiography*, **11**, 1125-1133.
- Abdurrahman L (1998) Pulmonary venous flow doppler velocities in children. *Journal of the American Society of Echocardiography*, **11**, 132-137.
- Adin DB, Thomas WP, Adin CA & Kass PH (2000) *Echocardiographic evaluation of cats with chronic renal failure*. In: Proceedings of the 18th Annual Veterinary Medical Forum (ed. by D J Davenport & M R Paradis), p. 243, Seattle.
- Agmon Y, Oh JK, McCarthy JT, Bailey KR & Seward B (1999) Are diastolic velocities of the mitral annulus load-dependent? A tissue-doppler study in hemodialysis patients [abstract]. *Journal of the American College of Cardiology*, **33**, 429A.
- Akasaka T, Yoshikawa J, Yoshida K, Maeda K, Takagi T & Miyake S (1994) Phasic coronary flow characteristics in patients with hypertrophic cardiomyopathy: A study by coronary doppler catheter. *Journal of the American Society of Echocardiography*, **7**, 9-19.
- Al-Ahmad A, Rand WM, Manjunath G, Konstam MA, Salem DN, Levey AS & Sarnak MJ (2001) Reduced kidney function and anemia as risk factors for mortality in patients with left ventricular dysfunction. *Journal of the American College of Cardiology*, **38**, 955-962.
- Alam M, Wardell J, Anderson E, Samad BA & Nordlander R (1999) Characteristics of mitral and tricuspid annular velocities determined by pulsed wave doppler tissue imaging in healthy subjects. *Journal of the American Society of Echocardiography*, **12**, 618-628.
- Alam M, Wardell J, Anderson E, Samad BA & Nordlander R (2000) Right ventricular function in patients with first inferior myocardial infarction: Assessment by tricuspid annular motion and tricuspid annular velocity. *American Heart Journal*, **139**, 710-715.
- Amann K, Kronenberg G, Gehlen F, Wessels S, Orth S, Munter K, Ehmke H, Mall G & Ritz E (1998) Cardiac remodelling in experimental renal failure-an immunohistochemical study. *Nephrology Dialysis Transplantation*, **13**, 1958-1966.
- Annonu AKMH, Fattah AA, Mokhtar MS, Ghareeb S & Elhendy A (2001) Left ventricular systolic and diastolic functional abnormalities in asymptomatic patients with non-insulin-dependent diabetes mellitus. *Journal of the American Society of Echocardiography*, **14**, 885-891.
- Appleton CP (1993) Estimation of left ventricular filling pressure using two-dimensional and doppler echocardiography in adult patients with cardiac disease. *Journal of the American College of Cardiology*, **22**, 1972-1982.

- Appleton CP (1997) Hemodynamic determinants of doppler pulmonary venous flow velocity components: New insights from studies in lightly sedated normal dogs. *Journal of the American College of Cardiology*, **30**, 1562-1574.
- Appleton CP, Carucci MJ, Henry CP & Olajos M (1991) Influence of incremental changes in heart rate on mitral flow velocity: Assessment in lightly sedated, conscious dogs. *Journal of the American College of Cardiology*, **17**, 227-236.
- Appleton CP, Firstenberg MS, Garcia MJ & Thomas JD (2000) The echo-doppler evaluation of left ventricular diastolic function. *Cardiology Clinics*, **18**, 513-546.
- Appleton CP, Hatle LK & Popp RL (1988) Relation of transmitral velocity patterns to left ventricular diastolic function; new insights from a combined hemodynamic and doppler echocardiographic study. *Journal of the American College of Cardiology*, **12**, 426-440.
- Appleton CP, Jensen JL, Hatle L & Oh JK (1997) Doppler evaluation of left and right ventricular diastolic function: A technical guide for obtaining optimal flow velocity recordings. *Journal of the American Society of Echocardiography*, **10**, 271-291.
- Atkins CE (1991) The role of noncardiac disease in the development and precipitation of heart failure. *Veterinary Clinics of North America: Small Animal Practice*, **21**, 1035-1080.
- Atkins CE, Gallo AM, Kurzman ID & Cowen P (1992) Risk factors, clinical signs, and survival in cats with a clinical diagnosis of idiopathic hypertrophic cardiomyopathy: 74 cases (1985-1989). *Journal of the American Veterinary Medical Association*, **201**, 613-618.
- Avdonin PV, Cottet-Maire F, Afanasjeva GV, Loktionova SA, Lhote P & Ruegg UT (1999) Cyclosporine a up-regulates angiotensin ii receptors and calcium responses in human vascular smooth muscle cells. *Kidney International*, **55**, 2407-2414.
- Averyhart-Fullard V, Fraker LD, Murphy AM & Solaro RJ (1994) Differential regulation of slow-skeletal and cardiac troponin i mrna during development and by thyroid hormone in rat heart. *Journal of Molecular Cellular Cardiology*, **26**, 609-616.
- Bach DS, Armstrong WF, Donovan CL & Muller DWM (1996) Quantitative doppler tissue imaging for assessment of regional myocardial velocities during transient ischemia and reperfusion. *American Heart Journal*, **132**, 721-725.
- Bagchi N (1982) Thyroid function in a diabetic population. *Special Topics in Endocrinology and Metabolism*, **3**, 45-55.
- Bahouth SW (1991) Thyroid hormones transcriptionally regulate the β_1 -adrenergic receptor gene in cultured ventricular myocytes. *Journal of Biological Chemistry*, **266**, 15863-15869.
- Barber PJ & Elliot J (1998) Feline chronic renal failure: Calcium homeostasis in 80 cases diagnosed between 1992 and 1995. *Journal of Small Animal Practice*, **39**, 108-116.
- Barber PJ & Elliott J (1996) Study of calcium homeostasis in feline hyperthyroidism. *Journal of Small Animal Practice*, **37**, 575-582.
- Bartges JW, Willis AM & Polzin DJ (1996) Hypertension and renal disease. *Veterinary Clinics of North America: Small Animal Practice*, **26**, 1331-1345.

- Bartges JW, Willis AM & Polzin DJ (1999) Hypertension and renal disease. *Hills "Canine and Feline Renal Disease"*, 51-60.
- Basset A, Blanc J, Messas E, Hagege A & Elghozi J (2001) Renin-angiotensin system contributes to cardiac hypertrophy in experimental hyperthyroidism: An echocardiographic study. *Journal of Cardiovascular Pharmacology*, **37**, 163-172.
- Baty CJ, Malarkey DE, Atkins CE, DeFrancesco TC, Sidley J & Keene BW (2001) Natural history of hypertrophic cardiomyopathy and aortic thromboembolism in a family of domestic shorthair cats. *Journal of Veterinary Internal Medicine*, **15**, 595-599.
- Beardow A (1993) Blood pressure measurement and its applications. *Veterinary Product News*, **January**, 21.
- Bing OHL (1994) Thyroid hormone effects on intracellular calcium and inotropic responses of rat ventricular myocardium. *American Journal of Medicine*, **267**, 1112-1120.
- Bland JM (2000) Clinical measurement. In: *An introduction to medical statistics* (ed. by M Bland), Oxford University Press, Oxford, 268-294.
- Bond BR & Fox PR (1984) Advances in feline cardiomyopathy. *Veterinary Clinics of North America-Small Animal Practice*, **14**, 1021-1037.
- Bond BR, Fox PR, Peterson ME & Skavaril RV (1988) Echocardiographic findings in 103 cats with hyperthyroidism. *Journal of the American Veterinary Medical Association*, **192**, 1546-1549.
- Brahimi M, Dahan M, Dabire H & Levy I (2000) Impact of pulse pressure on degree of cardiac hypertrophy in patients with chronic uraemia. *Journal of Hypertension*, **18**, 1645-1650.
- Branson KR, Wager-Mann CC & Mann FA (1997) Evaluation of an oscillometric blood pressure monitor on anaesthetised cats and the effect of cuff placement and fur on accuracy. *Veterinary Surgery*, **26**, 347-353.
- Bright JM, Golden AL & Daniel GB (1992) Feline hypertrophic cardiomyopathy: Variations on a theme. *Journal of Small Animal Practice*, **33**, 266-274.
- Bright JM, Herrtage ME & Schneider JF (1999) Pulsed doppler assessment of left ventricular diastolic function in normal and cardiomyopathic cats. *Journal of the American Animal Hospital Association*, **35**, 285-291.
- Brodin L, Lind M, Gaballa M, Jensen-Urstad M & van der Linden J (1999) A tissue-doppler based analysis of the longitudinal left ventricular shortening in patients with different forms of ecg bundle branch blocks. [abstract]. *European Heart Journal*, **20**, 262.
- Brown RS, Keating P, Livingston PG & Bullock L (1992) Thyroid growth immunoglobulins in feline hyperthyroidism. *Thyroid*, **2**, 125-130.
- Brown SA & Henik RA (1998) Diagnosis and treatment of systemic hypertension. *Veterinary Clinics of North America: Small Animal Practice*, **28**, 1481-1494.
- Brun P, Tribouilloy C, Duval A-M, Iserin L, Meguira A, Pelle G & Dubois-Rande J-L (1992) Left ventricular flow propagation during early filling is related to wall relaxation: A color m-mode doppler analysis. *Journal of the American College of Cardiology*, **20**, 420-432.
- Burggraaf J, Tulen JHM, Lalezari S, Schoemaker RC, De Meyer PHEM, Meinders AE, Cohen AF & PiJl H (2001) Sympathovagal imbalance in

- hyperthyroidism. *American Journal of Physiology: Endocrinology and Metabolism*, **281**, 190-195.
- Burk RL & Ackerman N (1996) The thorax. In: *Small animal radiography and ultrasound. A diagnostic atlas and text* (ed. by Burk & Ackerman), 23-214, W.B. Saunders Company, Philadelphia.
- Cardim N, Oliveira G, Longo S, Ferreira T, Pereira A, Palma Reis R & Correia JM (2003) Doppler tissue imaging: Regional myocardial function in hypertrophic cardiomyopathy and in athlete's heart. *Journal of the American Society of Echocardiography*, **16**, 223-232.
- Cardim N, Perrot A, Ferreira T, Pereira A, Osterziel KJ, Palma Reis R & Martins Correia JF (2002) Usefulness of doppler myocardial imaging for identification of mutation carriers of familial hypertrophic cardiomyopathy. *American Journal of Cardiology*, **90**, 128-132.
- Caso P, D'Andrea A, Galderisi M, Liccardo B, Severino S, De Simone L, Izzo A, D'Andrea L & Mininni N (2000) Pulsed doppler tissue imaging in endurance athletes: Relation between left ventricular preload and myocardial regional diastolic function. *American Journal of Cardiology*, **85**, 1131-1136.
- Castello A (1993) Perinatal hypothyroidism impairs the normal transition of glut4 and glut1 glucose transporters from foetal to neonatal levels in heart and brown adipose tissue. *Journal of Biological Chemistry*, **269**, 5905-5912.
- Chetboul V, Athanassiadis N, Carlos C, Nicolle AP & Lefebvre HP (2004) Quantification, repeatability and reproducibility of feline radial and longitudinal left ventricular velocities by tissue doppler imaging. *American Journal of Veterinary Research*, **65**, 566-572.
- Chetboul V, Concordet D, Pouchelon J-L, Athanassiadis N, Muller C, Benigni L, Munari AC & Lefebvre HP (2003a) Effects of inter- and intra-observer variability on echocardiographic measurements in awake cats. *Journal of Veterinary Medicine*, **50**, 326-331.
- Chetboul V, Lefebvre HP, Pinhas C, Clerc B, Boussouf M & Pouchelon J-L (2003b) Spontaneous feline hypertension: Clinical and echocardiographic abnormalities, and survival rate. *Journal of Veterinary Internal Medicine*, **17**, 89-95.
- Choong CY, Abascal VM, Thomas JD, Guerrero JL, McGlew S & Weyman AE (1988) Combined influence of ventricular loading and relaxation on the transmitral flow velocity profile in dogs measured by doppler echocardiography. *Circulation*, **78**, 672-683.
- Choong CY, Herrmann HC, Weymann AE & Fifer MA (1987) Preload dependence of doppler-derived indexes of left ventricular diastolic function in humans. *Journal of the American College of Cardiology*, **10**, 800-808.
- Crass MF, Moore PL, Strickland ML, Pang PKT & Citak MS (1985) Cardiovascular responses to parathyroid hormone. *American Journal of Physiology*, **249**, E187-194.
- Crispin SM & Mould JRB (2001) Systemic hypertensive disease and the feline fundus. *Veterinary Ophthalmology*, **4**, 131-140.
- DeMadron E, Bonagura JD & Herring DS (1985) Two-dimensional echocardiography in the normal cat. *Veterinary Radiology*, **26**, 149-158.

- Derumeaux G, Ovize M, Loufoua J, Andre-Fouet X, Miniarie Y, Criber A & Letac B (1998) Doppler tissue imaging quantitates regional wall motion during myocardial ischaemia and reperfusion. *Circulation*, **97**, 1970-1977.
- Dhalla NS, Golfman L, Liu X, Sasaki H, Elimban V & Rupp H (1999) Subcellular remodelling and heart dysfunction in cardiac hypertrophy due to pressure overload. *Annals of the New York Academy of Sciences*, **874**, 100-110.
- Dhein S, Rohnert P, Markau S, Kotchi-Kotchi E, Becker K, Poller U, Osten B & Brodde OE (2000) Cardiac beta-adrenoceptors in chronic uremia: Studies in humans and rats. *Journal of the American College of Cardiology*, **36**, 608-617.
- Dieckman LJ & Solaro RJ (1990) Effect of thyroid status on thin-filament Ca^{2+} regulation and expression of troponin i in perinatal and adult rat hearts. *Circulatory Research*, **67**, 344-351.
- Dillmann WH (1983) Thyroid hormones and the heart. *Thyroid Today*, **6**, 1-6.
- Dillmann WH (1990) Biochemical action of thyroid hormone in the heart. *American Journal of Medicine*, **88**, 626.
- Drozdz J, Ciesielczyk M, Kasprzak JD, Plewka M & Krzeminska-Pakula M (2000) Quantitative evaluation of myocardial contractility by tissue doppler echocardiography. *Polish Heart Journal*, **L111**, 210-219.
- Dukes J (1992) Hypertension: A review of the mechanisms, manifestations and management. *Journal of Small Animal Practice*, **33**, 119-129.
- Dukes McEwan J (1996) Advances in the treatment of feline cardiomyopathy. *The Veterinary Annual*, **36**, 217-244.
- Dukes McEwan J, French AT & Corcoran BM (2002) Doppler echocardiography in the dog: Measurement of variability and reproducibility. *Veterinary Radiology & Ultrasound*, **43**, 144-152.
- Edvardsen T, Aakhus S, Endresen K, Bjornerheim R, Smiseth OA & Ihlen H (2000) Acute regional myocardial ischemia identified by 2-dimensional multiregion tissue doppler imaging technique. *Journal of the American Society of Echocardiography*, **13**, 986-994.
- Edvardsen T, Skulstad H, Aakhus S, Urheim S & Ihlen H (2001) Regional myocardial systolic function during acute myocardial ischemia assessed by strain doppler echocardiography. *Journal of the American College of Cardiology*, **37**, 726-730.
- Eidem BW, McMahon CJ, Cohen RR, Wu J, Finkelshteyn I, Kovalchin JP, Ayres NA, Bezold LI, O'Brien Smith E & Pignatelli RH (2004) Impact of cardiac growth on doppler tissue imaging velocities: A study in healthy children. *Journal of the American Society of Echocardiography*, **17**, 212-221.
- Elliot J, Barber PJ, Syme HM, Rawlings JM & Markwell PJ (2001) Feline hypertension: Clinical findings and response to antihypertensive treatment in 30 cases. *Journal of Small Animal Practice*, **42**, 122-129.
- Elliot J, Rawlings JM, Markwell PJ & Barber PJ (2000) Survival of cats with naturally occurring chronic renal failure: Effect of dietary management. *Journal of Small Animal Practice*, **41**, 235-242.
- Factor SM, Bhan R, Minase T, Wolinsky H & Sonnenblick EH (1981) Hypertensive-diabetic cardiomyopathy in the rat. An experimental model of human disease. *American Journal of Pathology*, **102**, 219-228.

- Farias CA, Rodriguez L, Garcia MJ, Sun JP, Klein AL & Thomas JD (1999) Assessment of diastolic function by doppler tissue echocardiography: Comparison with standard transmitral and pulmonary venous flow. *Journal of the American Society of Echocardiography*, **12**, 609-617.
- Feldman EC & Nelson RW (2004) The thyroid gland. In: *Canine and feline endocrinology and reproduction*, Saunders, St Louis, Missouri, 152-218.
- Ferasin L, Sturgess CP, Cannon MJ, Caney SMA & Gruffydd-Jones TJ (2003) Feline idiopathic cardiomyopathy: A retrospective study of 106 cats (1994-2001). *Journal of Feline Medicine and Surgery*, **5**, 151-159.
- Fiebeler A, Schmidt F, Muller DN, Park J, Dechend R, Bieringer M, Shagdarsuren E, Breu V, Haller H & Luft FC (2001) Mineralocorticoid receptor affects ap-1 and nuclear factor- κ b activation in angiotensin ii-induced cardiac injury. *Hypertension*, **37**, 787-793.
- Fijii Y, Masuda Y, Takashima K, Ogasawara J, Machida N, Yamane Y, Chimura S, Awazu T, Yamane T & Wakao Y (2001) Hypertrophic cardiomyopathy in two kittens. *Journal of Veterinary Medicine and Science*, **63**, 583-585.
- Fleming AD, McDicken WN, Sutherland GR & Fenn L (1994a) Myocardial velocity gradients detected by doppler imaging. *The British Journal of Radiology*, **67**, 679-688.
- Fleming AD, McDicken WN, Sutherland GR & Hoskins PR (1994b) Assessment of colour doppler tissue imaging using test phantoms. *Ultrasound in Medicine & Biology*, **20**, 937-951.
- Flood SM, Randolph JF, Gelzer ARM & Refsal K (1999) Primary hyperaldosteronism in two cats. *Journal of the American Animal Hospital Association*, **35**, 411-416.
- Forfar JC (1982) Abnormal left ventricular function in hyperthyroidism. *New England Journal of Medicine*, **307**, 1165-1170.
- Fox PR (1999) Feline cardiomyopathies. In: *Textbook of canine and feline cardiology* (ed. by P R Fox, N S Moise & D Sisson), 621-678, W.B. Saunders Company, Philadelphia.
- Fox PR (2003) Hypertrophic cardiomyopathy. Clinical and pathological correlates. *Journal of Veterinary Cardiology*, **5**, 39-45.
- Fox PR, Broussard JD & Peterson ME (1993) Electrocardiographic and radiographic changes in cats with hyperthyroidism: Comparison of populations evaluated during 1979-1982 vs 1992 [abstract]. *Journal of Veterinary Internal Medicine*, **7**, 118.
- Fox PR, Broussard JD & Peterson ME (1999) Hyperthyroidism and other high output states. In: *Textbook of canine and feline cardiology* (ed. by P Fox, N Moise & D Sisson), W.B. Saunders Company, Philadelphia, 781-793.
- Fox PR, Liu S-K & Maron BJ (1995) Echocardiographic assessment of spontaneously occurring feline hypertrophic cardiomyopathy: An animal model of human disease. *Circulation*, **92**, 2645-2651.
- Fox PR, Petrie JP, Liu S-K, Hayes KC & Bond BR (1997) Clinical and pathological features of cardiomyopathy characterised by myocardial failure in 49 cats, 1990-1995. *Journal of Veterinary Internal Medicine*, **11**, 139.
- Fraser A, Cain P, Baglin T, Case C, Spicer D & Short L (2001) Application of tissue doppler to interpretation of dobutamine echocardiography and comparison

- with quantitative coronary angiography. *American Journal of Cardiology*, **87**, 525-531.
- Friedman MJ (1982) Left ventricular systolic and diastolic function in hyperthyroidism. *American Heart Journal*, **104**, 1303-1308.
- Fristenburg MS, Levine BD, Garcia MJ, Greenburg NL, Cardon L, Morehead AJ, Zuckerman J & Thomas JD (2000) Relationship of echocardiographic indexes to pulmonary capillary wedge pressures in healthy volunteers. *Journal of the American College of Cardiology*, **36**, 1664-1669.
- Frochlich ED, Apstein C, Chobanian AV, Devereux RB, Dustan HP, Dzau V, Fauad-Tarazi F, Horan MJ, Marcus M, Massie B, Pfeffer MA, Re RN, Savage D & Shub C (1992) The heart in hypertension. *The New England Journal of Medicine*, **327**, 998-1008.
- Fujino N, Shimizu M, Ino H, Yamaguchi M, Yasuda T, Nagata M, Konno T & Mabuchi H (2002) A novel mutation lys273glu in the cardiac troponin t gene shows high degree of penetrance and transition from hypertrophic to dilated cardiomyopathy. *American Journal of Cardiology*, **89**, 29-33.
- Galiuto L, Ignone G & DeMaria AN (1998) Contraction and relaxation velocities of the normal left ventricle using pulsed wave tissue doppler echocardiography. *American Journal of Cardiology*, **81**, 609-614.
- Gallagher KP, Osakada G, Matsuzaki M, Miller M, Kemper WS & Ross JJ (1985) Nonuniformity of inner and outer systolic wall thickening in conscious dogs. *American Journal of Physiology*, 241-248.
- Garcia M, Ares MA, Asher C, Rodriguez L, Vandervoort P & Thomas JD (1997) An index of early left ventricular filling that when combined with pulsed doppler peak e velocity may estimate capillary wedge pressure. *Journal of the American College of Cardiology*, **29**, 448-454.
- Garcia M, Palac RT, Malenka DJ, Terrell P & Plehn JF (1999) Colour m-mode doppler flow propagation velocity is a relatively preload-independent index of left ventricular filling. *Journal of the American Society of Echocardiography*, **12**, 129-137.
- Garcia M, Smedira N, Greenburg N, Main M, Firstenberg MS, Obadashian J & Thomas JD (2000) Color m-mode doppler flow propagation velocity is a preload insensitive index of left ventricular relaxation: Animal and human validation. *Journal of the American College of Cardiology*, **35**, 201-208.
- Garcia MJ, Rodriguez L, Ares M, Griffin BP, Klein AL, Stewart WJ & Thomas JD (1996) Myocardial wall velocity assessment by pulsed doppler tissue imaging: Characteristic findings in normal subjects. *American Heart Journal*, **132**, 648-656.
- Garcia MJ, Thomas JD & Klein A (1998) New doppler echocardiographic applications for the study of diastolic function. *Journal of the American College of Cardiology*, **32**, 865-875.
- Garot J, Derumeaux GA, Monin JL, Duval-Moulin AM, Simon M, Pascal D, Castaigne A, Dubois-Rande J-L, Diebold B & Guéret P (1999) Quantitative systolic and diastolic transmyocardial velocity gradients assessed by m-mode colour doppler tissue imaging as reliable indicators of regional left ventricular function after acute myocardial infarction. *European Heart Journal*, **20**, 593-603.

- Gavaghan BJ, Kittleson MD, Fisher KJ, Kass PH & Gavaghan MA (1999) Quantification of left ventricular diastolic wall motion by doppler tissue imaging in healthy cats and cats with cardiomyopathy. *American Journal of Veterinary Research*, **60**, 1478-1486.
- Gerber H, Peter H, Ferguson M.C. & Peterson M.E. (1994) Etiopathology of feline toxic nodular goitre. *Veterinary Clinics of North America; Small Animal Practice*, **24**, 542-565.
- Giles TD & Sander GE (1989) Myocardial disease in hypertensive-diabetic patients. *The American Journal of Medicine*, **87**, 23S-28S.
- Gonzalez-Vilchez F, Ares M, Ayuela J & Alonso L (1999) Combined use of pulsed and color m-mode doppler echocardiography for the estimation of pulmonary capillary wedge pressure: An empirical approach based on an analytical relation. *Journal of the American College of Cardiology*, **34**, 515-523.
- Gorscan JJ, Strum DP, Mandarin WA, Gulati VK & Pinsky MR (1997) Quantitative assessment of alterations in regional left ventricular contractility with color-coded tissue doppler echocardiography- comparison with sonomicrometry and pressure-volume relations. *Circulation*, **95**, 2423-2433.
- Grandy JL, Dunlop CI, Hodgson DS, Curtis CR & Chapman PL (1992) Evaluation of the doppler ultrasonic method of measuring systolic arterial blood pressure in cats. *American Journal of Veterinary Research*, **7**, 1166-1169.
- Gulati VK, Katz WE, Follansbee WP & Gorscan JJ (1996) Mitral annular descent velocity by tissue doppler echocardiography as an index of global left ventricular function. *American Journal of Cardiology*, **77**, 979-984.
- Gunn-Moore DA (2005) Feline endocrinopathies. *Veterinary Clinics of North America-Small Animal Practice*, **35**, 171-210.
- Häggström J, Hansson K, Karlberg BE, Kvart C & Olsson K (1994) Plasma concentrations of atrial natriuretic peptide in relation to severity of mitral regurgitation in cavalier king charles spaniels. *American Journal of Veterinary Research*, **55**, 698-703.
- Hamlin RL (1999) Normal cardiovascular physiology. In: *Textbook of canine and feline cardiology* (ed. by P R Fox, N S Moise & D Sisson), 25-37, W.B. Saunders Company, Philadelphia.
- Hammond HK (1987) Increased myocardial β -receptors and adrenergic responses in hyperthyroid pigs. *American Journal of Physiology*, **252**, 283-290.
- Han J (1994) Effects of thyroid hormone on the calcium current and isoprenaline-induced background current in rabbit ventricular myocytes. *Journal of Molecular Cellular Cardiology*, **26**, 925-935.
- Hanley DA & Sherwood LM (1978) Secondary hyperparathyroidism and chronic renal failure. Pathology and treatment. *Medical Clinics of North America*, **62**, 1319-1339.
- Harpster NK (1986) Feline myocardial disease. In: *Current veterinary therapy ix* (ed. by K R.W.), WB Saunders, Philadelphia, 380-398.
- Harpster NK (1990) Feline arrhythmias: Diagnosis and management. In: *Current veterinary therapy xi* (ed. by K R.W.), WB Saunders, Philadelphia.
- Hatle L & Sutherland GR (2000) Regional myocardial function-a new approach. *European Heart Journal*, **21**, 1337-1357.
- Havudrup O, Bundgaard H, Andersen PS, Larsen LA, Vuust J, Kjeldsen K & Christiansen M (2002) Outcome of clinical versus genetic family screening in

- hypertrophic cardiomyopathy with focus on cardiac β -myosin gene mutations. *Cardiovascular Research*, **57**, 347-357.
- Henein MY, O'Sullivan C, Sutton GC, Gibson DG & Coats AJS (1997) Stress-induced left ventricular outflow tract obstruction: A potential cause of dyspnoea in the elderly. *Journal of the American College of Cardiology*, **30**, 1301-1307.
- Henik RA (1997) Systemic hypertension and its management. *Veterinary Clinics of North America: Small Animal Practice*, **27**, 1355-1372.
- Henry WL, DeMaria A, Geramiak R, King DL, Kisslo JA, Popp RL, Sahn DJ, Tajik A.J., Teichholz LE & Weyman AE (1980) Report of the american society of echocardiography committee on nomenclature and standards in two-dimensional echocardiography. *Circulation*, **62**, 1054-1061.
- Hoit B, Shao Y, Gabel M & Walsh R (1992) Influence of loading conditions and contractile state on pulmonary venous flow; validation of doppler velocimetry. *Circulation*, **86**, 651-659.
- Hypertension Consensus Panel (2002) *Current recommendations for the diagnosis and management of hypertension in cats and dogs (report)*. In: 20th Annual Veterinary Medicine Forum, Dallas Texas.
- Iaccarino G, Barbato E, Cipoletta E, Fiorillo A & Trimarco B (2001) Role of the sympathetic nervous system in cardiac remodelling in hypertension. *Clinical and Experimental Hypertension*, **23**, 35-43.
- Isaaz K, Thompson A, Ethevenot G, Cloez JL, Brembilla B & Pernot C (1989) Doppler echocardiographic measurement of low velocity motion of the left ventricular posterior wall. *American Journal of Cardiology*, **64**, 66-75.
- Jacobs G & Knight DH (1985) M-mode echocardiographic measurement in nonanesthetized healthy cats: Effects of body weight, heart rate, and other variables. *American Journal of Veterinary Research*, **46**, 1705-1711.
- Jarcho JA, McKenna W & Pare JA (1989) Mapping a gene for familial hypertrophic cardiomyopathy to chromosome 14q1. *New England Journal of Medicine*, **321**, 1372-1478.
- Jayagopal V, Keevil BG, Atkin SL, Jennings PE & Kilpatrick ES (2003) Paradoxical changes in cystatin c and serum creatinine in patients with hypo- and hyperthyroidism. *Clinical Chemistry*, **49**, 680-681.
- Jensen J, Henik RA, Brownfield M & Armstrong J (1997) Plasma renin activity and angiotensin i and aldosterone concentrations in cats with hypertension associated with chronic renal disease. *American Journal of Veterinary Research*, **58**, 535-540.
- Kannel WB, Hjortland M & Castelli WP (1974) The role of diabetes in congestive heart failure: The framingham study. *American Journal of Cardiology*, **34**, 29-34.
- Kapusta L, Thijssen JM, Cuypers MHM, Peer PG & Daniels O (2000) Assessment of myocardial velocities in healthy children using doppler tissue imaging. *Ultrasound in Medicine & Biology*, **26**, 229-237.
- Karibe A, Tobacman LS, Strand J, Butters C, Back N, Bachinski LL, Arai AE, Ortiz A, Roberts R, Homsher E & Fananapazir L (2001) Hypertrophic cardiomyopathy caused by a novel α -tropomyosin mutation (v95a) is associated with mild cardiac phenotype, abnormal calcium binding to

- troponin, abnormal myosin cycling, and poor prognosis. *Circulation*, **103**, 65-71.
- Kass PH, Peterson ME, Levy J., James K., Becker D.V. & Cowgill L.D. (1999) Evaluation of environmental, nutritional and host factors in cats with hyperthyroidism. *Journal of Veterinary Internal Medicine*, **13**, 323-329.
- Kaul S (2001) *Coronary microcirculation for the clinical echocardiographer*. In: American Society of Echocardiography 12th Annual Scientific Sessions, pp. 16-22, Seattle, WA.
- Kedzierski RM & Yanagisawa M (2001) Endothelin system: The double edged sword in health and disease. *Annual Reviews of Pharmacology and Toxicology*, **41**, 851-876.
- Kennedy RL & Thoday KL (1988) Autoantibodies in feline hyperthyroidism. *Research in Veterinary Science*, **45**, 300-306.
- Kent RL, Mann DL & Copper G (1991) Signals for cardiac muscle hypertrophy in hypertension. *Journal of Cardiovascular Pharmacology*, **17**, S7-S13.
- Kent RL & McDermott PJ (1996) Passive load and angiotensin ii evoke differential responses of gene expression and protein synthesis in cardiac myocytes. *Circulatory Research*, **78**, 829-838.
- Keren G, Meisner, J., Sherez, J., Yellin E. And Laniado S. (1986) Interrelationship of mid-diastolic mitral valve motion, pulmonary venous flow, and transmitral flow. *Circulation*, **74**, 36-44.
- Keren G, Sherez J, Megidish R, Levitt B & Laniado S (1985) Pulmonary venous flow pattern - its relationship to cardiac dynamics. *Circulation*, **71**, 1105-1112.
- Khan S, Bess RL, Rosman HS, Nordstorm CK, Cohen GI & Gardin JM (2004) Which echocardiographic doppler left ventricular diastolic function measurements are most feasible in the clinical echocardiographic laboratory. *The American Journal of Cardiology*, **94**, 1099-1101.
- Kim S & Iwao H (2000) Molecular and cellular mechanisms of angiotensin ii-mediated cardiovascular and renal diseases. *Pharmacological Reviews*, **52**, 11-34.
- Kirk CA, Feldman EC & Nelson RW (1993) Diagnosis of naturally acquired type-i and type-ii diabetes mellitus in cats. *American Journal of Veterinary Research*, **54**, 463-467.
- Kitabatake A, Inoue M, Asao M, Tanouchi J, Masutama T, Abe H, Morita H, Senda S & Matsuo H (1982) Transmitral blood flow reflecting diastolic behaviour of the left ventricle in health and disease-a study by pulsed doppler technique. *Japanese Circulation Journal*, **46**, 92-102.
- Kittleson MD (1995) Cvt update: Feline hypertrophic cardiomyopathy. In: *Current veterinary therapy xii* (ed. by Kirk R.W. & Bonagura J.D.), WB Saunders, Philadelphia, 854-862.
- Kittleson MD (1998) Hypertrophic cardiomyopathy. In: *Small animal cardiovascular medicine* (ed. by M D Kittleson & R D Kienle), Mosby, St. Louis, 347-363.
- Kittleson MD, Meurs KM, Munro MJ, Kittleson JA, Liu S-K, Pion PD & Towbin JA (1999) Familial hypertrophic cardiomyopathy in maine coon cats: An animal model of human disease. *Circulation*, **99**, 3172-3180.
- Klahr S & Slatopolsky E (1986) Toxicity of parathyroid hormone in uremia. *Annual Review of Medicine*, **37**, 71-78.

- Klein A & Tajik JA (1991) Doppler assessment of pulmonary venous flow in healthy subjects and in patients with heart disease. *Journal of the American Society of Echocardiography*, **4**, 379-392.
- Klein AL, Abdalla I, Murray D, Chi Lee J, Vandervoort P, Thomas JD, Appleton CP & Tajik AJ (1998) Age independence of the difference in duration of pulmonary venous atrial reversal flow and transmitral a-wave flow in normal subjects. *Journal of the American Society of Echocardiography*, **11**, 458-465.
- Kobayashi DL, Peterson ME, Graves TK, Lesser M & Nichols CE (1990) Hypertension in cats with chronic renal failure or hyperthyroidism. *Journal of Veterinary Internal Medicine*, **4**, 58-62.
- Koffas H (2003) *An application of doppler echocardiography and tissue doppler imaging in the evaluation of cardiac function in normal cats and cats with hypertrophic cardiomyopathy [thesis]*. In: *Veterinary Clinical Studies*, p. 376. University of Edinburgh, Edinburgh.
- Koffas H, Dukes-McEwan J, Corcoran BM, Moran CM, French A, Sboros V, Anderson T, Smith P, Simpson K & McDicken WN (2003) Peak mean myocardial velocities and velocity gradients measured by color m-mode tissue doppler imaging in the left ventricular free wall of healthy cats. *Journal of Veterinary Internal Medicine*, **17**, 510-525.
- Koffas H, Dukes-McEwan J, Moran CM, French A, Sboros V, Thorp KE, Corcoran BM & McDicken WN (2001) *Left ventricular wall motion velocities measured by pulsed doppler tissue imaging in healthy cats. Normal values and the influence of ageing. [abstract]*. In: 11th European Society of Veterinary Internal Medicine, p. 101, Dublin, Ireland.
- Koffas H, Dukes-McEwan J., Corcoran B.M., Moran C.M., French A., Sboros V., Simpson K. & McDicken W.N. (2005) *Pulsed doppler tissue imaging in normal cats and cats with hypertrophic cardiomyopathy: Assessment of myocardial motion along the radial and longitudinal axis*. In: Submitted to the *Journal of Veterinary Internal Medicine*.
- Koide M, Carabello BA, Conrad CC, Buckley JM, DeFreyte G, Barnes M, Tomanek RJ, Wei C, Dell'Italia LJ, Cooper G & Zile MR (1999) Hypertrophic response to hemodynamic overload: Role of load vs. Renin-angiotensin system activation. *American Journal of Physiology*, **276**, H350-H358.
- Kunz K, Dimitrov Y, Muller S, Chantrel F & Hannedouche T (1998) Uraemic cardiomyopathy. *Nephrology Dialysis Transplantation*, **13**, 39-43.
- Laste NJ & Harpster NK (1995) A retrospective study of 100 cases of feline distal aortic thromboembolism:1977-1993. *Journal of the American Animal Hospital Association*, **31**, 492-500.
- Lesser M, Fox PR & Bond BR (1992) Assessment of hypertension in 40 cats with left ventricular hypertrophy by doppler-shift sphygmomanometry. *Journal of Small Animal Practice*, **33**, 55-58.
- Levin A & Foley RN (2000) Cardiovascular disease in chronic renal failure. *American Journal of Kidney Diseases*, **36**, S24-S30.
- Levin A, Thompson CR, Ethier J, Carlisle EJF, Tobe S, Mendelssohn D, Burgess E, Jindal K, Barrett B, Singer J & Djurdjev O (1999) Left ventricular mass index increase in early renal disease: Impact of decline in hemoglobin. *American Journal of Kidney Diseases*, **34**, 125-134.

- LeWinter MM, Kent RS, Kroener JM, Carew TE & Covell JW (1975) Regional differences in myocardial performance in the left ventricle of the dog. *Circulation Research*, **37**, 191-199.
- Lewis BS, Ehrenfeld EN, Lewis N & Gotsman MS (1979) Echocardiographic lv function in thyrotoxicosis. *American Heart Journal*, **97**, 460-468.
- Lewis BS, Milne FJ & Goldberg B (1976) Left ventricular function in chronic renal failure. *British Heart Journal*, **38**, 1229-1239.
- Lewis JF & Maron BJ (1994) Clinical and morphological expression of hypertrophic cardiomyopathy in patients >65 years of age. *American Journal of Cardiology*, **73**, 1105-1111.
- Lim D-S, Roberts R & Marian AJ (2001) Expression profiling of cardiac genes in human hypertrophic cardiomyopathy: Insight into the pathogenesis of phenotypes. *Journal of the American College of Cardiology*, **38**, 1175-1180.
- Lim HW, De Windt L, Steinburg L, Taigen T, Witt SA, Kimball TR & Molkentin JD (2000) Calcineurin expression, activation, and function in cardiac pressure-overload hypertrophy. *Circulation*, **101**, 2431-2437.
- Ling D, Rankin JS, Edwards CH, McHale PA & Anderson RW (1979) Regional diastolic mechanisms of the left ventricle in the conscious dog. *American Journal of Physiology*, **236**, H323-330.
- Lip GYH, Felmeden DC, Li-Saw-Hee FL & Beevers DG (2000) Hypertensive heart disease: A complex syndrome or a hypertensive 'cardiomyopathy'? *European Heart Journal*, **21**, 1653-1665.
- Littman MP (1994) Spontaneous systemic hypertension in 24 cats. *Journal of Veterinary Internal Medicine*, **8**, 79-86.
- Liu S-K (1970) Acquired cardiac lesions leading to congestive heart failure in the cat. *American Journal of Veterinary Research*, **31**, 2071-2088.
- Liu S-K (1977) Pathology of feline heart disease. *Veterinary Clinics of North America-Small Animal Practice*, **7**, 323-339.
- Liu S-K, Maron BJ & Tilley LP (1979) Canine hypertrophic cardiomyopathy. *Journal of the American Veterinary Medical Association*, **174**, 708.
- Liu S-K, Maron BJ & Tilley LP (1981) Feline hypertrophic cardiomyopathy; gross anatomical and quantitative histological features. *American Journal of Pathology*, **102**, 388-395.
- Liu S-K, Peterson M & Fox P (1984) Hypertrophic cardiomyopathy and hyperthyroidism in the cat. *Journal of the American Veterinary Medicine Association*, **185**, 52-57.
- Liu S-K, Roberts WC & Maron BJ (1993) Comparison of morphological findings in spontaneously occurring hypertrophic cardiomyopathy in humans, cats and dogs. *American Journal of Cardiology*, **72**, 944-951.
- Liu S-K, Tilley LP & Lord PF (1975) Feline cardiomyopathy. *Recent Advances in Studies on Cardiac Structure and Metabolism*, **10**, 627-640.
- Lord PF, Wood A, Tilley LP & Liu S-K (1974) Radiographic and hemodynamic evaluation of cardiomyopathy and thromboembolism in the cat. *Journal of the American Veterinary Medical Association*, **164**, 154-165.
- Lorell BH (1999) Role of angiotensin at₁ and at₂ receptors in cardiac hypertrophy and disease. *American Journal of Cardiology*, **83**, 48H-52H.
- Luis Fuentes V (1992) Feline heart disease: An update. *Journal of Small Animal Practice*, **33**, 130-137.

- Magnon AL, Meurs KM, Kittleson MD & Ware WA (2000a) *A highly polymorphic marker identified in intron 15 of the feline cardiac troponin t gene by sscp analysis*. In: International Society for Animal Genetics, Vol. 31: Animal Genetics, pp. 228-241.
- Magnon AL, Meurs KM, Kittleson MD & Ware WA (2000b) *Single nucleotide polymorphisms in intron 5 of the feline myosin regulatory light chain gene detected by sscp analysis*. In: International Society for Animal Genetics, Vol. 31: Animal Genetics, pp. 228-241.
- Mall G, Huther W, Schneider J, Lundin P & Ritz E (1990) Diffuse intermyocardiocytic fibrosis in uraemic patients. *Nephrology Dialysis Transplantation*, **5**, 39-44.
- Marian AJ, Yu Q-T, Mann DL, Graham FL & Roberts R (1995) Expression of a mutation causing hypertrophic cardiomyopathy disrupts sarcomere assembly in adult feline cardiac myocytes. *Circulatory Research*, **77**, 98-106.
- Marian AJ, Zhao G, Seta Y, Roberts R & Yu Q-T (1997) Expression of mutant (arg92gln) human cardiac troponin t, known to cause hypertrophic cardiomyopathy, impairs adult cardiac myocyte contractility. *Circulatory Research*, **81**, 76-85.
- Maron BJ, Gardin JM, Flack JM, Gidding SS, Kurosaki TT & Bild DE (1995) Prevalence of hypertrophic cardiomyopathy in a general population of young adults: Echocardiographic analysis of 4111 subjects in the cardia study. *Circulation*, **92**, 785-789.
- Martin L, VandeWoude S, Boon J & Brown D (1994) Left ventricular hypertrophy in a closed colony of persian cats [abstract]. *Journal of Veterinary Internal Medicine*, **8**, 143.
- Massart PE, Donckier J, Kyselovic J, Godfraind T, Heyndrickx GR & Wibo M (1999) Carvedilol and lacidipine prevent cardiac hypertrophy and endothelin-1 gene overexpression after aortic binding. *Hypertension*, **34**, 1197-1201.
- Matre K, Hexeberg E & Lekven J (1986) Fibre orientation in the left ventricle and its influence on local pressure-length loop analysis in the cat. *Clinical Physiology*, **6**, 293-301.
- Matsumura Y, Elliot PM, Virdee MS, Sorajja P, Doi Y & McKenna WJ (2002) Left ventricular diastolic function assessed using doppler tissue imaging in patients with hypertrophic cardiomyopathy: Relation to symptoms and exercise capacity. *Heart*, **87**, 247-251.
- McCann TM, Simpson KE, Butt JA & Gunn Moore D (2005) *Feline diabetes mellitus in the united kingdom*. In: British Small Animal Veterinary Association, p. 567, Birmingham.
- McDicken WN, Sutherland GR, Moran CM & Gordon L (1992) Colour doppler velocity imaging of the myocardium. *Ultrasound in Medicine & Biology*, **18**, 651-654.
- McEwan PE, Gray GA, Sherry L, Webb DJ & Kenyon CJ (1998) Differential effects of angiotensin ii on cardiac cell proliferation and intramyocardial perivascular fibrosis in vivo. *Circulation*, **98**, 2765-2773.
- McLaughlin RF, Tyler WS & Canada ROA (1961) A study of the subgross pulmonary anatomy in various mammals. *American Journal of Anatomy*, **108**, 149.

- Meluzín J, Špinarová L, Bakala J, Toman J, Krejčí J, Hude P, Kára T & Soucek M (2001) Pulsed doppler tissue imaging of the velocity of tricuspid annular systolic motion. *European Heart Journal*, **22**, 340-348.
- Meurs KM, Fox PR, Magnon A, Towbin JA & Liu S-K (1998) Polymerase chain reaction (pcr) analysis for feline viruses in formalin-fixed feline cardiomyopathic hearts identifies panleukopenia [abstract]. *Journal of Veterinary Internal Medicine*, **12**, 201.
- Meurs KM, Kittleson MD, Reiser PJ, Magnon AL & Towbin JA (2001) Myomesin, a sarcomeric protein, is reduced in maine coon cats with familial hypertrophic cardiomyopathy [abstract]. *Journal of Veterinary Internal Medicine*, **15**, 286.
- Meurs KM, Kittleson MD, Towbin JA & Ware W (1997) Familial systolic anterior motion of the mitral valve and/or hypertrophic cardiomyopathy is apparently inherited as an autosomal dominant trait in a family of american shorthaired cats [abstract]. *Journal of Veterinary Internal Medicine*, **11**, 138.
- Mildenberger RR, Bar-Shlomo B, Druck MN, Jablonsky G, Morch JE, Hilton JD, Kenshole AB, Frorbath N & McLaughlin PR (1984) Clinically unrecognised ventricular dysfunction in young diabetic patients. *Journal of the American College of Cardiology*, **4**, 234-238.
- Mishina M, Watanabe T, Fujii K, Maeda H & Takahashi M (1998) Non-invasive blood pressure measurements in cats: Clinical significance of hypertension associated with chronic renal failure. *Journal of Veterinary Medical Science*, **60**, 805-808.
- Mishiro Y, Oki T, Yamanda H, Onose Y, Matsuoka M, Tabata T, Wakatsuki T & Ito S (2000) Use of angiotensin ii stress pulsed tissue imaging to evaluate regional left ventricular contractility in patients with hypertrophic cardiomyopathy. *Journal of the American Society of Echocardiography*, **13**, 1065-1073.
- Miyatake K, Yamagishi M, Tanaka N, Uematsu M, Yamazaki N, Mine Y, Sano A & Hirama M (1995) A new method for the evaluation of left ventricular wall motion by tissue doppler imaging: In vitro and in vivo studies. *Journal of the American College of Cardiology*, **25**, 717-724.
- Moise NS & Dietze AE (1986) Echocardiographic, electrocardiographic, and radiographic detection of cardiomegaly in hyperthyroid cats. *American Journal of Veterinary Research*, **47**, 1487-1494.
- Moise NS & Fox PR (1999) Echocardiography and doppler imaging. In: *Textbook of canine and feline cardiology* (ed. by Fox PR, Moise NS & Sisson D), 130-171, W.B. Saunders Company, Philadelphia.
- Møller JE, Poulsen SH, Sondergaard E & Egstrup K (2000) Preload dependence of colour m-mode doppler flow propagation velocity in controls and in patients with left ventricular dysfunction. *Journal of the American Society of Echocardiography*, **13**, 902-909.
- Moreno H, Metze K, Bento AC, Antunes E, Zatz R & De Nucci G (1996) Chronic nitric oxide inhibition as a model of hypertensive heart disease. *Basic Research in Cardiology*, **91**, 248-255.
- Morgan RV (1986) Systemic hypertension in four cats: Ocular and medical findings. *Journal of the American Animal Hospital Association*, **22**, 615-622.
- Mori K, Hayabuchi Y, Kuroda Y, Masaki N & Manabe T (2000) Left ventricular wall motion velocities in healthy children measured by pulsed wave doppler

- tissue echocardiography: Normal values and relation to age and heart rate. *Journal of the American Society of Echocardiography*, **13**, 1002-1011.
- Moustapha A, Lim M, Saikia S, Kaushik V, Kang S-H & Barasch E (2001) Interrogation of the tricuspid annulus by doppler tissue imaging in patients with chronic pulmonary hypertension: Implications for the assessment of right-ventricular systolic and diastolic function. *Cardiology*, **95**, 101-104.
- Munagala VK, Jacobsen SJ, Mahoney DW, Rodeheffer RJ, Bailey KR & Redfield MM (2003) Association of newer diastolic function parameters with age in healthy subjects: A population based study. *Journal of the American Society of Echocardiography*, **16**, 1049-1056.
- Murat A, Pellieux C, Brunner HR & Pedrazzini T (2000) Calcineurin blockade prevents cardiac mitogen-activated protein kinase activation and hypertrophy in renovascular hypertension. *The Journal of Biological Chemistry*, **275**, 40867-40873.
- Myreng YS & Smiseth OA (1990) Assessment of left ventricular relaxation by doppler echocardiography. *Circulation*, 260-266.
- Nagueh MF, Kopelen. H.A., Zoghbi WA, Quinones MA & Nagueh SF (1999a) Estimation of mean right atrial pressure using tissue doppler imaging. *The American Journal of Cardiology*, **84**, 1448-1451.
- Nagueh SF, Bachinski LL, Meyer D, Hill R, Zoghbi WA, Tam JW, Quinones MA, Roberts R & Marian AJ (2001a) Tissue doppler imaging consistently detects myocardial abnormalities in patients with hypertrophic cardiomyopathy and provides a novel means for an early diagnosis before and independently of hypertrophy. *Circulation*, **104**, 128-130.
- Nagueh SF, Issam M, Kopelen HA, Middleton KJ, Quinones MA & Zoghbi WA (1998) Doppler estimation of left ventricular filling pressure in sinus tachycardia: A new application of tissue doppler imaging. *Circulation*, **98**, 1644-1650.
- Nagueh SF, Kopelen HA, Lim D, Zoghbi WA, Quinones MA, Roberts R & Marian AJ (2000) Tissue doppler imaging consistently detects myocardial contraction and relaxation abnormalities, irrespective of cardiac hypertrophy, in a transgenic rabbit model of human hypertrophic cardiomyopathy. *Circulation*, **102**, 1346-1350.
- Nagueh SF, Lakkis NM, Middleton KJ, Spencer WH, Zoghbi WA & Quinones MA (1999b) Doppler estimation of left ventricular filling pressures in patients with hypertrophic cardiomyopathy. *Circulation*, **99**, 254-261.
- Nagueh SF, Middleton KJ, Kopelen HA, Zoghbi WA & Quinones MA (1997) Doppler tissue imaging: A noninvasive technique for evaluation of left ventricular relaxation and estimation of filling pressures. *Journal of the American College of Cardiology*, **30**, 1527-1533.
- Nagueh SF, Sun H, Kopelen HA, Middleton KJ & Khoury DS (2001b) Hemodynamic determinants of the mitral annulus diastolic velocities by tissue doppler. *Journal of the American College of Cardiology*, **37**, 278-285.
- Nelson OL, Reidesel E, Ware WA & Christensen WF (2002) Echocardiographic and radiographic changes associated with systemic hypertension in cats. *Journal of Veterinary Internal Medicine*, **16**, 418-425.

- Nelson RW, Griffey SM, Feldman EC & Ford SL (1999) Transient clinical diabetes mellitus in cats: 10 cases (1989-1991). *Journal of Veterinary Internal Medicine*, **13**, 28-35.
- Nishimura R, Abel MD, Hatle LK & Jamil TA (1989a) Assessment of diastolic function of the heart: Background and current applications of doppler echocardiography. Part ii, clinical studies. *Mayo Clinic Proceedings*, **64**, 181-204.
- Nishimura R, Abel MD, Hatle LK & Jamil Tajik A (1990) Relation of pulmonary vein to mitral flow velocities by transesophageal doppler echocardiography; effect of different loading conditions. *Circulation*, **81**, 1488-1497.
- Nishimura R & Appleton CP (1996) "diastology": Beyond e and a. *Journal of the American College of Cardiology*, **27**, 372-374.
- Nishimura R, Housmans PR, Hatle LK & Jamil Tajik A (1989b) Assessment of diastolic function of the heart: Background and current applications of doppler echocardiography. Part i. Physiologic and pathophysiologic features. *Mayo Clinic Proceedings*, **64**, 71-81.
- Oki T, Mishiro Y, Yamanda H, Onose Y, Matsuoka M, Wakatsuki T, Tabata T & Ito S (2000) Detection of left ventricular regional relaxation abnormalities and asynchrony in patients with hypertrophic cardiomyopathy with the use of doppler tissue imaging. *American Heart Journal*, **139**, 497-502.
- Oki T, Tabata T, Mishiro Y, Yamanda H, Abe H, Onose Y, Wakatsuki T, Iuchi A & Ito S (1999) Pulsed tissue doppler imaging of left ventricular systolic and diastolic wall motion velocities to evaluate differences between long and short axis in healthy subjects. *Journal of the American Society of Echocardiography*, **12**, 308-313.
- Oki T, Tabata T, Yamanda H, Wakatsuki T, Mishiro Y, Abe H, Onose Y, Iuchi A & Ito S (1998) Left ventricular diastolic properties of hypertensive patients measured by pulsed tissue doppler imaging. *Journal of the American Society of Echocardiography*, **11**, 1106-1112.
- Oki T, Tabata T, Yamanda H, Wakatsuki T, Shinohara H, Nishikado A, Iuchi A, Fukuda N & Ito S (1997) Clinical application of pulsed doppler tissue imaging for assessing abnormal left ventricular relaxation. *American Journal of Cardiology*, **79**, 921-928.
- Olivetti G, Cigola E, Maestri R, Lagrasta C, Corradi D & Quaini F (2000) Recent advances in cardiac hypertrophy. *Cardiovascular Research*, **45**, 68-75.
- Olsen MH, Wachtell K, Hermann KL, Frandsen E, Dige-Petersen H, Rokkedal J, Devereux RB & Ibsen H (2002) Is cardiovascular remodelling in patients with essential hypertension related to more than high blood pressure? A life substudy. *American Heart Journal*, **144**, 530-537.
- Ommen SR, Nishimura MD, Appleton CP, Miller FA, Oh JK, Redfield MM & Tajik AJ (2000) Clinical utility of doppler echocardiography and tissue doppler imaging in the estimation of left ventricular filling pressures- a comparative simultaneous doppler-catheterisation study. *Circulation*, **102**, 1788-1794.
- Ommen SR & Tajik AJ (2001) Hypertrophic cardiomyopathy. From bench to bedside.....And now back again? *Circulation*, **104**, 126-127.
- Opie LH (1998a) Chapter 3: Heart cells and organelles. In: *The heart: Physiology from cell to circulation*, Lippencott-Raven, Philadelphia PA, 43-68.

- Opie LH (1998b) Chapter 14; blood pressure and the peripheral circulation. In: *The heart physiology from cell to circulation*, Lippencott-Raven, Philadelphia PA, 421-447.
- Orlowski J & Lingrel JB (1990) Thyroid and glucocorticoid hormones regulate the expression of multiple na,k-atpase genes in cultured neonatal rat cardiac myocytes. *Journal of Biological Chemistry*, **265**, 3462-3470.
- Ortlepp JR, Vosburg HP, Reith S, Ohme F, Mahon NG, Schroder D, Klues HG, Hanrath P & McKenna WJ (2002) Genetic polymorphisms in the renin-angiotensin -aldosterone system associated with expression of left ventricular hypertrophy in hypertrophic cardiomyopathy: A study of five polymorphic genes in a family with a disease causing mutation in the myosin binding protein c gene. *Heart*, **87**, 270-275.
- Pai RG & Gill KS (1998a) Amplitudes, durations and timings of apically directed left ventricular myocardial velocities: I their normal pattern and coupling to ventricular filling and ejection. *Journal of the American Society of Echocardiography*, **11**, 105-111.
- Pai RG & Gill KS (1998b) Amplitudes, durations and timings of apically directed left ventricular myocardial velocities: II systolic and diastolic asynchrony in patients with left ventricular hypertrophy. *Journal of the American Society of Echocardiography*, **11**, 112-118.
- Palka P, Lange A, Fleming AD, Fenn LN, Bouki KP, Shaw TRD, Fox KAA, McDicken WN & Sutherland GR (1996) Age-related transmural peak mean velocities and peak gradients by doppler myocardial imaging in normal subjects. *European Heart Journal*, **17**, 940-950.
- Panciera DL, Thomas CB, Eicker SW & Atkins CE (1990) Epizootiologic patterns of diabetes mellitus in cats: 333 cases (1980-1986). *Journal of the American Veterinary Medical Association*, **197**, 1504-1508.
- Pastan SO & Braunwald E (1988) Renal disorders and the heart. In: *Heart disease: A textbook of cardiovascular medicine* (ed. by Braunwald E.), WB Saunders, Philadelphia, 1828-1847.
- Paternostro G, Pagano D, Gneccchi-Ruscone T, Bonser RS & Camici PG (1999) Insulin resistance in patients with cardiac hypertrophy. *Cardiovascular Research*, **42**, 246-253.
- Pedersen KM, Pedersen HD, Häggström J, Koch J & Ersbøll AK (2003) Increased mean arterial blood pressure and aldosterone-to-renin ratio in persian cats with polycystic kidney disease. *Journal of Veterinary Internal Medicine*, **17**, 21-27.
- Pederson D (1984) The cardiovascular system ch 7. In: *Textbook of veterinary anatomy* (ed. by Dyce K.M., Sack W.O. & Wensing C.J.G.), W.B. Saunders, Philadelphia.
- Peterson EN, Moise NS, Brown CA, Hollis NE & Slater MR (1993) Heterogeneity of hypertrophy in feline hypertrophic heart disease. *Journal of Veterinary Internal Medicine*, **7**, 183-189.
- Peterson ME, Keene BW, Ferguson DC & Pipers FS (1982) Electrocardiographic findings in 45 cats with hyperthyroidism. *Journal of the American Veterinary Medical Association*, **180**, 934-937.
- Pion PD, Kittleson MD & Rogers QR (1987) Myocardial failure in cats associated with low plasma taurine: A reversible cardiomyopathy. *Science*, **237**, 764.

- Pipers FS, Reef V & Hamlin RL (1979) Echocardiography in the domestic cat. *American Journal of Veterinary Research*, **40**, 882-886.
- Polzin DJ, Osborne CA, Bartges JW, James KM & Churchill JA (1995) Chronic renal failure. In: *Textbook of veterinary internal medicine* (ed. by E C Feldman), WB Saunders, Philadelphia.
- Poulsen SH, Andersen NH, Ivarsen PI, Mogensen C-E & Egeblad H (2003) Doppler tissue imaging reveals systolic dysfunction in patients with hypertension and apparent "isolated" diastolic dysfunction. *Journal of the American Society of Echocardiography*, **16**, 724-731.
- Rahimtoola S (2001) *Viable myocardium-pathophysiology and clinical relevance*. In: American Society of Echocardiography 12th Annual Scientific Sessions, pp. 31-38, Seattle, WA.
- Raij L (2001) Hypertension and cardiovascular risk factors; the role of angiotensin ii-nitric oxide interaction. *Hypertension*, **37**, 767-775.
- Rajagopalan N, Garcia MJ, Rodriguez L, Murray RD, Apperson-Hansen C, Stugaard M, Thomas JD & Klein AL (2001) Comparison of new doppler echocardiographic methods to differentiate constrictive pericardial heart disease and restrictive cardiomyopathy. *American Journal of Cardiology*, **87**, 86-94.
- Rambaldi R, Bax JJ, Boersma E, Valkema R, Dunker DJ, Sutherland GR, Roelandt JRTC & Poldermans D (2003) Value of pulse-wave doppler tissue imaging to identify dyssynergic but viable myocardium. *The American Journal of Cardiology*, **92**, 64-67.
- Rand JS (2002) Understanding feline diabetes [suppl]. *Compendium of Continuing Education for the Practicing Vet*, **24**, 2-6.
- Rand JS, Bobbermein LM, Hendrikz JK & Copland M (1997) Over representation of burmese cats with diabetes mellitus. *Australian Veterinary Journal*, **75**, 402-405.
- Richardson P, McKenna W, Bristow M, Maisch B, Mautner B, O'Connell J, Thiene G, Goodwin J, Gyarsas I, Martin I & Nordet P (1996) Report of the 1995 world health organisation/international society and federation of cardiology task force on the definition and classification of cardiomyopathies. *Circulation*, **93**, 841-842.
- Rishniw M, Porciello F, Herndon WE, Birretoni F, Antognoni MT, Simpson K.W. & Fruganti G (2004) *Cardiac troponin i concentrations in dogs and cats with renal insufficiency [abstract]*. In: Proceedings of the 14th ECVIM Congress-CA, p. 197, Barcelona.
- Rishniw M & Thomas WP (2002) Dynamic right ventricular outflow obstruction: A new cause of systolic murmurs in cats. *Journal of Veterinary Internal Medicine*, **16**, 547-552.
- Rodriguez L, Garcia M, Ares M, Griffin BP, Nakatani S & Thomas JD (1996) Assessment of mitral annular dynamics during diastole by doppler tissue imaging: Comparison with mitral doppler inflow in subjects without heart disease and in patients with left ventricular hypertrophy. *American Heart Journal*, **131**.
- Rossvoll O & Hatle LK (1993) Pulmonary venous flow velocities recorded by transthoracic doppler ultrasound; relation to left ventricular diastolic pressures. *Journal of the American College of Cardiology*, **21**, 687-696.

- Rozengurt N & Hayward AHS (1984) Primary myocardial disease in cats in britian: Pathological findings in twelve cases. *Journal of Small Animal Practice*, **25**, 617-626.
- Rush JE, Freeman LM, Fenollosa NK & Brown DJ (2002) Population and survival characteristics of cats with hypertrophic cardiomyopathy:260 cases (1990-1999). *Journal of the American Veterinary Medical Association*, **220**, 202-207.
- Rush JE, Keene BW & Fox PR (1990) Pericardial disease in the cat: A retrospective evaluation of 66 cases. *Journal of the American Animal Hospital Association*, **29**, 39-46.
- Rushmer RF, Crystal DK & Wagner C (1953) The functional anatomy of ventricular contraction. *Circulation Research*, **1**, 162-170.
- Rychik J & Tian Z-Y (1996) Quantitative assessment of myocardial tissue velocities in normal children with doppler tissue imaging. *The American Journal of Cardiology*, **77**, 1254-1257.
- Sahn DJ, DeMaria AN, Kisslo JA & Weyman AE (1978) Recommendations regarding the quantitation in m-mode echocardiography: Results of a survey of echocardiographic measurements. *Circulation*, **58**, 1072-1083.
- Sanderson JE, Brown DJ, Rivellesse A & Kohner E (1979) Diabetic cardiomyopathy? An echocardiographic study of young diabetics. *British Medical Journal*, **1**, 404-407.
- Sansom J (1997) Ocular manifestations of systemic hypertension in the dog and cat. *Friskies*, **9**, 24-29.
- Sansom J, Barnett KC, Dunn KA, Smith KC & Dennis R (1994) Ocular disease associated with hypertension in 16 cats. *Journal of Small Animal Practice*, **35**, 604-611.
- Santilli RA & Bussadori C (1998) Doppler echocardiographic study of left ventricular diastole in non-anaesthetized healthy cats. *The Veterinary Journal*, **156**, 203-215.
- Santilli RA, Galavotti P, Bussadori C & D'Agnolo G (2000) Hyperthyroidism in the cat. A retrospective study on 38 cases (1997-1998). *European Journal of Companion Animal Practice*, **X**, 159-166.
- Sasson Z, Hatle L, Appleton CP, Jewitt M, Alderman EL & Popp RL (1987) Intraventricular flow during isovolumic relaxation: Description and characterisation by doppler echocardiography. *Journal of the American College of Cardiology*, **10**, 539-546.
- Saunders TG, Ferguson MJ, Rush JE & Lesser MB (2001) *Severe hypertrophic cardiomyopathy in 10 young ragdoll cats*. In: American College of Veterinary Internal Medicine, p. 148, Denver CO.
- Sawyer DC (1993) Indirect blood pressure measurements in dogs, cats and horses: Correlation with direct and indirect arterial pressure measurement.
- Schillaci G, Pasqualini L, Verdecchia P, Vaudo G, Marchesi S, Porcellati C, De Simone G & Mannarino E (2002) Prognostic significance of left ventricular diastolic dysfunction in essential hypertension. *Journal of the American College of Cardiology*, **39**, 2005-2011.
- Schirmer H, Lunde P & Rasmussen K (2000) Mitral flow derived doppler indexes of left ventricular diastolic function in a general population; the tromso study. *European Heart Journal*, **21**, 1376-1386.

- Schmitz L, Schneider MBE & Lange PE (2003) Isovolumic relaxation time corrected for heart rate has a constant value from infancy to adolescence. *Journal of the American Society of Echocardiography*, **16**, 221-222.
- Schober K, Luis Fuentes V & Bonagura JD (2003) Comparison between invasive hemodynamic measurements and noninvasive assessment of left ventricular diastolic function by use of doppler echocardiography in healthy anesthetised cats. *American Journal of Veterinary Research*, **64**, 93-103.
- Schober K, Luis Fuentes V, Dukes McEwan J & French AT (1998) Pulmonary venous flow characteristics as assessed by transthoracic pulsed doppler echocardiography in normal dogs. *Veterinary Radiology & Ultrasound*, **39**, 33-41.
- Schober KE & Luis Fuentes V (2001a) Effects of age, body weight, and heart rate on transmitral and pulmonary venous flow in clinically normal dogs. *Journal of Veterinary Research*, **62**, 1447-1454.
- Schober KE & Luis Fuentes V (2001b) Mitral annulus motion as determined by m-mode echocardiography in normal dogs and dogs with cardiac disease. *Veterinary Radiology & Ultrasound*, **42**, 52-61.
- Segal J (1989) Acute effect of thyroid hormone on the heart: An extranuclear increase in sugar uptake. *Journal of Molecular Cellular Cardiology*, **21**, 323-334.
- Segal J (1990) Calcium is the first messenger for the action of thyroid hormone at the level of the plasma membrane: First evidence for an acute effect of thyroid hormone on calcium uptake in the heart. *Endocrinology*, **126**, 2693-2702.
- Sen S (1999) Myocardial response to stress in cardiac hypertrophy and heart failure. *Annals of the New York Academy of Sciences*, **874**, 125-133.
- Senbonmatsu T, Ichihara S, Price E, Gaffney FA & Inagami T (2000) Evidence for angiotensin ii type 2 receptor-mediated cardiac myocyte enlargement during in vivo pressure overload. *The Journal of Clinical Investigation*, **106**, R25-R29.
- Seneviratne BIB (1977) Diabetic cardiomyopathy; the preclinical phase. *British Medical Journal*, **1**, 1444-1446.
- Sennello KA, Schulman RL, Prosek R & Siegel. A.M. (2003) Systolic blood pressure in cats with diabetes mellitus. *Journal of the American Veterinary Medical Association*, **223**, 198-201.
- Sessoms MW, Lissauskas J & Kovacs SJ (2002) The left ventricular color m-mode doppler flow propagation velocity v(p): In vivo comparison of alternative methods including physiologic implications. *Journal of the American Society of Echocardiography*, **15**, 339-348.
- Severino S, Caso P, Galderisi M, De Simone L, Petrocelli A, De Divitiis O & Mininni N (1998) Use of pulsed doppler tissue imaging to assess regional left ventricular diastolic dysfunction in hypertrophic cardiomyopathy. *American Journal of Cardiology*, **82**, 1394-1398.
- Shan K, Bick RJ, Poindexter BJ, Shimoni S, Letsou GV, Reardon MJ, Howell JF, Zoghbi WA & Nagueh SF (2000) Relation of tissue doppler derived myocardial velocities to myocardial structure and beta-adrenergic receptor density in humans. *Journal of the American College of Cardiology*, **36**, 891-896.

- Simone G, Ganau A, Roman MJ & Devereux RB (1997) Relation of left ventricular longitudinal and circumferential shortening to ejection fraction in the presence or in the absence of mild hypertension. *Journal of Hypertension*, **15**, 1011-1017.
- Sisson DD, Knight DH & Helinski C (1991) Plasma taurine concentrations and m-mode echocardiographic measurements in healthy cats and cats with dilated cardiomyopathy. *Journal of Veterinary Internal Medicine*, **5**, 232-238.
- Slatopolsky E, Martin K & Hruska K (1980) Parathyroid hormone metabolism and its potential as a uremic toxin. *American Journal of Physiology*, **239**, F1-12.
- Smiseth O, Thompson CR, Lohavenichbutr K & Bowering J (1999) The pulmonary venous systolic flow pulse-its origin and relationship to left atrial pressure. *Journal of the American College of Cardiology*, **34**, 802-809.
- Smith SA, Stoner JE, Russell AE, Sheppard JM & Aylward PE (1989) Transmitral velocities measured by pulsed doppler in healthy volunteers: Effects of acute changes in blood pressure and heart rate. *British Heart Journal*, **61**, 344-347.
- Snyder PS, Sadek D & Jones GL (2001) Effect of amlodipine on echocardiographic variables in cats with systemic hypertension. *Journal of Veterinary Internal Medicine*, **15**, 52-56.
- Sohn D-W, Chai I-H, Lee D-T, Kim H-C, Kim H-S, Oh B-H, Lee M-M, Park Y-B, Choi Y-S, Seo J-D & Lee Y-W (1997) Assessment of mitral annulus velocity by doppler tissue imaging in the evaluation of left ventricular diastolic function. *Journal of the American Colleges of Cardiology*, **30**, 474-480.
- Sohn D-W, Chung W-Y, Chai I-H, Zo J-H, Lee M-M, Park Y-B, Choi Y-S & Lee Y-W (2001) Mitral annulus velocity in the noninvasive estimation of left ventricular dp/dt. *The American Journal of Cardiology*, **87**, 933-936.
- Sokal RR & Rohlf FJ (1995) Biometry. (ed. by R R Sokal & F J Rohlf), 382, W.H. Freeman and Co., New York.
- Solomon SD, Wolff S, Watkins H, Ridker PM, Come P, McKenna WJ, Seidman CE & Lee RT (1993) Left ventricular hypertrophy and morphology in familial hypertrophic cardiomyopathy associated with mutations of the beta-myosin heavy chain gene. *Journal of the American College of Cardiology*, **22**, 498-505.
- Song J-M, Kim JH, Kim Y-H, Lee S-W, Yoon Y-J, Kim J, Kang D-H & Song J-K (2003) Temporal changes and histologic relation of postsystolic thickening in an animal model of acute ischemia and reperfusion. *Journal of the American Society of Echocardiography*, **16**, 409-414.
- Sparkes AH, Caney SMA, King MCA & Gruffydd-Jones TJ (1999) Inter- and intraindividual variation in doppler ultrasonic indirect blood pressure measurements in healthy cats. *Journal of Veterinary Internal Medicine*, **13**, 313-318.
- Steen T & Steen S (1994) Filling of a model left ventricle studied by colour m-mode doppler. *Cardiovascular Research*, **28**, 1821-1827.
- Stepien RL (2004) *Blood pressure measurement: Equipment, methodology and clinical recommendations of the american consensus panel*. In: 22nd Annual Forum of the American College of Veterinary Internal Medicine.
- Stoddard MF, Pearson AC, Kern MJ, Ratcliff J, Mrosek DG & Labovitz AJ (1989) Influence of alteration in preload on the pattern of left ventricular diastolic

- filling as assessed by doppler echocardiography in humans. *Circulation*, **79**, 1226-1236.
- Stoddard MF, Risoe C, Ihlen H & Smiseth O (1994) Intracavity filling pattern in the failing ventricle assessed by colour m-mode doppler echocardiography. *Journal of the American College of Cardiology*, **24**, 663-670.
- Streeter DDJ, Spotnitz HM, Patel DP, Ross JJ & Sonnenblick EH (1969) Fiber orientation in the canine left ventricle during diastole and systole. *Circulatory Research*, **24**, 339-347.
- Stugaard M, Risoe C, Ihlen H & Smiseth O (1993) Intraventricular early diastolic filling during acute myocardial ischemia; assessment of multigated color m-mode doppler echocardiography. *Circulation*, **88**, 2705-2713.
- Stugaard M, Risoe C, Ihlen H & Smiseth O (1994) Intracavity filling pattern in the failing left ventricle assessed by colour m-mode doppler echocardiography. *Journal of the American College of Cardiology*, **24**, 663-670.
- Sugden MC, Holness MJ, Liu YL, Smith DM, Fryer LG & Kruszynska YT (1992) Mechanisms regulating cardiac fuel selection in hyperthyroidism. *Biochemical Journal*, **286**, 513-517.
- Suko J (1973) The calcium pump of the sarcoplasmic reticulum: Functional alterations at different levels of thyroid state in rabbits. *Journal of Physiology*, **228**, 563-568.
- Sundell J & Knuuti J (2003) Insulin and myocardial blood flow. *Cardiovascular Research*, **57**, 312-319.
- Sutherland GR, Bijnens B & McDicken WN (1999) Tissue doppler echocardiography: Historical perspective and technological considerations. *Echocardiography*, **16**, 445-453.
- Sutherland GR & Hatle L (2002) Normal data. In: *Doppler myocardial imaging: A textbook* (ed. by Sutherland GR, Hatle L, Rademakers FE, Claus P, D'hooge J & Bijnens BH), 59-97, Leuven University Press, Leuven, Belgium.
- Syme HM, Barber PJ, Markwell PJ & Elliott J (2002) Prevalence of systolic hypertension in cats with chronic renal failure. *Journal of the American Veterinary Medicine Association*, **12**, 1799-1804.
- Tabata T, Oki T, Yamada H, Abe H, Onose Y & Thomas JD (2000) Subendocardial motion in hypertrophic cardiomyopathy: Assessment from long- and short-axes views by pulsed doppler tissue imaging. *Journal of the American Society of Echocardiography*, **13**, 108-115.
- Tahiliani AG & McNeill JH (1986) Diabetes-induced abnormalities in the myocardium. *Life Sciences*, **38**, 959-974.
- Takatsuji H, Maikami T, Urasawa K, Teranishi J-I, Onozuka H, Takagi C, Makita Y, Matsuo H, Kusuoka H & Kitabatake A (1996) A new approach for evaluation of left ventricular diastolic function: Spatial and temporal analysis of left ventricular filling flow propagation by color m-mode doppler echocardiography. *Journal of the American College of Cardiology*, **27**, 365-371.
- Taugner F (2001) Stimulation of the renin-angiotensin system in cats with hypertrophic cardiomyopathy. *Journal of Comparative Pathology*, **125**, 122-129.
- Taugner F, Baatz G & Nobiling R (1996) The renin-angiotensin system in cats with chronic renal failure. *Journal of Comparative Pathology*, **115**, 239-252.

- Thoday KL & Mooney CT (1992) Historical, clinical and laboratory features of 126 hyperthyroid cats. *Veterinary Record*, **131**, 257-264.
- Thomas JD, Choong CY, Flachskampf FA & Weyman AE (1990) Analysis of the early transmitral doppler velocity curve: Effect of primary physiologic changes and compensatory preload adjustment. *Journal of the American College of Cardiology*, **16**, 644-655.
- Thomas JD, Newell JB, Choong CYP & Weyman AE (1991) Physical and physiological determinants of transmitral velocity; numerical analysis. *American Journal of Physiology*, **29**, 1718-1730.
- Thomas JD & Weyman AE (1991) Echocardiographic doppler evaluation of left ventricular diastolic function. *Circulation*, **84**, 977-990.
- Thomas WP, Gaber GJ, Jacobs PM, Kaplan CW, Lombard CW, Moise NS & Moses BL (1993) Recommendations for standards in transthoracic two-dimensional echocardiography in the dog and cat. Echocardiography committee of the speciality of cardiology; american college of veterinary internal medicine. *Journal of Veterinary Internal Medicine*, **7**, 247-252.
- Thomas WP, Mathewson JW, Suter PF, Reed JR & Meierhenry EF (1984) Hypertrophic obstructive cardiomyopathy in a dog: Clinical, haemodynamic, angiographic, and pathological studies. *Journal of the American Animal Hospital Association*, **20**, 253-260.
- Tilley LP (1976) Feline cardiology. *Veterinary Clinics of North America-Small Animal Practice*, **6**, 415-432.
- Tilley LP (1992) Essentials of canine and feline electrocardiography. (ed. by L P Tilley), Lea and Febiger, Philadelphia.
- Tilley LP & Liu S-K (1975) Cardiomyopathy and thromboembolism in the cat. *Feline Practice*, **September-October**, 32-41.
- Tiska RW, Bahl JJ, Leinwand LA & Morkin E (1990) Thyroid hormone regulates expression of a trans fected human α -myosin heavy-chain fusion gene in foetal rat heart cells. *Proceedings of the National Academy of Science USA*, **87**, 379-383.
- Trambaiolo P, Tonti G, Salustri A, Fedele F & Sutherland GR (2001) New insights into the regional systolic and diastolic left ventricular function with tissue doppler echocardiography: From qualitative analysis to a quantitative approach. *Journal of the American Society of Echocardiography*, **14**, 85-96.
- Uematsu M & Miyatake K (1999) Myocardial velocity gradient assessed by a tissue doppler imaging technique. *Echocardiography*, **16**, 465-472.
- Uematsu M, Miyatake K, Tanaka N, Matsuda H, Sano A, Yamazaki N, Hiramata M & Yamagishi M (1995) Myocardial velocity gradient as a new indicator of regional left ventricular contraction: Detection by a two-dimensional tissue doppler imaging technique. *Journal of the American College of Cardiology*, **26**, 217-223.
- Van Vleet JF & Ferrans VJ (1986) Myocardial disease of animals. *American Journal of Pathology*, **124**, 98-178.
- Van Vleet JF, Ferrans VJ & Weirich WE (1980) Pathological alterations in hypertrophic cardiomyopathy and congestive cardiomyopathy of cats. *American Journal of Veterinary Research*, **41**, 2037-2048.

- Vanoverschelde JJ, Raphael D, Robert A & Cosyns J (1990) Left ventricular filling in dilated cardiomyopathy; relation to functional class and hemodynamics. *Journal of the American College of Cardiology*, **15**, 1288-1295.
- Verhelst J, Berwaerts J, Marescau B, Abs R, Neels H, Mahler C & De Deyn PP (1997) Serum creatine, creatinine, and other guanidino compounds in patients with thyroid dysfunction. *Metabolism: Clinical and Experimental*, **46**, 1063-1067.
- Vierendeels JA, Dick E & Verdonck PR (2002) Hydrodynamics of colour m-mode doppler flow wave propagation velocity $v(p)$: A computer study. *Journal of the American Society of Echocardiography*, **15**, 219-224.
- Vinereanu D, Florescu N, Sculthorpe N, Tweddel AC, Stephens MR & Fraser AG (2001) Differentiation between pathologic and physiologic left ventricular hypertrophy by tissue doppler assessment of long-axis function in patients with hypertrophic cardiomyopathy or systemic hypertension and in athletes. *American Journal of Cardiology*, **88**, 53-58.
- Vinereanu D, Khokhar A & Fraser AG (1999) Reproducibility of pulsed wave tissue doppler echocardiography. *Journal of the American Society of Echocardiography*, **12**, 492-499.
- Wandt B, Bojö L, Hatle L & Wranne B (1998) Left ventricular contraction pattern changes with age in normal adults. *Journal of the American Society of Echocardiography*, **11**, 857-863.
- Weber KT, Brilla CG & Janicki JS (1991) Signals for the remodelling of the cardiac interstitium in systemic hypertension. *Journal of Cardiovascular Pharmacology*, **17**, S14-S19.
- WHO/ISFC task force (1980) Report of the who/isfc task force on the definition and classification of cardiomyopathies. *British Heart Journal*, **44**, 672-673.
- Wilkenshoff UM, Hatle L, Sovany A, Wranne B & Sutherland GR (2001) Age-dependant changes in regional diastolic function evaluated by colour doppler myocardial imaging: A comparison with pulsed doppler indices of global function. *Journal of the American Society of Echocardiography*, **14**, 959-969.
- Wilkins RJ (1977) Clinical pathology of feline cardiac disease. *Veterinary Clinics of North America-Small Animal Practice*, **7**, 285-290.
- Woo A, Radowski H, Liew JC, Zhao M-S, Liew C-C, Parker TG, Zeller M & Wigle ED (2003) Mutations of the β myosin heavy chain gene in hypertrophic cardiomyopathy: Critical functional sites determines prognosis. *Heart*, **89**, 1179-1185.
- Yamanda H, Oki T, Mishiro Y, Tabata T, Abe M, Onose Y, Wakatsuki T & Ito S (1999) Effect of aging on diastolic left ventricular myocardial velocities measured by pulsed tissue doppler imaging in healthy subjects. *Journal of the American Society of Echocardiography*, **12**, 574-581.
- Yamanda H, Oki T, Tabata T, Iuchi A & Ito S (1998) Assessment of left ventricular systolic wall motion with pulsed doppler imaging: Comparison with peak dp/dt of the left ventricular pressure curve. *Journal of the American Society of Echocardiography*, **11**, 442-449.
- Yamauchi-Takahara K, Nakajima-Taniguchi C, Matsui H, Fujio Y, Kunisada K, Nagata S & Kishimoto T (1996) Clinical implications of hypertrophic cardiomyopathy associated with mutations in the α -tropomyosin gene. *Heart*, **76**, 63-65.

- Yamazaki T, Komuro I, Shiojima I & Yazaki Y (1999a) The molecular mechanism of cardiac hypertrophy and failure. *Annals of the New York Academy of Sciences*, **874**, 38-48.
- Yamazaki T, Komuro I & Yazaki Y (1999b) Role of the renin-angiotensin system in cardiac hypertrophy. *American Journal of Cardiology*, **83**, 53H-57H.
- Yoshida T, Mori M & Nimura Y (1961) Analysis of heart motion with ultrasonic doppler method and its clinical application. *American Heart Journal*, **61**, 61-75.
- Yoshikawa J, Akasaka T, Yoshida K & Takagi T (1993) Systolic coronary flow reversal and abnormal diastolic flow patterns in patients with aortic stenosis: Assessment with an intracoronary doppler catheter. *Journal of the American Society of Echocardiography*, **6**, 516-524.
- Zou Y, Hiroi Y, Uozumi H, Takimoto E, Toko H, Zhu W, Kudoh S, Mizukami M, Shimoyama M, Shibasaki F, Nagai R, Yazaki Y & Komuro I (2001) Calcineurin plays a critical role in the development of pressure overload-induced cardiac hypertrophy. *Circulation*, **104**, 97-101.